Alma Mater Studiorum – Università di Bologna

DOTTORATO DI RICERCA IN

SCIENZE BIOTECNOLOGICHE FARMACEUTICHE

Ciclo XXXII

Settore Concorsuale: 03/D1 - CHIMICA E TECNOLOGIE FARMACEUTICHE, TOSSICOLOGICHE E NUTRACEUTICO-ALIMENTARI

Settore Scientifico Disciplinare: CHIM/08

Multitarget and network-driven medicinal chemistry strategies for the treatment of neuroinflammatory diseases

Presentata da: Michele Rossi

Coordinatore Dottorato

Prof. Maria Laura Bolognesi

Supervisore

Prof. Maria Laura Bolognesi

Esame finale anno 2020

Abstract

Neuroinflammatory based-diseases are a very challenging area for medicinal chemists. Several efforts have been made during the years; however, an effective treatment for these diseases, such as Alzheimer's disease (AD) and multiple sclerosis (MS), does not exist yet. Neuroinflammatory -based diseases are multifactorial in nature with still unclear pathogenic mechanisms and scarce information on how neuroinflammation is interconnected with other concomitant events, such as neurodegeneration.

Polypharmacology is one of the milestones for the development of therapies able to combat multifactorial diseases. Particularly, the development of multitarget compounds through different strategies (linking, fusing, merging) has permitted to expand the potential arsenal to treat multifactorial diseases.

Based on these considerations, this thesis was focused on the development of multitarget molecules for combating neuroinflammatory diseases through different and innovative polyphamacological approaches in four projects.

Projects 1 & 2 focused on the development of fatty acids (FAs)/drug conjugates for the treatment of MS and AD, respectively. Particularly, we applied a conjugation strategy among omega-3 FAs and valproic acid (project 1) or $P2Y_6$-agonists (project 2), in order to obtain innovative multitarget molecules with potentially increased property in terms of efficacy and pharmacokinetics, and less cytotoxicity.

Projects 3 & 4 focused on the design and synthesis of multitarget molecules derived from food byproduct (cashew nut-shell liquid) for the treatment of AD. Particularly, we developed different series of molecules as potentially globally accessible drugs, by applying a hybridization strategy. Notably, we developed a small library of dual sustainable HDAC/ferroptosis inhibitors (project 3), and a library of cholinergic inhibitors with potential anti-inflammatory profile (project 4) as multitarget hybrids for the treatment of AD.

TABLE OF CONTENTS

ABBREVIATIONS

Aβ: amyloid β; **AA**: arachidonic acid; **AD**: Alzheimer's diseases; **ALA**: alpha-linolenic acid; **APP**: amyloid precursor protein; **BACE**-1: aspartyl protease β-secretase; **BBB**: Blood-brain barrier; **CNS**: central nervous system; **CNSL**: cashew nut-shell liquid; **DDIs**: drug–drug interactions ; **DHA**: docosahexaenoic acid; **EPA**: eicosapentaenoic acid; **FAs**: Fatty acids; **FDA**: Food and Drug Administration; **GSK-3β**: kinase-3 beta; **HDACi**: histone deacetylases inhibitor; **IL**: interleukin; **iNOS**: inducible nitric oxide synthase; **LA**: linoleic acid; **LC-FA**: long-chain fatty acids; **LC-PUFAs**: Long-chain polyunsaturated fatty acids; **LDL**: low-density lipoprotein; **MAO-B**: monoamine oxidase-B; **MC-FA**: medium-chain fatty acids; **MS**: multiple sclerosis; **MTDL**: multitarget-direct ligand; **MUFAs**: monounsaturated fatty acid; MW: molecular weight; **OEA**: oleic acid; **OPCs**: oligodendrocyte progenitor cells; **PA**: palmitic acid; **PPAR-α**: proliferator-activated receptor-alpha; **PD**: pharmacodynamic; **PK** pharmacokinetic; **PUFAs**: polyunsaturated fatty acids; **ROS**: reactive oxygen species, **SC-FAs**: short-chain fatty acids; **SA**: Stearic; **TNF-α**: tumors necrosis factor-alpha; **TREM2**: Triggering receptor expressed on myeloid cells 2; **VLC-FAs**: very long chain fatty acids; **VPA**: valproic acid; **MW**: microwave

Chapter 1

Introduction

1.1 Neuroinflammatory diseases

The functional decline of the central nervous system (CNS) is characterized by a chronic progressive loss of the structure and functions of neuronal materials.[1, 2] This event is generally observed in numerous humans CNS diseases characterized by a chronic form of inflammation,[1] [2] and is particularly related to a set of neurodegenerative and neurological disorders, such as Alzheimer's disease (AD),[3] and multiple sclerosis (MS).[4] Neuroinflammation is defined as a CNS inflammatory condition where the immune cellular defense respond to harmful stimuli, such as: pathogens, damaged cells, or toxic compounds.[5] These pathogenic conditions are primarily recognized by the innate-immune system of the CNS such as: microglia, and astrocytes, but also by oligodendrocytes, neurons, and endothelial cells.[6] The condition of neuroinflammation is generally characterized by abundant production of cytokines (i.e. IL-1β, IL-18), chemokines, reactive oxygen species (ROS), and secondary messengers.[7]

As it is well known, inflammation in neurological disorders is considered a double-edged sword.[8] Indeed, inflammation is a physiological defense reaction against many insults, but an altered expression of different inflammatory factors can either promote or counteract neurodegenerative processes.[8] Therefore, the intensity and duration of inflammation are the main factor that contributes to a physiological or pathological effect in the CNS.[5] Indeed, a controlled inflammatory responses process is generally considered a benefit for the organism. For instance, immuno-brain signals after inflammation lead to the subsequent reorganization of host priorities such as: regulation of interleukin expression (i.e. IL-1 and IL-4), and reprogramming of microglia activity.[5] On the contrary, a characteristic of neurodegenerative diseases is the higher degree of chronic inflammation due to the high level of damaged neurons. Indeed, chronic uncontrolled inflammation is characterized by increased production of cytokines (IL-1 and TNF), reactive oxygen species (ROS), and other inflammatory mediators (e.g. inducible nitric oxide synthase, (iNOS)). These markers are highly evident following trauma to the CNS and are associated with a significant recruitment and trafficking of peripheral macrophages and neutrophils to the site of injury.[5]

Microglia are the main actors for any argument about neuroinflammation. This is because these innate immune cells perform the primary immune surveillance and macrophage-like activities of the CNS, including the production of cytokines and chemokines.[5] These cells are local CNS cells that are placed in the white matter and gray matter of the brain and spinal cord. Overall,

microglia comprise 5–12% of the CNS population and are involved in homeostasis and in host defense against pathogens and CNS disorders.[5, 9] Microglia have the ability to shift into three different functional states, modifying its proliferation, morphology, phagocytic activity, and antigen presentation.[10] The first functional state occurs when microglia are characterized by a quiescent morphology with several thin ramified processes, typical in healthy adult CNS.[11] Although commonly considered "resting", emerging evidence suggests that quiescent microglia are active and are actively involved in many physiological processes that include making dynamic contacts with neuron.[11] Upon appropriate stimulation, the second type of microglia are the proinflammatory phenotype (M1). The M1 phenotype is the first line of defense of the innate immune system that often occurs within the first few hours or days.[12] Indeed, resident microglia or macrophages infiltrating cells after injury, trauma, ischemia-reperfusion injury, chemical exposure or infections start a massive production of proinflammatory cytokines (TNF-α, interleukin (IL)-1β, IL-12), present antigen, and express high levels of inducible NO (iNOS) for NO production.[12] This action is aimed to kill the pathogen and restore the physiological condition. Unfortunately, in several neurological diseases a chronic and uncontrolled inflammatory condition can importantly contribute to disease pathogenesis. This is the case for AD, MS, or other phatologies.[2] Finally, the third type of microglia are an alternative form discovered in the early 1990s, called M2 phenotype.[13] The M2 phenotype has been found to be induced after stimulation by IL-4 with inducing expression of the anti-inflammatory cytokines (IL-4, IL-10, IL-13 and TGF-β) as well as, arginase-1 (Arg1), CD206, MRC1 and TREM2.[12] M2 microglia play a critical role in allergy response, parasite clearance, inflammatory dampening, tissue remodeling, angiogenesis, and immunoregulation. In addition to these, M2 phenotype facilitates the resolution of inflammation through anti-inflammatory factors (e.g. IL-10, IL-13, TGF-β, VEGF, EGF) to deactivate pro-inflammatory cell phenotypes and re-establish homeostasis.[12] In a few studies, the effects, particularly on neuroprotection, repair and anti-inflammatory, of M2 microglia have been demonstrated.[14, 15] These have suggested that targeting microglia could represent an innovative potential target for treatment for neuroinflammatory-based diseases.

1.1.1 Alzheimer's disease

AD is a neurodegenerative disease primarily characterized by formation of amyloid β (Aβ)-containing plaques, neurofibrillary tangles comprising intracellular hyperphosphorylated tau protein, and neuronal loss.[16] The brain regions that are associated with higher mental functions,

particularly the neocortex and hippocampus, are those most affected by the characteristic cholinergic neuron degeneration in AD.[16] Actually, despite the several potential treatments in clinical trials, only four acetylcholinesterase inhibitors (tacrine, donepezil, rivastigmine, galantamine) and an N-methyl-D-aspartate (NMDA) receptor antagonist (memantine) have shown sufficient safety and efficacy to allow marketing approval (Figure 1).[17] Tacrine was the first drug approved by the FDA in 1993 from the treatment of AD, then withdrawn in some countries, due to concerns over safety.[17] Then, donepezil was approved in 1996, rivastigmine in 1998, galantamine in 2001, and memantine in 2003.[17] From 2003 to now, no new treatments have been approved. Moreover, for the period from 2002 to 2012, a very high attrition rate was found, with an overall success rate of 0.4% (99.6% failure), thus making AD one of the most unsuccessful therapeutic areas of drug discovery.[18] Actually, there are no new drugs and disease-modifying approved by Food and Drug Administration (FDA) for the treatments of AD.[19]

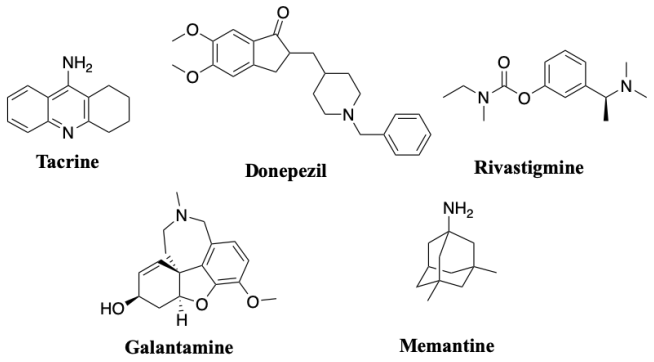

Figure 1. Chemical structures of the approved drugs for AD.

AD progression is typically painted as a sequence of events that starts from the accumulation of Aβ.[16] This process leads to a microglial response, which promotes tau hyperphosphorylation and formation of neurofibrillary tangles, leading to neurodegeneration and cognitive impairment.[9] Another key feature of AD is the presence of prominent neuroinflammation.[3, 20] Indeed, although not fully appreciated, the neuroinflammation process in AD contributes to the pathogenesis as much as the Aβ plaques and tangles do themselves.[21]

Aβ is generated by a parent protein called amyloid precursor protein (APP), which is cleaved in two steps by the secretase enzymes.[22] In physiological condition APP is cleaved by α- and γ-secretases resulting in the generation of a long-secreted form of soluble APP (APPsα).[22] Instead,

in pathological conditions, the APP is cleaved sequentially by β- followed by γ-secretases, leading to release of the Aβ fragment and different soluble APP (APPsβ).[22] The resulting Aβ fragments are predominantly 40 amino acids-long (but peptide length can range from 38 to 43 amino acids) and are the main component of Aβ-plaques after oligomerization. Aβ itself has been shown to have proinflammatory properties into the CNS and can bind to several innate immune receptors present on microglia, such as TLR2, TLR4, TLR6, and CD14.[23] The binding of Aβ with the microglia transmembrane receptors results in activation of microglia which starts to produce proinflammatory cytokines, chemokines, ROS, and neurotoxic reactive nitrogen species (RNS).[23] Moreover, Aβ-induced proinflammatory cytokines reduce microglial Aβ clearance ability causing Aβ aggregation and leading to further amyloid 'seeding' and spreading of amyloid pathology.[24] Similarly, Aβ-induced cytokines promote tau hyperphosphorylation and pathology, thus initiating a self-perpetuating loop that culminates in worsening disease.[25] Other proinflammatory cytokines, such as IFNγ and TNFα not only inhibited uptake of Aβ, but also prevents the internalized Aβ degradation.[26] This demonstrates that M1 microglia phenotype might be less able to take up and degrade Aβ properly.[26] While M1 microglia appear to be impaired in their ability to remove Aβ, M2 microglia have been demonstrated to be efficient phagocytes. Furthermore, many studies have demonstrated that modulation of microglial polarization from the M1 to the M2 phenotype ameliorates neuroinfammatory responses, Aβ deposits and tau hyperphosphorylation in AD.[27] Hence, modulation of microglial phenotypes may represent a promising therapeutic approach for the treatment of AD.[27]

1.1.2 Multiple sclerosis

MS is a chronic, inflammatory, neurodegenerative and demyelinating disease of the CNS.[28] Although MS etiology is not fully elucidated, its multifactorial nature is well-acknowledged.[28] Demyelination is the key of histopathological feature, in which the immune system attacks either the myelin or the oligodendrocytes that produce it.[28] Physiologically, when axonal damage occurs, a remyelinating process starts, with oligodendrocyte progenitor cells (OPCs) engaging the demyelinated axons and differentiating into oligodendrocytes.[29] However, in MS, this natural self-repair process is hampered and fails. Importantly, in the progressive stages, both active demyelination and neurodegeneration are observed, together with pronounced inflammation in the brain.[29] This occurs through the activation of microglial cells and the pathological infiltration of immune system cells into the CNS.[30]

The mechanism of action of the actual MS's drugs can be summarized into two interdependent processes: immunosuppression and anti-inflammation. Indeed, the drugs such as interferon-β, glatiramer, fingolimod, dimethyl fumarate, teriflunomide, laquinimod, siponimod, and ocrelizumab are able to interact with B- or T-cells and lymphocyte in order to immunosuppress the overactivated immune system decreasing the neuroinflammatory status (Figure 2). [31] Other drugs used for the treatment of MS are the monoclonal antibody: alemtuzumab and natalizumab. Alemtuzumab is an anti-CD52 antibody and cause a robust peripheral depletion of lymphocytes and monocytes, while natalizumab selectively binds the α4 subunit of the cell adhesion molecule very late antigen 4 (VLA-4), which is expressed on the surface of lymphocytes and monocytes blocking the entry of lymphocytes into the CNS.[31] Although reducing inflammation or brain-cells perfusion, none of the currently available therapies has been shown to effectively enhance lesion repair. Therefore, there is an unmet clinical need to develop new disability-reversing therapies also aiming at the preservation and/or regeneration of both neurons and oligodendroglia cells.[32]

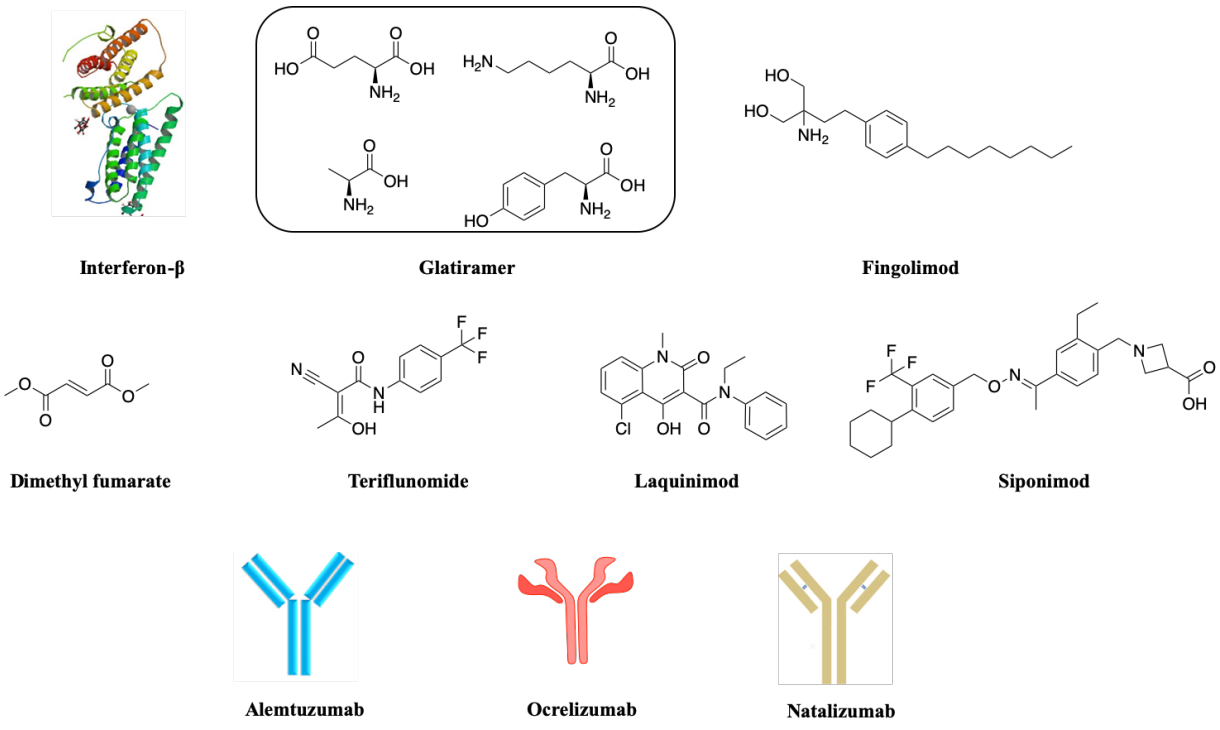

Figure 2. Principal actual treatments for MS disease.

In the research of such restorative interventions, one emerging possibility is targeting both protection and regeneration of neurons and oligodendrocytes, by acting at the same time on immunomodulation.[33] Clearly, the simultaneous activation of endogenous neuroprotective

pathways, the support of brain neurogenesis and gliogenesis, and the decrease of neuroinflammation may be more effective than blocking only one of these multiple networked events underlying complex MS pathogenesis. It is appreciated that during the immune-driven and neurodegenerative processes, MS-specific deregulation of gene expressions and resulting protein dysfunction play a central role.[34] These deviations in gene expression support the CNS inflammatory response. Epigenetic mechanisms are considered crucial in MS-disease pathogenesis.[34] Indeed, changes in histone acetylation patterns in normal-appearing white matter and in early MS lesions have been documented.[35] Furthermore, it has been found an increase of immunoreactivity for acetylated histone H3 in nuclei of mature oligodendrocytes.[35] A particular attention has been also paid to the pharmacological regulation of microglial activation, which, as already discussed, is recognized as a double-edged sword, exerting both beneficial and detrimental effects on neurons, the latter through neruoinflammation.[36] Microglia are thought to be protective when properly activated M2. However, inappropriate activation worsens neuropathological processes and increases neuronal death (as observed in AD) and has been largely incriminated for the MS pathology. Moreover, the complexity of the microglia phenotype and its regulation, from proinflammatory (M1) to anti-inflammatory phenotype (M2) may account for its protective and detrimental effects toward neurons, respectively.[37] The mechanisms of action of some of the drugs in Figure 2 can be summarized into anti-inflammatory activity by acting directly on immunomodulation (Glatiramer, interferon (IFN) beta, dimethyl fumarate) or blocking the entry of lymphocytes into the CNS hampered the inflammation (Natalizumab, Laquinimod) or preventing lymphocyte egression (Fingolimod, Ocrelizumab).[31] Therefore, the reduction of neuroinflammation by modulation of microglia phenotype represents a validated target for the treatment of MS.

1.2 Polypharmacological approach for the treatment of complex diseases

Among the drug discovery community, there is a full understanding that the traditional approach *one-drug one-target one-disease* may be inadequate for the treatment of complex diseases such as neuroinflammatory diseases. This principle is based on the dogma that the causes and/or the symptoms of a given disease can be tackled by a drug rationally designed to modulating an individual biological target, previously identified as responsible of a given disease.[38, 39] Such a so-called *target-based approach* to discover new drugs promoted from important technological advances: such as the arrival of omics and structural biology techniques.[40] It has led to the successfully identify a series of top selling drugs which, by hitting a single disease-relevant target with high potency and selectivity, entirely fulfilled the idea of the "magic bullet" proposed by Ehrlich.[41, 42]

The solid and rational foundation of *(single)target-based drug discovery* coupled with an essentially finished version of the human genome sequence in 2003, led to an increase enthusiasm among the pharmaceutical community and was expected to open new frontiers.[43]

Conversely, a lower number of new molecular entities approved over the last decades has been the tangible symbol of a gradual decline of the pharma's productivity.[44] In parallel to these evidences, the cost of bringing a drug to the market has steadily increased, with a recent estimate of $2.6 billion.[45] The evident inefficiency of the drug discovery process, together with the consideration that most diseases are multifactorial in nature has highlighted that this approach is reductionist, oversimplifying the disease mechanisms.[39, 46] Nowadays, the most accepted view on this matter is based on network medicine. Under an general perspective, diseases are viewed as the result of the systemic collapse of physiological networks, due to the suppression or activation of certain pathway and a consequent imbalance of input-output.[47] Thus, it is intuitive that diseased networks cannot be efficiently restored by acting with a drug that interact with a single target protein. This is because robustness and redundancy are distinctive features of complex biological network systems. As a consequence, the modulation of several targets through a well-concerted multitarget approach is more likely to achieve the desired therapeutic effect.[48, 49] The notion that the most currently incurable human diseases, such as cancer and neurological diseases are complex in nature, i.e. are caused by a combination of events such as genetic, environmental, and lifestyle factors and therefore must be attacked with similarly complex therapeutic approaches, is another important argument to further support this drug discovery paradigm change. In addition, different widely prescribed and effective drugs have been retrospectively shown to interact more than one protein target, with their therapeutic

efficiency. One example is the anti-cancer drugs imatinib, which was originally developed as a selective inhibitor of the BCR-Abl kinase, but then shown to also inhibit other protein kinases. These additional properties were reported to be essential for imatinib's clinical activity, for the drug's multitarget profile potentially forming the basis of its therapeutic activity. A more recent multitarget drug for cancer therapy is midostaurin. Midostaurin, a semi-synthetic derivative of the pan-kinase inhibitor staurosporine, is a multi-kinases inhibitor for the treatment of acute myeloid leukemia, approved in the 2017. It was shown to inhibit the protein kinase C alpha (PKC alpha), VEGFR2, KIT, PDGFR and WT and/or mutant FLT3 tyrosine kinases.[50] Another example is the neuropsychiatric drug clozapine, which acts against schizophrenia by modulating more than a dozen of different central nervous system (CNS) receptors.[51] A more recent example concerns safinamide, registered in 2017 (first drug approved for neurodegeneration from 2007 to 2017) for the treatment of Parkinson's disease. Safinamide combines dopaminergic effects, comprising a selective and reversible MAO-B inhibition and a dopamine reuptake inhibition, which are largely responsible for its beneficial effects on motor symptoms (Figure 3).[52]

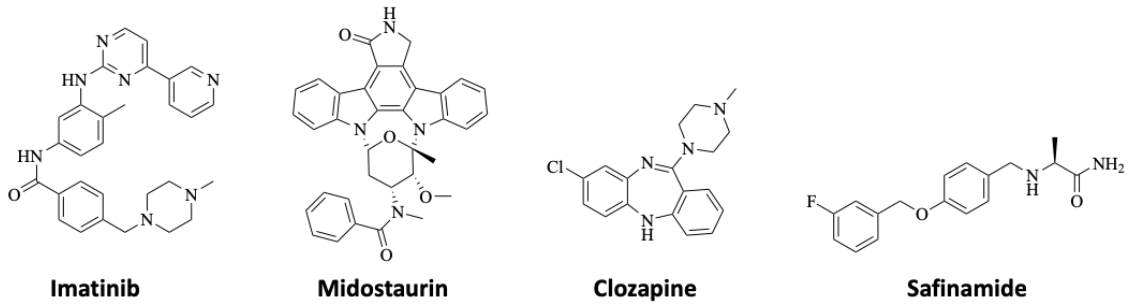

Figure 3. Chemical structure of multitarget drugs: imatinib, midostaurin, clozapine, and safinamide.

All these considerations have supported the acceptance of the quite unusual concepts of polypharmacology at the beginning of the new century. The definition of polypharmacology reported in the National Library of Medicine (NLM) vocabulary refers to "the design or use of pharmaceutical agents that act on multiple targets or disease pathways". Hence, polypharmacology includes two possible scenarios: numerous drugs binding to multiple targets (drug combination) and one drug binding to multiple targets.[53] In the first case two or more monotherapies are combined in a therapeutic regimen either as drug cocktail (combinations of two or more active pharmaceutical ingredients (APIs)) or fixed-dose combination (a dosage form with multiple APIs), whereas the second approach is based on so-called multitarget-

directed ligands (MTDLs, one dosage form, one API able to simultaneously modulate multiple targets) (Figure 4).[54]

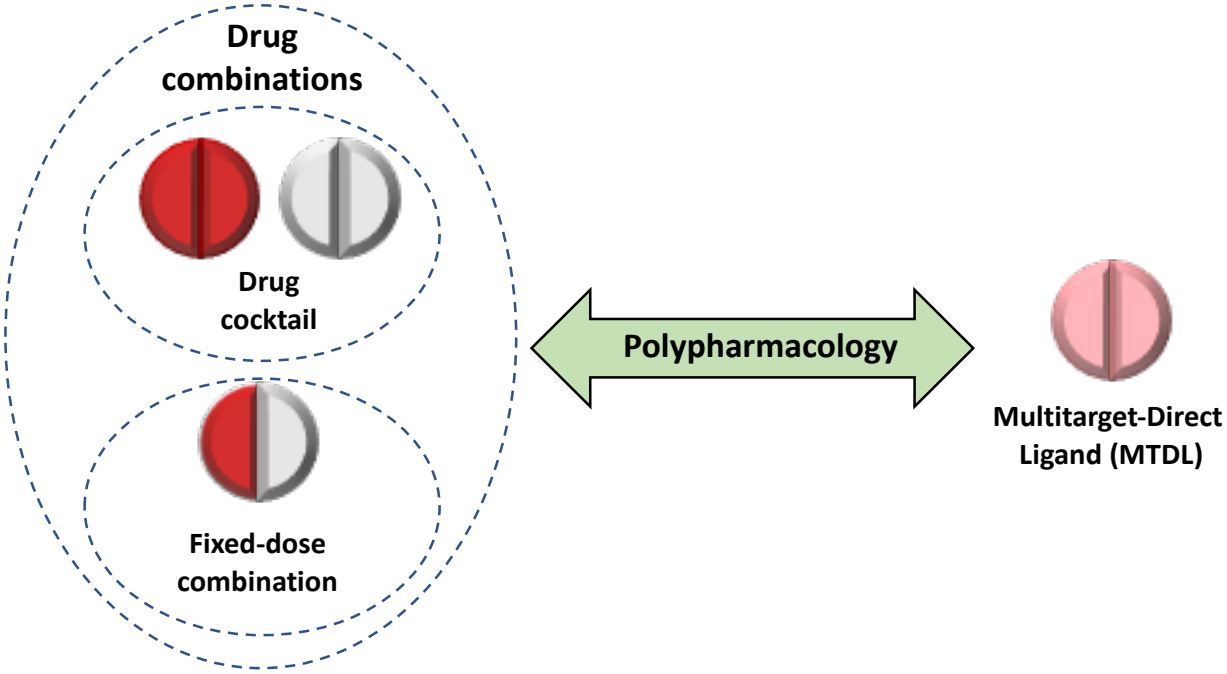

Figure 4. Possible clinical strategies for a polypharmacological therapy.

In principle, both drug combinations and MTDLs are equally possible for reaching the desired polypharmacological effect. Indeed, both have been pursued, and both have already been used for the clinical treatment of complex diseases, such as neoplastic[55] and neurological diseases.[56-58] However, in a risk/benefit analysis, MTDLs may be superior to drug combinations for a series of reasons.[59]

Although drug combinations present more elasticity for what concerns dosing, they have the intrinsic risk of drug–drug interactions (DDIs). DDIs are commonly caused by the inhibition or induction of the hepatic drug metabolism by cytochrome P450-dependent (CYP450) enzymes. These enzyme are monooxygenases that utilize heme as a cofactor and that are responsible of metabolism of all xenobiotics, including drugs.[60] Drugs may induce or inhibit CYP450 enzymes and in turn, decrease or increase the concentrations of co-administered drugs that are CYP450 substrates. Thus, alterations in drug concentrations can lead to treatment failures or toxicities. For these reasons, combinations often cause concern to prescribers, especially in the case of polymedicated aged patients where DDIs can be serious and even life-threatening. [61] Patients aged ≥65 use an estimated 4.5 drugs and 2 over-the-counter preparations per day,[62] and the number of daily used drugs is a significant predictor of adverse drug reactions due to DDIs. Thus, an MTDL will be desirable to drug cocktail in the treatment of complex diseases. Another

clinically relevant advantage of MTDLs over drug cocktail relates to the simplification of the therapeutic regimen. It is very well-known that simplifying drug regimens is one method of improving patient compliance and adherence, which are fundamental for the therapeutic success.[59]

Moving to peculiar drug discovery issues, the advantages of biological study by a standardized approval process of a multitarget drug with respect to a drug combination cannot be excluded. The prediction of pharmacodynamic (PD) and pharmacokinetic (PK) relationships should be substantially less complex when dealing with a single agent, rather than two or more. Similarly, manufacturing and formulation of MTDL should be less complicated compared to a mixture of two or more molecules, with inherent economic advantages.

In light on the potential to overcome some of the major limitations of traditional "one target, one drug" strategies, the multitarget drug discovery research field has since grown rapidly. As a key indicator of this phenomenon, we have seen an ever-increasing number of articles, which have contributed to establish these research field as a accepted branch of medicinal chemistry.[63] In addition, when considering another performance indicator referring to the late stages drug discovery pipeline, i.e. the number of Food and Drug Administration (FDA)-approved New Molecular Entities (NME) with a polypharmacological activity, a similar steady increase is evident.[63]

However, the difficulties of the MTDL approach should also be mentioned. The major criticism is in the initial stages of the drug discovery process. This is because the rational design of MTDLs poses hitherto unexplored challenges to medicinal chemists. In fact, a well-known challenge is related to the design of ligands able to interact with two proteins belonging to different target families. Indeed, if the starting frameworks present different structure functionalities, required for the interaction with the structurally unrelated targets, it might be particularly problematic to integrate them in a new single molecule and to further optimize the MTDL of high and balanced potencies.[64] Indeed, previously mentioned examples of multi-kinase inhibitors (i.e. imatinib and midostaurin) are a particular and reductive examples of MTLDs. In spite of these challenges, a certain number of design strategies have already been proposed and successfully developed. The first examples were explored by the pioneers Morphy and Rankovic delineating two possible broadly different strategies: a *knowledge-based approach* and *random screening approach*.[53]

For a *knowledge-based approach* the following flowchart can be envisaged. (i) First, two validated target proteins are chosen. They can either belong to the same or to different pathways or better involved in a target network, recognized as being critically involved in the disease's

pathogenesis. The regulation of these targets by a MTDL should potentially lead to additive effects or, even better, to synergistic potentiation. MTDLs could certainly show synergistic potentiation in the case they modulate the two targets at different key points. In the case of additive effects "only", an MTDL is expected to show major efficacy and safety profiles than a single-target drug. (ii) Second, the pharmacophoric groups responsible for binding to the selected targets must be identified. These pharmacophoric groups can be structurally joined into a single new molecule through medicinal chemistry strategy (see below). (iii) Third, the new MTDLs are tested using first biochemical and then cell-based assays. This stage is fundamental for balancing the biological profile of the new MTDLs against the selected targets.

An alternative to this previous approach, a *random screening approach* is equally feasible. This approach uses appropriate assays to search large compound collections, focused libraries, and libraries of approved drugs for discover new MTDL candidates. In this case, molecules that are already known to hit one of the targets of interest are screened against the second one in an unbiased mode. Certainly, repurposing drugs that are already on the market shows the clear advantages of reducing the cost of development, time to launch, and the uncertainty associated with safety and pharmacokinetics over a new drug.[65]

Another very well validated alternative is to start from natural products.[66] Indeed, as natural products provide plants and animals with potent defense molecules with intrinsic multifunctional activity, they are widely-predictable as prototypical multitarget molecules.[67] The biosynthesis of natural products has been evolved so that they usually possess a complex molecular structure featuring more than one active functional group, which allows them to recognize numerous molecular targets. In most cases, their synthesis involves a lot of enzymes (synthetases), each with distinct structure and binding pockets, and to permit the natural product synthesis, these enzymes must be able to bind to the molecules. Therefore, natural products have inherently more potential than synthetic compounds to bind multiple target proteins due to their mode of generation.[68] On the other hand, their poor drug likeness properties and the difficulty to synthesize them have limited their use in drug discovery.[66]

1.2.1 Strategies to design multitarget-directed ligands

Although the concept of designing MTDLs is almost recent, the existence of a series of ligands able to interact at the same time with multiple targets is well-appreciated. In this context, the most exploited rationale medicinal chemistry strategy is the *molecular hybridization* (Figure 5).[64] This approach is a very well-known medicinal chemistry strategy, which, through the

combination of two pharmacophoric moieties, aims to produce a new hybrid compound. These hybrid compounds should show improved affinity and efficacy and reduced toxicity with respect to the starting drugs.[69] With the advent of network pharmacology,[48] this strategy has been elegantly denominated as *framework combination.*[46] Basically, this approach aims to "integrate the framework and underlying pharmacophores of two molecules, each selective for a different target of interest, into a single molecules with dual activity".[70] Then, the resulting hybrid compounds can be classified as *linked*, *fused* and *merged* according to the degree of integration between the starting pharmacophores (Figure 5).[46, 71, 72] Clearly, the choice of *linked*, *fused* and *merged* hybrids is driven by the possibility of the starting frameworks, their chemical tractability, and the nature of the target.

The *linking* strategy is characterized by the typical presence of a linker (or spacer) able to bridge the two pharmacophoric groups. The nature and the position of the linker in the pharmacophore are the main issues for the success of this strategy. Indeed, it is necessary to identify a structurally tolerant position in the structure of the starting framework where the modification by the linker does not hinder the interaction with the targets. Another fundamental feature is related to the chemical nature of the linker. First, the difference between a flexible linker and a rigid one affects the PD properties of the hybrid compound, by allowing or not the recognition with both targets. Second, the difference among stable and *in vivo*-metabolizable linkers plays a fundamental role in the PK profile. In fact, a cleavable linker allows (after the appropriate *in vivo* metabolism) the release of the two starting frameworks, which will be able to interact with their targets, at the same time, and in the same tissue. This kind of hybrids are sometimes reported in the literature as *codrugs*. It is intuitive that the principal limit of the *linking* strategy is the high molecular weight (MW) of the final hybrid compounds (Figure 5). According to the Lipinski's rule of five, a molecule with an optimal oral PK profile should possess a MW less than 500 Da. Clearly, if the MW is much higher than this threshold, it could hamper membrane permeation, and compromise the reach of the desired targets.[73, 74]

Hybrid compounds can be obtained using two strategies defined as *fused* and *merged* when the structure of the frameworks shows some scaffold similarities (Figure 5). If the two frameworks are integrated by small portions or by no discernable linkers, they are called *fused hybrids*. Conversely, when the frameworks possess an evident overlapping degree, the new hybrids are defined as *merged.* Certainly, hybrid molecules derived from *fusing* or *merging* strategy, will present lower MW and consequently potentially better PK properties than those obtained via a

linking strategy. This would be of particular importance when designing compounds acting on CNS.[75, 76]

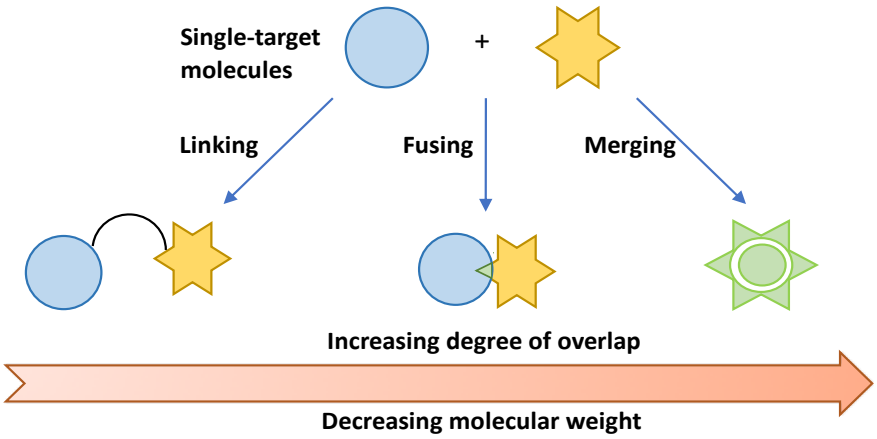

Figure 5. Design strategy to obtain hybrid compounds.

The concepts discussed above may be exemplified using the approved drug sultamicillin and two investigational drugs, i.e. edasalonexent and ladostigil (Figure 6, 7). Particularly, sultamicillin is one of the first example of an antibacterial agent (Unasyn®) designed by a *linking* strategy. It is shown that, after its administration and gastro-intestinal absorption, it can be hydrolyzed with the simultaneous liberation of two APIs, i.e. the β-lactam antibiotic ampicillin and the β-lactamase inhibitor sulbactam upon hydrolysis of the methylene diester linker.[77] The most recent example of *linking* strategy is edasalonexent, a hybrid compound in phase three clinical trial (NCT03703882) for the Duchenne muscular dystrophy, in which salicylic acid and docosahexaenoic acid are covalently linked through an ethylenediamine linker. The aim of this molecule is to release in the selected tissue and in equimolar concentration the starting molecule in order to exploit a synergistic effect after inhibition of NF-κB.[78] Finally, ladostigil has been designed by *fusing* the molecular frameworks of neuroprotective drug rasagiline (a selective inhibitor of MAO-B) with the acetylcholinesterase inhibitor rivastigmine, with the aim of achieving a dual-targeted action against AD.[79]

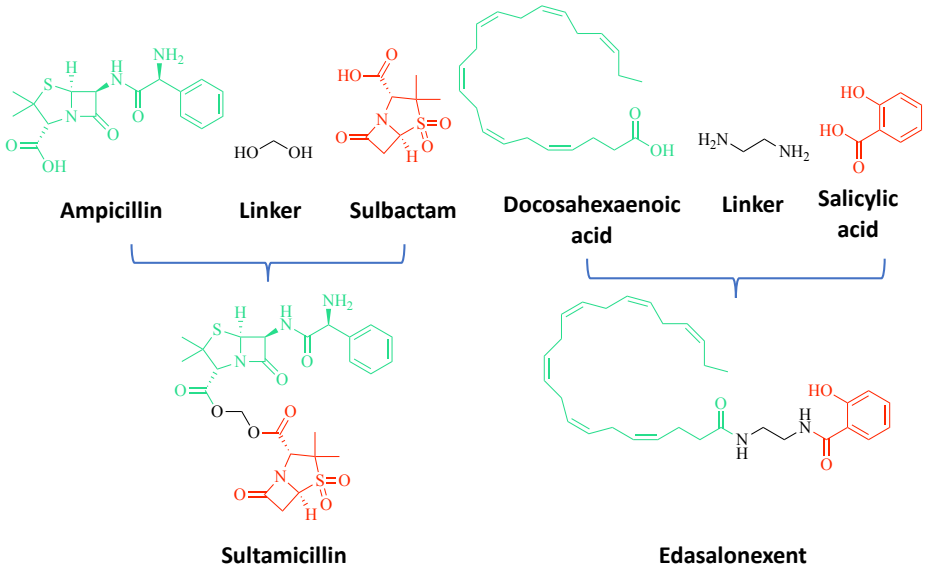

Figure 6. Molecular examples of *linking* strategy: rational design of sultamicillin and edasalonexent.

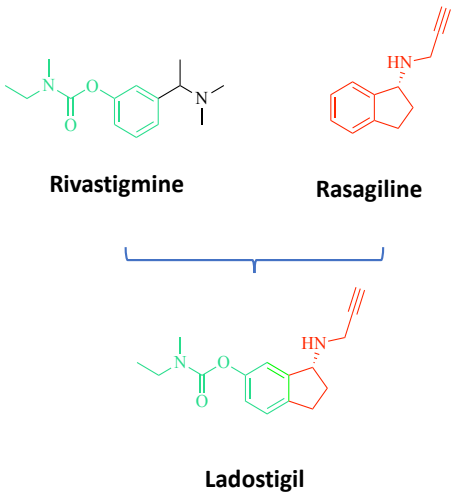

Figure 7. Molecular example of the *fused* strategy: rational design of ladostigil.

1.2.2 The fragment-based strategy to design multitarget-directed ligands

During the last decade another investigated strategy for the development of MTDL was the fragment-based drug design (FBDD). Indeed, this strategy has gained increasing attention not only as a successful strategy to discover new drugs, but also as a way to overcome the limitations related to the sub-optimal PK profile of large MTDLs.[80] The application of FBDD has already allowed to bring two drugs to the market,[81, 82] and to develop at least 30 drug candidates.[83] Fragments are defined as molecules characterized by well-defined chemical

properties. According to the so-called rule of three, fragments have: (i) a MW < 300, (ii) ≤ 3 H-bond acceptors and donors, (iii) a log P ≤ 3, (iv) ≤ 3 rotatable bonds, and also (v) a polar surface area ≤ 60. Hence, by definition, fragments are very small molecules with less complex molecular scaffold, and so with an innate propensity to binding to multiple targets (multitarget profile), as well a high possibility to cross the BBB.[71] However, being smaller compare to lead-like molecules, usually they bind very weakly to their targets, with affinity among 100 μM -10 mM.[80] Thus, once the activity against two targets of interests has been verified, fragments need to be modified into larger molecules by step-wise addition of functional groups, in order to increase affinity and balance it among the two targets. To do this *fragment evolution*, it is possible to use several strategies including: *fragment optimization*, *linking*, *growing*, and *merging*. All of these evolution strategies are aimed to transform a hit-fragment into a lead-like molecule, and finally to a drug candidate.[83]

An important example of FBDD strategy has been applied to develop the first class of dual-target fragments able to simultaneously inhibit the aspartyl protease β-secretase (BACE-1) and glycogen synthase kinase-3 beta (GSK-3β) enzymes for the treatment of AD (Figure 8).[84, 85] BACE-1 and GSK-3β are considered ideal targets for multitarget approaches because they are extremely involved in AD pathogenesis and progression and their network has been demonstrated. Thus, the simultaneous and balanced inhibition of both these crucial, networked enzymes could represent a polypharmacological advance for AD treatment.[85] Particularly, this class of molecules has been obtained by merging in a single MTDL (i) a guanidino motif which binds to the aspartic dyad of BACE-1 and (ii) a cyclic amide group, as a structural element responsible for the interaction of GSK-3β. Merging these functional groups led to a series of 6-amino-4-phenyl-3,4-dihydro-1,3,5-triazin-2(1H)-one derivatives as dual BACE-1/GSK-3β inhibitors for the treatment of AD (Figure 8).

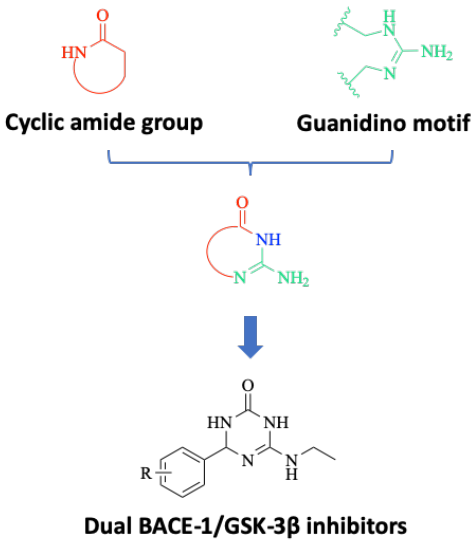

Figure 8. Design of the dual BACE-1/GSK-3β inhibitors.

1.2.3 How to test multitarget compounds for neuroinflammation?

In the search of multitarget compounds, particularly of those active against complex diseases, the set-up of a proper screening pipeline is a critical step. It should be proved by the performed experiments that the efficacy is the result of a simultaneous modulation of both the targets of interest and that their advantages compared to single-target drugs is clear. Cellular studies may be very helpful in this connection.[63] Different from isolated protein assays (where the initial proof of a balanced affinity needs to be previously obtained), cell-based screening systems allows to evaluate the disease target network as a result of molecular-pathway interactions.[71] Clearly, *in vivo* studies using whole, living organisms are even better suited for observing the overall multitarget effect. However, cell-based assays, thanks to a continuous technological evolution, can act in a quicker, low cost, and more efficient manner. In addition to the choice of a suitable cellular system, another fundamental point while dealing with multitarget compound testing, is the use of proper controls. Comparison with the starting frameworks alone and in combination represents the standard to estimate the actual superior activity of multitarget drugs.[63]

In light of these consideration, a *phenotypic* screening represents a possible strategy for investigate the multitarget drugs activity for neuroinflammatory-based diseases such as AD or MS.

The *phenotypic screening* could start with the evaluation of viability profiles in neural cultures in order to proceed only with the molecules that shows no neurotoxicity. Based on the nature of neuronal culture (immortalized or primary culture) the outcome results different.[86] Indeed, immortalized cells or those derived from tumors differ biologically from the primary one, the latter also having the advantage of being more sensitive to pharmacological intervention than immortalized cell lines.[86] However, the ethical constraints related to the manipulation of primary cultures cannot be ignored.

If possible, primary pure neuronal cells are a reliable model for studying cellular and molecular mechanisms of survival/apoptosis and neurodegeneration.[87] Therefore, a cytotoxicity test on primary neuron cell line, in comparison to the appropriate standard compounds, represents a good starting point of a biological screening strategy for anti-neuroinflammatory drugs. In addition to neurotoxicity, hepatic cell lines are useful to asses drug-likeness and to exclude other relevant toxicities. In case of neuroinflammatory-based diseases, that affect mostly elderly

people with comorbidity and subsequent polytherapy, there is a significant higher risk of pharmacological side effects (i.e., liver injury). So, together with neurotoxicity, the evaluation of hepatotoxicity in hepatoma cell line (i.e., HepG2) is extensively used to evaluate viability and drug-likeness of new MTDLs.[87-89]

Following these preliminary steps, the anti-neuroinflammatory properties of the less toxic compounds is also extensively explored in the study of multitarget drugs against AD or MS. As it is known, in *in vivo* conditions, glial cells, especially microglia, strongly affect CNS environment through their activation.[90, 91] Microglia are able to engulf and phagocyte the extracellular Aβ, via stimulation of triggering-receptor-expressed on myeloid cells 2 (TREM2). TREM2 is a cell surface protein that is selectively and highly expressed by microglia and is linked to an anti-inflammatory phenotype.[92] In fact, microglial polarization, i.e., the shift from a neurotoxic M1 to a neuroprotective phenotype M2, is crucial to make the brain microenvironment not permissive to neurodegeneration.[93] To this end, it is possible and relevant to investigate the ability to modulate the glial phenotypic switch from the proinflammatory M1 to the anti-inflammatory M2 type, by following TREM2 expression.[89] The first limit while investigating the role of microglia in these models is that studying cell lines separately (neurons and microglia) does not encompass the complexity of CNS physiological network. In this respect it would be a benefit to use a co-culture system that allows to study how microglia and the factors they release in a shared environment mediate the effects of drugs on neuronal function and survival.[94, 95]

Another phenotype largely explored is the study of the neuroprotective activity. Therefore, it is possible to evaluate the neuroprotective effect following peculiar insults (i.e., β-amyloid (Aβ) for AD, 6-hydroxydopamine for Parkinson disease, and glutamate for excitotoxicity) mimicking distinct aspects of neurodegeneration.

In addition to target-based and phenotypic screens, drug discovery platforms that also include evaluation of absorption, distribution, metabolism, and excretion–toxicity (ADME-Tox) properties may accelerate drug discovery. An assay panel comprising physicochemical characterization, solubility, in vitro off-target liability enzyme panel, in vitro cytotoxicity assay panel, mitochondrial toxicity, cytochrome P450 (CYP) inhibition (1A2, 2C9, 2C19, 2D6, and 3A4 isoforms) or cardiotoxicity is being routinely used also at an academic drug discovery level. [96]

The concepts discussed in this chapter have been largely reported in the following review articles:

- Ivasiv V, Albertini C, Goncalves AE, **Rossi M**, Bolognesi ML. Molecular hybridization as a tool for designing multitarget drug candidates for complex diseases. Curr. Top. Med. Chem. 2019, 19(19), 1694-1711
- **Rossi M,** Bolognesi ML. Sonde bifunzionali: l'unione fa la forza. La Chimica & l'industria. DOI: 10.17374/CI.2019101.3.26

Chapter 2

Objectives

Considering the clear medical needs discussed in Chapter 1, this PhD project has been devoted to the development of small molecules with a polypharmacological profile against two neuroinflammatory diseases, i.e. AD and MS. Starting from this rationale, the following specific objectives have been pursued:

1. In the first project, we applied a conjugation strategy to develop omega-3 FAs/VPA drug conjugates for MS. Indeed, several scientific evidences support the potential synergistic role of omega-3 FAs and VPA to modulate multiple pathways involved in neuroinflammation. Starting from these evidences, a polypharmacological approach based on the combination of the two drugs could be an innovative starting point for fighting neuroinflammation. On this basis, the aim of this project was to realize a single multitarget drug conjugate which, *in vivo*, could release the starting VPA and omega-3 FAs drugs, able to interact with several targets involved in neuroinflammation. Toward this aim, we have covalently linked a fragment of VPA, with ALA or DHA through a purposely selected linker. In this way, we have obtained VPA-ALA or -DHA conjugates, where, VPA is covalently linked by ethylene diester, diamide or ester-amide groups with the carboxylic group of ALA or DHA (Figure 9). According to the approach proposed by Catabasis researchers[78] (see § 1.2.1), these VPA-conjugates should be inactive in the circulation, so that safety may be improved compared to the individual starting drugs. Once delivered inside the brain, they potentially become substrate of specific intracellular enzymes that release the omega-3 FAs and VPA in equimolar concentration, which, in turn, should be able to simultaneously modulate multiple targets.

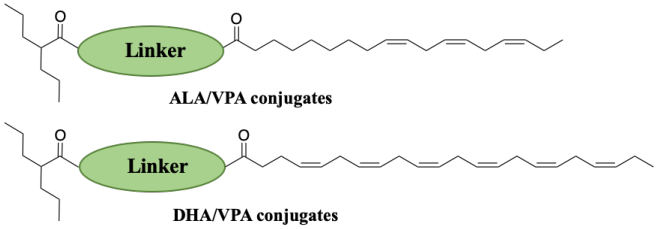

Figure 9. General chemical structure of VPA/ALA and VPA/DHA conjugates.

2. In a second project, we applied a similar conjugation strategy in order to develop FA/P2Y$_6$ agonist conjugates as modulators of neuroinflammation. Microglia cells are involved in the homeostasis of the brain microenvironment, by taking part in phagocytosis of misfolded

proteins, neurotrophic factor and cytokine secretion. $P2Y_6$ is a purinergic/pyrimidinergic receptor expressed in microglia and activated by uridine 5′-diphosphate (UDP), which mediates inflammation and regulation of phagocytosis. For these reasons, it is considered a druggable target for neuroinflammatory diseases. Recent study has demonstrated that the $P2Y_6$ receptor agonist GC021109 (NCT02386306) has showed positive results in the stimulation of phagocytosis and in the suppression of proinflammatory cytokine release in a recent Alzheimer's disease (AD) trial. However, it has not being progressed to the market, while repurposed for asthma. Reasonably, the PK and the BBB permeation problems of GC021109 and other UDP-like $P2Y_6$ receptor agonists have hampered the development of UDP-like drugs. FAs are essential nutrients and components of neuronal and glial cell membranes regulating several processes in the brain, including neuroinflammation. Particularly, omega-3 FAs is associated with a decreased risk of AD in animal models. Thus, the co-administration of supplementation and drugs may lead a novel therapeutic approach for AD.

Building on these considerations, the aim of this project was to develop a new class of lipid−drug conjugates obtained by combining the structures of UDP-like $P2Y_6$ agonists with FA. This strategy is in principle particularly promising for the following reasons: (i) it would allow to exploit a polypharmacological approach by combining the beneficial activities of both structures against neuroinflammation; (ii) it might overcome the pharmacokinetic challenges of UDP-like molecules as CNS-directed drugs (Figure 10).

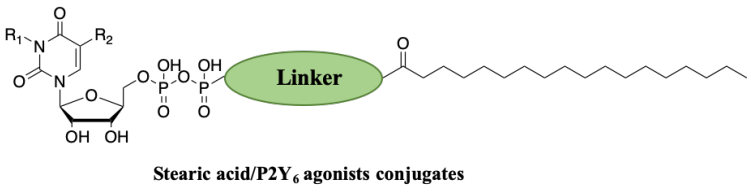

Figure 10. General chemical structure of stearic acid/$P2Y_6$ agonist conjugates.

3. In a third project, we applied a multitarget strategy in order to design and synthesize the first class of sustainable multitarget compounds able to hit histone deacetylation enzymes and ferroptosis. In particular, these molecules were rationally designed for a potential use for neurodegenerative diseases, including AD. The lack of an effective treatment and the increasing life expectancy are the reason of an ever-increasing number of people affected by AD not only in the Western societies, but also in the developing countries. Moreover,

the cost of currently treatments is too high for the people affected in developing countries, hence the possibility to develop new drugs based on inexpensive resources has gained increasing attention. Brazil is one of the main producers of cashew nuts. During the cashew nut processing, an enormous amount of a dark viscous fluid, called cashew nut-shell liquid (CNSL), is obtained as a byproduct material. Long-chain phenolic compounds contained in the inexpensive CNSL show innate multitarget mechanisms of action, becoming innovative molecules with potential applications for the treatment of AD. In addition, the structural homology between CNSL components and SAHA (suberoylanilide hydroxamic acid), caught our attention. Indeed, recent studies with the approved histone deacetylases inhibitor (HDACi) SAHA showed an improvement in memory, and cognition in several AD animal models.

In light of this, the aim of this work was the design and synthesis of accessible and sustainable multitarget compounds obtained by combining CNSL derivatives with the well know SAHA structure. The target compounds have been synthesized using a cross metathesis synthetic strategy in order to bridge the capping group, derived from CNSL compounds and different zinc-binding groups. The molecules obtained were innovative dual HDACIs with potential antiferroptotic activity, thanks to their potential metal chelating activity. (Figure 11).

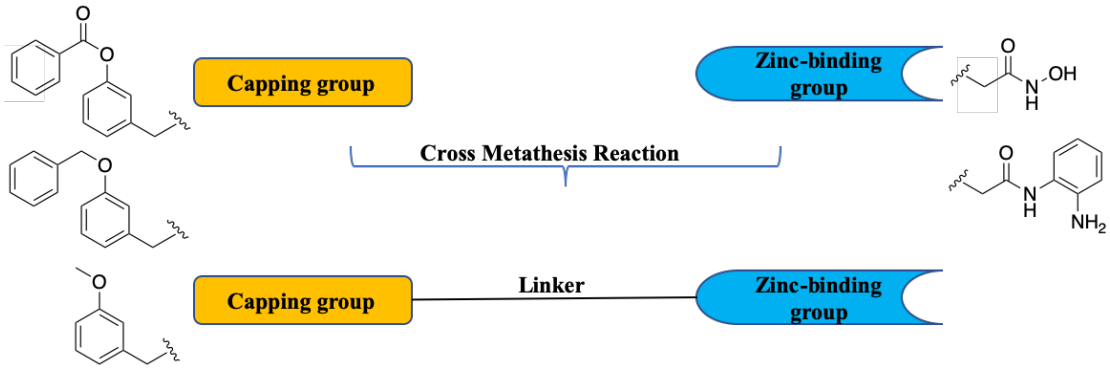

Figure 11. Cross metathesis design strategy for the synthesis of dual sustainable HDAC/ferroptosis inhibitors.

4. In the fourth project, we applied a molecular hybridization strategy to the design and synthesis of a class of sustainable and globally accessible CNSL compounds-tacrine hybrids for the treatment of AD. The lack of the efficacy of the actual drugs, their elevated cost and the ever-increasing number of people affected by AD in the developing countries has guided medicinal chemist in the develop of globally accessible multitarget compounds. Tacrine is a withdrawn drug for the treatment of AD, but actually represent a good scaffold

for the development of new anticholinesterase drugs inhibitors. Indeed, tacrine has been largely exploited to obtain tacrine-hybrids with increased bioactive properties, thanks to a chemically versatile scaffold, easy to functionalize. CNSL compounds, as highlighted in above, have been reported as bioactive molecules with several biological functions including anti-inflammatory and antioxidant activities. Moreover, these long-chain phenolic compounds are easy to chemically modify and becoming a zero-cost starting material for the synthesis of globally accessible drugs.

In light of this, the aim of this work was the design and synthesis of accessible and sustainable multitarget compounds obtained by combining CNSL derivatives with the well know acetylcholinesterase inhibitor drug, tacrine. The conjugation strategy (Figure 12) allowed us to obtain innovative CNSL-tacrine hybrids with potential acetylcholinesterase inhibition, and anti-inflammatory, antioxidant profiles.

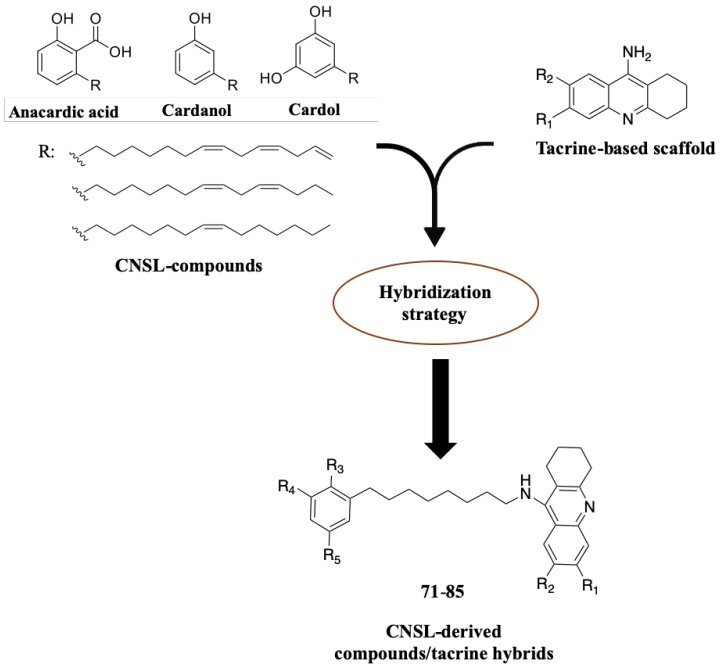

Figure 12. Molecular hybridization design approach for the synthesis of CNSL-derived compounds/tacrine hybrids.

Chapter 3

Project 1: Omega-3 FAs/VPA conjugates as a potential treatment for multiple sclerosis

3.1 Introduction to fatty acids

Fatty acids (FAs) are a class of natural lipids characterized by a hydrocarbon chain (lipophilic tail) and a terminal carboxy acid function (hydrophilic head). FAs can be classified based on i) the number of carbons, and ii) the number and position of double bonds in the carbon chain. (Figure 13, Table 1).[97]

The FAs that differ by length, can be categorized as:

- Short-chain fatty acids (SC-FAs) are fatty acids with aliphatic tails of five or less carbons (e.g. butyric acid).

- Medium-chain fatty acids (MC-FAs) are fatty acids with aliphatic tails of 6 to 12 carbons, which can form medium-chain triglycerides.

- Long-chain fatty acids (LC-FAs) are fatty acids with aliphatic tails of 13 to 21 carbons.

- Very-long chain fatty acids (VLCFAs) are fatty acids with aliphatic tails of 22 or more carbons.

Moreover, FAs can be classified according to the number of double bonds. There are three classes of fatty acids:

- Saturated FAs: are a type of fat in which the fatty acid chains have all single bonds (e.g. palmitic acid (PA) and stearic acid (SA)).

- Monounsaturated FAs: are a type of fat in which the fatty acid chains have only one double bond (MUFA, e.g. oleic acid (OEA)).

- Polyunsaturated FAs: are a type of fat in which the fatty acid chains have more than two double bonds (PUFA, e.g. alpha-linolenic acid (ALA), arachidonic acid (AA), and docosahexaenoic acid (DHA)).

The unsaturated FAs can be also classified in according to the position in the carbon-chain of the double bond. Indeed, three predominant family can be classified starting to count from the terminal methyl carbon, called omega (ω or n-). These families are:

- omega-9: the first double bound is in position 9 counting from the end of the carbon tail (e.i. OEA)

- omega-6 FAs: the first double bound is in position 6 counting from the end of the carbon tail (e.i. linoleic acid (LA), and AA)

- omega-3 FAs: the first double bound is in position 3 counting from the end of the carbon tail (e.i. ALA, eicosatetraenoic acid (EPA), and DHA)

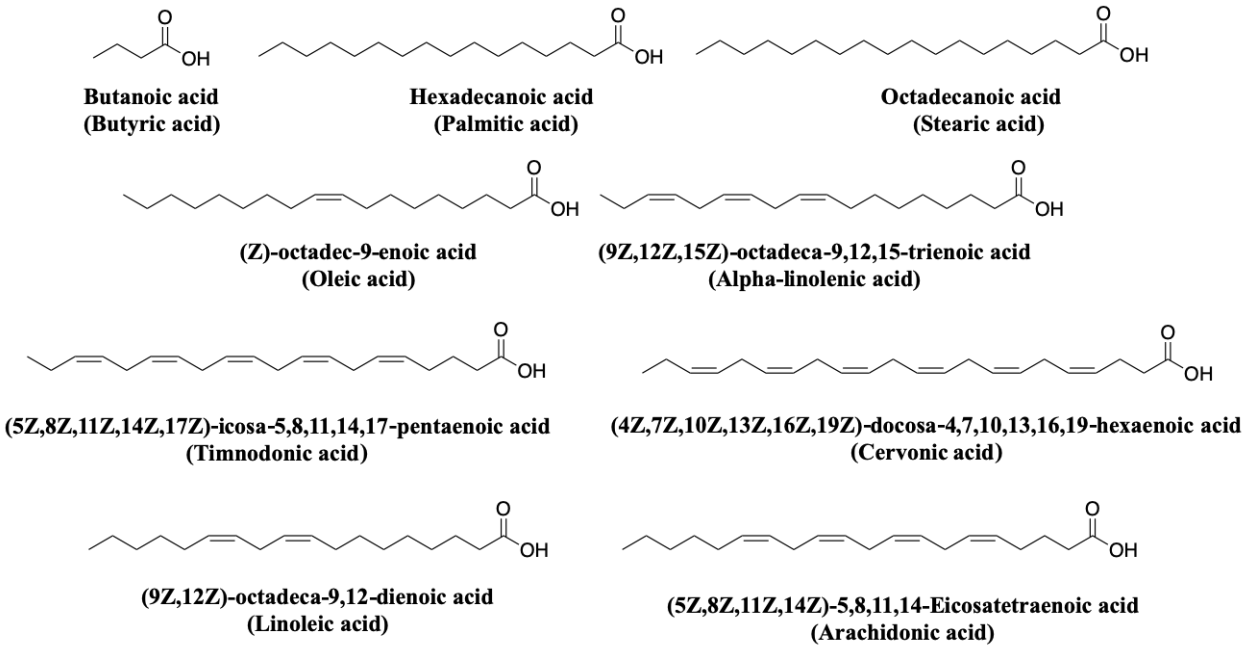

Figure 13. Structures of principal FAs.

Table 1. List of principals FAs.

IUPAC Name (Traditional name)	Type	Number of carbons	Number of double bonds	Symbol
Butanoic acid **Butyric acid**	Saturated	4	0	4:0 (BA)
Hexadecanoic acid **Palmitic acid**	Saturated	16	0	16:0 (PA)
Octadecanoic acid **Stearic acid**	Saturated	18	0	18:0 (SA)
(Z)-octadec-9-enoic acid **Oleic acid**	n-9 monounsaturated	18	1	18:1 (OEA)
(9Z,12Z,15Z)-octadeca-9,12,15-trienoic acid **Alpha-linolenic acid**	n-3 polyunsaturated	18	3	18:3 (ALA)
(5Z,8Z,11Z,14Z,17Z)-icosa-5,8,11,14,17-pentaenoic acid **Timnodonic acid**	n-3 polyunsaturated	20	5	20:5 (EPA)
(4Z,7Z,10Z,13Z,16Z,19Z)-docosa-4,7,10,13,16,19-hexaenoic acid **Cervonic acid**	n-3 polyunsaturated	22	6	22:6 (DHA)
(9Z,12Z)-octadeca-9,12-dienoic acid **Linoleic acid**	n-6 polyunsaturated	18	2	18:2 (LA)
(5Z,8Z,11Z,14Z)-5,8,11,14-Eicosatetraenoic acid **Arachidonic acid**	n-6 polyunsaturated	20	4	20:4 (AA)

Among FAs, the omega-3 and -6 PUFAs are considered essential. Indeed, they are nutrients necessary for maintaining the normal homeostasis, but cannot be produced by mammals and need to be provided by the diet.[98] In particular, LA is the dietary-essential PUFA precursor of AA (omega-6 FAs), whereas ALA is the dietary-essential PUFA precursor of EPA and DHA (omega-3 FAs). As represented in Figure 14, the biosynthetic process from LA and ALA to the production of AA, EPA, and DHA, respectively, share common biosynthetic pathway. The liver is the primary organ involved in the synthesis of PUFAs from FAs circulating precursors.[99]

Other organs, including the brain and kidney, can synthesize PUFAs because they express the same liver enzymes for completing the synthesis of PUFAs.[99] The principal biosynthetic enzymes are a series of desaturation, and elongation enzymes, and only for the biosynthesis of DHA a beta-oxidation enzyme. The PUFA LA and ALA result essential for the biosynthesis of LC-PUFA because the lack in the human genes of delta-12 and -15 desaturases enzymes prevent the formation of them starting from OEA (Figure 2).[100]

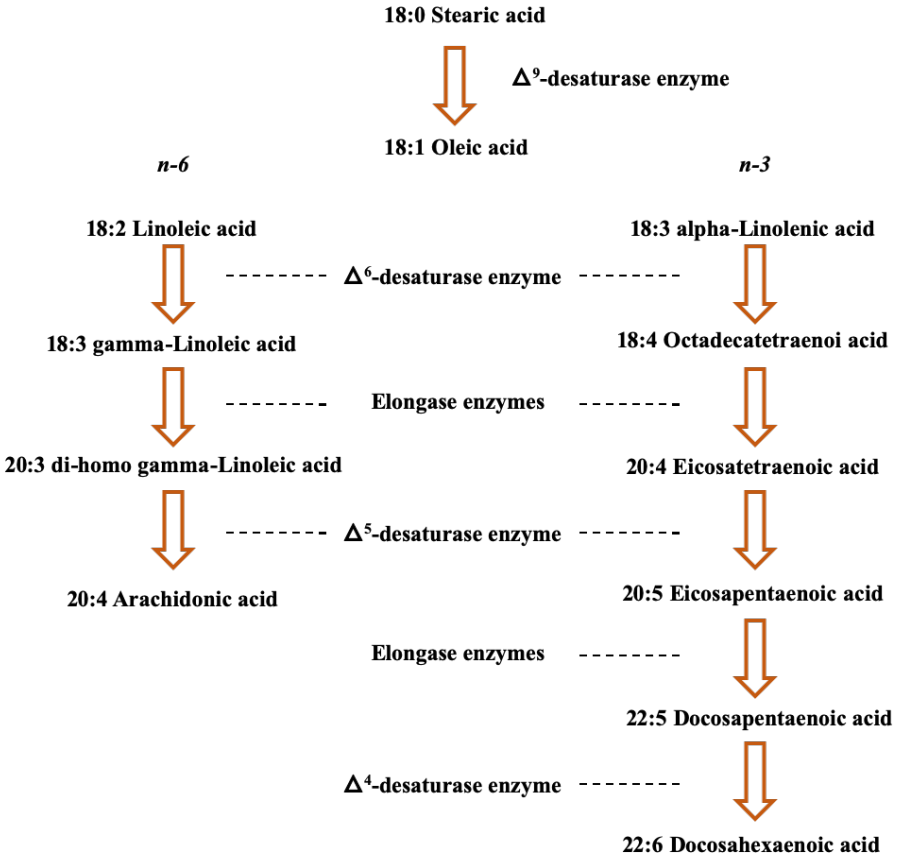

Figure 14. Scheme of biosynthesis of PUFAs in mammals.

Therefore, the principle source of PUFAs, especially AA and DHA, come from the diet (nuts and fish oil respectively), while LA and ALA are plentiful in green vegetables and seeds. Although human metabolism can synthesize the more complex PUFA (e.g. AA and DHA) starting from LA and ALA, the biosynthetic conversion efficiency is very low (1%) even in healthy adults.[101]

In general, after the dietary absorption, FAs are preliminary transported by lipoprotein such as chylomicron or albumin in their esterified form.[102] FAs can be also transported as esters of

lysophosphatidylcholine (lyso-PC) or as free FAs form in a rapidly dissociable lipid-protein complex in the blood.[102] Then, PUFAs accumulate principally in cell membranes, adipose tissue, brain, cardiovascular system, immune system, muscular mass, and bone.[103,104] Particularly, ALA and EPA are found in the blood as triacylglycerols and cholesteryl esters, becoming the building blocks for cell membrane phospholipids of all tissues.[105] However, in phospholipids, ALA is minimally present, whereas DHA and EPA are both prominent components. In the organs of human body, DHA is the most abundant n-3 PUFA, especially in brain and retina, where it is several hundred-fold more present than EPA.[106]

The brain is the most PUFA-rich organ of our body. Particularly, AA and DHA are esterified as phospholipid in neuronal cell membranes. Once PUFAs are released from the membrane, they can participate in signal transduction, either directly or after enzymatic transformation to a variety of bioactive derivatives ('mediators'). PUFAs and their mediators regulate several processes in the brain, such as neurotransmission, cell survival, neuroinflammation, and cognition. PUFA levels and the signaling pathways that they regulate are altered in various neurological disorders, including Alzheimer's disease.[97]

Unfortunately, since the *de novo* synthesis of PUFA is very low in the brain,[101] the blood must supply PUFA to the brain either from exogenous PUFA obtained through diet or from endogenous liver synthesis of PUFA from dietary precursors. The mechanisms by which generally FAs cross the BBB and enter into the brain has been partially identified and characterized. Several theories have been investigated regarding the involvement of several proteins and transports for the delivery of FAs into the brain.

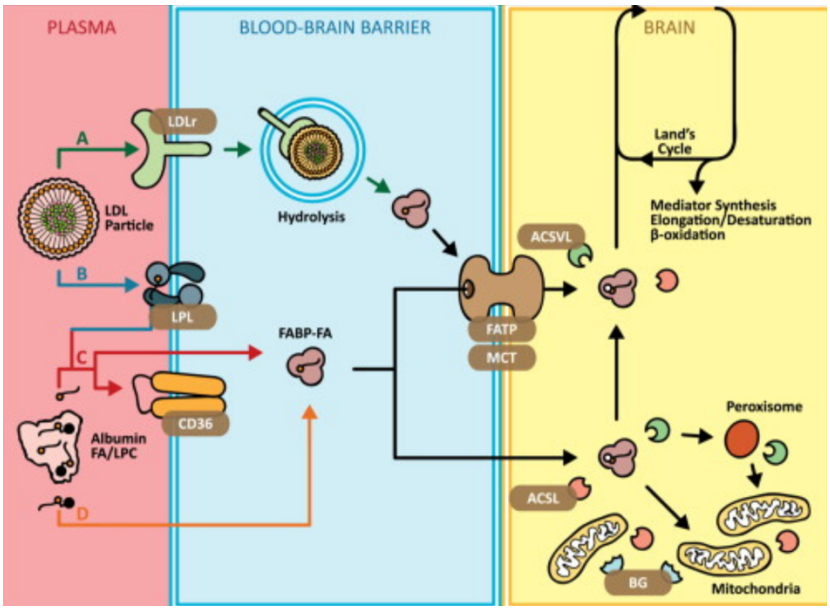

Figure 15. General FAs mechanisms to entry from the plasma into the brain.[107]

The Edmond′s theory (A, Figure 15) concern the involvement of lipoprotein receptor mediated FA uptake. The binding of low-density lipoprotein (LDL) particles to LDL receptor (LDLr) induces endocytosis of LDL particles into the BBB where it is hydrolyzed and releases unesterified FAs.[107] The Eckel′s theory (B) hypothesizes that lipoprotein lipase (LPL) mediates PUFA uptake. Circulating LDL particles binds to lipoprotein lipase where FAs are de-esterified and taken up into the BBB via passive diffusion or transporter (such as CD36).[107] The theory of Hamilton (C) proposed that albumin-bound unesterified PUFA may be the primary source of PUFA for the brain. Albumin-bound unesterified PUFA passively diffuse across the BBB via a "flip-flop" mechanism or transporter, (such as CD36).[107] (D) Lagarde′s theory of albumin-bound lysophosphatidylcholine (LPC) uptake. Albumin-bound LPC containing FA is taken up into the BBB by passive diffusion. Upon entry into the endothelial cells of BBB, unesterified FAs are bound to fatty acid binding protein (FABP) and shuttled to the brain by fatty acid transport protein (FATP) or monocarboxylic acid transporter (MCT) transport. Finally, PUFAs are converted in different mediators (i.e. Acyl-CoA) able to explain several biological activities in the CNS.[107]

3.2 Omega-3 FAs role in the brain

During the last ten years from both *in vivo* and epidemiological research, the implication of long chain (LC) -PUFAs in the development and function of normal brain has emerged.[97, 98] The principal LC-PUFA found in mammalian brain grey matter is DHA, an omega-3 FAs which comprises approximately 10%-20% of total PUFA composition in the adult frontal cortex.[97, 98] Although the omega-3 FAs precursors of DHA, ALA and EPA and docosapentaenoic acid (22:5n-3), are able to cross the BBB, they are rapidly oxidized in DHA and consequently represent < 1% of total brain PUFAs composition.[107, 108] The free DHA is esterified in the sn-2 position of brain phospholipids and it is maintained at low levels of other PUFAs in the brain.[107, 108] Omega-3 FAs, especially DHA, regulate both the structure and the function of neurons, glial cells and endothelial cells. Moreover, once arrived into the brain, PUFAs can explicate several biological actions such as regulation of neuroinflammation, membrane dynamics, neurogenesis and neuroprotection.[1]

3.2.1 The role of omega-3 FAs in neuroinflammation

The higher dietary intakes of PUFAs are associated with an inferior risk of neurological disorders that shared an inflammatory component, including Alzheimer's disease, Parkinson's disease, multiple sclerosis, epilepsy and major depression.[109] Hence, limiting inflammation by PUFAs is very important, and may provide new targets in brain damage prevention and treatment. Several reviews have discussed the role of omega-3 FAs in the regulation of neuroinflammation compared to omega-6 FAs.[110] Indeed, omega-3 FAs are anti-inflammatory FAs and they are precursors of lipid derivatives with anti-inflammatory properties, whereas omega-6 FAs are commonly the precursors of the proinflammatory prostaglandins, leukotrienes and stimulate the production of inflammatory cytokines.[110] This has led to the hypothesis that DHA or its metabolites may have anti-inflammatory and pro-resolving effects in the brain.[111] Indeed, several experiments have shown that the pre-treatment with DHA in rodent models of brain ischaemia–reperfusion, spinal injury, and ageing is associated with a reduction of the proinflammatory marker expression after systemic lipopolysaccharide (LPS) administration.[111] Another large number of studies supports the hypothesis that PUFAs or their metabolites are candidates for limiting neuroinflammation by downregulation of inflammatory gene expression, such as those of cytokines or enzymes involved in the synthesis of eicosanoids, in parallel to the induction on lipid mediators involved in the resolution of inflammation.[112, 113]

The same results have been found in people with higher omega-3 FAs levels in blood and with lower proinflammatory cytokine production.[114, 115] Moreover, supplementation of DHA-rich diet in AD patients led to a reduced release of proinflammatory cytokines from blood mononuclear leukocytes.[116]

The main mediators of neuroinflammation are microglial cells. Microglia cells are the resident macrophages of the brain and constitute the first line of immune defense of the brain.[117] Once stimulated by an immune insult, microglia are capable of acquiring diverse and complex phenotypes as well as performing several macrophage-like functions including inflammatory and anti-inflammatory cytokine production. The anti-inflammatory effects of DHA could be due to a direct action of DHA on microglia cells. Indeed, *in vitro* and *in vivo* results have shown that DHA blocks microglia-induced activation of NF-κB in the CNS of rodents after the neuroinflammatory induction by LPS or by spinal cord injury.[118, 119] Moreover, DHA promotes the switching of microglia polarization from M1 proinflammatory phenotype to an anti-inflammatory M2 phenotype. This phenotypic alteration results in a low production of proinflammatory cytokine and an increased phagocytosis of amyloid-β isoform 42 (Aβ42).[120] One beneficial effect of DHA in AD consists in enhancing removal of Aβ42, increasing neurotrophin production, decreasing proinflammatory cytokine production, and inducing a shift in phenotype from a proinflammatory M1 to M2.[120]

3.2.2 Synaptic effect of omega-3 FAs

PUFAs and their metabolites act through several mechanisms in the brain. One of these is the regulation of membrane dynamics; indeed, DHA is the most abundant esterified FA in the neuron plasma membrane.[97] As reported by *Salem et al*. in the human brain the DHA-phosphatidylserines ester results to be the 42.2% while the DHA-phosphatidylethanolamines the 27.7%.[121] Once esterified into phospholipids, DHA has been demonstrated to significantly alter the order and fluidity of the membrane through modification of the elastic compressibility, permeability, fusion, flip-flop and protein activity of the membrane.[122] PUFAs are also involved in the modulation of many membrane and nuclear receptors, in the signal transduction mechanisms in neuronal membranes and in the synapses regulation. Particularly, PUFAs affect adenylate cyclase as they influence a series of metabotropic receptors like serotoninergic (5-HT1 and 5-HT4), beta-adrenergic and dopaminergic (D1 and D2) that are all coupled to the cAMP messenger system.[123, 124] Moreover, PUFAs and/or their metabolites can directly interact

as agonists with the oxysterols receptor LXR, peroxisome proliferator-activated receptor (PPAR), hepatic nuclear factor 4A (NR2A1), chemokine- like receptor 1 (CHEMR23), G-protein- coupled receptor 32, (GPR32) and inhibit nuclear factor-κB (NF-κB).[97, 113, 125] PUFAs can also influence brain function through modulation of neurons, glial cells and astrocytes by modulation of endocannabinoid system. The endogenous ligand of endocannabinoids system directly derives from the metabolism of PUFA.[126] Indeed, the endocannabinoids involve the fatty acid ethanolamides anandamide (AEA), synaptamide (DHEA), oleylethanolamide (OEA) and palmitoylethanolamide (PEA), as well as 2-arachidonoylglycerol (2-AG).[127, 128] The most abundant endocannabinoids in the brain are AEA, DHEA and 2-AG, which bind to cannabinoid receptor type 1 (CB1) and cannabinoid receptor type 2 (CB2).[32] The endocannabinoid system has an important role in the synaptic regulation of the neurotransmitter release (including the release of glutamate, GABA, opioids, monoamine neurotransmitters, and acetylcholine).[129] Recent studies have also shown that endocannabinoids can modulate synaptic transmission through TRPV1 (transient receptor potential cation channel sub-family V member 1), which is located in the post-synaptic cliff, through CBs.[130] Recent studies demonstrate that synaptamide presents bioactive functions completely different compared to the analog AEA. Particularly, synaptamide is involved in the neuritogenesis and synaptogenesis processes.[131, 132] Despite the structural similarity between synaptamide and AEA, these bioactive molecules interact independently with the endocannabinoid receptor system. Indeed, as proposed by *H.S. Moon*, *H.Y. Kim et al.,* synaptamide is a very weak binder on CB1 and CB2 receptors, compared to AEA.[127] In addition, AEA at high concentrations (1–1.5 μM) does not stimulate neurite growth or synaptogenesis in cultured embryonic hippocampal neurons.[127, 133] These results indicate that synaptamide, and not AEA, promotes neurite growth and synaptogenesis by a cannabinoid-independent mechanism.[127]

3.2.3 The role of omega-3 FAs in neurogenesis and neuroprotection

Although DHA is involved in learning and memory brain function, the cellular and molecular mechanisms of these effects are poorly understood.[134] One of the first described protective effects of DHA is the promotion of neurogenesis[135] and neuronal survival.[136] DHA, the main PUFA in phosphatidylserine, enhances phosphatidylserine synthesis *in vitro*, and the depletion of DHA from the membrane impairs phosphatidylserine-mediated AKT and RAF1.[97, 137] The phosphorylation of this two proteins modifies the translocation and activation of them, promoting neurogenesis.[97, 137] Potential neuroprotective mechanisms include anti-oxidative,

anti-inflammatory, and anti-apoptotic properties of DHA.[138] Moreover, part of the DHA neuroprotective effect is thought to be linked to its active oxygenated derived mediators, such as protectin D1 (PD1, called neuroprotectin D1 in brain), resolvins, and maresins.[139, 140]
Another neurogenesis mechanism is mediated by synaptamide, as highlighted in § 3.2.2. This DHA-ethanolamide is a more potent promoter of neurite growth, synaptogenesis and synaptic function than DHA itself, and is able to promote neuro and synaptogenesis, [131, 133] and neuronal differentiation.[131, 141] DHA was converted to synaptamide in the brain and retina, but also in adipocyte, macrophage, and prostate and breast cancer cell lines.[142] Synaptamide results at least 10-times more potent than DHA in stimulating hippocampal neurite growth, synapse formation and synaptic activity,[131] and inhibits the production of proinflammatory mediators and protein markers in challenged microglia cultures.[143] The N-acylethanolamines of other FA including AEA, PEA and OEA are not effective, indicating the fundamental role of synaptamide in neurogenesis and neuroprotection. Other mechanisms of action of synaptamide involve several targets such as: G-protein coupled receptor GPR110 (ADGRF1), increasing cAMP production in neural cells,[144] activation of peroxisome proliferator-activated receptor alpha and gamma (PPARα, γ), 5-lipoxygenase,[145] and COX-2.[146]

To the end, these considerations suggest the importance and the involvement of omega-3 FAs as key molecules for the maintenance of physiological condition of the brain. Moreover, the broad spectra of activity and the anti-neuroinflammatory and neuroprotective profile make these molecules promising for the development of innovative treatments for neurological disorders with neuroinflammatory etiopathology.

3.3 Omega-3 FAs as potential drugs for neuroinflammatory diseases

In the last decades, the hypothesis that omega-3 FAs could be used for the treatment of neurological diseases has been highly investigated. Considering the role of DHA and of its principal ethanolamide metabolite (synaptamide) in the brain, the dietary approach or supplementation regimen of omega-3 FAs represents an innovative potential strategy to control neuroinflammatory processes in neurological disease. While omega-6 FAs are relatively abundant in the diet and there is no substantial evidence of their therapeutic potential, instead, omega-3 FAs supplementation has been studied as a potential treatment or preventive strategy for numerous diseases.[147]

Indeed, ReportLinker prospect that Omega-3 FAs supplement will be the fastest ingredient type during next years, reaching USD 1.2 billion dollars (https://www.reportlinker.com/p05778223/Algae-Omega-3-Ingredients-Market-Growth-Trends-and-Forecasts.html?utm_source=PRN). The most recent approved drug by the Food and Drug Administration (FDA) is omegaven. Omegaven is a fish oil triglycerides injectable emulsion for intravenous use as a source of calories and FAs for pediatric patients with parenteral nutrition-associated cholestasis. Another example is lovazan, approved by FDA in the 2004, is a mixture of omega-3 FAs ethyl esters, in oral capsules formulation. This drug is composed principally by EPA and DHA ester and is indicated as an adjunct to diet to reduce triglyceride (TG) levels in adult patients with severe (≥ 500 mg/dL) hypertriglyceridemia.

During these years the interest to develop omega-3 FAs-based therapy for several disease is continuing under investigation. In order to better understand the involvement of omega-3 FAs in clinical trials we performed an analysis using Clinicaltrials.gov web site (September 2019). The goal of this analysis was focused on the quantification of clinical trials where the omega-3 FAs are involved in order to understand their implication. Moreover, have been investigated the major class of disease where omega-3 FAs are involved with a particular interest for neurological diseases. The analysis was performed searching directly on the website the following keywords: DHA, EPA, docosahexaenoic acid, eicosapentaenoic acid, alpha-linolenic acid, omega-3 FAs, and adopting the boolean operator we found 1847 studies. The principal diseases where the omega-3 FAs are implicated results the metabolic disorders (275 clinical trials), followed by: cardiovascular disorders (244 clinical trials), cancer (211 clinical trials), neurological disorders (149 clinical trials) and eye disorders (63 clinical trials). In detail,

between the neurological disorders, we found that the high numbers of trials are related to Alzheimer's disease (13 clinical trials) and among these 5 are ongoing (Figure 16). Remarkably, all the 13 trials have been started during the last 10 years highlighting the increased therapeutic role of omega-3 FAs. The other diseases included multiple sclerosis (11 clinical trials and 3 of those are ongoing), epilepsy (9 clinical trials and 3 of those are ongoing), stroke (6 clinical trials and 3 of those are ongoing), dementia (3 clinical trials and 1 of those are ongoing), CNS inflammation (3 clinical trials and 1 of those is ongoing), and Parkinson (2 clinical trials and 1 of those is ongoing). Clearly, all of these are neuroinflammatory-based pathologies that could benefit from the anti-neuroinflammatory and neuroprotective effect of omega-3 FAs.

To note, the number of clinical trials involving omega-3 FAs is high, despite same inconclusive evidences and failures. All in all, several trials are ongoing and the use of omega-3 FAs for the treatment of neurological diseases remains a very promising field.

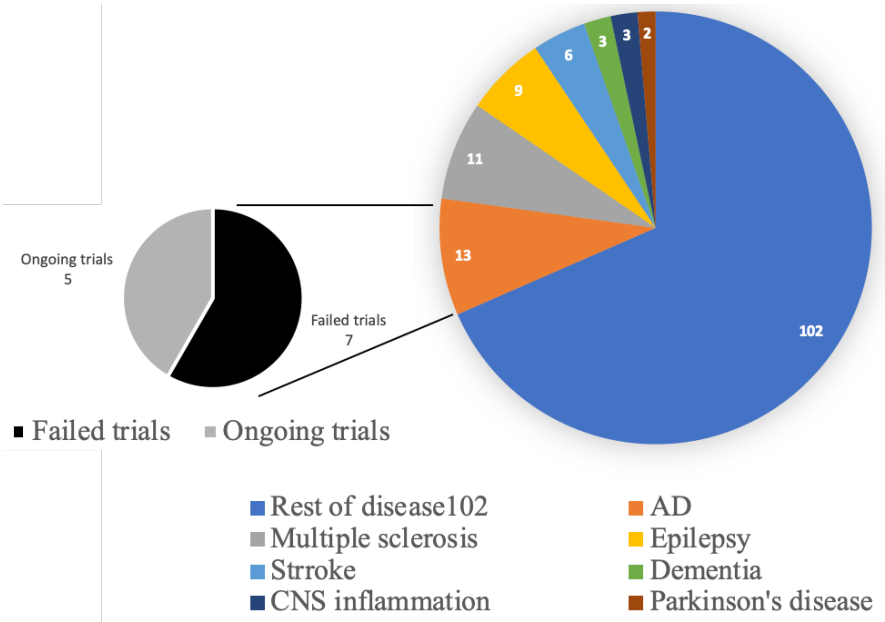

Figure 16. Pie charts distribution data referred to the use of omega-3 FAs clinical trials.

3.3.1 The use of omega-3 FAs in combination therapy: a polypharmacological strategy

All the trials discussed in the previous paragraph refer both to the use of a single omega-3 FAs or a mixture of them (DHA and EPA). The lack of efficacy of a single omega-3 FAs against multifactorial diseases might be easily explained by considering that it is not adequate to contrast the underlying complex pathogenesis. Despite the intrinsic multipotent activity of omega-3 FAs and their ability to interact with numerous targets, the challenges to exploit them as a new treatment, in particular for neurological disease, remains open. Starting from these considerations, a polypharmacological strategy could have increased possibilities to treat multifactorial disorders. The so-called combination therapy (or drug cocktail) is not a new polypharmacological strategy in the field of drug discovery.[46, 53, 54, 148] Indeed, a therapeutic regime composed by two or three different drugs that combine different therapeutic mechanisms might produce a stronger treatment for a disease than an individual one.[54] In particular, several studies indicate that the drug therapeutic regime supplemented by the use of omega-3 FAs could produce a better response compared to individual drug and with potential reduction of side effects. These studies reported the potential use of omega-3 FAs as supplement for the treatment of different neuroinflammatory diseases like: AD, epilepsy and multiple sclerosis.

There is a growing interest in lifestyle and dietary components as possible protection factors for AD, including the use of omega-3 FAs. Moreover, epidemiological and animal studies have suggested that dietary fish or fish oil, rich in omega-3 FAs DHA and EPA, may have effects for the treatment of AD.[116, 149] As reported in several articles, the use of omega-3 FAs could interfere directly with the AD's pathologic hallmarks like Aβ's excessive production or deposition, neurodegeneration, and neuroinflammation, although the mechanisms still remain unknown.[82, 150] A pilot study was designed to evaluate the effects of supplementation with omega-3 FAs, in particular DHA, in mild to moderate AD.[151] The trial participants chronically used a cholinesterase inhibitor or a NMDA-receptor antagonist (memantine). A total of 295 participants completed the trial (DHA: 171; placebo: 124). Unfortunately, the collected results indicated that DHA supplementation is not useful for that AD population.[151] The same result has been obtained in another clinical trial in which the cohort of AD patients has been treated with a fixed-dose mixture of DHA and EPA and an acetylcholinesterase inhibitor among donepezil, galantamine or rivastigmine.[152] Even in this case, supplementation of DHA and EPA

in patients with mild to moderate AD did not seem to influence psychiatric, behavior or functional abilities.

Another neurological disorder where omega-3 FAs seem to be highly involved is epilepsy.[153] Relevant to epilepsy, omega-3 FAs reduce neuronal excitability. Reduction in excitability is heavily dependent on sodium and calcium ion channels, which can be modulated by EPA and DHA.[154, 155] In animal models of epilepsy, the result obtained after treatment with omega-3 FAs have been highly controversial. Indeed, in a mouse model of epilepsy, *Taha A., Y. et al.* reported a 45% nonsignificant increase in time to the onset of seizures (prolonged seizure latency) in fat-1 mice.[156] However, *El-Mowafy et al.* and *Abdel-Dayem* found that high dose of EPA (125–200 mg/kg) or DHA (120–250 mg/kg) administration delayed the onset of seizures by 49%, and synergistically enhanced the anticonvulsant activity of valproic acid.[157, 158] In addition, in both papers, the co-administration of DHA or EPA with VPA markedly alleviated VPA-induced hepatotoxicity, oxidative stress, and inflammation. In conclusion, these experiments highlight the protective and synergistic profile of the drug combination compared to the single use of VPA.[157, 158]

Analogous result has been observed in a combination therapy between omega-3 FAs (fixed-dose mixture of DHA and EPA) with the antiepileptic drug levetiracetam.[159] As reported by *Habeeb M., S. et al*., combined treatment of levetiracetam with omega-3 FAs has shown an additive protective effect to levetiracetam against pentylenetetrazol (PTZ) kindling-induced seizures compared to the single antiepileptic drug. This effect was accompanied by a decrease in hippocampal glutamate, oxidative stress, and improvement in antioxidant defenses in young rat models.[159]

Another application of omega-3 FAs in combination therapy for neurological disorders is multiple sclerosis. Important for multiple sclerosis is the immune-modulatory effect of omega-3 FAs, and their anti-inflammatory and neuroprotective activities. In clinical trials studies the has been studied the efficacy of co-administration of omega-3 FAs and interferon-beta, the multiple sclerosis first line therapeutic drug. In general, what is emerged from these studies is the no differences in clinical efficacy after the drug combination.[4, 160] However, in only one trial, where the primary outcome was not to evaluate the efficacy on the clinical outcomes, the decrease of neuroinflammatory markers was observed.[69]

3.4 Lipid/drug conjugate as drug discovery strategy

The development of drug optimally targeting the CNS remains one of the most formidable challenges for medicinal chemistry.[161] In several cases, the scarce CNS distribution is one of the most complicated aspects. To overcome this problem, medicinal chemists have established several strategies, such as the so-called prodrug strategy. Particularly, masking a polar or hydrophilic group responsible of the low BBB permeability, is possible to increase the brain permeation of a given drug. One very well-known strategy is the development of lipid-drug conjugate (LDC).[162] LDCs are drug molecules that have been covalently modified with lipids. The resulting conjugate will gain several advantages including improved oral bioavailability, enhanced CNS targeting, reduced toxicity, and enhanced drug loading into delivery carriers.[162] Based on the chemical structures and the nature of the starting drugs and lipids, various conjugation strategies and chemical linkers can be utilized to develop LDCs.[162] Among lipids, the most investigated source of lipids are: steroids, FAs, glycerides and phospholipids.
In many cases, the use of a chemical linker is a promising strategy to join covalently the drugs and the lipids. Moreover, depending from the nature of the linker, the profile of the LDCs could be very variegated. Ester or amide bonds have been the most investigated functions to form LDCs.[162, 163] They are usually formed by reaction between a carboxylic acid and an alcohol or amine group, respectively. These kinds of linkers can be easily degraded by enzymatic hydrolysis. Another common linker is hydrazine.[162, 163] This linker is stable at neutral pH but is hydrolyzed in acid conditions. Alternative responsive-pH linkers are silyl ether, acetal or Schiff base. Disulfide bonds is another class of linker. Disulfide lipid conjugates are stable in the extracellular oxidative environments but will be hydrolyzed after cellular internalization in response to the reductive intracellular environment.[162, 163]

Another positive feature of LDC is the possibility to develop drug delivery system.[164, 165] Indeed, joining a lipid to a hydrophilic drug leads to the formation of an amphiphilic molecule that can self-assemble into nanoparticles without or with minimal use of stabilizer.[162] This results very useful for the preparation of emulsion, liposome, micelle, lipid nanoparticle, polymer nanoparticle, and carbon nanotube.[162]

3.4.1 Omega-3 FAs/drug conjugates for the treatment of multifactorial diseases

The drug combination strategy to combat multifactorial disease is a milestone of the polypharmacological field since the first publications.[46, 53] Moreover, the interest to develop drug combinations by the pharmaceutical companies is witnessed by the increased number of drugs approved in the last years.[63] However, this is not the case for neurological disorders. Indeed, all the trials proposed in this therapeutic area have inexorably failed.

Omega-3 FAs have been proposed as adjuvant in combination with usual therapy for many neurological diseases. Unfortunately, the results are usually very promising until the *in vivo* studies, then become controversial or with no clinical impact when translated to the clinical trials. Probably, this is related to some disadvantages deriving from the combination therapy and the use of supplements. The limitations of combination therapy are well-known and have been discussed in Chapter 1.[59] On the other side, the main problem of omega-3 FAs supplementation is related to its bioavailability. As reviewed by *Tamargo M. et al.,* short-term and long-term studies have analyzed the oral bioavailability of different omega-3 FAs formulation (i.e. free-FAs, triglycerides) in healthy volunteers.[166] Unfortunately, these studies present multiple limitations which explain why contradictory results are frequently reported and is difficult to extrapolate them. Clearly, additional studies with larger sample sizes are needed to identify the PK differences in omega-3 FAs bioavailability among the most common formulations.[166]

A polypharmacological strategy to overcome these problems might be the development of multitarget drugs.
Clearly, therapy with a single drug with multiple biological properties would have numerous advantages compared to combination therapy. It would avoid the problem of administering complex combination therapy, which could have different drug bioavailability, DDI, and metabolism. Furthermore, a single chemical entity can solve a difficult problem that appears with the simple coadministration of two drugs, namely the different PK and tissue distribution profile. The complex PK and tissue distribution of combination therapy could hamper the synergistic activity of the drug combination therapy due to the heterogeneous concentration distribution of the single drugs in different tissues. This undesired process is obviously avoided with the use of a multitarget drug, which is a single molecular entity.

In light of this, a polypharmacological strategy seems to be in principle very promising also for omega-3 FAs. Indeed, several studies have been performed with the aim to develop omega-3 FAs-drug conjugates for the treatment of several disorders. One of the most recent examples relates to the treatment of Duchenne muscular dystrophy. The drug candidate edasalonexent (Figure 5) has been developed as NF-κB inhibitor by Catabasis company.[167] Edasalonexent is the result of the conjugation between three main elements: i) the drug (salicylic acid), ii) the omega-3 FA (DHA), and iii) the ethylendiamine linker used to covalently bridge the two carboxylic functions. The rational design of this molecule has been realized and successfully demonstrated. Indeed, edasalonexent is stable in the plasma, and once it is internalized into the target tissue it becomes substrate of hydrolytic enzymes, releasing at the same time and in equimolar concentration the two active drugs.[167] Actually this drug is investigated in the phase III clinical trial study NCT03703882.

This design strategy has been exploited to link other omega-3 FAs with bioactive molecules or drugs for the treatment of neuroinflammatory diseases such as AD, Parkinson's disease, and multiple sclerosis.[168] An example reported by *Meijerink J et al*. propose the N-docosahexaenoyl dopamine (DHDA) as anti-inflammatory molecules for the treatment of neuroinflammatory diseases. This study was performed by evaluating the anti-inflammatory activity of DHDA in both RAW264.7 macrophages and BV-2 microglial cells. DHDA results able to reduce several key neuroinflammatory markers like NO, IL-6, MCP-1, and CCL-20. Moreover, has been deeply investigate the immune-modulatory activity of DHDA analyzing the level of COX-2 mRNA expression, its metabolite PGE2 and the involvement of NF-κB. In conclusion, DHDA displays marked immune-modulatory effects by attenuating the neuroinflammatory marker detected and their mechanism of action involve the COX-2 enzyme (Figure 17).[168]

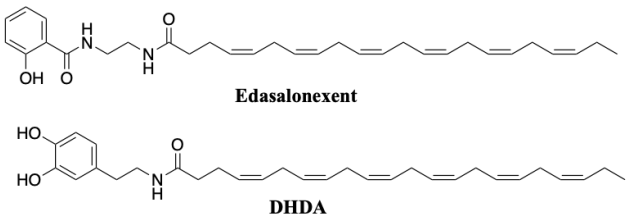

Figure 17. Chemical structure of edasalonexent e DHDA.

The conjugation strategy has been also highly investigated for the development of anti-cancer drugs (Figure 18).[169] Based on the fact that omega-3 FAs uptake is considerably elevated in cancer tissues, numerous omega-3 FAs/drug conjugates have been developed. Therefore, conjugation of anticancer drugs to omega-3 FAs has been found to considerably change the PK and distribution of the drugs, resulting in specific accumulation of the drugs in tumor tissues

and cells. Noteworthy, among the numerous of examples, the drug candidate Taxoprexin® is the most advanced in clinical trials (phase III). Taxoprexin® was designed by joining DHA with the anticancer drug paclitaxel.

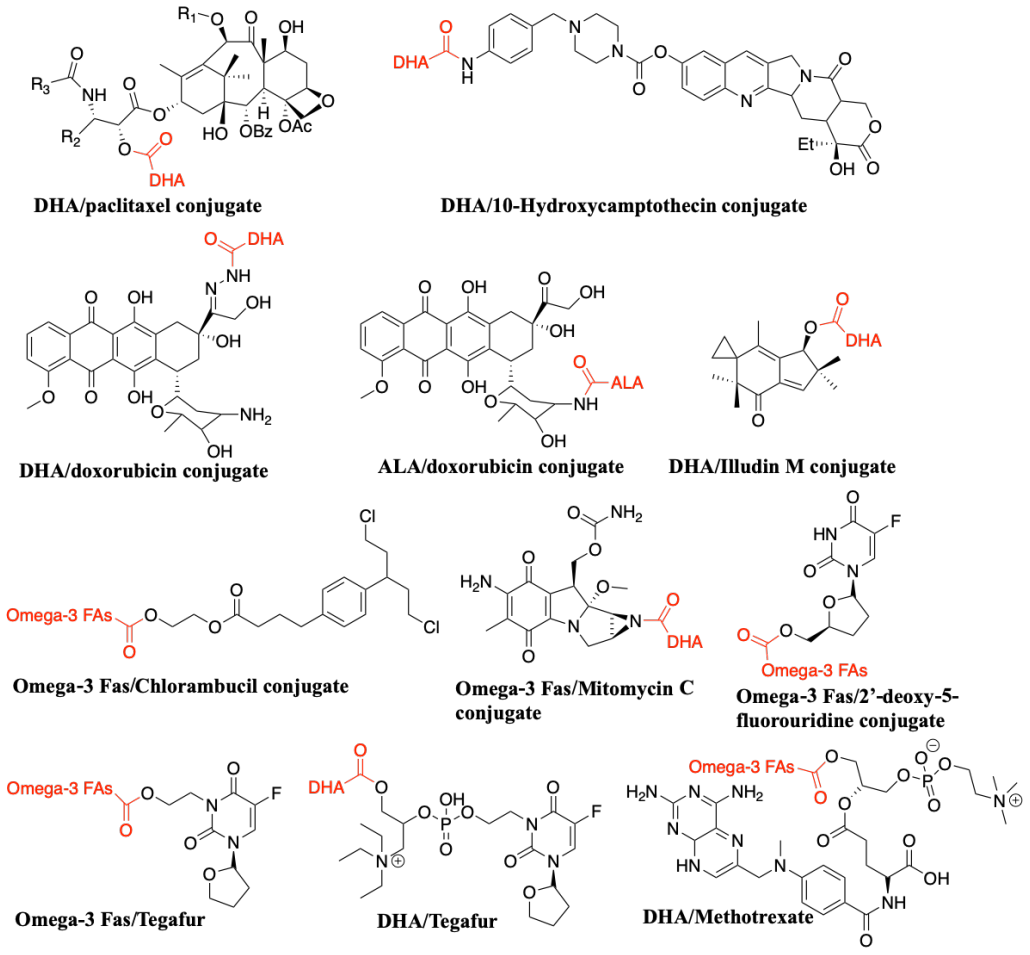

Figure 18. Example of FAs/anticancer drug conjugates.

From the conjugation strategy between omega-3 FAs and drugs we took inspiration for the develop of our series of omega-3 FAs/drug conjugates directed towards neuroinflammation.

3.5 Design of omega-3 FAs/VPA conjugates

Harnessing the polypharmacological approach, the aim of this project was the development of a completely new class of anti-neuroinflammatory lipid-drug conjugates against neurological disorders. Particularly, we have investigated the possibility to join in a single molecule the well-known effect of omega-3 FAs with the multipotent activity of VPA.

As highlighted before, neuroinflammation is a common element spanning all the neurological and neurodegenerative disorders, and it is becoming one of the major targets for drug discovery. As largely discussed before, the omega-3 FAs are effective anti-neuroinflammatory supplements. Moreover, the use of omega-3 FAs are an attractive strategy for novel drug development for the following reasons: (i) omega-3 FAs are FDA-approved food supplement and so are non-toxic compounds;[170] (ii) omega-3 FAs possess anti-inflammatory activity via a myriad of signaling pathways; (iii) synergism has been observed with a variety of drugs against neurological disorders; (iv) omega-3 FAs appear to have protective effects on healthy cells by preventing drug-induced specific organ injury; (v) conjugation may limit systemic toxicity by altering the pharmacokinetic properties of the conjugated drugs.

Building on this rationale, in this project among the omega-3 FAs we have selected ALA and DHA. ALA is the founder of omega-3 FAs family and, although less studied compared to its derivatives EPA and DHA, it has demonstrated neuroprotective, anti-inflammatory, and antidepressant properties.[171] Conversely, DHA is the most abundant omega-3 FA in the brain and is role has been deeply investigate with better result in *in vivo* neurological model compared to other omega-3 FAs analogs.[106]

On the other end, the histone deacetylase (HDAC) inhibitor VPA is a well-known multipotent compound actually registered as an antiepileptic drug and for mood disorder. The VPA has been also deeply investigated as potential drug for neuroinflammatory diseases. Indeed, VPA has demonstrated anti-neuroinflammation, neuro-regenerative and neuroprotective effect in several neurological models.[172, 173] Moreover, the role of VPA as HDAC inhibitor results fundamental for the prevention on neuronal death in in *vivo* models.[174] However, the molecular mechanisms underlying this anti-inflammatory effect and the HDAC responsible are not completely understood.[174]

Recent studies have shown the role of VPA for the treatment of AD obtaining controversial results. Indeed, as reported by *Zhang H., Y* et al. VPA promote neurogenesis and neuroprotection suggest it could prove beneficial in AD patients.[172] Unfortunately, several clinical trials demonstrate that the chronic stimulation with the VPA attenuated human microglial phagocytosis,[175] and accelerate brain atrophy in AD patients with potentially greater cognitive decline.[176]

Another study investigates the potential role of VPA for the treatment of spinal cord injury.[177] From the study conducted by *Shun Li et. al*. emerged that VPA treatment attenuated the inflammatory response by modulating microglia polarization through STAT1-mediated acetylation of the NF-κB pathway, dependent on HDAC3 activity. These outcomes led to neuroprotective effects in spinal cord injury *in vivo* model.[177]

Recently, VPA has been also tested in the experimental allergic encephalomyelitis (EAE) multiple sclerosis model. *Schluesener et al*. reported that VPA greatly reduces the severity and duration of EAE.[178] Moreover, VPA administration also reduces demyelination and suppresses mRNA levels of the proinflammatory cytokines IFNγ, TNFα, IL-1β and IL-17, while increasing the anti-inflammatory cytokine IL-4, with a neuroprotective effect.[178] In spite of these promising data, recent evidences have highlighted the reduced remyelinating activity for VPA.[179] This might be responsible (at least in part) of the inconclusive results of the first human study.[173]

Generally, a great deal of attention has been paid to the pharmacological regulation of microglial activation by VPA. Indeed, the possibility to modulate the microglia polarization from proinflammatory (M1) to anti-inflammatory phenotype (M2) has put VPA in a new light for the treatment of neuroinflammatory-based diseases. Starting from these scientific evidences, the aim of this project was to design and synthesize a first set of omega-3 FAs/VPA conjugates (**1**-**8**) for the treatment of neuroinflammatory diseases. To obtain this goal, we chemically linked through proper spacers (ethylene glycol, ethanolamine and ethylenediamine) the marketed VPA drug and ALA or DHA food supplements via their carboxylic acid functions (Figure 19).

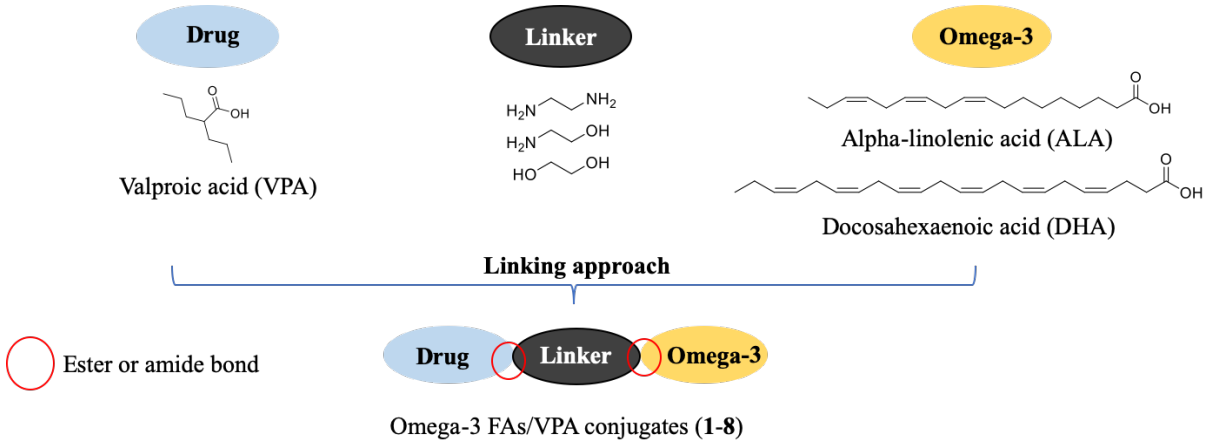

Figure 19. Design of omega-3 FAs/VPA conjugates **1-8**.

We expected that, due to the nature of the formed ester and/or amide bonds, hydrolysis will occur *in vivo*. Thus, each released starting framework would retain the ability to interact with its specific target and, collectively, to produce multiple, synergistic pharmacological effects. We believe that such a concerted, simultaneous modulation of multiple critical pathways affected by VPA and ALA or DHA can result in a truly immunomodulatory, protective and anti-neuroinflammatory effect.

In principle, the effect of the combination of these individual drugs should be well described.[180] However, the herein proposed single-molecule conjugates should have several advantages with respect to a classical drug combination for the following reasons: VPA and ALA or DHA are delivered intracellularly at the same time and in equimolar concentrations. Since multiple biological pathways in multiple brain cell types will be simultaneously hit by this type of delivery, the resulting pharmacology that can be produced is peculiar and cannot be replicated by administering VPA and ALA or DHA in combination, where each one has an individual pharmacokinetic profile.

For the specific case of the DHA/VPA conjugate, when ethanolamine is used to link VPA and DHA, the conjugate *in vivo* can release three active ingredients: VPA, DHA and synaptamide. This is an N-acyl omega-3 FAs endogenous mediator whose immunomodulatory effect is well-known. It promotes neurogenesis, neuritogenesis, synaptogenesis and axonal morphogenesis.[127, 142] Moreover, it is an agonist of cannabinoid receptors, which in turn if activate can positive modulate decreasing the neuroinflammation. Importantly, while each bioactive can exert an individual peculiar beneficial profile, we expect that the whole effect of

this tripartite combination on neurons, oligodendrocytes and microglia is much greater than the sum of its parts. Such a single-molecule combination encompassing a well-known drug, a food supplement and an endogenous neurorigenerative compound could have a breakthrough mechanism of action.

Another important advantage to combine in a single molecule VPA and omega-3 FAs is to obtain codrug (or prodrug). In this case both codrug and mutual prodrug assumes the same importance and relevance.[181] This because the drug design approach proposed allowed us to chemically bind two drugs to improve theoretically the therapeutic efficiency, improve the PK tissue distribution, and potentially decrease side effects.[181] The codrug obtained also can potentially better targeting the CNS.[161] The BBB represents a formidable impediment for the develop of CNS drugs. Experimental tests have shown that the carboxylic acid groups in a molecular structure, due to their dissociated form, hinder the BBB crossing and the consequent distribution in the CNS of a drug.[161] Therefore, the strategy to develop codrug masking the carboxylic acid functions of VPA and omega-3 FAs, such as ester or amide, represent a solution to overcome the PK tissue distribution problem.

3.6 Chemistry

The synthesis of compounds **1-8** was easily realized using a linear synthetic strategy, by applying a modified Steglich coupling reaction. The conventional protocol is based on the nucleophilic acyl substitution between a carboxylic acid and an amine or alcohol, in presence of N,N'-dicyclohexylcarbodiimide (DCC) and a catalytic amount of 4-dimethylaminopyridine (DMAP) in order to obtain an amide or ester derivative, respectively. However, the reported protocol suffers principally from long reaction time, and a boring work-up filtration protocol to remove the N,N'-dicyclohexylurea (DCU) coupling side product. Moreover, the risk to find DCU in the final product remains an important problem to solve. Thus, taking inspiration from the literature, we modified the protocol using 1-ethyl-3-(3-dimethylaminopropyl)carbodiimide (EDC) and a catalytic amount of DMAP.[167] Clearly, the major advantage using EDC compared to DCC is the simplification of the work-up. Indeed, The EDC side products are soluble in the organic solvent and easily removed during the purification step by column chromatography.

In details, the final conjugates **1-8** were synthesized starting from the appropriate valproic-linker derivative **22-25** and ALA or DHA omega-3 FAs (Scheme 1). The synthesis starts from the three linkers **11-13** that were protected with the appropriate protecting group as: di-tert-butyl decarbonate (Boc_2O) or tert-butyldimethylsilyl chloride (TBSCl) obtaining the N-Boc- and O-TBS-protected derivatives **14-17** with a typical protection protocol in very good yields (87-98%). The obtained protected-linker **14-17** was coupled with valproic acid (VPA) after activation with EDC/DMAP obtaining the ester or amide intermediates **18-21** in good yields (42-68%). Therefore, a deprotection reaction, using trifluoracetic acid (TFA) or tetrabutylammonium fluoride (TBAF) in order to remove respectively the Boc- or TBS-protecting groups, were performed, obtaining in very good yield the intermediates **22-25** (89-98%). The deprotection reactions were conducted under anhydrous condition and at 0°C in order to limit the valproic acid hydrolysis as side reaction. Finally, compound **22-29** were synthesized starting from ALA or DHA and the valproic-linker conjugate **18-21** using the previous coupling reaction condition with EDC/DMAP.

Scheme 1. Synthesis of omega-3 FAs/VPA conjugates **1-8**.

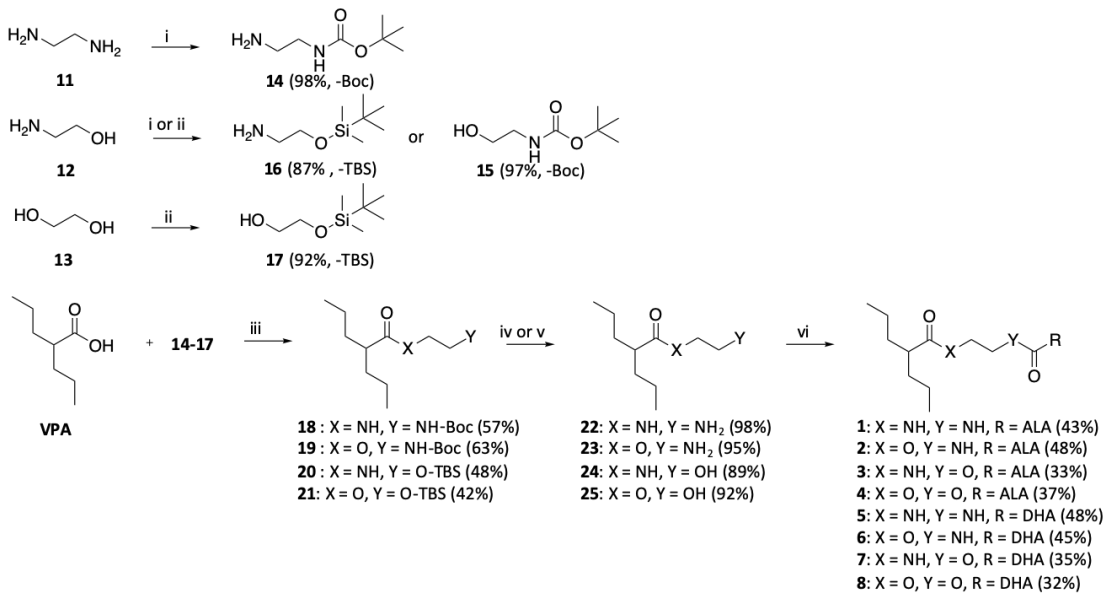

Reagent and conditions: i) TBSCl, Imidazole, DCM, r.t., 24 h; ii) Boc_2O, DCM, r.t., 24 h. iii) EDC, DMAP, DCM, r.t., 8 h, N_2; iv) TFA, DCM, r.t., 2h; v) TBAF, r.t., 24h; vi) ALA or DHA, 1-EDC, DMAP, DCM, r.t., 8 h, N_2.

The final reaction was conducted from 0°C during the acid activation to room temperature under nitrogen atmosphere and in the dark, in order to limit the formation of oxidation-side products. The four final products have been purified by low-pressure column chromatography always in the dark, the solvent was evaporated in a low-temperature bath, and finally stored at -20°C. Finally, Compound **9**-**10** have been synthesized with the same synthetic strategy starting from the protected linker. Then, the intermediate obtained was reacted with ALA or DHA by modify Steglich coupling reaction obtaining **26**-**27** (Scheme 2). The last step was the deprotection reaction using the appropriated reagent in order to remove the terminal O-protecting group.

Scheme 2. Synthesis of N-acyl omega-3 FAs derivatives **9**, **10.**

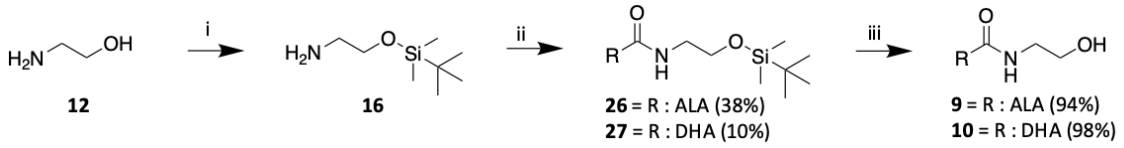

Reagent and conditions i) TBSCl, Imidazole, DCM, rt, 24 h; ii) ALA or DHA, EDC, DMAP, DCM, rt, 8 h, N_2; v) TBAF, DCM, rt, 24h.

All compounds were characterized using analytical (HPLC) and spectroscopic data (1H- and 13C-NMR) (see Chapter 8).

3.7 Results and discussion

The small series of omega-3 FAs/VPA conjugates **1-8** were designed and synthesized with the aim to develop a new treatment for neuroinflammatory diseases, in particular MS. Thus, we decided to first analyze the neuro- and hepatotoxicity profile of **1-8**. After that, the HDAC inhibitor activity has been evaluated, followed by a cannabinoid receptor (CB1/2) affinity assay of the less cytotoxic conjugates.

As second step, the potential therapeutic profile of compounds **1-4** (ALA/VPA conjugates) has been examined in detail. After excluding cytotoxic effects in Oli-Neu and microglia cell line (N9), **1-4** were screened in order to evaluate their neuroprotective and immune-modulation activity. Then, the most promising conjugates have been analyzed to evaluate their proliferation, and differentiation activity in Oli-Neu cells.

Finally, the hydrolysis kinetic profile of the best conjugates (**1**, **2**) was tested in rat blood, liver, and brain lysate by LC-DAD-MS/MS.

3.7.1 Neurotoxicity assay

Being these conjugates designed to combat neurological diseases, a preliminary neurotoxic screening has been performed on **1-8**, the ethanolamide **9** and **10 and** reference compounds **(**VPA, ALA and DHA). Increasing concentrations of each compounds have been tested in cerebellar granule neurons (CGNs). Primary cultures of CGNs were established a few decades ago as one of the most useful *in vitro* models to study neuronal death.[182] Positively, none of them (up to 10 μM) showed significant neurotoxic effects when viability was measured through a (3-(4,5-dimethythiazol-2-yl)-2,5-diphenyltetrazolium bromide) MTT assay (Figure 20). However, DHA derivatives **5** and **6,** that present di-amide or ethanolamide linker, resulted the most cytotoxic conjugates among the tested compounds. On the other side, the corresponding ALA derivatives **1** and **2**, maintain cells viability on CGNs over 100% at 10 μM after 24h. This assay has been performed by the group of Prof. Monti of the University of Bologna.

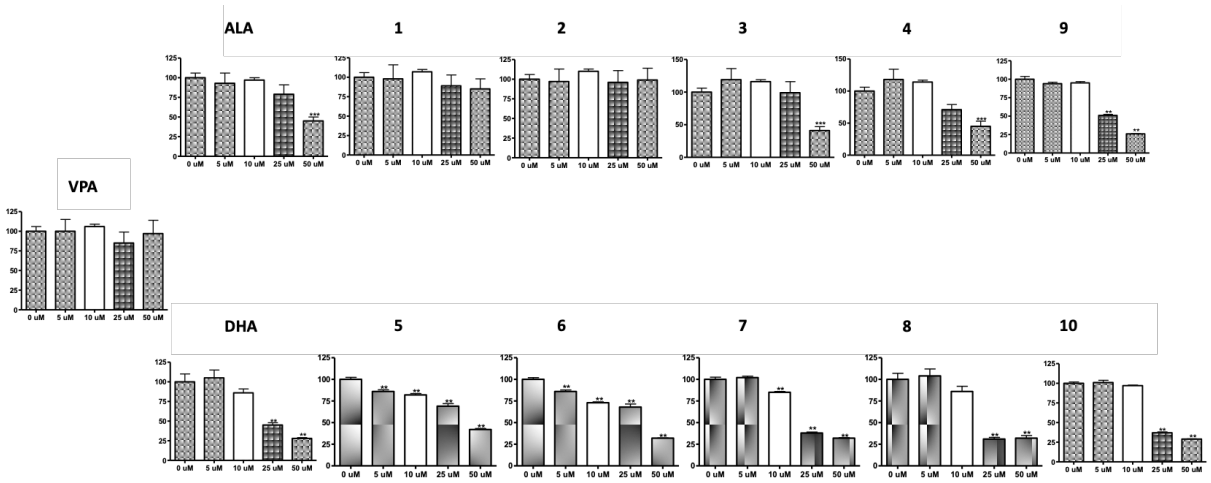

Figure 20. Effect of conjugates **1-8** on cell survival/death through MTT assay in CGN cells at the concentrations 0, 5, 10, 25 and 50μM of **1-10** for 24h. Each point is the mean ± S.E. of two independent experiments, each run-in quadruplicate and is expressed as the percentage of control (0μM). Bonferroni's test after ANOVA.

3.7.2 Hepatotoxicity assay

In a parallel assay, we evaluated the hepatotoxicity of compounds **1-10** by MTT assay on human hepatocellular liver carcinoma immortalized cell line (HepG2). The assay has demonstrated no significant hepatotoxicity effect through MTT assay at 5 and 10 μM concentrations (Figure 21). At higher concentrations (25 and 50 μM) the tested compounds start to display some sign of cytotoxicity after 24h. Notably, the conjugate **8** results the safest, similarly to DHA. This assay has been performed by the group of Prof. Monti of the University of Bologna.

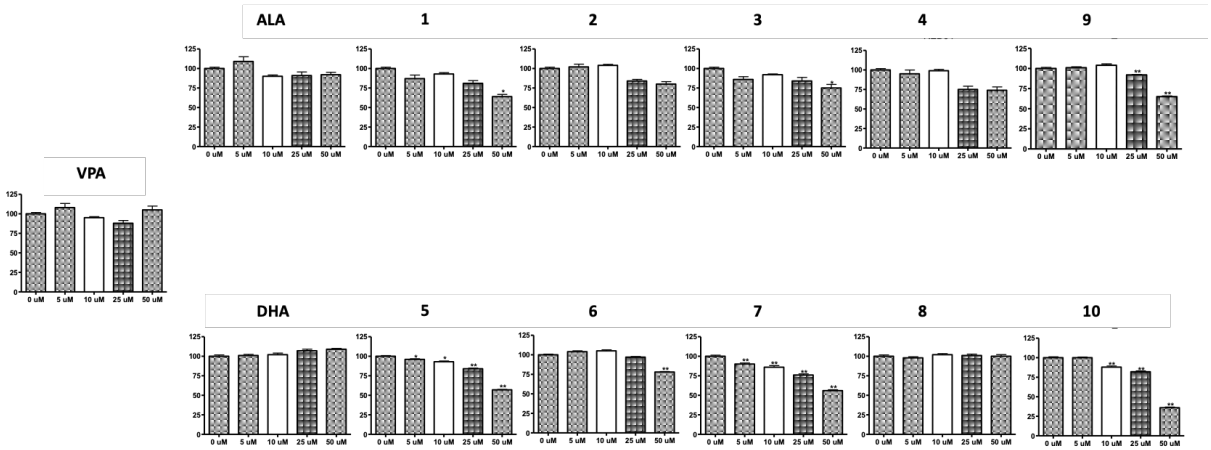

Figure 21. Effect of conjugates **1-8** on cell survival/death through MTT assay in HepG2 cells at the concentrations 0, 5, 10, 25 and 50µM of **1-10** for 24h. Each point is the mean ± S.E. of two independent experiments, each run-in quadruplicate and is expressed as the percentage of control (0µM). Bonferroni's test after ANOVA.

3.7.3 HDAC inhibition profile

We wanted to evaluate whether the VPA-conjugates **1-8** maintain the HDAC inhibitory activity of the parent drug VPA. The HDAC inhibition is a fundamental aspect to evaluate because it is highly involved in neuroprotective and neuroinflammatory processes, and oligodendrocyte precursor cells (OPCs) differentiation into oligodendrocytes.[172, 174] The Western blot analysis and the relative densitometries of acetylated histones clearly indicate that compounds **1** (ALA di-amide derivative), **2** (ALA ethanolamide derivative), **5** (DHA di-amide derivative) show an activity similar or even better than VPA. Conversely **3, 4, 6-8** are significantly less effective than VPA (Figure 22). From these data we can speculate that at least the presences of one amide bond between the FA and the linker (and not the amide between the VPA and the linker as in **3** and **7**) is essential for HDAC activity. Indeed, both the ALA and DHA di-ester derivatives do not show significant HDAC activity. Possible explanations could be: (i) the more active "amide-type" conjugates undergo to more efficient hydrolysis mediated by specific fatty acid amide hydrolases (e.g. FAAH) to release the active molecule VPA (potent HDAC inhibitor); (ii) the higher activity of ALA derivatives **1** and **2** support a possible contribution to the epigenetic effect by this FA.[183, 184] Apparently, this does not apply to DHA. In fact, the equimolar combination of DHA and VPA results equally active compared to the single treatment with only VPA. This assay has been performed in collaboration with the group of Prof. Spampinato of the University of Bologna.

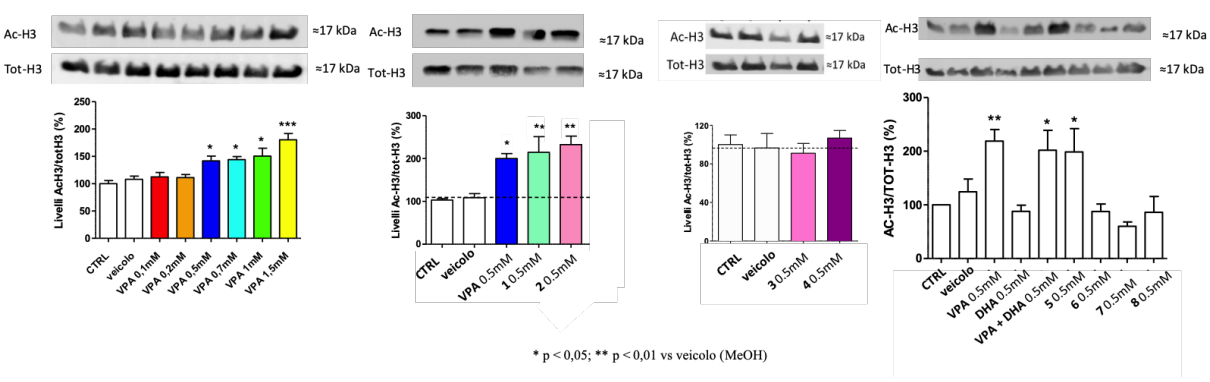

Figure 22. Effect of conjugate **1-8** on HDAC inhibition, evaluated through analysis of pan-acetylated Histone H3 and total histone H3 in neuroblastoma (DAOY) cells. Cells were exposed to 0.5mM for 48h and analyzed through western blot analysis of pan-acetylated Histone H3 or total-histone H3. In the densitometry, each column is the mean ± S.E. of three independent experiments and are expressed as the percentage of control (0μM). * $p < 0,05$; ** $p < 0,01$ vs vehicle (Student's t-test).

3.7.4 Cannabinoid receptor binding assay

For the following experiment, we selected the less toxic and most active compounds based on the previous experiments, i.e. the "amide-type" conjugates **1**, **2**, **5**, **6** and the validated reference compounds GW and WIN. As highlighted before, these compounds are omega-3 FAs conjugates that after the *in vivo* hydrolysis can release important omega-3 FAs metabolites. Notably, it has been observed that omega-3 ethanolamide FAs metabolites can interact as direct agonists with the cannabinoid receptors.[127] Thus, in collaboration with Prof. Contino of the University of Bari, a binding assay on CB1/2 cannabinoid receptors was performed. Remarkably, only compound **10** (synaptamide) resulted to be a good binder for CB2 receptor and a weak binder of CB1 receptor (Table 2), in agreement with what is reported in the literature. The rest of the tested molecules show less than 50% of binding at 10μM. The conjugates are probably not active due to the lack of hydrolysis at the experimental conditions.

Table 2. CB1/2 receptor binding affinity values for compounds 1,2 5, 6, 9, 10 and reference compounds.

Compounds	**CB2R[a,b]**	**CB1R[a,b]**
	Ki ± SEM, nM	
1	**39%**	**nd[c]**
2	**6%**	**41%**
9	**28%**	**NA[d]**

5	**25%**	**NA[d]**
6	**30%**	**27%**
10	**443nM**	**2,6µM**
GW	**7.7nM**	**nd**
WIN	**nd**	**75nM**

[a] Data represent mean values of n ≥ 3 separate experiments in duplicate (±SEM for CB2R).

[b] Percentage of displacement at the concentration of 10 µM.

[c] nd: no determined

[d] NA: without affinity at the repecptor

3.7.5 Immuno-modulatory assay

After collecting the data described above, we performed the preliminary experiments to evaluate whether the selected ALA/VPA "amide-type" conjugates **1** and **2** were able to modulate microglial activation from the M1 neurotoxic to the M2 neuroprotective phenotype. Therefore, N9 microglial cells were treated with 100ng/mL lipopolysaccharides (LPS) in presence or absence of increasing concentrations (0.5, 1, 5, and 10 µM) of **1** and **2**, the reference compounds (ALA and VPA) and a mixture 1:1 of reference compounds, for 24h. Microglial phenotype has been evaluated through Western blot analysis of the M1 marker iNOS (responsible for nitrite production) and Triggering receptor expressed on myeloid cells-2 (TREM2, Figure 23) M2 marker. Compounds **1**, VPA, ALA and their mixture does not affect the concentration of nitrites, whereas slightly **2** does. Regarding, marker expression, all of compounds seem to decrease iNOS expression at 10 µM more than the equimolar mixture of VPA and ALA. More importantly, **2** presents another biological function, particularly significant for a possible anti-neuroinflammatory activity. It maintain constant the level the expression of TREM2, an immunomodulatory activity marker of microglia shifts towards the M2 phenotype, whereas the rest of compounds decrease this anti-inflammatory maker. We

might interpret the increases expression of TREM2 by considering the hydrolysis pattern of **2**. From the hydrolysis of **2** three active metabolites could be released: ALA, VPA and the ALA-ethanolamide. As discussed, omega-3 FAs ethanolamides are potent endogen stimulator of immune-modulation, and are involved in remyelination process in the CNS.[185] This peculiar biological effect can be appreciated by considering that diamide derivative **1**, unable to release an endogenous ethanolamide metabolite, is not active.

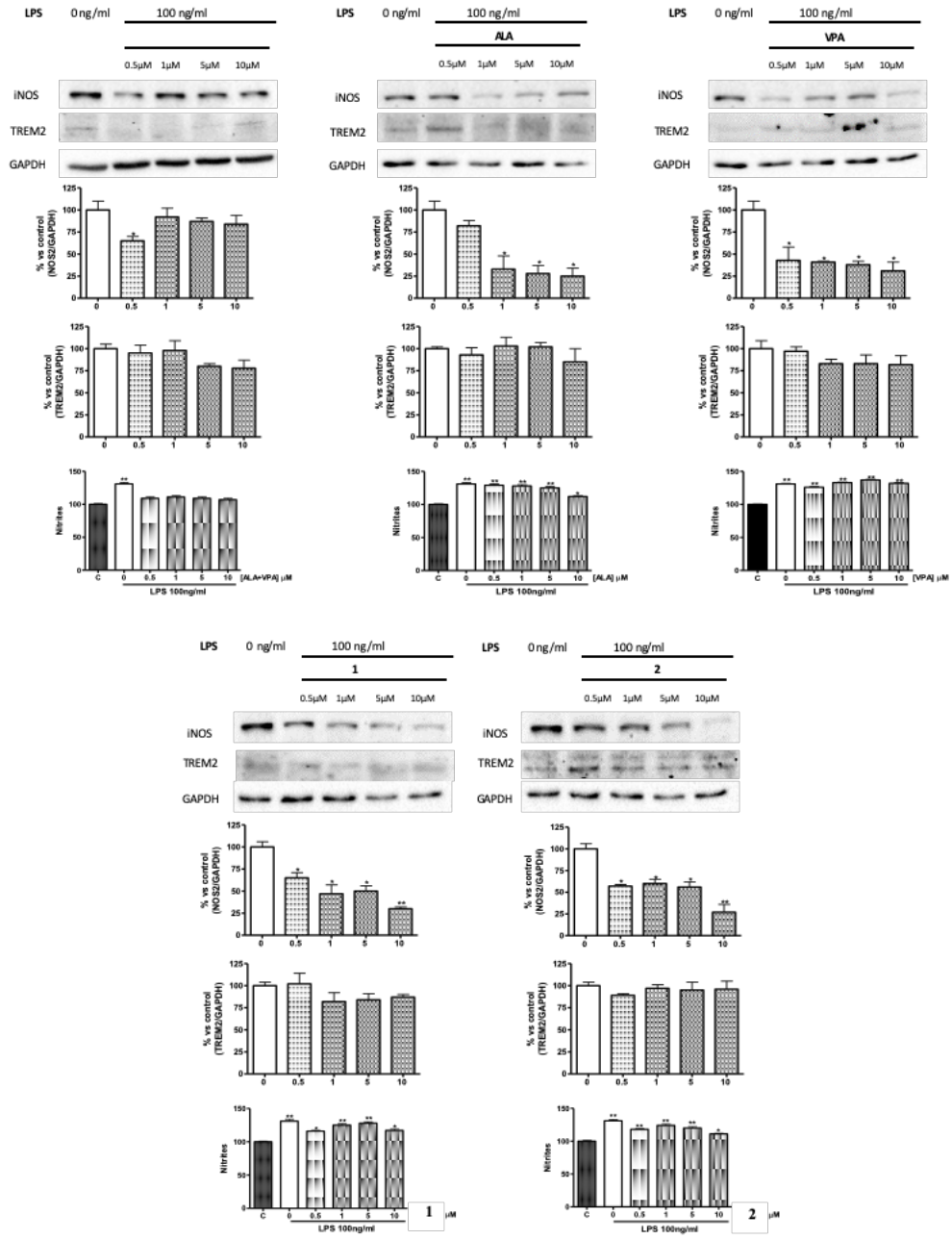

Figure 23. Effect of **1**, **2** and parent compounds on microglia activation. Western blot analysis and the relative densitometries of iNOS (M1 marker), TREM2 (M2 marker) and nitrite

concentration in N9 microglial cells. Densitometric data are expressed percentage of LPS only of one experiment.

3.7.6 Microglia cell neuroprotective assay

As further step, we evaluated the neuroprotective activity of conjugates **1** and **2** and their parent compounds ALA and VPA in N9 cell line. A typical neuroprotective assay involves the use of H_2O_2 as stressor agent that induces cell injury (Figure 25). After pre-treatment with the tested compounds, the cells were treated with 500 μM of H_2O_2 and viability evaluated by MMT assay. From the data of Figure 25, we can conclude that all compounds do not show a significant neuroprotective effect in this experimental cell model.

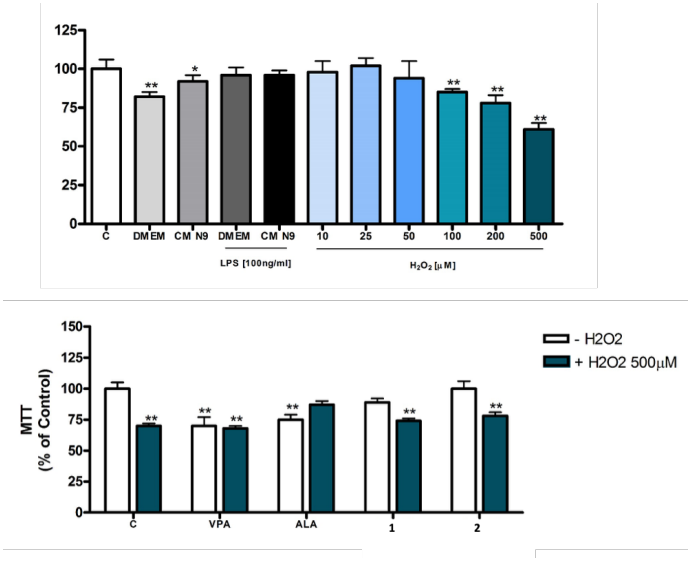

Figure 25. Effect of compounds **1**, **2** on cell survival/death through MTT assay in Oli-Neu cells, immortalized. Cells were exposed to 10μM of 1, 2 and the reference compounds, then treated with 500μM of H_2O_2. Each point is the mean ± S.E. of two independent experiments, each run-in quadruplicate and is expressed as the percentage of control (0μM). * P <0.05, ** P <0.01).

3.7.7 Oli-Neu cell cytotoxicity assay

Next, we tested whether the conjugates **1**, **2** could be toxic in a model of immortalized murine OPCs, by using Oli-Neu cells. Indeed, the use of Oli-Neu cells is considered a good *in vitro* preliminary model to screen potential MS drug candidates.[186] After treatment with increasing concentrations of compounds **1** and **2** and reference compounds (ALA and VPA) for 24h, the

MTT assay clearly shows that, while the VPA and ALA are significantly toxic for these cells even at low concentration (5µM), conjugates **1,** and especially **2,** show no toxicity even at higher concentrations (Figure 24).

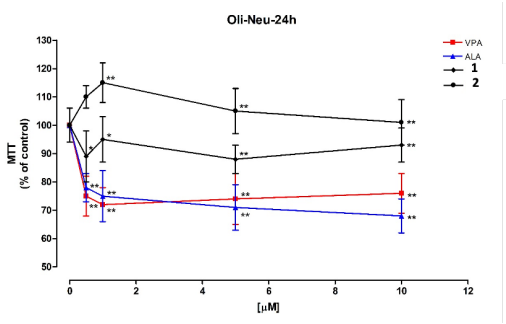

Figure 24. Effect of compounds **1** and **2** on cell survival/death through MTT assay in Oli-Neu cells, immortalized mouse oligodendrocyte precursor cells. Cells were exposed to increasing concentrations (0.5, 1, 5 and 10µM) of the selected compounds. Each point is the mean ± S.E. of two independent experiments, each run-in quadruplicate and is expressed as the percentage of control (0µM). * P <0.05, ** P <0.01.

3.7.8 Proliferation and differentiation assay

After the preliminary promising result obtained by Oli-Neu cytotoxicity assay, we performed an experiment to evaluate the effect of "amide-type" ALA conjugates **1** and **2** on Oli-Neu proliferation and on their spontaneous differentiation in oligodendrocytes, in comparison with their equimolar mixture (Figure 26). Clearly, this assay will allow to preliminary assess the therapeutic potential of these conjugates against MS. Compounds **1** and **2** slightly reduced the proliferation of the cells and the number of their filaments (Figure 26). Conversely, by analyzing filaments length as an index of differentiation, we observed that: (i) ALA alone does not affect the length of the filaments (low differentiation); (ii) the VPA/ALA mixture reduces differentiation; (iii) VPA and diamide **1** only slightly increase differentiation; (iv) conjugate **2** increases differentiation more then 20 % compared the other molecules and the control.

Remarkably, again **2** is the conjugate that can release the ALA-ethanolamide metabolite, which can have a role of in Oli-Neo differentiation.

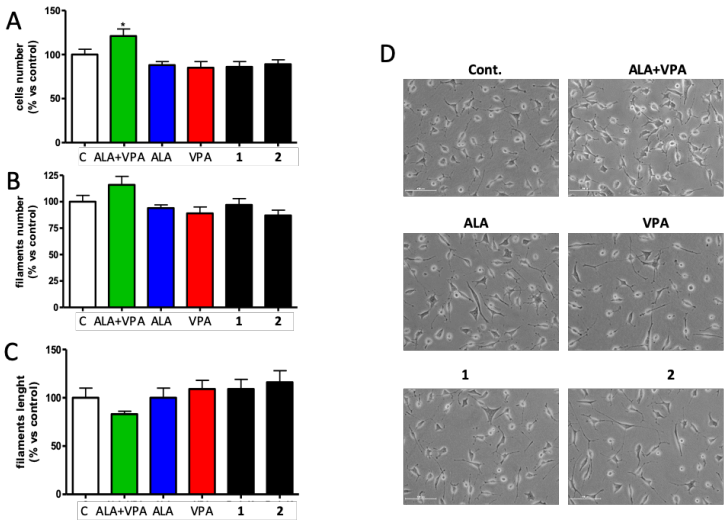

Figure 26. Effect of tested molecules on cells and filaments proliferation and differentiation in Oli-Neu cells. Cells were exposed to 5µM of **1** and **2** or VPA or ALA for 48h. The cells and number of filaments proliferation (A-B) were evaluated by cell counting, while differentiation by measuring the filaments length (C), as shown by illustrative figures of each treatment (D). For quantification, each point is the mean ± S.E. of two independent experiments, five different image fields for each experiment and is expressed as the percentage of control (0µM). Bonferroni's test after ANOVA. Scale bar = 100µm.

3.6.9 Blood stability assay

Our was to develop plasma-stable conjugates that would be hydrolyzed in the brain. Thus, selective, localized hydrolysis of conjugates **1** and **2** in the brain would permit a better efficacy profile and less side effects following a targeted distribution. Therefore, we have evaluated the plasma stability of the most promising compounds **1** and **2**. From analysis by LC-DAD-MS/MS we evaluated the percentage of starting compounds after 1h of treatment in *in vitro* rat blood. Encouragingly, the remaining quantity of **1** and **2** after 1h of treatment is over 85% (Figure 27); as expected, the diamide derivative **1** is slightly more stable. (< 90%). These data highlight that the rational design strategy to obtain plasma-stable conjugates has been fulfilled.

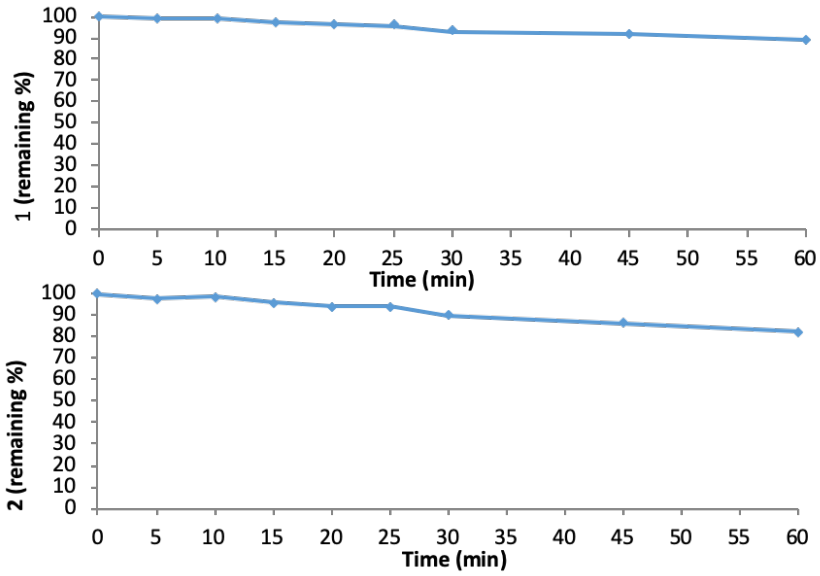

Figure 27. *In vitro* stability of compounds **1**, **2** in rat blood (37 °C): percentage remaining upon incubation, assessed by means of LC-DAD-MS/MS.

3.6.10 Hydrolysis kinetic assay

We have also demonstrated the desired hydrolysis profile of the conjugates **1** and **2** by hydrolysis kinetics assay. To establish the hydrolysis profile of the two synthesized conjugates we treated the rat-liver and brain lysate with **1** and **2** and determined the percentage of compounds remaining upon incubation at 37 °C using LC-DAD-MS/MS (Figure 28, 29). As expected, the different nature of the linkers resulted in different hydrolysis kinetics. Indeed, the diamide bonds of **1** resulted more stable compared to the ester-amide linkage of **2**. The further step will be the determination of the structure and the quantification of the parent drugs and metabolites after the hydrolysis.

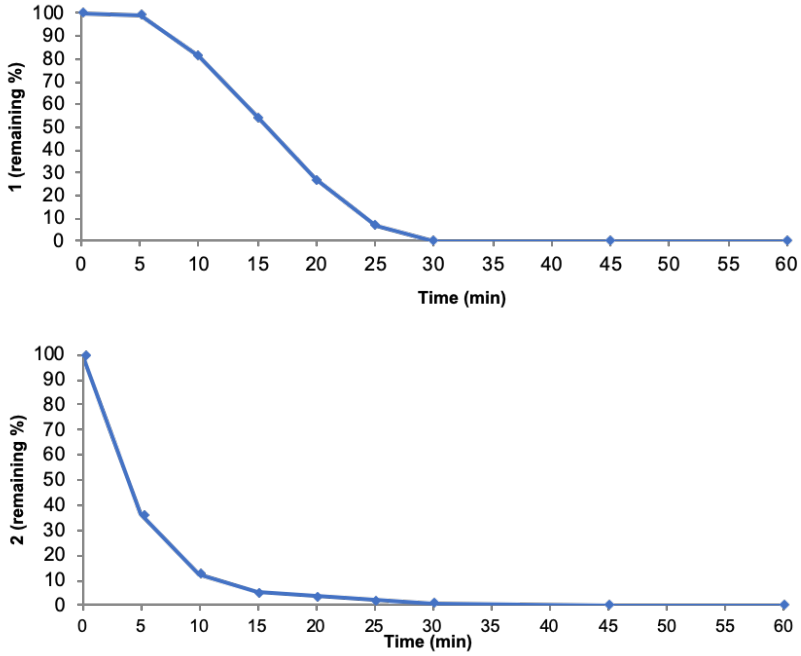

Figure 28. Kinetics hydrolysis of conjugate **1**, **2** in rat liver homogenate (37 °C): percentage remaining upon incubation, assessed by means of LC-DAD-MS/MS.

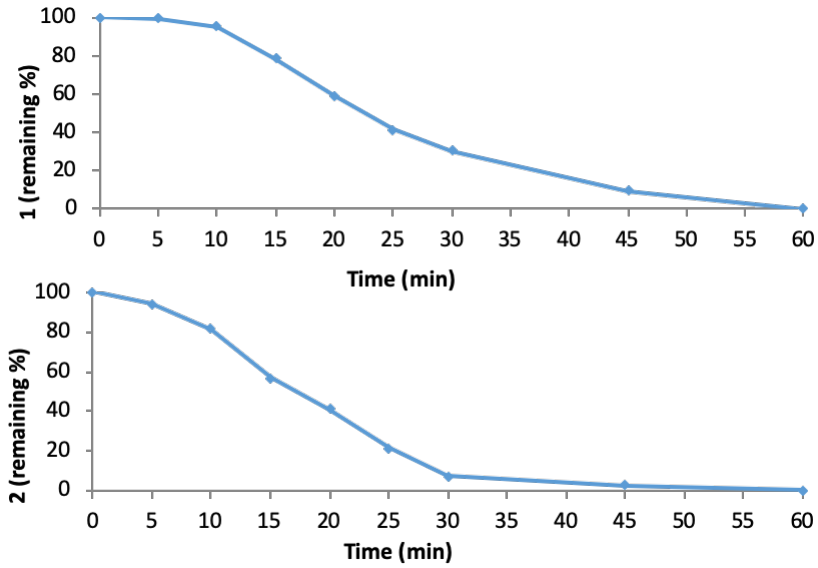

Figure 29. Kinetics hydrolysis of conjugate **1**, **2** in rat brain homogenate (37 °C): percentage remaining upon incubation, assessed by means of LC-DAD-MS/MS.

By recognizing the heterogeneity and the multifactorial nature disease, single chemical entities directed to multiple disease-relevant targets offer a promising approach to the treatment of a multifactorial disease such as MS. Notably, the VPA-ALA "amide-type" conjugate **2** emerges

as a very promising hit compound for the treatment of MS pathology. Particularly, **2** proved to be the less cytotoxic in two different CNS cell lines (CGN and Oli-Neu cells) and one hepatic cell line (HepG2 cells) compared to the reference compounds (ALA and VPA) also at high concentration. Moreover, the conjugate **2** demonstrated to be able to modulate the microglia polarization from a pro-inflammatory phenotype M1 to an anti-inflammatory phenotype M2 through decreasing of the expression of iNOS and increasing the level of TREM2. Furthermore, **2** reveled to be the most promising compound also after analysis of cell differentiation assay in Oli-Neu cell model (validated MS cell model). Indeed, it can decrease cell proliferation and trigger differentiation (by increasing the length of the filament) in Oli-Neu cells. Finally, conjugate **2** proved to be a stable molecule after preliminary in vitro PK evaluation using *in vitro* rat blood after 1 h, and it seem to be hydrolyzed in specific tissue (rat brain and liver lysate).

Chapter 4

Project 2: FAs/UDP-like conjugates as potential treatment for Alzheimer's disease

This project has been performed during a Short-Term Scientific Mission (STSM) funded by Multi-Target Paradigm for Innovative Ligand Identification in the Drug Discovery Process (Mu.Ta.Lig.) COST ACTION (CA15135), in collaboration with the laboratory of the Prof. Christa Müller at the University of Bonn.

4.1 The role of $P2Y_6$ receptor in microglia and neuroinflammation

Neurodegenerative diseases such as AD, Parkinson's disease, amyotrophic lateral sclerosis, and neurological disorders like MS, are among the most pressing problems in the word.[187] Neurons play an essential role such as signal transmission and network integration in the CNS and are the main targets of neurodegenerative disease, in particular AD. Moreover, it is interesting to understand how the brain environment could contribute to a neurodegenerating process. Indeed, it largely emerged that neurodegeneration occurs in part because the environment is affected during the disease in a cascade of processes called neuroinflammation.[187] In light of this, neuroinflammation is considered nowadays one of the main component to the cause and progression of neurodegenerative diseases.

Microglia cells are the resident immune cells in the CNS and are considered the main controllers of the inflammatory responses in the brain.[188] They exhibit multiple activation phenotypes (M1 or M2) to accommodate functions in response to environmental changes. The physiological functions of microglia, which include phagocytosis of cell fragments, misfolded proteins, neurotrophic factors, cytokine secretion, and synaptic pruning, are crucial for maintaining homeostasis of the brain microenvironment. Targeting microglia might represent a therapeutic strategy for the treatment of several of these multifactorial diseases like AD.[188, 189]

Microglia express a plethora of cell-surface proteins related to innate immunity that constantly survey the surrounding extracellular environment. Certain receptors mediate microglial Aβ phagocytosis and release of anti-inflammatory cytokines, thereby enhancing Aβ clearance in AD models.[188, 190]

In particular, $P2Y_6$ is a purinergic/pyrimidinergic receptor expressed on microglia that mediates inflammation and regulates microglial activation and phagocytosis.[191, 192] Shortly, P2YRs belong to the δ-branch of class A rhodopsin-like GPCRs.[193] They have an extracellular, glycosylated N-terminal domain, the characteristic seven hydrophobic transmembrane domains, three intra- and three extracellular loops, and an intracellular C-terminus that possesses consensus binding motifs for protein kinases. The mammalian P2YR family consists of eight subtypes: $P2Y_1$, $P2Y_2$, $P2Y_4$, $P2Y_6$, $P2Y_{11}$, $P2Y_{12}$, $P2Y_{13}$, and $P2Y_{14}$. The numbers

missing in the sequence belong to non-mammalian receptors.[193] The human P2YRs can be further categorized into two groups based on sequence homology and the type of G coupled protein.[194] The $P2Y_1$, $P2Y_2$, $P2Y_4$, $P2Y_6$, and $P2Y_{11}$ receptors signal principally through Gq/11 with successive activation of phospholipase C_β. This enzyme, through the production of the second messengers inositol 1,4,5-trisphosphate (IP3) and diacyl-glycerol (DAG), mediates the release of calcium ions from intracellular stores and activation of protein kinase C, respectively.[194] The $P2Y_{12}$, $P2Y_{13}$, and $P2Y_{14}$ receptors are coupled to Gi/o proteins, thereby inhibiting adenylate cyclase and reducing 3′,5′-cyclic adenosine monophosphate (cAMP) levels (Figure 30).[195]

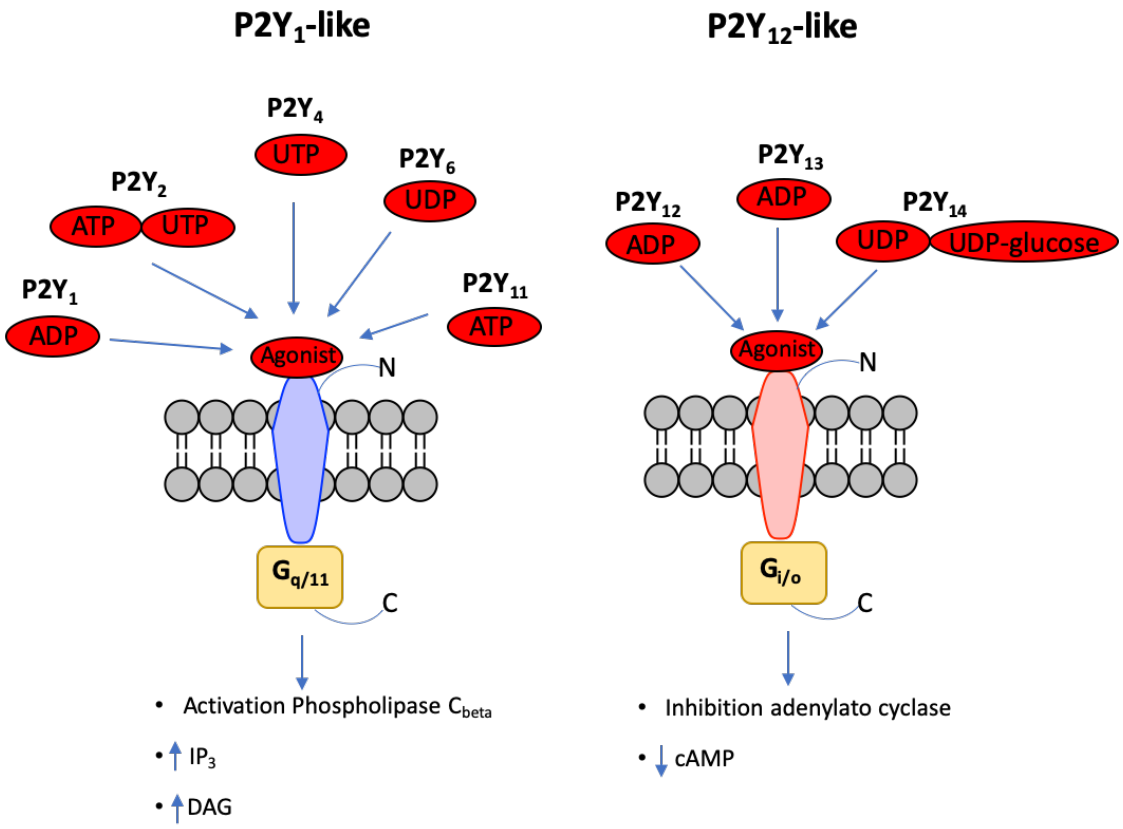

Figure 30. The P2Y receptor subtypes categorized into two groups based on sequence homology and main signaling cascades.

Furthermore, P2YRs may form homo- or hetero- oligomers, as is the case for other GPCRs. This may alter their pharmacological, signaling, desensitization, and trafficking properties (i.e. formation of homodimers of $P2Y_6$).[196]

Another approach to classifying the human P2YR family is based on their natural ligands. The $P2Y_1$, $P2Y_{11}$, $P2Y_{12}$, and $P2Y_{13}$ receptors are activated by adenine di- or tri-phosphates. The

$P2Y_2$ receptor responds to both ATP and UTP. In contrast, the receptors $P2Y_4$, $P2Y_6$, and $P2Y_{14}$ are activated by the endogenous agonist uracil nucleotides.[193]

In particular, the uracil nucleotide uridine 5′-diphosphate (UDP) is the most selective endogenous agonist for $P2Y_6$ receptor. The activation by UDP on $P2Y_6$ receptor mediate only the phagocytosis but not the chemotaxis or migration of microglia.[191] However, *Kim et al*. (2011) found in primary cultured microglia, astrocytes and cortical slice cultures that UDP induces expression of the chemokines CCL2 (MCP-1) and CCL3 (MIP-1α), which are important for monocyte infiltration into the damaged brain.[197]

On these bases, $P2Y_6$ receptor represent an innovative, potential target for the treatment on neuroinflammatory disease, as it is highly involved in the regulation of neuroinflammatory process, microglia chemotaxis and increase of the phagocytosis. All these aspects have made this receptor a potential druggable target for the treatment of AD.[189]

Unfortunately, two main problems have hampered the development of UDP-like agonist for the treatment of CNS diseases, both linked to the structure of the ligand. The first one is related to the synthesis of more active agonist,[193] while the second one is correlated to the high hydrophilicity due to the present of two deprotonated phosphoric functions.[198] The first problem is at least in part solved through a long and difficult optimization process of lead optimization to obtain UDP-like molecules. Indeed, during the last year several UDP-like derivatives, able to bind very tightly and with high selectivity the $P2Y_6$ receptor, (see Figure 31 for recent examples) have been developed. Moreover, a new UDP dimer nucleotide (MRS2957) structure has been found to be very active on $P2Y_6$ receptor.

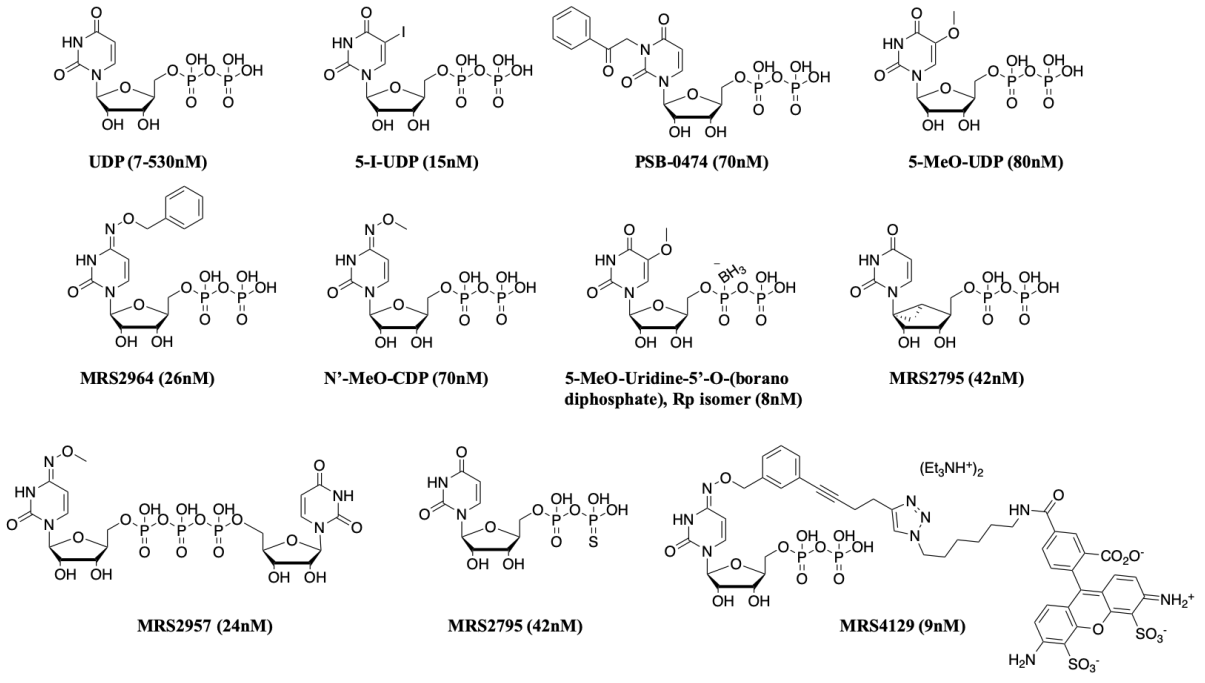

Figure 31. Chemical structure and EC50 of $P2Y_6$ agonists.

The second problem, related to the low BBB penetration and consequent CNS distribution, remain a barrier for the development of UDP-like drugs.

4.1.1 Compound GC021109: the race to victory

One year ago, the company GliaCure started a clinical trial (NCT02386306) investigating the therapeutic effect of the $P2Y_6$ agonist GC021109. This compound is able to recruit microglia to phagocytose cell debris and regulate neuroinflammation. The peculiarity of this structure is that GC021109 is an uracil-like nucleoside where in position N3 is present the 3-ethylbenzo(*d*)isoxazole group.[199] GC021109 is a prodrug, with the foremost advantage to cross the BBB by an active transport system.[200] However, it is a nucleoside, this means that in this form it does not activate $P2Y_6$ receptor, nor over 70 channels, transporters, or receptors assayed in an off-target screen. Nevertheless, when administered to cells, or *in vivo*, the nucleoside is phosphorylated into the actual more active nucleotide (GC011002) that selectively activates the $P2Y_6$ receptor (EC_{50} 12 nM). Like the endogenous agonist, once the GC011002 is released from cells it is rapidly hydrolyzed by endogenous ectonucleotidases enzymes back to the original inactive nucleoside (Figure 32).[199]

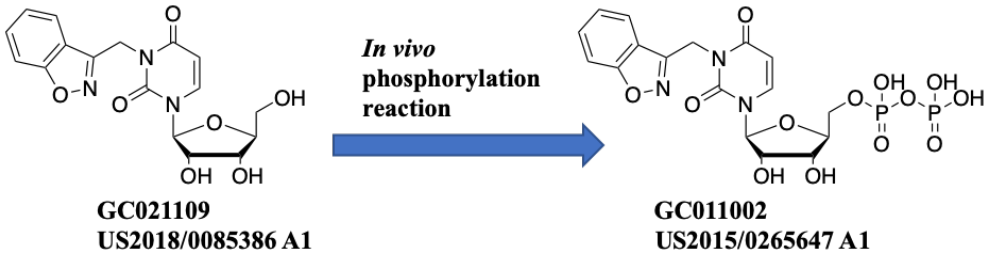

Figure 32. Chemical structure of the $P2Y_6$ agonist GC011002 and its nucleoside GC021109.

However, GC021109 has not being progressed to the market, while repurposed for asthma.[199] Reasonably, the complex PK profile and the BBB permeation problems of this and other UDP-like $P2Y_6$ receptor agonists, have hampered the development of UDP-like drugs.

4.2 Design of FAs/UDP-like conjugates

The world-wild impact, together with its future relevance makes AD the principal medical need of our society. Moreover, the lack of new treatment and the absence of new targets, make it the most formidable challenge for the drug discovery field. Thus, the aim of this project was focused to the design and synthesis of a new class of lipid/drug conjugates obtained by combining the structure of UDP-like $P2Y_6$ agonists with FA. The final idea also in this project would been the use of omega-3 FAs in order to obtain omega-3 FAs/$P2Y_6$ agonist conjugates with multipotent activities for the treatment of AD. We decided to start by using stearic acid as FA model to conjugate with the $P2Y_6$-like molecules. Being an unexplored project, we have preferred to set up the reaction with the lower cost materials to obtain first a reliable and optimized synthetic strategy. Similarly, to the previous project, also in this case, the final molecules have been designed as inactive conjugates. Once arrived in the target tissue, they will become substrate of hydrolytic enzymes releasing the two active parent drugs.

In detail, these conjugates are characterized by the following parts: (i) the polar head: constituted by an UDP-like structure, able to maintain the interaction with the $P2Y_6$ receptor, (ii) the lipophilic tail constituted by stearic acid (FA), that in principle should increase the lipophilicity of the molecule, and (iii) an ethanolamine linker able to bridge the two different parts of the structure (Figure 33).

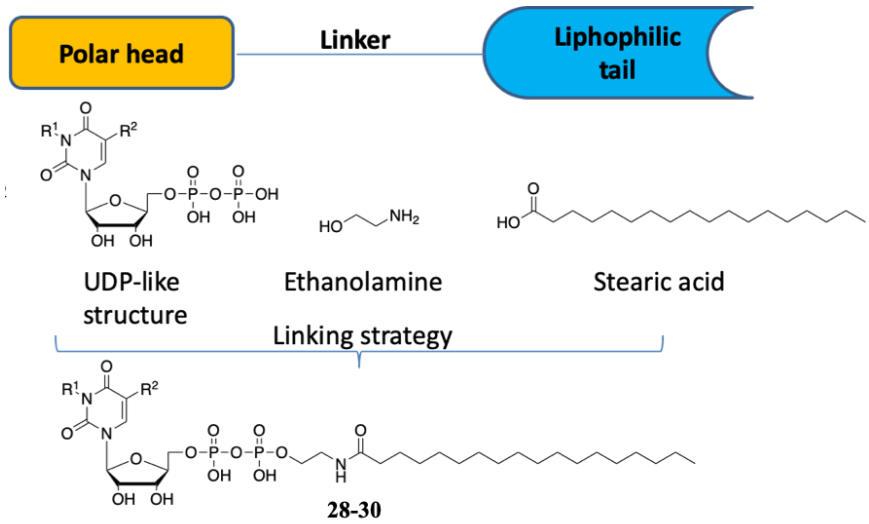

Figure 33. Design of stearic acid/$P2Y_6$ agonist conjugates **28-30**.

In this way, the strategy aims to create new chemical entities with a better profile in order to overcome the PK problems highlighted before. In fact, the new conjugates should be stable in the plasma and the increased lipophilicity would facilitate the brain penetration.[162] Moreover, once the conjugate will arrive in the target tissue, it would potentially become substrate of specific enzymes releasing the two molecules, able to exert their functions.[201]

To achieve this goal, we chosen to start with the UDP molecule as reference compound and two other UDP-derivatives. The first one is the well-known active compound synthesized in the lab. of Prof. Müller: 3-phenacyl-UDP, where in position N3 of the uridine heterocycle (R^1) a phenacyl group is present.[202, 203] The second derivative is a new UDP-derivatives that present in position 3 (R^1) a phenacyl group and in position 5 (R^2) an iodine atom. The rational modification in position 5 is due to the high activity and selectivity of compounds with halogen atoms in that position, particularly the iodine.[204]
Moreover, also the choice of the linker is not casual: ethanolamine will be used in order to create a phosphor-ester bond on the polar head part and an amide bond on the lipophilic tail side. In this way, as reported in literature, phosphor-ester bond result stable in different pH conditions avoiding a possible premature degradation (i.e. plasma hydrolysis) of the conjugates.[205]

4.3 Chemistry

In details, the designed synthetic strategy to obtain the target compounds was a convergent one. In one branch of the synthetic route the synthesis of the nucleotide scaffold has been investigated, while in the other part of the scheme the synthesis of the N-stearyl-ethanolamide intermediate has been performed.

The synthesis of the intermediate nucleotide has represented the main challenge of all the synthetic procedure. The synthesis started form the functionalization of the uridine in the position N3 adding a phenacyl group. The reaction proceeded in basic conditions and after column chromatography provided the desired compound in very good yield. The second step was the iodination in position 5 using iodine in acid conditions. The iodination is selective for the position 5 of the uracil ring, but the acid condition hindered the reaction, increasing the side products after 5 hours (Scheme 3).

Scheme 3. Preparation of UDP-like derivatives **31** and **32**.

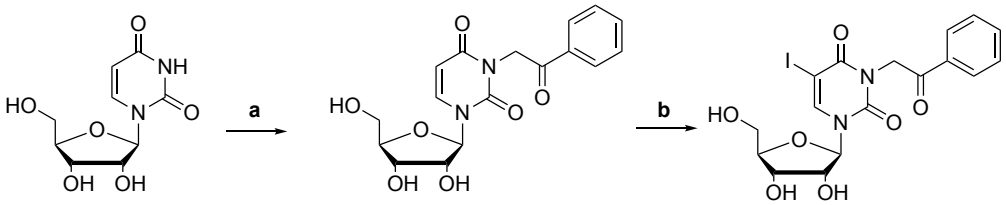

Reagent and conditions: a) K_2CO_3, DMF: Acetone (1:1), 120°C, 5h; b) I_2, HNO_3 (1 N), DCM, reflux, 5h.

Intermediates **31** and **32** were obtained, they were subjected to phosphorylation reaction, according to the Ludwig procedure (Scheme 4).

Scheme 4. Synthesis of uridine-nucleotide **33-36.**

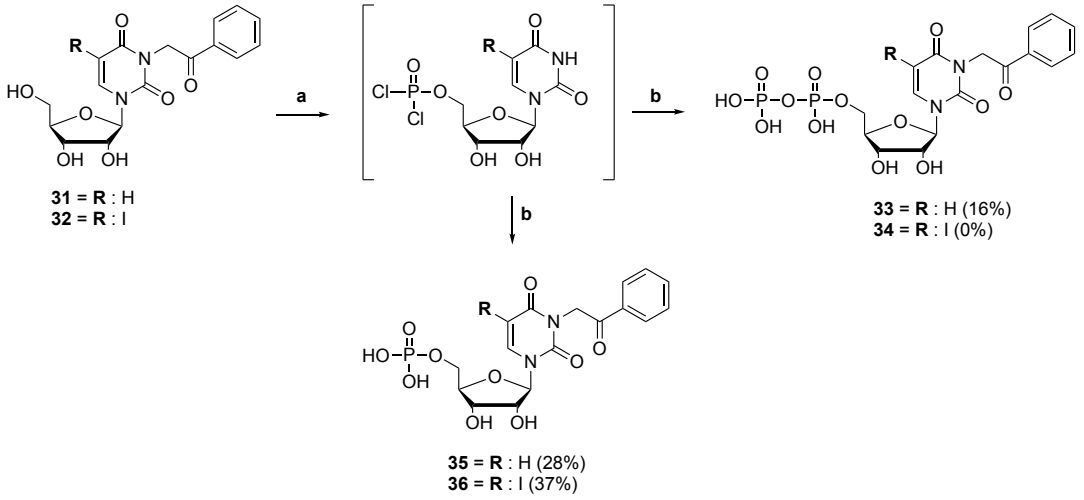

Reagent and conditions: (a) $POCl_3$, $(C_2H_5O)_3PO$, 1,8-bis-(dimethylamino)naphthaline, 0 °C, 5 h. (b) Two steps: (i) $(HNBu_3)_2HPO_4$, Bu_3N; (ii) (Et_3NHHCO_3), pH 7.4−7.6, H_2O, room temperature, 1 h.

The lyophilized nucleosides **31** and **32** were dissolved in triethyl phosphate and reacted with phosphorus oxychloride in presence of 1,8-bis-(dimethylamino)naphthaline, yielding the reactive 5′-dichlorophosphate intermediates. Those were immediately reacted with a mixture of tri-n-butylamine and bis(tri-n-butylammonium) phosphate in DMF to afford, after hydrolysis with triethylammonium hydrogencarbonate (TEAC), the desired nucleoside diphosphates (**33**, **34**).[202, 203] Unfortunately, the reaction of diphosphorylation of compound **34** did not work but stopped as monophosphates (**36**). Probably, the reaction was hampered by iodine impurity, making the color of the reaction violet. During the reaction most of the formed products are the nucleoside monophosphates (**35**, **36**) that were collected and purified. Particularly, **33**, **35**, **36** have been purified by anion exchange chromatography (FPLC condition: the column was washed with deionized water, followed by a solvent gradient of 5%−100% mM NH_4HCO_3 buffer (0.5 M) using approximately 1000 mL of solvent to elute the mono and diphosphates. Finally, to remove inorganic salts (inorganic phosphates and buffer) they were further purified by reverse phase high-performance liquid chromatography (RP-HPLC column Knauer 20 mm ID, Eurospher-100 C18; condition: the column was eluted with a solvent gradient of 0−40% of acetonitrile in 50 mM aqueous NH_4HCO_3 buffer for 30 min at a flow rate of 5 mL/min).

As it was not possible to obtain compound **34** using the Ludwig procedure, a new one synthetic procedure has been evaluated (Scheme 5). Unfortunately, also in this case the yield of the reaction was 0%.

Scheme 5. Alternative synthetic strategy to obtain **34**.

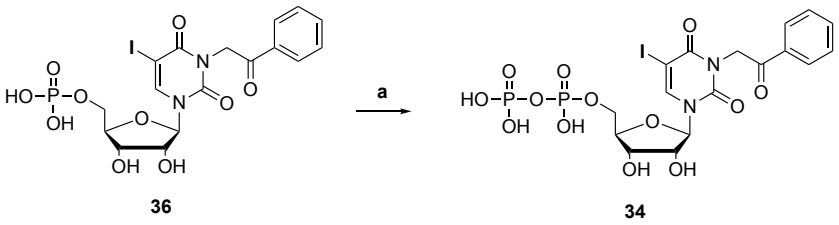

Reagent and conditions: (a) DIC, $MgCl_2$, DMF, $(HNBu_3)_2HPO_4$, 16 h, room temperature.

In parallel to the nucleotide synthesis, the lipophilic tail has been prepared, starting from stearic acid. To obtain the target intermediate **38** two strategies have been investigated (Scheme 6).

Scheme 6. Synthesis of N-(2-bromoethyl)stearamide (**38**).

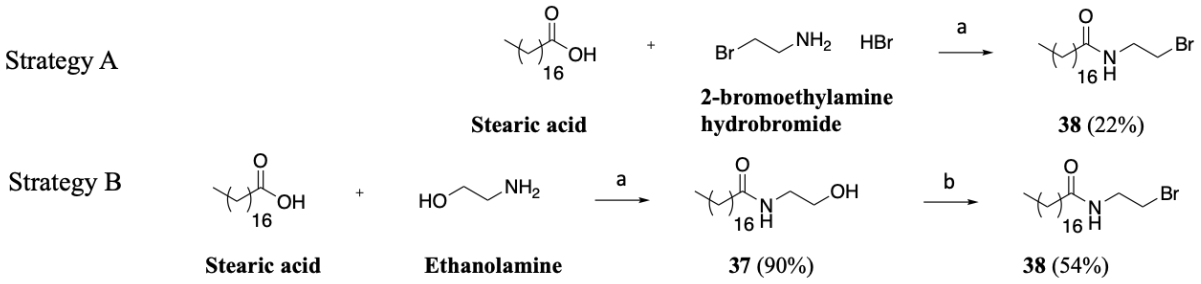

Reagent and conditions: a) Ethyl chloroformate, NEt_3, DCM, overnight, r.t.; b) PBr_3, DCM dry, Ar, overnight, r.t.

The first one synthetic strategy (A) involved a direct amidation reaction between stearic acid and 2-bromoethylamine hydrobromide, using several coupling reagents. Despite it seems an easy reaction, all the coupling reagent investigated in Table 3 did not work, except for TBTU and isobutyl chloroformate, with triethylamine (NEt_3) as base, obtaining the target compound in low yield (22%). However, also using ethyl chloroformate, this reaction not only provides the target intermediate, but also the derivative with chlorine as leaving group. These two molecules were impossible to separate (Table 3).

Table 3. Synthetic strategy (A) optimization.

Reagent	Base	Solvent	Temperature	yield
EDC/DMAP	/	DCM	r.t	0%
DCC	NEt_3	DCM	r.t and 45°C	0%
TBTU	NEt_3	DCM	r.t	15%
$SOCl_2$	NEt_3	DCM	r.t	0%
T3P	NEt_3	DCM	r.t	0%
Ethyl chloroformate	NEt_3	DCM	r.t and 45°C	Not quantified
Isobutyl chloroformate	NEt_3	DCM	r.t	22%

On the contrary, the second strategy (B) allowed us to obtain **38** in acceptable yield. Indeed, stearic acid has been reacted with ethanolamine, using ethyl chloroformate and NEt_3, obtaining the stearyl-ethanolamide intermediate (**37**) in very good yield (90%). Finally, **37** has been reacting with PBr_3 under anhydrous condition, obtaining the key intermediate **38** (with bromide as leaving group for the following reaction), in acceptable yield (54%).

The final reaction to obtain the target conjugates **28** and **29** is an alkylation at the beta-phosphate (nucleophilic substitution) between an alkyl bromide **38** and the commercially available UDP or **31** (Scheme **7**). As reported in literature this reaction proceeds only if the UDP-derivatives is converted in the tetrabutylammonium form, and if the reaction runs in DMF under strictly anhydrous conditions. Thus, all the starting material has been solubilized 12 h before in dry DMF and treated with molecular sieves 3Å to remove completely the water.[205]

Scheme 7. Synthesis of target conjugates **28**, **29**.

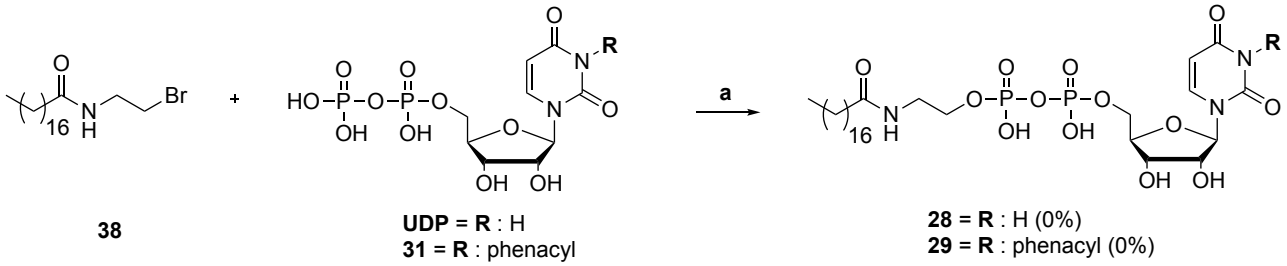

Reagent and conditions: a) NBu_3, DMF dry, Ar, 45°C, 24h.

After 24 hours of reaction a new molecule has been detected by TLC (eluent iso- propanol/ NH_3 25% H_2O/ H_2O = 6/3/1). The crude reaction has been purified first using FPLC followed by

RP-HPLC. Unfortunately, from micrOTOF-Q analysis the product obtained was not the target compound.

During my period at the University of Bonn I synthesized several intermediate compounds. In particular I obtained two nucleosides (**31**, **32**) three nucleotides (**33**, **35**, **36**) and an optimize synthetic protocol for the synthesis of compound **38**. Despite the reported reaction in the literature, the synthetic strategy proposed for the synthesis of compounds **28**, **29** results actually incomplete. As future outlook, the synthetic strategy to obtain the target compounds **28**, **29** will be modify taking inspiration from the papers publish from Prof. Chris Meier.[206, 207]

All compounds synthesize have been characterized by using analytical HPLC, 1H- and 13C-NMR, ESI-MS) (see Chapter 8) and have been included to the chemical library of Prof. Christa Müller.

Chapter 5

Project 3: Dual sustainable HDAC/ferroptosis inhibitors for the potential treatment of Alzheimer's disease

This project has been performed during a Short-Term Scientific Mission (STSM) funded by Epigenetics Chemical Biology (EpiChemBio.) COST ACTION (CM1406), in collaboration with the laboratory of the Prof. Philippe Bertrand of the University of Poitiers, France.

5.1 The global impact of Alzheimer's disease

AD is the most common cause of dementia worldwide and the most dominant neurodegenerative disorder, representing one of the most formidable challenges for drug discovery.[208] Since the first description by Alois Alzheimer in 1906 to the most recent knowledge of etiopathology mechanisms, an effective drug has not been developed yet, despite an ever-increasing global socioeconomic and clinical burden. [19, 208]

As for 2019, AD is the most common dementia in late life, and it is becoming increasingly common as the global population ages. The report edited by the World Alzheimer's Disease International reveals the results of the largest studies to dementia survey ever undertook with almost 50 million people in the world with dementia.[209, 210] Moreover, the number of people affected by AD is destined to increase form the actual estimates to 152 million people by 2050.[209, 210] These results derived from the increased life-expectancy in the developing countries with the consequence risk to be affected by aging diseases (i.e. AD) and from the absence of effective therapies. The current cost of the disease is about a trillion US dollars a year, and that's forecast to double by 2030.[209, 210] The estimates about the growth of AD population are dramatic. Particularly, between 2015 and 2050, the amount of older people living in higher income countries is forecast to increase by just 56%, compared with 138% in upper middle-income countries, 185% in lower middle-income countries (Figure 34).[211]

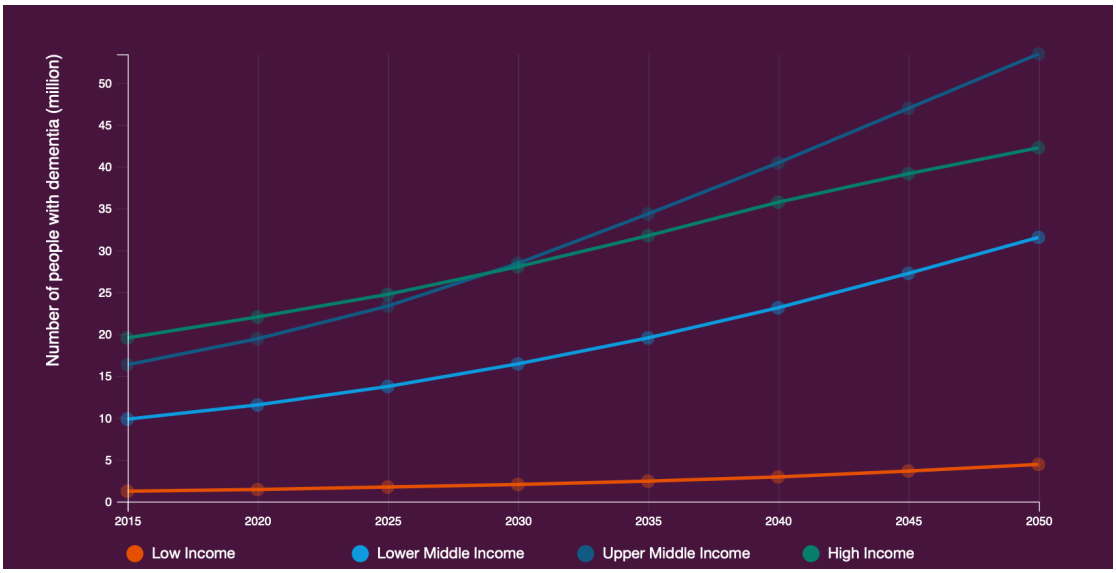

Figure 34. The growth of people with dementia (millions) in high income, upper-middle income, middle income and low-income countries.[211]

According to the World Bank 2019-2020 classification, the high-income countries are represented by a country with over US$12,375 Gross National Income per Capita, the Upper-middle income corresponds to a country with between US$ 3,996 - 12,375 Gross National Income per Capita, lower-middle income are represented by a country with between US$ 1,026 - 3,995 Gross National Income per Capita, and low income is equal to a country with less than US$1,025 Gross National Income per Capita.[212]

Low income countries tend to have a lower life expectancy, which reduces the possibility of dementia. In upper middle-income countries, life expectancy and populations are increasing, leading to a greater number of people with dementia compared with the high income countries.[211] This indicates that the future actors affected by AD will be the people living in the developing countries. The geographic picture of global dementia is more complex due to the considerable differences between countries in the same global region (Figure 35). The number of people with dementia is expected to rise more rapidly in Asia compared to the rest of the world due to the rapidly rising population growth rate and increasing life-expectancy.[209, 210]

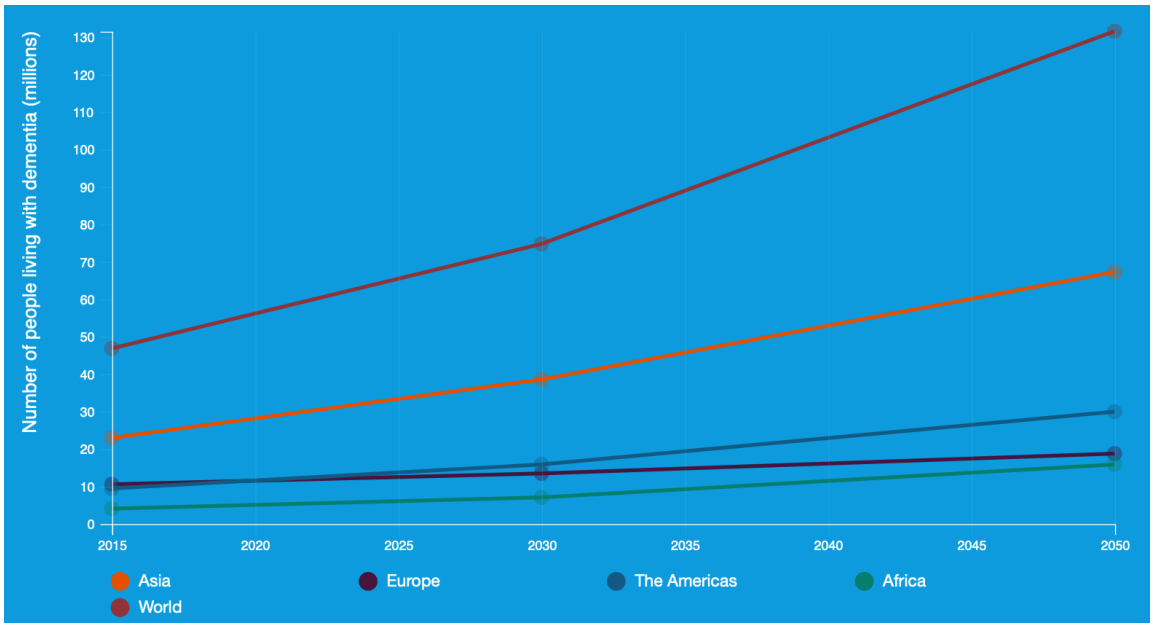

Figure 35. Geographical distribution of people with dementia (millions) in different counties.[211]

What clearly emerge from these data is that, if AD was initially thought of as the epidemic of the developed world, with its aging population, nowadays it particularly impacts middle- and upper-middle income countries.[205, 213] As a consequence of an increasing life expectancy, 62% of people with dementia already live in India, Brazil, and China, but by 2050 this will reach 71%.[210, 213] Therefore, AD emerges as a global tragedy, because it is actually incurable and also because the actual palliative treatments cost is too high to guarantee a universal coverage and equity of access of treatments to the global AD population.[214]

5.1.1 The cost of drug production

The drug production cost represents a problem for researchers and industries, but also for consumers. Several high profiles news stories have highlighted the exorbitant cost of pharmaceuticals.[215, 216] According to a recent study by Tufts Center for the Study of Drug Development, developing a new prescription medicine that gains marketing approval is estimated on average to cost 2.6 billion dollars.[45]

As highlighted earlier in the chapter, the frequency of cases of AD is increasing as such as the world's population ages and poses a major threat to the public health, especially for the developing countries. Among the drawbacks of the current AD scenario, one important issue is

the cost of the drugs. Indeed, the total costs of AD drug development program are estimated to be $5.6 billion, and the process takes 13 years from preclinical studies to approval by the FDA.[217] This cost results extremely high if compared with the estimated cost of cancer treatment development of $793.6 million per agent.[218] AD drug development costs significantly exceed the most estimates for drugs production compared to the other therapeutic areas. The most recent successful drug's example for the treatment of AD is Namzaric.[219] Namzaric is a fixed-dose combination of Memantine and Donepezil both hydrochloride (10 mg, 7 mg, respectively) and is marketed as extended release oral capsule. The cost is around 282 US dollar for a supply of 30 capsules.[219] Despite the palliative activity and considering the high drug cost and the chronic use for AD patients, it is an option for only a part of the global AD's problem.[219]

Unfortunately, all these events collectively (high drug development costs, a failure rate of about 99,6%;[18] and a failure rate of disease-modifying therapies of 100%), has led the big pharma to pull out of AD research.[220]

Despite these discouraging outcomes in the drug discovery and development area, the urgent need to address the socioeconomic crisis posed by AD requires a continued effort.

5.2 Food byproduct as a valuable resource for drug production

Despite the limitations and the persistent problems in the development of new drugs for the treatment of the AD, the research in this field should not stop. In parallel, the potential production of innovative low-cost and effective drugs, in order to bridge the persistent gap to access affordable medicines, represents the new challenge in drug discovery. In this context, a possibility is represented by the valorization of food byproduct material.[221, 222] Food byproducts are the raw-material obtained after various industrial food processing with a very low-economic value.[221] For the industries this raw-material is an important problem because it represents a potential source of pollution, a material prone to bacterial contamination, with a not very well-known chemical composition.[221] It also represents a logistic problem because of the accumulation, as well as an economic problem because of the disposal.[221] Therefore, the valorization of food byproduct, as low-cost starting material for the production of drugs or chemicals could be considered a revolution in the drug discovery field.[216] In addition, an innovative environmental ecofriendly process that allows the recycling of the food byproduct could affect the final cost of the product and facilitate the disposal process of the food byproduct.

Several examples can be found in the literature about the valorization of byproduct, and most of them are related to food- or plant-derivatives.[221, 222] Cashew nut-shell liquid (CNSL) is one of the most investigated case of a food byproduct obtained during the cashew nut industrial process. [221-223] Cashew (*Anacardium occidentale*) is a tree native to Brazil, and it was introduced to other parts of the world, such as Asia, Africa and South America.[223] Cashew is mainly grown for its nuts, which have a well-established market in the United States and European Union countries with a great variety of uses. The other product, cashew apple (fruit), is generally processed and consumed locally.[216, 223] During the cashew nut industry processing, tons of a dark viscous fluid, called CNSL, is obtained as a byproducts. The composition of CNSL is different and the concentration of the main components such as cardanol, cardol, anacardic acid and 2-methyl-cardol depends by the industry process (see Figure 36 for structures).[223] Natural CNSL, which is extracted by using cold solvents or mechanical extraction, contains anacardic acid (60–65%), cardanol (10–15%), cardol (20%) and traces of 2-methyl-cardol. On the other hand, technical CNSL is extracted by roasting the cashew nuts at higher temperature causing decarboxylation of most anacardic acid to cardanol as a major component (60–65%).[224]

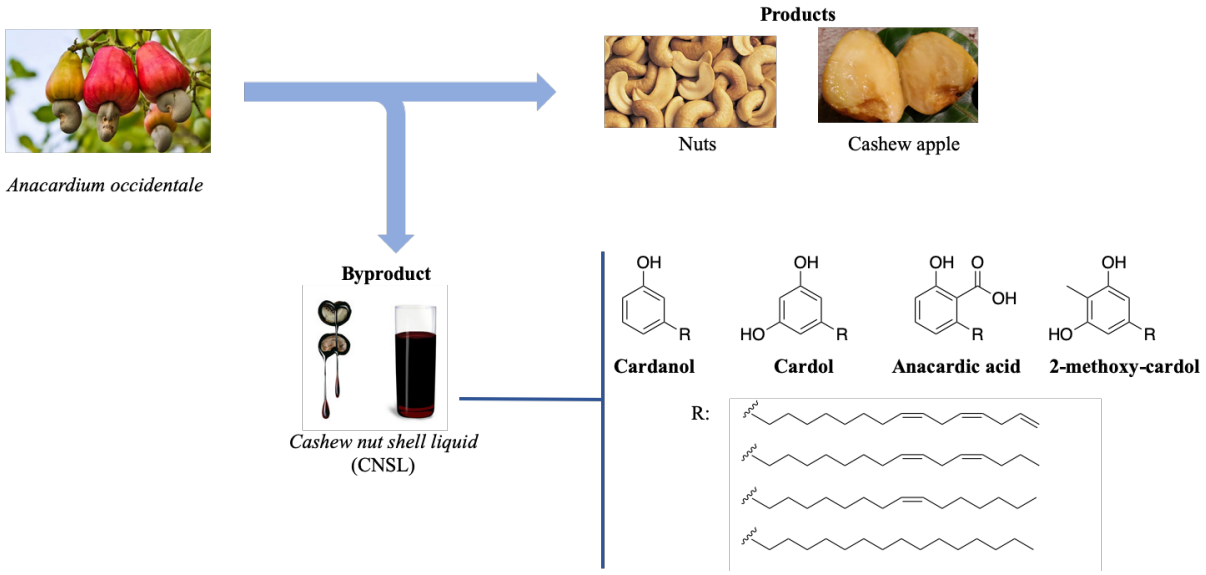

Figure 36. Cashew products and component of the CNSL.

Chemically, CNSL components are phenolic compounds with in *meta* position a fifteen-carbon linear chain with a varying degree of unsaturation, depending on the origin of the cashew nuts.[224] This peculiar amphiphilic structure leads the CNSL to be used for many applications.[223] Indeed, CNSL is used in the construction sector, laminating industry, foundry industry and in automobiles as resin for brake lining.[223] Pharmaceutical application might be another important use for CNSL. Indeed, emerging evidence suggests that all three CNSL constituents could be potent bioactive compounds with bactericide, fungicide, insecticide, anti-termite and molluscicide properties and with activity towards more serious disorders like cancer, oxidative damage and inflammatory diseases.[225] Based on that, very recently medicinal chemists have started to use CNSL components as starting material for the design and synthesis of new bioactive molecules (Figure 37).

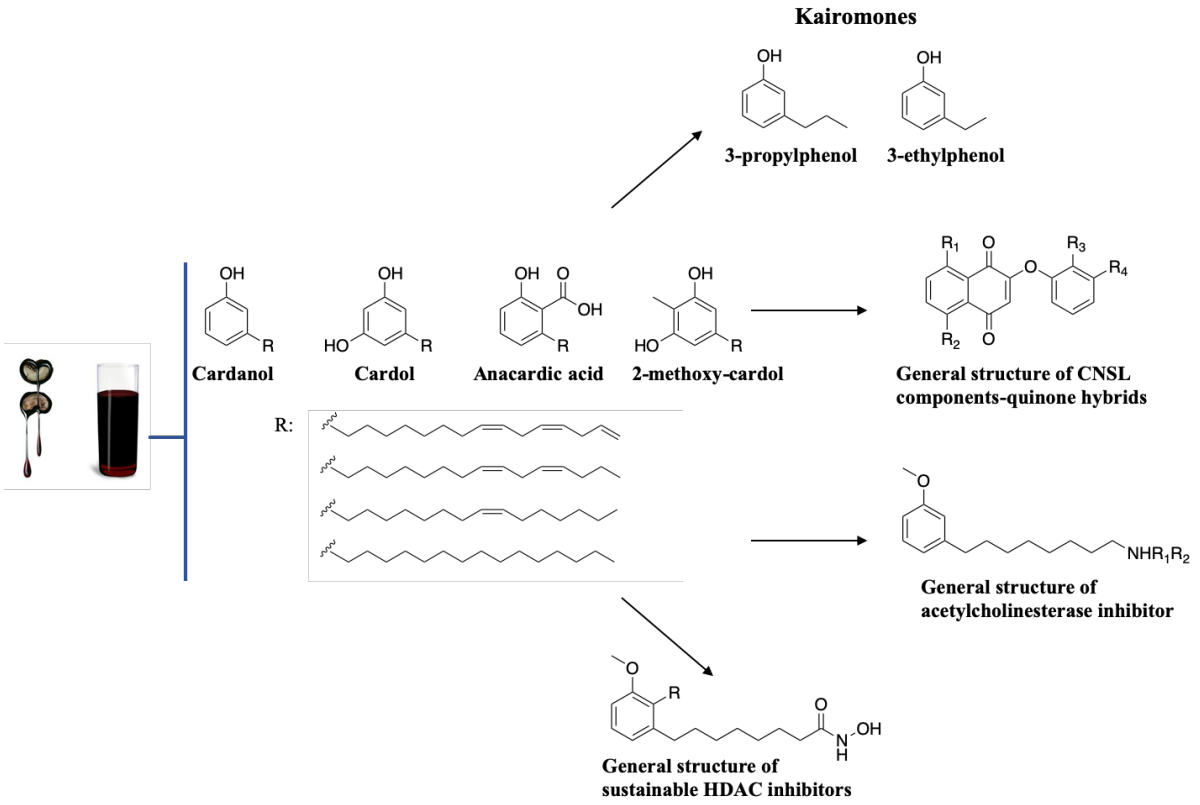

Figure 37. Examples of the use of CNSL components for pharmaceutical applications.

An example is the production of kairomones as attractors for tsetse flies.[226] Tsetse flies, the main vector of African sleeping sickness (trypanosomiasis), inhabit sub-Saharan Africa, the region where CNSL is predominantly produced (Nigeria, Ivory Coast, and Tanzania). Traps charged with the kairomones might be used as a sustainable and eco-friendly way to control the tsetse flies population.[226] Therefore, the synthesis of kairomones starting from the byproduct cardanol through a green chemistry approach might represent an important success in the fight against trypanosomiasis. [226]

Tsetse flies are the main vector of parasites such as: *Trypanosoma brucei rhodesiense* and *Trypanosoma brucei gambiense* responsible of Human African trypanosomiasis.[227] Human African trypanosomiasis is one of the most neglected tropical diseases, endemic in sub-Saharan Africa, but its diffusion in Mediterranean area (due to climate change and migratory flux) represents a risk for public health.[227] The actual anti-trypanosomiasis treatments suffer from toxic side effects, lack of efficacy, and development of multiple-resistance. Moreover, even though almost all control programs subsidize the cost of drugs and hospitalization, the development of new drugs based on inexpensive resources is a valuable approach to be pursued. Thus, the group of Professor Bolognesi in collaboration with Professor Romeiro synthesized a

series of sustainable CNSL components-quinone hybrids for the treatment of trypanosomiasis (see Figure 37 for general structure) .[227]

Another example of CNSL application has been the realization of potential drugs for the treatment of AD. Particularly, Professors Bolognesi and Romeiro have tightly collaborated at the realization of acetylcholinesterase inhibitors and histone deacetylase inhibitors (HDACi) for the treatment of AD.[228, 229] Both researches are focused on the functionalization of the long carbon-chain of CNSL compounds through the addition of functional groups able to interact with a target involved in the AD. Indeed, adding an amine or a hydroxamic function to the carbon chain has permitted to targeting efficacy the acetylcholinesterase and the HDAC enzymes, respectively (see Figure 37 for general structure).[228, 229]

Considering these examples, it is possible to understand how the use of food byproducts (i.e. CNSL) represents a valid alternative for the design and synthesis of bioactive molecules. Moreover, starting from a low-cost material, the molecules obtained could be represent examples of globally accessible drugs for the treatment of diverse diseases.

5.3 The current strategies for targeting Alzheimer's disease

As reported in Chapter 1, AD and other dementias represent the main challenge for drug discovery in terms of healthcare systems, research, drug-discovery infrastructures, drug development, and public policy.[230] Despite decades of study of basic biology of AD and significant pharmaceutical industry efforts to develop therapies, there is no effective therapy available to cure AD or to significantly inhibit the progression of the symptoms.[230] Only four drugs are currently approved and their utility is limited.

At the moment, the clinical trials AD situation results multifaceted because of the high number of different targets investigated.[19] The analysis of the therapeutic indication of the most promising drug candidates (phase 3) published by Cummings et al. 2019, shows 28 agents in 42 trials.[19] Among the 28 drug candidate, 61% (18 drug candidates) are proposed as diseases-modifying therapies and 32% anti-amyloid activity, 4% presented anti-tau activity, 4% presented anti-amyloid activity & anti-tau activity, and 21% presented other mechanisms of action such as anti-inflammatory, neuroprotection and antibiotic activity.[19] The remaining drug candidates are proposed as symptomatic cognitive enhancers (11%) and present different mechanisms of action such as neurotransmitter-based, and anti-oxidant, and drug candidates for the treatment of neuropsychiatric symptoms (28%, Figure 38).[19]

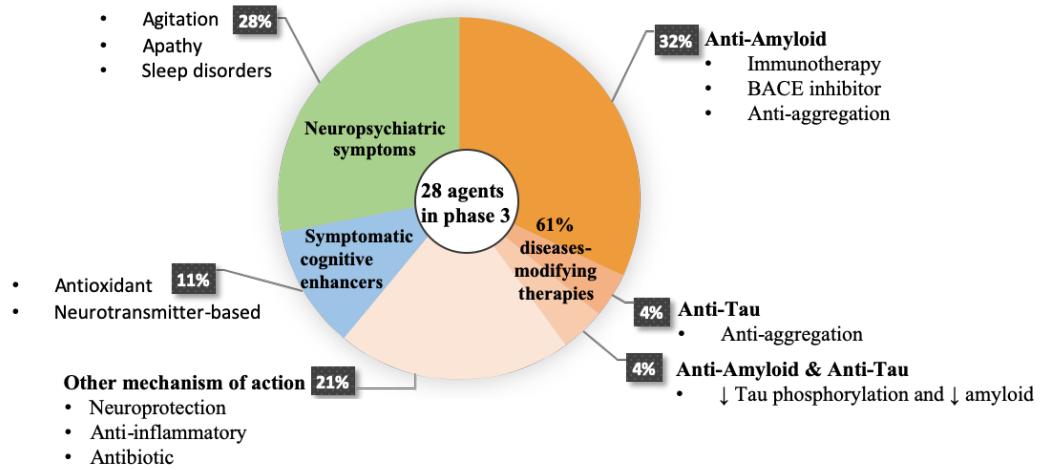

Figure 38. Mechanisms of action of agents in phase 3 (Source: Cummings et al. 2019).[19]

What comes out from this study is that the amyloid cascade hypothesis is the most investigated strategy for targeting AD, despite the number of failures collected.[231] In light of the enduring failures, the Alzheimer Drug Discovery Foundation (ADDF) has decided to not support anti-

amyloid projects.[232] However, different approaches have already been investigated for blocking the β-amyloid production such as: inhibiting β- or γ-secretases, increasing β-amyloid clearance with immunotherapy or using anti-amyloid aggregation therapy. Another investigated strategy is targeting the tau protein.[19] Neurofibrillary tangles are one of the primary histological marker of AD and are composed of tau protein.[233] Hyperphosphorylated tau leads to cytoskeletal disruptions along axons and consequence collapse of neuron structure.[233] A reasonable therapeutic approach would be to re-stabilize the microtubules to preserve neuronal health and axonal transport. To this aim different approaches are investigated such as: using tau anti-aggregation molecules or inhibiting the post transcriptional modification (hyperphosphorylation) by inhibition of glycogen synthase kinase 3β.[233] Other areas of interest include neuroprotection, inflammation, proteostasis, mitochondria and metabolic function, vascular function, epigenetics, APOE, synaptic activity and neurotransmitters, other aging target (e.g. senescent cells) and epigenetic.[232]

The sporadic nature of the AD, the differential susceptibility and disease course, as well as the late age onset and the influence of lifestyles, highlight that genetic causes alone fail to explain AD etiology and reinforce the hypothesis that epigenetics mechanism might play a main role.[234, 235] Several research suggest that targeting epigenetic mechanisms, namely, DNA methylation, histone acetylation/deacetylation, or noncoding RNA, may be of potential benefit in AD.[236] Particularly, restoring the perturbed acetylation homeostasis of the neurodegenerative state by histone modification has become one of the most significant research.[236] Indeed, if epigenetic treatments represent fewer than 2% of current drugs in Alzheimer's trials, ADDF considers this as an emerging area holding great expectation.[237] Two epigenetic drugs are currently in AD clinical trials: the HDAC inhibitor (HDACi) vorinostat (SAHA, NCT03056495) and nicotinamide (NCT00580931, Figure 39).

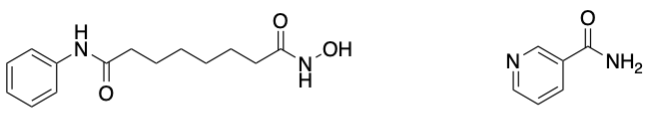

Vorinostat (SAHA) **Nicotinamide**

Figure 39. Chemical structures of HDACis in current clinical trials.

SAHA's target in AD are the class I histone deacetylases (HDACs) and HDAC6 (class IIb),[238] while nicotinamide is a selective inhibitor of class III HDAC proteins.[239] Actually, the trial with

nicotinamide has completed the phase 1, while the trials with SAHA is currently recruiting participants for the phase 1.

Among the strategies for targeting AD the cholinesterase persists inexorably. Even if ADDF has decided to not support new cholinergic therapeutic approaches,[232] this strategy remains the more prolific one, considering that the number of marketed drugs have acetylcholinesterase as target. Actually, the number of acetylcholinesterase inhibitors in clinical trials are three and are one in phase 1, one in phase 2 and one in phase 3, respectively.[19] Thus, the cholinergic strategy remain again a milestone to combat AD.

The complex cellular pathophysiological nature of AD, involving a causal and temporal sequence of Aβ aggregation, tau pathology, and neuroinflammation, is not fully understood. Unfortunately, this problem has caused the high failure rate of drugs in clinical trials, and has hampered the development of drugs for AD. Therefore, the challenge to find correct sequence of event and the correlated targets for the treatment of AD remains open.

5.3.1 Ferroptosis: a new target for the treatment of Alzheimer's disease

Such lack of effective treatments and the continued failures of clinical trials have inspired the investigation of new targets for the treatment of AD or repurposing and deeply investigate old hypothesis. Even if the dysregulation of brain metal homeostasis is one of the older hypotheses,[240] there is a renovated interest in this theory. From 2012, Stockwell et al. defined this dysregulation, which particularly involve the iron in the brain, ferroptosis, in order to better identify this pathologic condition.[241] More precisely, ferroptosis is a nonapoptotic, iron-catalyzed form of regulated necrosis that is critically dependent on glutathione peroxidase 4 (GPX4).[241] Ferroptosis is also a mode of cell death that involves the production of iron-dependent ROS, followed by accumulation of lipid hydroperoxides to lethal levels.[241] Moreover, abnormal iron level in the brain can also interact with several metal-binding proteins (such as Aβ peptide or neuromelanin) that lead to oxidative stress. These have recently emerged as important potential mechanisms in brain ageing and neurodegenerative disorders.[240]

In healthy brain, iron plays a fundamental role in maintaining several biological functions, which includes oxygen transport, mitochondrial respiration, cell growth and differentiation, as well as the active site of metalloenzymes.[242] The biological function of iron is linked to its redox

potential, which allows the reversible transition from the ferrous (Fe^{2+}) to the ferric (Fe^{3+}) state, thus catalyzing electron-transfer reactions.[243] However, the same redox chemistry process can trigger deleterious reactions with oxygen and hydrogen peroxide leading to the formation of ROS and RNS via Haber–Weiss and Fenton chemistry.[243] Thus the iron homeostasis is finely regulated by keeping its levels less to toxic threshold and chelated in safe environment as within metalloproteins.[243]

Iron accumulation or dysregulation in several brain regions, as well as aging, is considered one of the common starting event for several neurodegenerative disorders.[244]

The mechanism of ferroptosis is recently defined as an iron-dependent form of cell death, which is distinct from apoptosis, necrosis, autophagy, and other forms of cell death, with different morphological, biochemical, and genetic criteria.[241] Ferroptosis involves metabolic dysfunction that results in the production of both cytosolic ROS and lipid peroxidation by mitochondria independent patways.[241, 244] The main feature of ferroptosis is the accumulation of iron-induced lipid peroxidation, the depletion of glutathione (GSH), and inactivation of the phospholipid peroxidase glutathione peroxidase 4 (GPX4), creating a dysregulation redox process triggering cell death.[241, 244] The mechanism of ferroptosis has been for the first time identified through serendipity by researchers during the screening of antitumor agents.[245] Indeed, from this screening the molecule erastin emerged as a molecule with a completely new profile to induce cellular death (Figure 40). [241, 244] Following erastin, other molecules (such as RSL3 and RSL5) have been identified as triggering new cellular death profiles (Figure 40).[246]

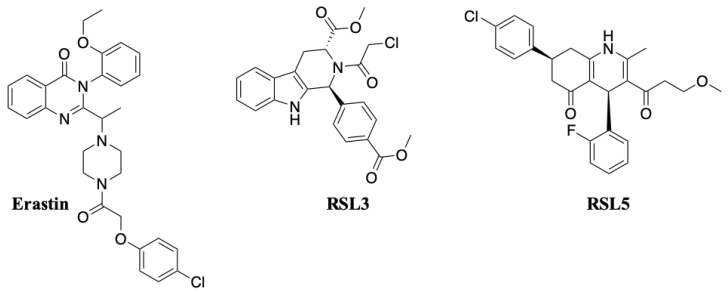

Figure 40. Chemical structure of erastin, RSL3 and RSL5.

Even if the mechanisms of action of erasitin and RSLs are different, they share common ferroptosis features, such as iron, MEK, and ROS dependence.[244, 247] Indeed, erastin acts by depleting glutathione (GSH), inhibiting GPXs and targeting the voltage-dependent anion channels 2 and 3 (VDAC2/3).[247] RSL's mechanism has been for long time unknown because it

is not dependent by VDAC2/3 and the level of GSH after insult with RSLs remains unaffected.[247] Only in the 2017, the common mechanism of erastin and RSLs to induce ferroptosis has been disclosed.[247] Indeed, by inhibiting the isoform 4 of GPX enzymes, resulting the cell death has been found to be different compared the other well-known forms of cell death.[247]

Therefore, a renewed interest about metal-dysregulation conditions, particularly iron, opens a new direction for AD drug discovery.[248, 249] Consequently, the research of new molecules as ferroptosis inhibitors could represent an innovative strategy for the researchers. The first molecule identified as ferroptosis inhibitor was ferrostatin-1 (Fer-1). [241] This molecule derived from the screening of 3,372,615 commercially available compounds that were filtered in silico on the basis of drug likeness and solubility. Fer-1 resulted as the most potent inhibitor of erastin-induced ferroptosis in HT-1080 cells (EC_{50} = 60 nM).[241] Although the exact mechanism of action of Fer-1 is unknown, the same ferroptosis inhibition evidence has been obtained by using deferoxamine (an iron chelating agent) after insults by erastin (Figure 41).

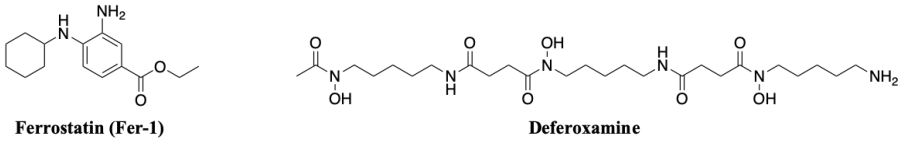

Figure 41. Chemical structure of ferrostatin-1 (Fer-1) and deferoxamine.

Novel inhibitors derived from Fer-1 are currently designed and synthesized with the aim of increasing the potency and improving several critical issues such as solubility and stability.[248, 249]

In conclusion, despite the pathological mechanisms of the process remain not completely clear, as well as the mechanism of action of Fer-1, ferroptosis represents a potential new strategy for targeting AD.

5.4 Design of dual sustainable HDAC/ferroptosis inhibitors

The world-wide AD impact, and its future impact in the developing countries is considered the most formidable challenge in the drug discovery field (see chapter 5.1). In particular, the interest to produce globally and eco-sustainable AD drugs, starting from inexpensive resources, is one of the most important future challenges. CNSL is a food byproduct produced in tons during the cashew nut processing. This dark viscous fluid is composed by long-chain phenolic compounds with innate multitarget mechanisms of action, which could become innovative molecules with potential applications for the treatment of AD.[229] In addition to this, the structural homology between CNSL components (cardanol) and the capping group of SAHA, as well as the recent studies showing an improvement in memory and cognition in SAHA-treated animal models, caught our attention (Figure 42). [238]

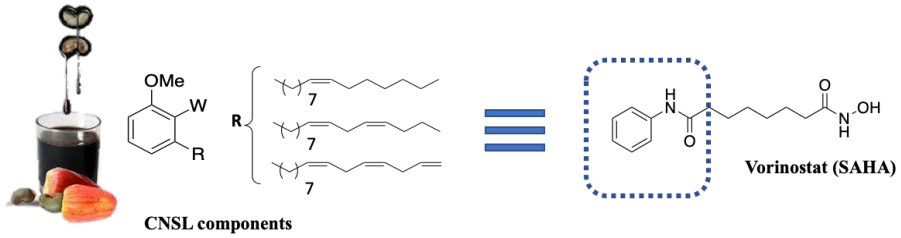

Figure 42. Structure homology between CNSL derivatives and SAHA.

Thus, during a visit in the laboratory of Prof. Bertrand, we focused in the design and synthesis of a small library of accessible and sustainable multitarget compounds obtained by combining the CNSL derivatives (cardanol derivatives), as capping group, with different zinc-binding group in order to obtain AD drugs from CNSL.

The designed molecule can act as dual, sustainable HDAC/ferroptosis inhibitors (**39-46**). Particularly, these molecules could act as multitarget molecules able in principle to simultaneously inhibit the HDAC enzymes and inhibit the ferroptosis condition.

In detail, the small library of compounds **39-46** are derived from cardanol, an inexpensive resource, linked with several zinc-binding groups (Figure 43).

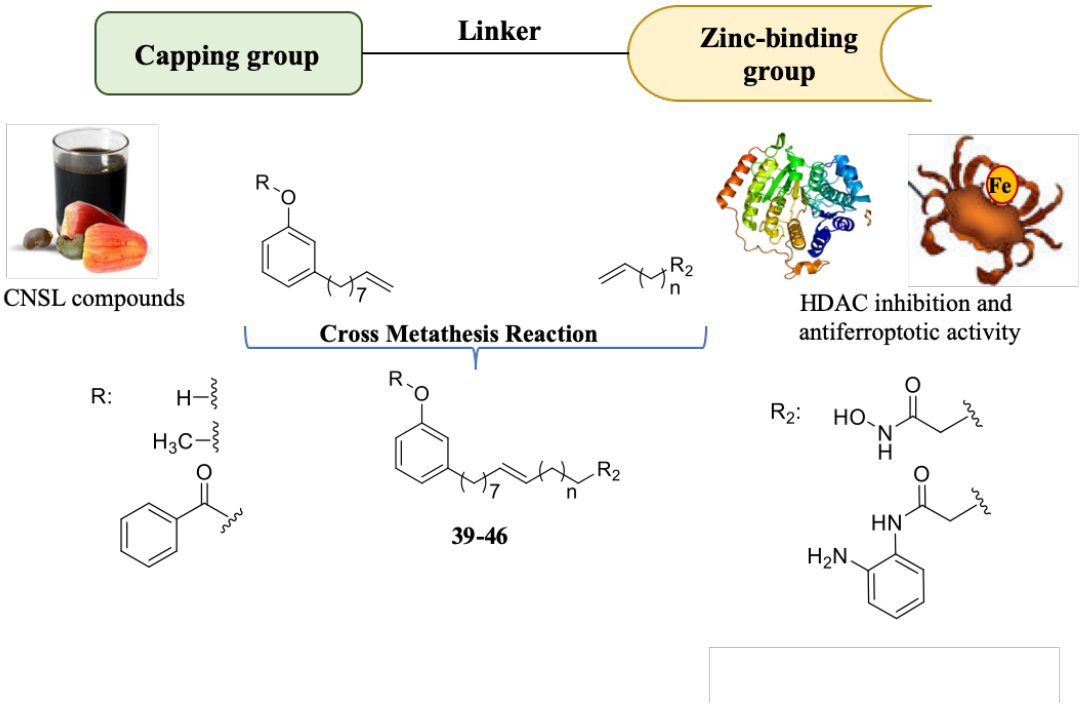

Figure 43. Cross metathesis design strategy for the synthesis of dual, sustainable HDAC/ferroptosis inhibitors.

The role of the two main functional groups in these molecules is very peculiar. Indeed, the zinc-binding group have a dual role: the first one will be the interaction with the zinc present in the HDAC enzyme, permitting interaction and consequent inhibition, and the second will be the potential metal chelating activity against iron, zinc and copper responsible of the oxidative stress and potentially ferroptosis. Moreover, a very recent study has highlighted how HDACis can protect neurons from ferroptosis induced by erastine.[250, 251] Thus, the concomitant interaction with both biological targets can synergistically act on AD models.

In addition, the capping group could be an important function to obtain different selectivity profiles among the different HDAC isoforms. For the design of compounds **39-46**, we considered particularly effective the strategy to link the capping group derived from cardanol and the zinc-binding groups through the cross-metathesis reaction. Cross metathesis reaction is an optimal way for this type of purposes, because it allows to easily join two pharmacophore functions via formation of carbon-carbon double bond. The cross metathesis synthetic strategy developed by Prof. Bertrand has been exploited to easily provide the target compounds **39-46**.

5.5 Chemistry

In details, the synthetic strategy to obtain compounds **39-46** was a convergent starting from the cross-metathesis reaction between capping group derivatives **47-49** (Figure 44), and different Boc-protected hydroxamate and benzamide **50** and **51.**

The starting cardanol mono-ene derivatives **47-49** have been provided by Prof. Romeiro from the University of Brasilia, while the characterization via ^{1}H-NMR, ^{13}C-NMR, and GC-MS was accomplished by us.

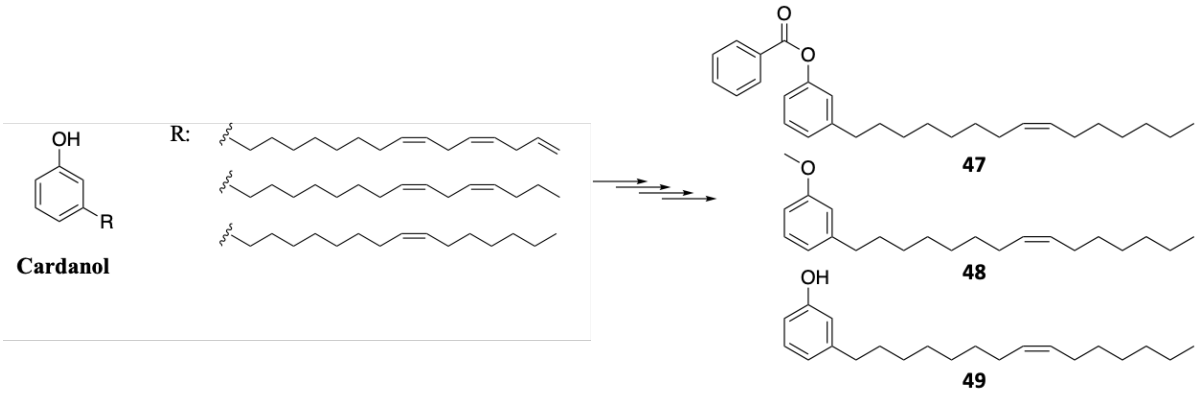

Figure 44. Structure of cardanol mono-ene derivatives (**47-49**).

The zinc binding groups (**50, 51**) were obtained by protection of hydroxylamine and N-phenylenediamine with Boc_2O, followed by pentenoylation with pentenoyl chloride, affording compounds **50** and **51**. The zinc binding groups were already present in the laboratory of Prof. Bertrand (Scheme 8).

Scheme 8. Synthetic procedure to obtain protected zinc binding groups (**50**, **51**).

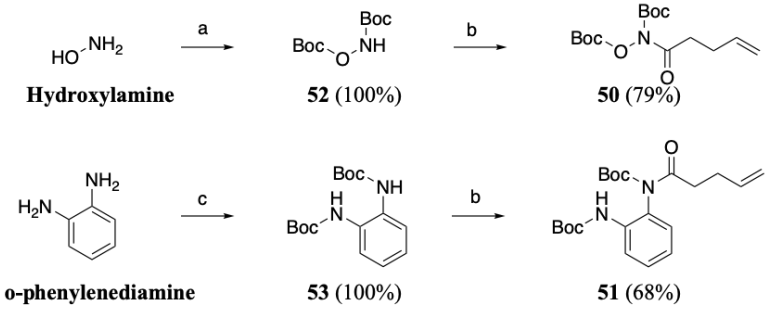

Reagents and condition: a) Boc_2O, triethylamine, petroleum ether/ Tert-butyl methyl ether (4/1); b) Pentenoyl chloride, pyridine, DCM; c) Boc_2O, THF; d) Triphenylmethanethiol, K_2CO_3, CH_3CN.

To verify the effectiveness of the cross-metathesis reaction, we have performed some cross-metathesis reaction models. The cross-metathesis reactions were performed using Grubbs catalyst between two terminal double bonds. The mechanism is a [2+2] cycloaddition between an alkene double bond and a transition metal alkylidene (Ru, Mo, W) to form a metallocyclobutane intermediate. A second alkene double bond will recruit obtaining the desired a transalkylidenation compounds. (Figure 45).

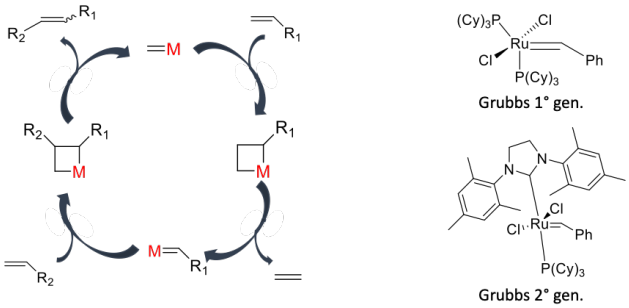

Figure 45. Catalytic mechanism of cross-metathesis reaction and structures of some Grubbs 1° and 2° gen. catalysts.

Most of the cross-metathesis have been performed between terminal double bond, but in our case starting from non-terminal double bond reagent could hampered the reaction, thus we perform a series of reaction models (scheme 9).

Compounds **47** was reacted with Grubbs 1° gen. catalyst, in order to obtain the symmetric cross metathesis products **54**. At the same time, compound **49** was reacted with the zinc-binding group **50** to obtain the intermediate compound **55**. These two cross-metathesis reaction models have allowed us to understand that: i) the cross-metathesis reaction between non-terminal double bond compounds works, and ii) the presence of free-phenoxy group hampered the reaction, which has been necessary protect the phenolic group of compound **49** as benzylic ether derivatives (**56**), otherwise the cross-metathesis reaction did not work.

Scheme 9. Cross metathesis reaction models, and benzyl protection of compound **49.**

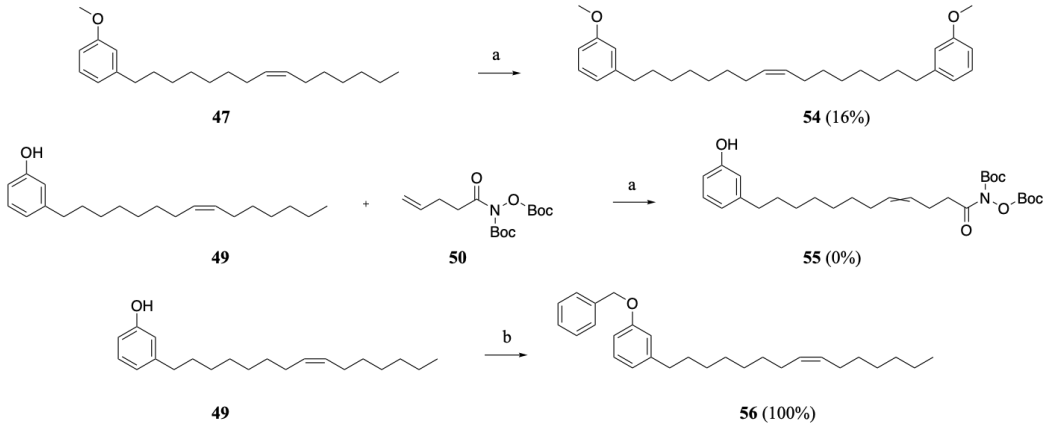

Reagents and condition: a) Grubbs 1° gen. (0,5ml/h), DCM, 7h, reflux; b) Benzyl bromide, K_2CO_3, DMF, 12h, room temperature.

Considering the positive results observed in the cross-metathesis reaction models, we began to synthesize the small library of compounds **39-46**.

The synthetic strategy starts with the cross-metathesis among the capping group **47**, **48**, **56** and the zinc-binding group **50**, **51** (Scheme 10). In particular, Grubbs 1° gen catalyst has been used to join the capping group **47**, **48**, **56** with the zinc-binding group **50** and the 2° gen. catalyst for the compounds **51**. These reaction conditions are necessary otherwise, as reported from the literature, that benzamide zinc-binding group do not react with the Grubbs 1° gen. catalyst.[252, 253] Moreover, the cross-metathesis reaction was performed with an optimized continuous catalyst injection protocol used to obtain good yields (20%-47%) of the Grubbs 1° and 2° gen. at 7.5% mol (flow injection 0.5 ml/h).[252, 253] From the cross-metathesis reaction has been obtained the intermediate compounds **57-62**. The intermediate compounds were obtained in very good yields after purification of the crude reaction mixture by gradient column chromatography (pentane/AcOEt, 100/0, 95/5, 90/10). The compounds **57-62** were obtained as a mixture of isomer E/Z, in light of the non-stereoselectivity reaction protocol.

Scheme 10. Synthetic strategy to obtain hydroxamic and benzamide derivatives (**39-46**).

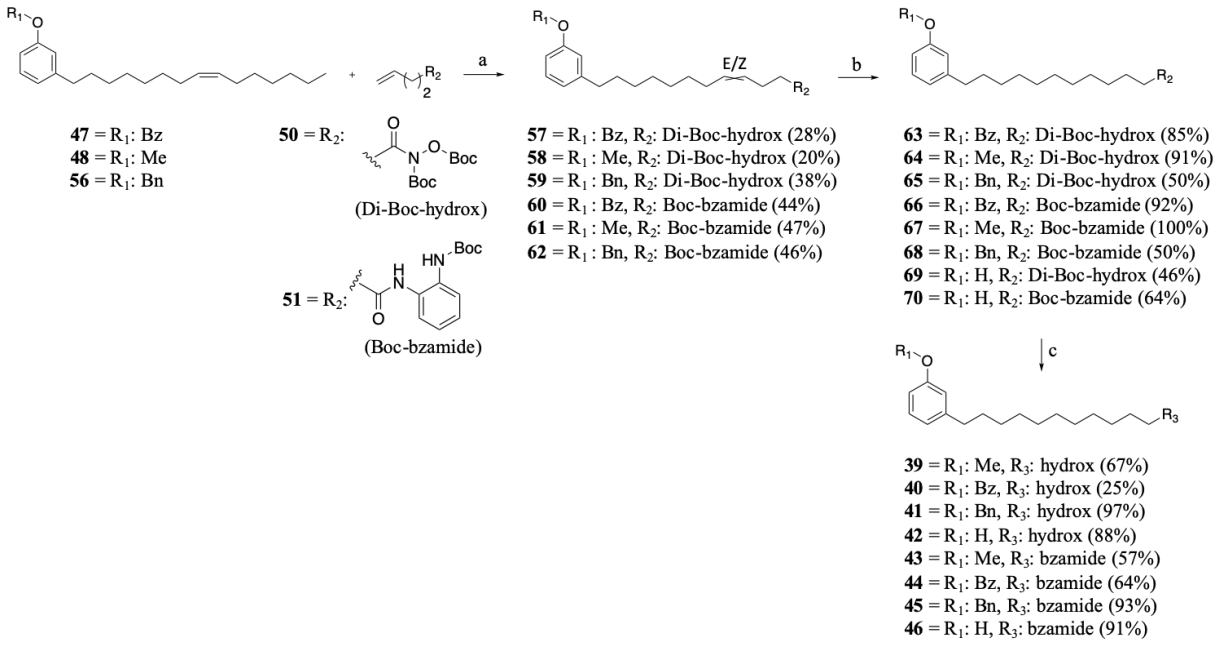

Reagents and condition: a) Grubbs 1st or 2nd gen. catalyst (0,5ml/h), dry CH_2Cl_2, reflux, 8 h; b) H_2, Pd/C, 5%, AcOEt, 3h; d) Trifluoroacetic acid, CH_2Cl_2, 2h, room temperature.

The second reaction step was the reduction of the intermediate compounds **57**-**62**. The reduction reaction was performed using H_2, Pd/C 5% for 3h at room temperature and the crude was purified only filtrating on silica the catalyst from the reaction mixture. In this way was obtained the intermediate compounds **63**-**70** in very good yields (50%-100%). Moreover, starting from compounds **59**, **62** and monitoring the reaction every 30 minute by H-NMR, allowed us to get four more compounds: **65**, **68**-**70**. Particularly, the intermediates **59** and **62** are two benzylated derivatives with the double bond in the carbon chain and during the reduction reaction is possible to observe the complete reduction of the double bond on the carbon chain and also the partial de-benzylation of the starting compounds. In this way, after 1.5h of reaction we isolated from compounds **59** the products **65**, **69** (respectively 50%, 46%), while for compound **62** the products **68** and **70** (respectively 46%, 22%).

The last reaction step was the deprotection of the Boc-group of the capping group by trifluoroacetic acid in DCM at room temperature for 2h obtaining the final compounds **39**-**46**.

All compounds synthesize have been characterized by using analytical HPLC, 1H- and 13C-NMR, ESI-MS) (see Chapter 8).

5.6 Results and discussion

5.6.1 Neurotoxicity assay

A preliminary neurotoxicity screening has been performed on compounds **39-46**. At the concentrations of 10 μM, each compound has been tested for evaluate their cytotoxicity against human cell neuroblasts (IMR-32) using MTT assay. All the tested compounds showed no significant neurotoxic effect, except for compounds **39** (Figure 46). This assay has been performed in collaboration with the group of Prof. Fato of the University of Bologna.

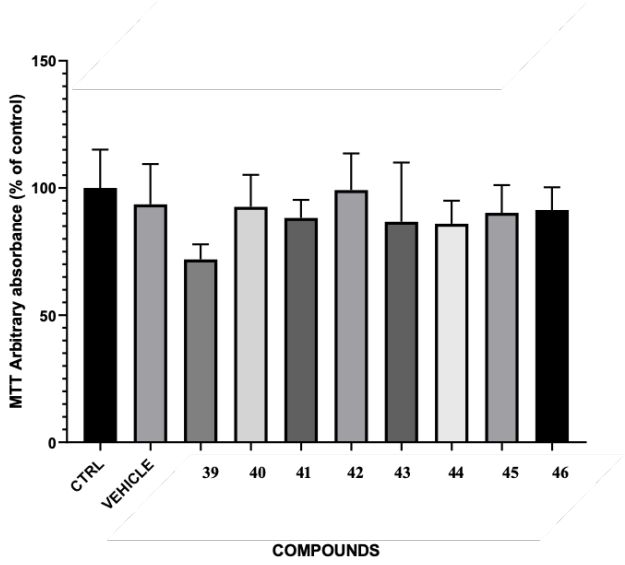

Figure 46. Effect of compounds **39-46** on cell survival/death through MTT assay in IMR-32 cells at the concentrations of 10 μM for 24h.

5.6.2 Hepatotoxicity assay

In a parallel assay, we evaluated the hepatotoxicity of **39-46** by MTT assay Hep G2. The assay has demonstrated no significant hepatotoxicity effect through at the concentrations of 10 μM. (Figure 47). This assay has also been performed by the group of Prof. Fato.

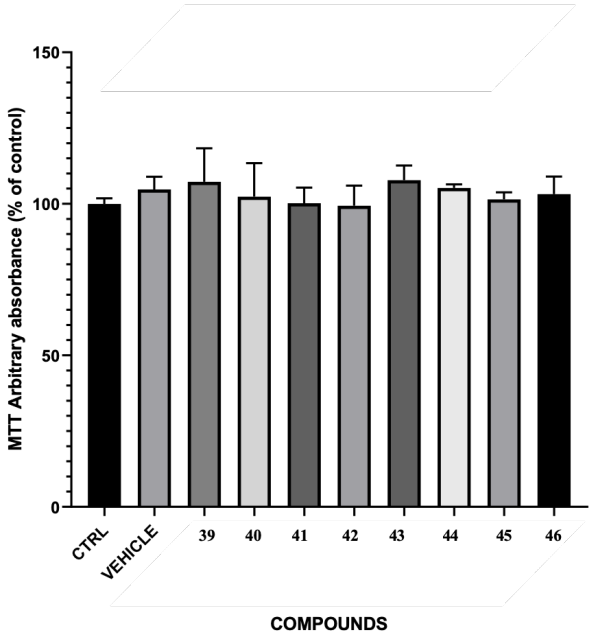

Figure 47. Effect of compounds **39-46** on cell survival/death through MTT assay in HepG2 cells at the concentrations of 10 μM for 24h.

5.6.3 Global HDAC inhibition in cells by BRET assay

In order to evaluate the HDAC inhibition profile of compounds **39-46**, a bioluminescence resonance energy transfer (BRET) has been used. The luminescence being obtained directly in living cells transfected with a histone H3 tagged with a yellow fluorescent protein (YFP) and a bromodomain tagged with *Renilla Luciferase* protein. The treatment with an HDACi permits the interaction of the two complex and the consequence energy transfer from the YFP to the *luciferase* indicating the degree of acetylation in the system using an HDACi. The BRET signal was expressed in milliBRET units (mBu), and the intensity of the signal is directly correlated with the potency of the inhibitor used (Figure 48).

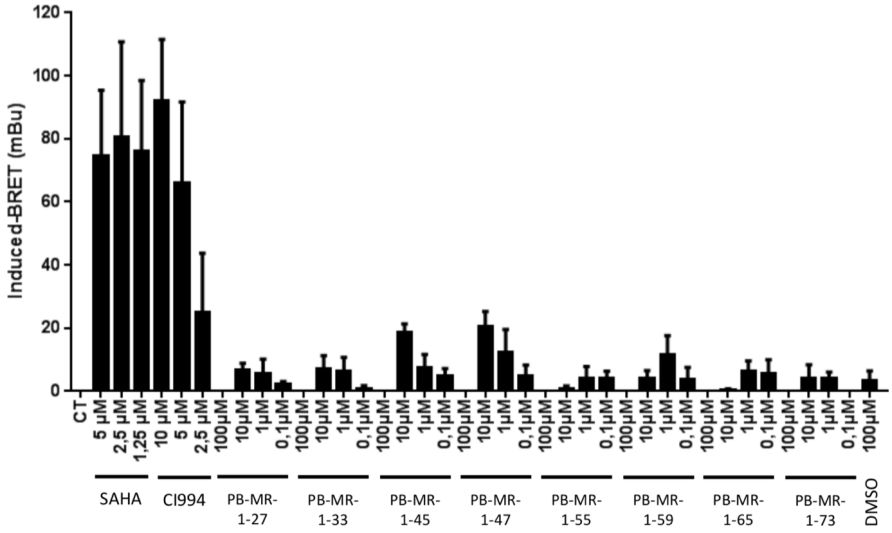

Figure 48. Histone H3 acetylation BRET assay of compounds **39-46** at different concentrations.

Unfortunately, all of the tested compounds present a very low activity compared to the reference compounds used (SAHA and CI-994) at all concentration. Probably, the lack of activity could be due to the longer linker, formed during the synthesis, between the capping group and the zinc binding group that could hampers the interaction with the enzyme. Another reason for the lack of activity could be the low permeability of the compounds in the nucleus of the cells.

This assay has been performed in collaboration with the group of Prof. Blanquart of the University of Nantes. Actually, the molecules **39-46** are under evaluation to analyze their ferroptosis inhibitor profile using the erastin model proposed by Prof. Stockwell,[244] the BBB permeability assay and the HDAC6 inhibitor profile.

Chapter 6

Project 4: Cashew nut-shell liquid-derived compounds/tacrine hybrids as sustainable multitarget hybrids for the treatment of Alzheimer's disease

The following project has been developed by Stefano Perna and Carlo Faggiotto, two graduate students in Chemistry and pharmaceutical technology at the University of Bologna, under my direct supervision. Moreover, also for this project, the CNSL-derived compounds have been kindly provided by Prof. Luiz Antonio Soares Romairo of the University of Brasilia.

6.1 The cholinergic strategy to combat Alzheimer's disease

As briefly highlight in the paragraph 5.3 "The current strategies for targeting Alzheimer's Diseases" the cholinergic strategy still remains a validated strategy for the treatment of AD. Even if also this strategy suffers of the famine of new drugs that infected all the AD drug discovery process. Indeed, the younger AChE drug inhibitor synthesized was galantamine in the 2001.

Historically, the aim of the cholinergic strategy was the design and synthesize drugs able to interact with AChE in order to repristinate the cholinergic tone lost in AD patients.[254] During the last 20 years it is emerged that the isoform butyrylcholinesterase (BuChE),[255] also belong to the cholinesterase family of enzymes, could play a role in acetylcholine regulation and in the cholinergic signaling, representing a good target for the treatment of AD.[255] Indeed, the two enzymes isoforms are extraordinarily efficient and they are able to hydrolyze more than 10000 acetylcholine molecules per second.[256] Acetylcholine is the specific substrate of AChE and it is found in high concentrations in the post-synaptic neuron in the brain, while BuChE is not-specific and is widely distributed all over the body.[257] In a healthy brain, the AChE enzyme dominantly hydrolyze the acetylcholine in acetate and choline, while BuChE plays only a minor role during the regulation of the cholinergic tone. The two enzymes display diverse kinetic characteristics depending on acetylcholine concentrations.[258] At low acetylcholine concentrations, AChE's activity becomes highly dominant, while BuChE is more efficient in the hydrolysis at high acetylcholine concentrations.[257] Initial studies underestimated the importance of BuChE in human brain owing to its low expression.[258] However, other studies have demonstrate the importance of BuChE within the nervous system to be pivotal in the late stages of AD.[259] Indeed in patients with AD, BuChE activity progressively increases, while AChE activity remains unchanged or decreased.[259, 260]

The two enzymes AChE and BuChE share nearly 65% sequence homology.[261] Both enzymes present similar binding sites: the active site on the bottom of the gorge with the catalytic site

and the peripheral anionic site (PAS) situated at the entry of the gorge for AChE and several peripheral aromatic site for BuChE.[261] The main difference between the structure of these two enzymes is situated in the acyl-binding site, which accommodates the acetylcholine moiety. In detail, two bulky amino acids (Phe) in AChE are replaced with two smaller amino acids; Val and Leu, which allows BuChE accommodate large and chemically different molecules. [257, 261] However, the active site of both enzymes is built of two subsides: the first one is the catalytic anionic site (CAS) where the acetylcholine moiety is stabilized by Trp-Glu-Phe (or Val-Leu instead of Phe in BuChE), while the second subsite is present in the catalytic triad made of Ser–His–Glu which hydrolyzes acetylcholine. [257, 261]

Thus, targeting the BuChE in order to ameliorate the condition of AD patients represent a valid alternative in the field of AD drug discovery. Indeed, over the course of the disease, the concentration of AChE sometimes decreases by 85%, whereas the levels of BuChE were found to be stable and could influence the aggregation of Aβ, the main component of the amyloid plaques found in the brains of AD patients.[259, 260] Therefore, the possibility to design new molecular scaffold able to inhibit not only the AChE but also the BuChE represent a validate strategy in the AD drug development.

6.1.1 Tacrine hybrids: an old but gold medicinal chemistry strategy

The cholinergic hypothesis was defined over 40 years ago as the first AD hypothesis.[262] The damage of the cholinergic neurons is observed in the hippocampus, amygdala, frontal cortex, and other structures responsible for learning, memory, or conscious awareness.[263] Has been observed in cholinergic neuron that the main change was related to the choline uptake, impaired acetylcholine release, and deficits in the expression of nicotinic and muscarinic receptors. Indeed, the low levels of acetylcholine results in the cognitive impairment and memory problems that occur decades after the beginning of the neurodegenerative process.[263]

Currently, the most popular treatment for AD is using inhibitors of AChE. Tacrine was the first AChE inhibitor drug (IC_{50} = 500nM)[87] approved by the FDA in 1993, but after 5 years, it was withdrawn from the market because of its hepatotoxicity caused by the stimulation of ROS production and glutathione depletion.[264] Despite these side effects, tacrine still remain a simple drug to synthesis, with a good inhibitory activity, and potential to attenuate Aβ-induced neurotoxicity.[265] Thus, tacrine and its derivatives 6-chlorotacrine (6-Cl-THA, IC_{50} = 7.18nM)[87]

and 7-methoxytacrine (7-MEOTA, IC_{50} = 10500nM)[87] (Figure 49) are still widely investigated by the researchers worldwide, especially for the design and synthesis of MTDLs for AD treatment. The 6-Cl-THA even if was more potent, results more hepatotoxic compared to tacrine, while the 7-MEOTA resulted more safer compared the two congeners but with a very low inhibit activity.[266] Several examples are reported in literature which, tacrine or its derivatives, are used as substrate in order to obtain hybrids with improved biological profile compared the starting tacrine and its derivatives and with less side effects.[265, 267]

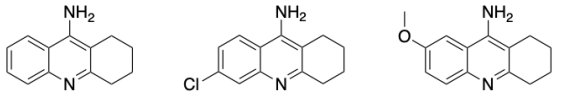

Figure 49. Chemical structures of tacrine and its derivatives.

The list of tacrine hybrids examples is very long considering that the first hybrid molecule was the bis-tacrine in the 1996.[268] Moreover, bis-tacrine represents the first example of dual-binding site inhibitor, designed to interact at the same time with the CAS and PAS of AChE. Indeed, several linkers have been tested until to understand that the perfect one was the methylene chain with 7 atoms of carbon.[268] The simultaneous interaction in two important sites have permitted to obtain one of the highest potent and selective AChE inhibitors (IC_{50} = 0.40nM, Figure 50).[268] From this first example dozens of tacrine hybrids have been designed and synthesized modifying several functions, in order to obtain new multitarget compounds for the treatment of AD (Figure 50).[265] Indeed, maintaining the AChE and BuChE inhibition, a second biological activity such as anti-inflammatory, anti-amyloid β, anti-aggregatory, anti-oxidant activity is expressed. Therefore, substituting one tacrine and introducing different substructures, such as: lipoic acid (Lipocrine),[269] quinone,[87] gallamine, resveratrol,[89] indole,[270] flurbiprofen,[271] phenylbenzoheterocycle,[272] or donepezil[273] subunits has been possible to obtain multitarget hybrids for the treatment of AD.

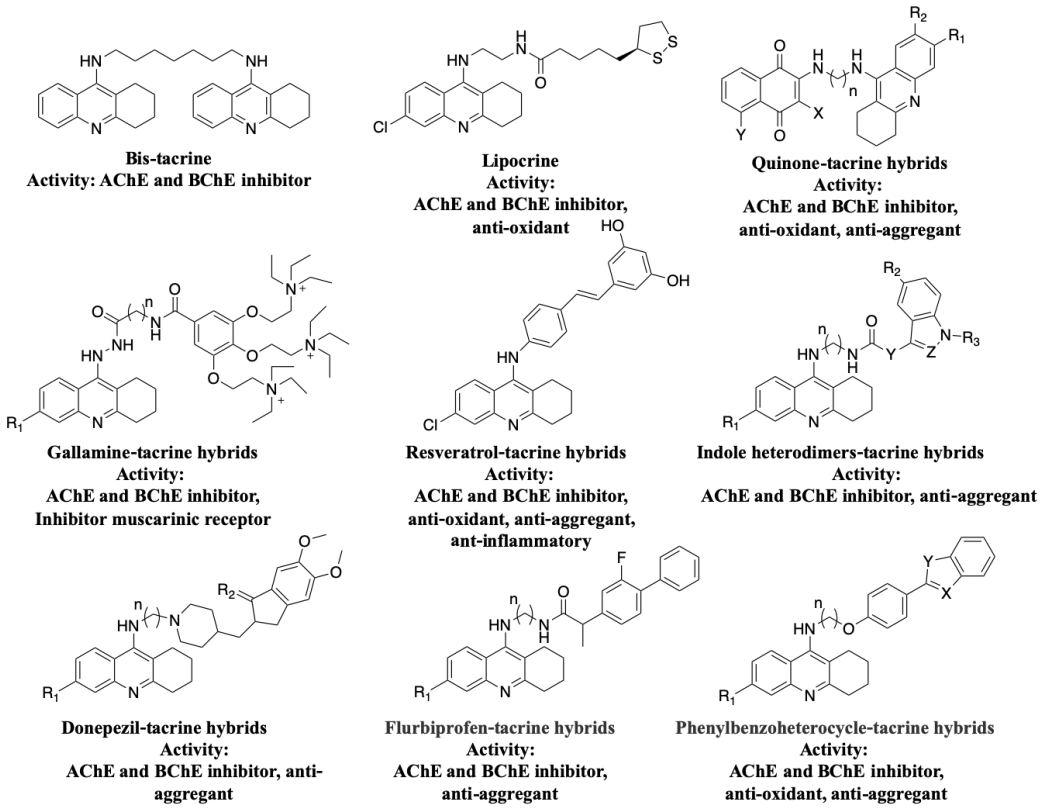

Figure 50. General chemical structure of different tacrine hybrids and own activity.

As we have appreciated from these limited series of examples the tacrine-hybrids strategy has been investigated from long time ago. Moreover, original research on novel tacrine derivatives has been still carried out.

6.2 Design of cashew nut-shell liquid-derived compounds/tacrine hybrids

Harnessing the polypharmacological approach, promoted in the chapter 1, the aim of this project was the development of a completely new class of CNSL compounds-tacrine hybrids for the treatment of AD. Moreover, beginning from inexpensive starting material compounds, as in the previous project, the possibility to obtain globally accessible drugs by food byproduct material could represent a solution for the people affected by AD in low and middle country.

To obtain this goal we decided to design and synthesize a CNSL compounds/tacrine hybrids **71-85** through a hybridization strategy. To do this, we have decided to integrate in a single chemical entity the modified structure of the CNSL compounds with the tacrine moieties (Figure 51).

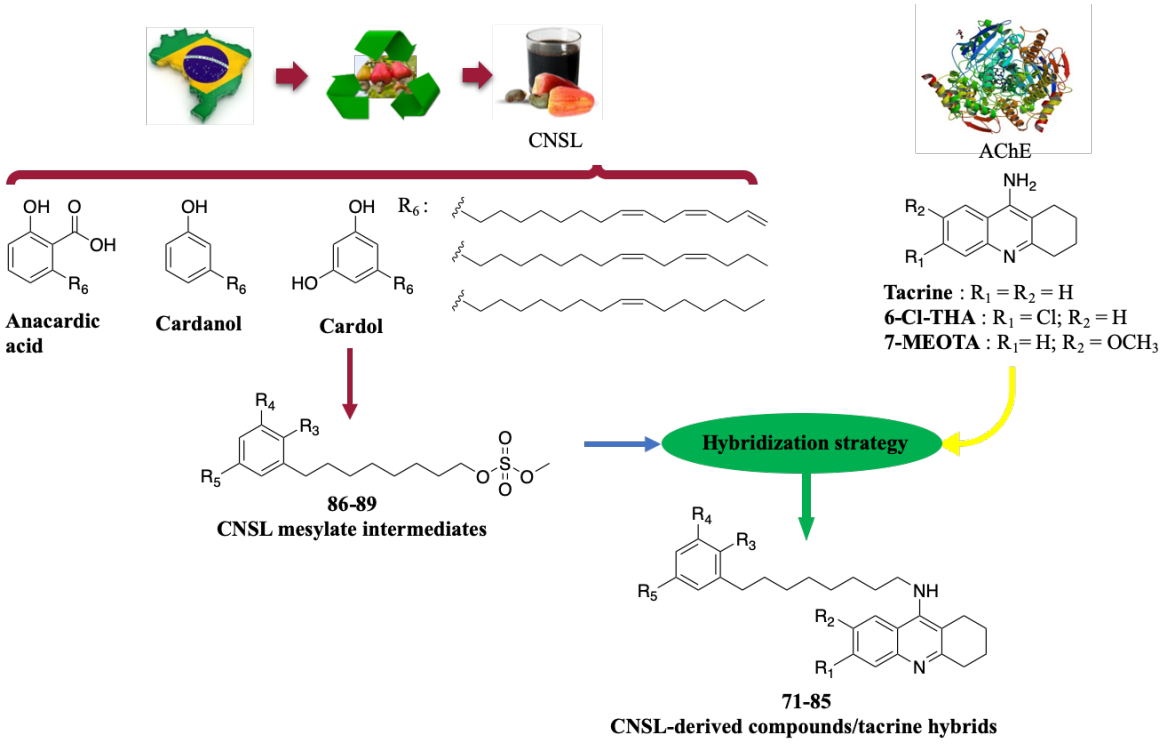

Figure 51. Design strategy to obtain CNSL-derived compounds/tacrine hybrids as sustainable multitarget molecules.

The hybridization strategy has been rationally thought in order to obtain compounds with an appropriate medicinal chemistry profile. Indeed, the long chain of the CNSL derivatives has been reduced from 15 to 8 atom of carbon and introducing a good leaving group (mesyl group)

obtaining the intermediate compounds **86-89**. The mesyl group will be useful for the reaction of aromatic nucleophilic substitution in order to join in one step the CNSL-derived compounds with the tacrine's moieties.

This strategy will permit to create multitarget hybrids maintaining the tacrine biological activities and integrating with the well-known anti-inflammatory activity derived from the phenolic portion of the CNSL-derived compounds. Particularly, the tacrine's portion will permit the interaction with the CAS of the AChE and the BuChE, while the phenolic portion of the CNSL-derived compounds present other biological functions. Indeed, the phenolic group other that interact with the PAS, stabilizing the interaction, it could present a validate anti-inflammatory activity useful for the treatment of neuroinflammatory-based diseases like AD.[274]

Therefore, starting from unexpansive compounds, derived from food byproduct (CNSL), and combining by hybridization strategy with the acetylcholinesterase inhibitor tacrine's moieties will permit us to obtain another example of innovative globally accessible drug for the treatment of AD.

6.3 Chemistry

The synthetic strategy purposed to obtain compounds **71-85** was a linear synthetic strategy that begins with the aromatic nucleophilic substitution between the tacrine and its derivatives and the CNSL mesyl-derivatives (**86-89**). Particularly, tacrine and its derivatives 6-Cl-THA have been synthesized starting with cyclohexanone and 2-aminobenzonitril or 2-amino-4-chlorobenzonitril in order to obtain in high yield tacrine and 6-Cl-THA, respectively (Scheme 11). The reaction proceeds via Friedländer mechanism in which the lewis acid $ZnCl_2$ increase the reactivity of the cyclohexanone promoting the formation of an imine intermediate. Then, by intramolecular cycloaddition permit to obtain the 9-amino-tetrahydroacridine scaffold. The crude products were purified by crystallization in ethanol/water in order to remove the $ZnCl_2$ and impurities. The compounds 7-MEOTA was kindly donated from Professor Kamil Kuca of the department of pharmaceutical chemistry and drug control, faculty of pharmacy in Hradec Kralove, Charles University in Prague, Czech Republic.

Scheme 11. Synthetic strategy to obtain tacrine and 6-Cl-THA.

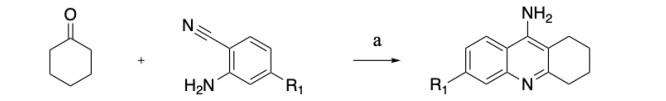

Cyclohexanone **2-aminobenzonitril** : R_1 = H **2-amino-4-chlorobenzonitril** : R_1 = Cl **Tacrine** : R_1 = H (70%) **6-Cl-THA** : R_1 = Cl (60%)

Reagents and conditions: a) $ZnCl_2$, 3h, 140°C, NaOH (pH = 13).

The second substrate to obtain the final compounds are the CNSL-derived compounds as mesyl-derivatives **86-89**. Compounds **86-88** are kindly synthesized by Prof. Luiz Antonio Soares Romeiro of the University of Brasilia. The first step for the synthesis of the intermediaries was an ozonolysis reaction with reductive work-up; by using $NaBH_4$ and isolating the intermediate primary alcohol. Then, the CNSL primary alcohol intermediate was treated with mesyl chloride in order to obtain the desiderated compounds **86-88** (Scheme 12).

Scheme 12. Synthetic strategy to obtain compounds **86-89**.

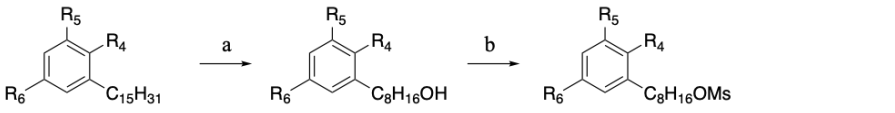

CNSL compounds mixture | **CNSL primary alcohol intermediates**

86 : R_3 = H; R_4 = OCH_3; R_5 = H
87 : R_3 = $COOCH_3$; R_4 = OCH_3; R_5 = H
88 : R_3 = H; R_4 = OBn; R_5 = H
89 : R_3 = H; R_4 = R_5 = OCH_3

Reagents and conditions: a) two steps: i) O_2/O_3, MeOH 2h; ii) $NaBH_4$, MeOH, -15°C to room temperature, 3h; b) mesyl chloride, triethylamine, DCM, 12h, room temperature.

The last CNSL mesyl derivatives **89** has been obtained through different protocol reaction. Indeed, starting from the **LDT-71**, donated from Prof. Romeiro Lab., has been first selectively benzylated in the phenolic function and finally introduced the mesyl function in the aliphatic alcohol using the previous mesylation protocol. Compounds **89** would be useful to obtain a series of cardanol-tacrine derivative hybrids in which the benzyl group will be removed by hydrogenation reaction (Scheme 13). This strategy permits us to maintain the natural free phenolic function responsible of the anti-inflammatory activity of the CNSL compounds.

Scheme 13. Synthetic strategy to obtain compound **89**.

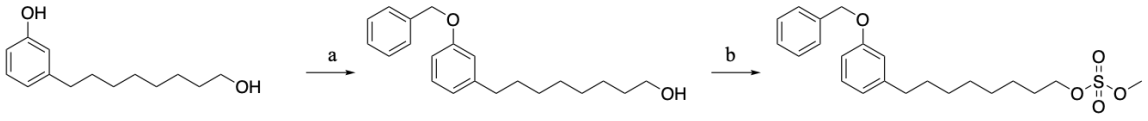

LDT-71 | **90** (92%) | **89** (87%)

Reagents and conditions: a) benzyl bromide, K_2CO_3, acetone, 12h, reflux; b) mesyl chloride, triethylamine, DCM, 12h, room temperature.

With the starting material in our hands, the synthetic strategy began with the nucleophilic aromatic substitution between the compounds **86-89** and the tacrine derivatives (Scheme 14). This reaction was performed under microwave (MW) condition in which a solution of KOH in DMSO dry was necessary to deprotonate the aniline function of the tacrine derivatives permitting the nucleophilic substitution with the electrophilic carbon in alpha-position to the mesyl group of compounds **86-89**. The reaction carried out at 100°C for 12 minutes followed by several extraction with water in order to remove the DMSO before the purification by column chromatography. From this first reaction we obtained the final compounds **71-78** and the intermediates **91-93**. The benzylic

intermediates **91-93** have been hydrogenated using the H-CUBE system: a flow chemistry hydrogenation process that permitted as to remove the benzylic group and obtain the free phenyl derivatives **79-81**. The free phenolic derivatives should present an increased anti-inflammatory activity as reported in literature.[274]

Scheme 14. Synthetic strategy to obtain the CNSL compounds-tacrine hybrids **71-85**.

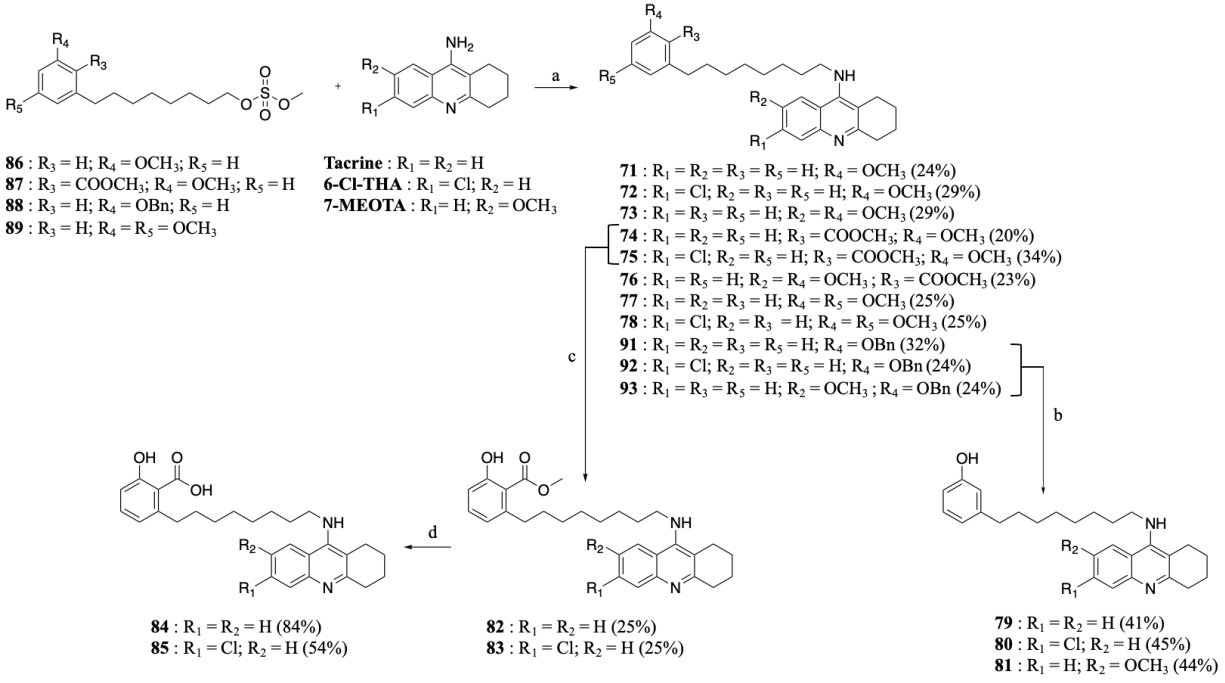

Reagents and conditions: a) KOH, DMSO dry, MW: 100° C, 80 W, 12 min; b) H-CUBE: H_2, 6 bar, Pd/C 10%, flow 1 ml/min c) BBr_3, DCM, from 0° C to room temperature, 40 min; d) two steps: i) KOH 3,5 M, MeOH/H_2O (2:1) MW: 100°C, 100W, 10 min, ii) HCl 2N 0°C, 20 min.

Considering that the anti-inflammatory activity seems derive from the free phenolic and benzoic acid functions, we disassembled the compounds synthesized before **74**, **75** removing at first the methyl ether function and then the methyl ester function. The structure-activity relationship expansion will permit as to validate the hypothesis about the role of the CNSL portion for the anti-inflammatory activity. The structure-activity relationship expansion started with the demethylation of the ether derivatives **74**, **75** using BBr_3, in order to obtain the compounds **82**, **83** after purification by column chromatography. Then, the methyl ester has been removed starting from the compounds previous synthesized **82**, **83** after treatment with KOH 3,5 M, MeOH/H_2O (2:1) under MW condition (100°C, 100W, 10 min). The crude of the reaction was purified adding HCl until the complete precipitation of the final products **84**, **85**.

All compounds synthesize have been characterized by using analytical HPLC, 1H- and 13C-NMR, ESI-MS and HRMS) (see Chapter 8).

6.4 Results and discussion

6.4.1 Cytotoxicity assay in hepatocyte cell line (Hep G2)

We evaluated the hepatotoxicity of the hybrids **72-85** by MTT assay on HepG2. Positively, none of them (up to 1 µM) showed significant hepatotoxicity effect (Figure 52). At the concentration of 10 µM, only compounds **73**, **77** and **79** results cytotoxic, decreasing the viability of the 40% compared the resto of compounds. At the higher concentration (100 µM) all compounds result toxic. This assay has been performed by the group of Prof. Fato of the University of Bologna.

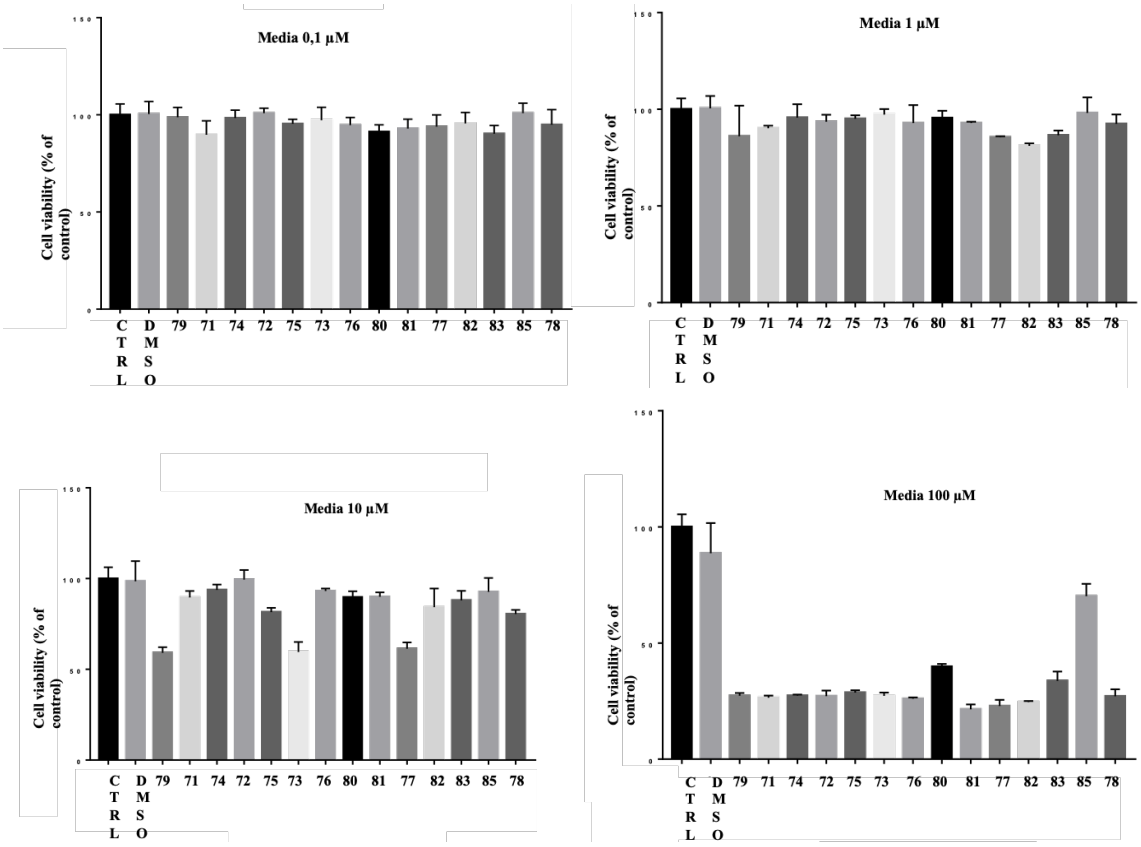

Figure 52. Effect of hybrid molecules on cell survival/death through MTT assay in Hep9 cells at the concentrations 0,1, 1, 10 and 100µM of **79-85** for 24h.

6.4.2 Cytotoxicity assay in SH-SY5Y cells

The molecules resulted less toxic in the previous cytotoxicity assay has been studied by MTT assay on Homo sapiens neuroblastoma cells (SH-SY5Y). The hybrids **72, 74, 75, 80-83, 85**

have been tested in three different concentration 0,1, 1, and 10 µM. Tacrine and the natural and anti-inflammatory compound anacardic acid (LDT_11) have been used as reference compounds. From the results emerged that at the low concentrations (0,1 and 1 µM) the molecules are no cytotoxic. At the concentration of 10 µM the viability of all compounds decrees more than 70% compared to the reference compounds, except for compounds **80** and **85** (Figure 53). The reference compounds tested results more toxic compared the new hybrids compounds at all concentrations tested. This assay has been performed by the group of Prof. Hrelia of the University of Bologna.

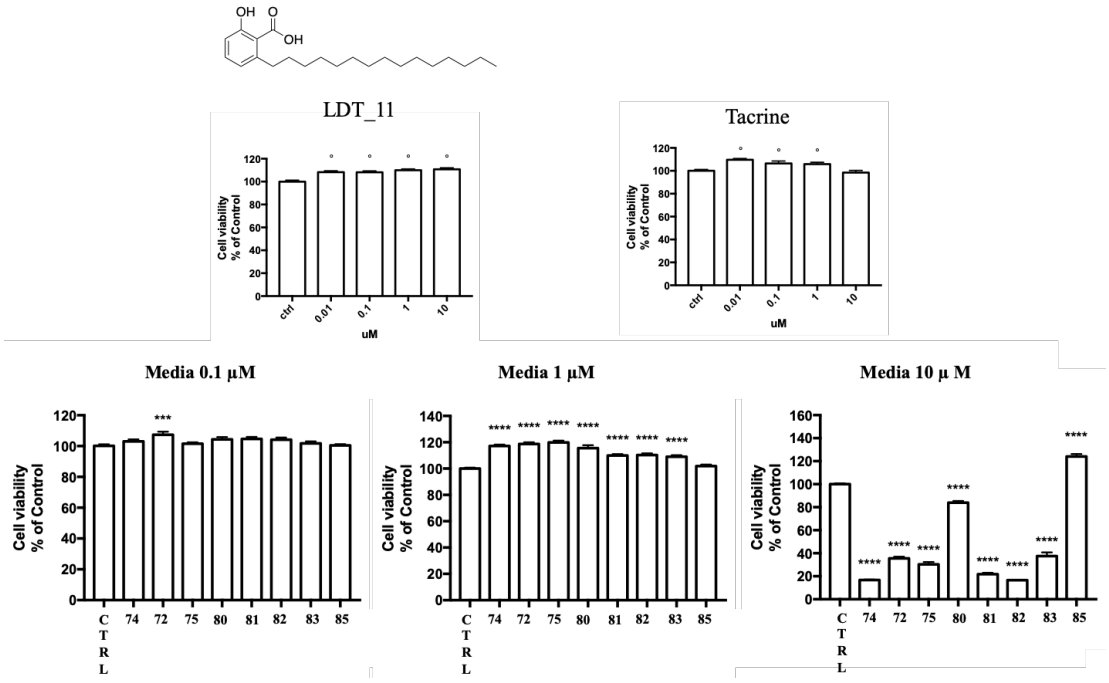

Figure 53. Effect of hybrid molecules on cell survival/death through MTT assay in SH-SY5Y cells at the concentrations 0,1, 1, and 10 µM of the references tacrine and LDT_11 and **72, 74, 75, 80-83, 85** for 24h.

6.4.3 Cytotoxicity assay in BV2 cells

In parallel with the previous assay was also evaluated the cytotoxicity by MTT assay on murine microglia cell lines (BV2). The hybrids **72, 74, 75, 80-83, 85** have been tested in three different concentration 0,1, 1, and 10 µM. From the results obtained emerges that at the low concentrations (0,1 and 1 µM) the molecules are not toxic, while it became toxic at 10 µM except for compound **85** (Figure 54). This assay has been performed by the group of Prof. Hrelia of the University of Bologna.

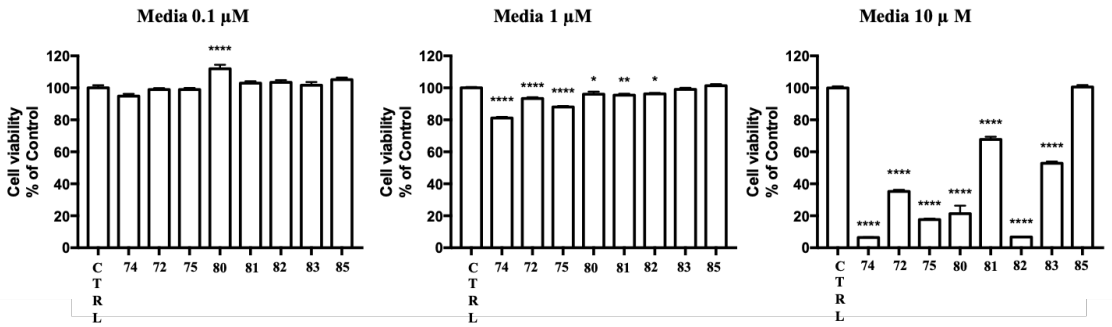

Figure 54. Effect of hybrid molecules on cell survival/death through MTT assay in BV2 cells at the concentrations 0,1, 1, and 10 µM of **72, 74, 75, 80-83, 85** for 24h.

6.4.4 Neuroprotection assay in BV2 cells after LPS insults

The tacrine hybrids tested previously **72, 74, 75, 80-83, 85** does not show any cytotoxic effect at low concentrations in neurons and microglia cells lines. Thus, these selected hybrids have been tested to evaluate their potential protective effects on BV2 cell lines after LPS insults. The reference compounds tacrine and LDT_11 have been analyzed highlighting the moderate neuroprotective effect of LDT_11 and a slightly neuroprotective effect of the tacrine at all concentration tested. As shown in Figure 55, treated BV2 cells with hybrids **74, 75, 82, 85** at 0.01 µM results protective showing a restored cell viability, while the rest of compounds results less neuroprotective and more cytotoxic also at the high-dose concentration used (1 µM). In a structure-activity relationship (SAR) point of view, compounds **74, 75, 82, 85** shear the same anacardic acid motif in the phenolic subunit representing an indispensable functional group for the neuroprotective activity compared the rest of phenolic functions investigated. Conversely, the presence of the chlorine in the tacrine subunit does not influence the activity. This assay has been performed by the group of Prof. Hrelia of the University of Bologna.

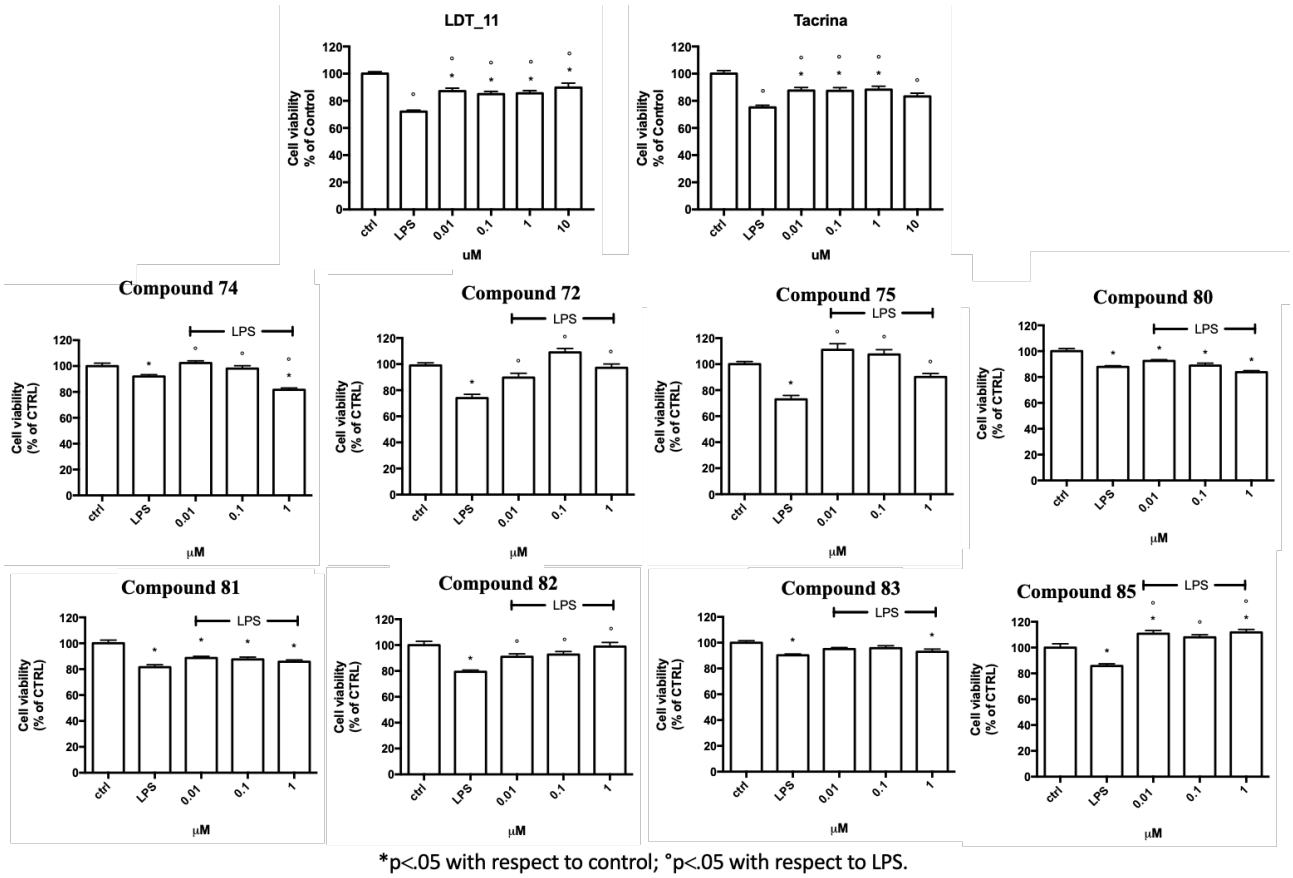

Figure 55. Effect of hybrid molecules on cell survival/death through MTT assay in BV2 cells at the concentrations 0,01, 0,1, and 1 μM of the reference compounds tacrine and **LDT_11** and the hybrids **72, 74, 75, 80-83, 85** for 24h after LPS insults 100ng/ml.

6.4.5 Genes expression assay in BV2 cells after LPS insults

Targeting neuroinflammation in AD represent one of the most important strategy for the treatment of this neuroinflammatory-based diseases. Thus, the evaluation of the genes expression of typical inflammatory markers represent a validate assay to evaluate the anti-inflammatory profile. Consequently, BV2 cell line has been treated with the most protective compounds **72, 74, 75, 82, 85** at 0.1 μM and then insulted with LPS in order to evaluate the mRNA expression level of IL-1β and TNF-α. All compounds decrease the expression of mRNA levels of both markers, but particularly hybrids **85**. **85** display in the CNSL portion the free anacardic acid function resulting structurally similar to the salicylic acid. Thus, the possibility that **85** is the more potent anti-inflammatory compounds was reinforced by the similarity with the anti-inflammatory salicylic acid molecule.[274] Moreover, the starting CNSL derivative, saturated anacardic acid, has been reported in literature as potent anti-inflammatory molecule

decreasing the mRNA levels of IL-1β and TNF-α (Figure 56).[274] This assay has been performed in collaboration with the group of Prof. Hrelia of the University of Bologna.

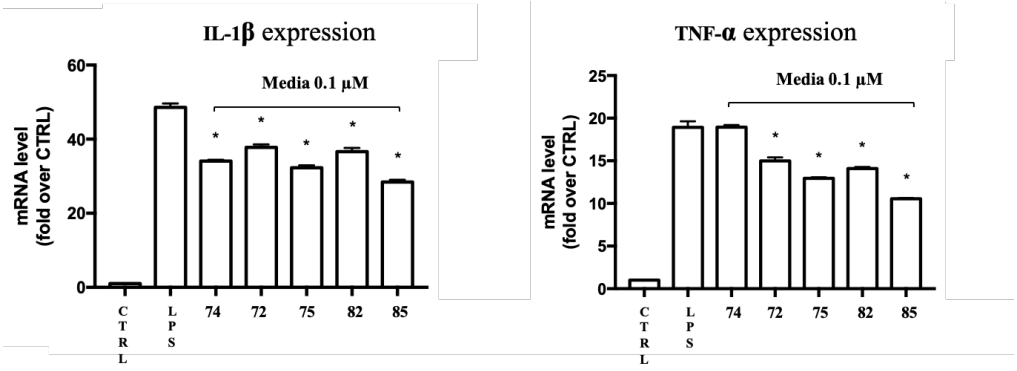

Figure 56. Effect of hybrid molecules on cell mRNA gene expression (**IL-1β** and **TNF-α**) in BV2 cells at the concentration 0,1 μM of **72, 74, 75, 82, 85** for 24h after LPS insults 100ng/ml.

6.4.6 Cholinesterase inhibitory activity

It is well known that AChE inhibitors are effective in temporarily improving behavior and well-being and slowing cognitive decline in patients with dementia. In addition to AChE, mounting preclinical evidence suggests that BuChE may be important in order to maintain normal cholinergic function in AD, becoming more pronounced during the disease course.[275] Tacrine and its derivatives acts as a dual AChE/BuChE inhibitor. In according to this, the inhibitory activities of the synthesized hybrids and of the reference tacrine's derivatives against human recombinant AChE and human serum BuChE were evaluated by the method of Ellman in by the Prof. Bartolini of the University of Bologna.

All the tested hybrids **71**, **72**, **74-85** turned out to be effective inhibitor of BuChE and AChE with an IC_{50} values spanning from a wide range (from nanomolar to picomolar, Table 4).

Table 4. Inhibition of human BChE and AChE activities by **71**, **72**, **74-85**

	IC_{50} hAChE (nM)[a]	**IC_{50} hBuChE** (nM)[a]
Tacrine	230 ± 12	45.8 ± 3.0

79	19.2 ± 4.0	3.74 ± 0.10
71	40.0 ± 3.3	7.72 ± 0.96
77	47.2 ± 9.8	29.2 ± 5.4
74	20.8 ± 3.8	0.0352 ± 0.0077
82	17.0 ± 2.7	0.177 ± 0.005
84	184 ± 59	11.2 ± 2.3
6-Cl-THA	14.5 ± 0.9	505 ± 28
80	4.19 ± 0.81	19.4 ± 4.0
72	5.71 ± 0.43	25.8 ± 0.5
78	5.10 ± 0.99	83.2 ± 3.5
75	2.54 ± 0.07	0.265 ± 0.027
83	2.81 ± 0.14	4.25 ± 0.48
85	13.4 ± 4.2	120 ± 12
7-MEOTA	8000 ± 650	8860 ± 640
76	1260 ± 10	3.49 ± 0.09

[a] Results are expressed as the mean of at least three experiments
[b] Results are expressed as preliminary data.

According to the data contained in Table 4 we were able to draw preliminary SAR (Figure 57). All hybrids obtained were significantly more potent compared to the corresponding tacrine's reference compounds. The hybrids that presents tacrine results more active on BuChE, while the hybrids that present 6-Cl-THA are more active on AChE. The activity and selectivity of the hybrids, towards the investigated enzymes, is due to the nature of the connected tacrine's scaffold in the hybrids reflecting the trend already deeply explored in literature.[276, 277]

What predominantly emerged from the SAR is the presence of a modified phenolic fragment derived from the CNSL-derive molecules. Indeed, the different structure of the modified phenolic fragment seems to deeply affect the inhibitory activity and selectivity of the hybrids. In fact, the hybrids carrying di-methylated anacardic acid moiety (**74-76**) display the highest potency and selectivity for BuChE, and at the same time the best activity over AChE.

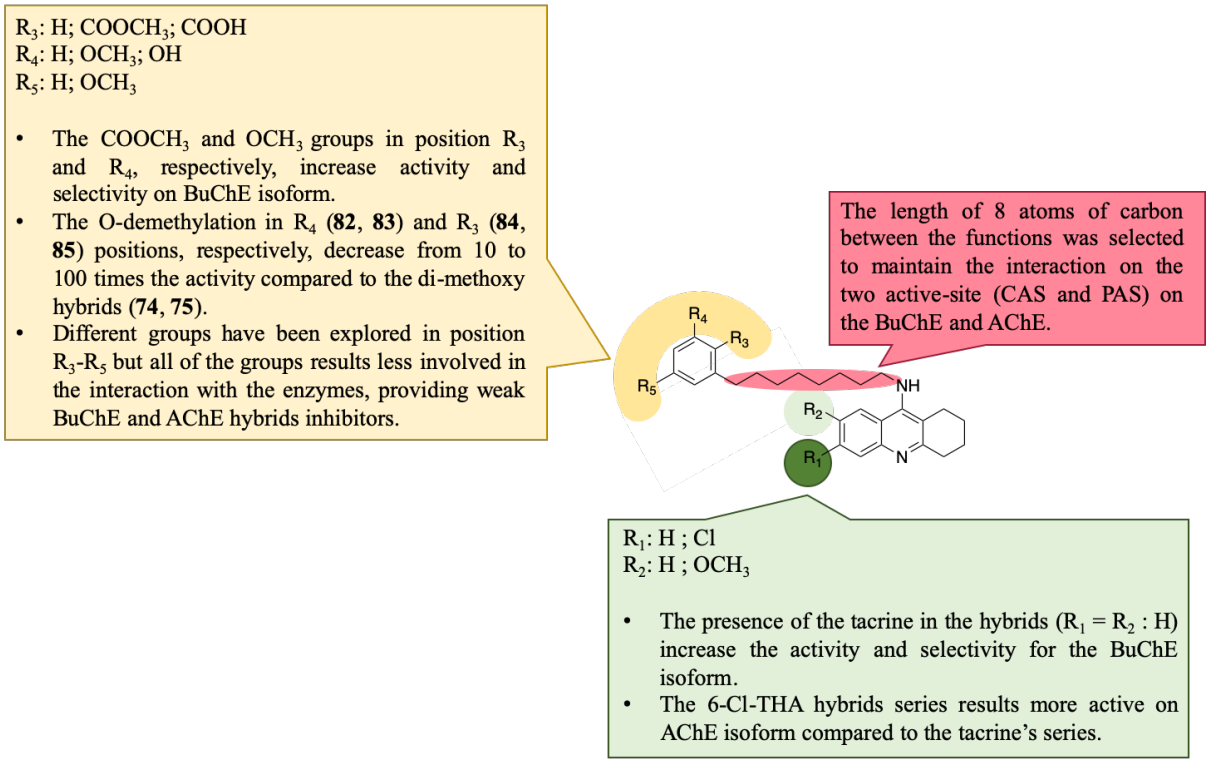

Figure 57. Structure-activity relationships of the CNSL/Tacrine hybrids.

Compared with the di-methoxy anacardic acid hybrids **74**, **75** (IC_{50} = 0.0352 nM and 0.265 nM, respectively), the introduction of the hydroxy substituent in position R_4 in the phenyl ring decrease the enzyme inhibition of 10 times, as evident for **82** and **83** (IC_{50} = 0.177 nM and 4.25 nM). Moreover, any other O-demethylation in position R_3 (**84**, **85**) decrease the activity of 100 times compared the starting hybrids **74**, **75**. Monosubstituted methoxy- **71-73** and hydroxy-hybrids **90-92** in position R_4 shows a weak enhancement respect to starting tacrine's reference compounds. The disubstituted methoxy-hybrids in position R_3 and R_5 (**77**, **78**) presents a similar profile of the monosubstituted hybrids **71-73**.

In light of the data collected, le most promising compounds **74**, **75** are already under biological investigation in order to detect their ability to cross the BBB by using PAMPA assay by Prof. Prof. Ondrej of the University of Hradec kralove (Czech Republic), and an *in vivo* proof of concept by using Drosophila Melanogaster model by the group of Prof. Hrelia. Moreover, for the hybrids **74** will be result determined the X-ray crystal structure with the BuChE in collaboration with Prof. Florian from the Institut de Recherche Biomédicale des Armées (France).

Chapter 7

Conclusions

Neuroinflammatory based-diseases are a very challenging area for medicinal chemists. Several efforts have been made during the years, however, an effective treatment for these diseases, such as AD and MS does not exist yet. Neuroinflammatory based-diseases are multifactorial in nature with still unclear pathogenic mechanisms and scarce information on how neuro-inflammation is interconnected with other concomitant events, such as neurodegeneration.
Polypharmacology is one of the milestones for the development of therapies able to combat multifactorial diseases. Particularly, the development of multitarget compounds through different strategy (linking, fusing, merging) has permitted to expand the potential arsenal to treat multifactorial diseases.

Based on these considerations, this thesis was focused on the development of small molecule for combat neuroinflammatory diseases through different and innovative polyphamacological approaches:

1. Based on a peculiar interest in developing multitarget molecules for the treatment of MS and aiming to target microglia immunomodulation and Oli-Neu differentiation, we have synthesized and tested a small series of omega-3 FAs/VPA conjugates. Among the developed compounds, the omega-3 FAs/VPA conjugate **2** display features relevant in terms of very low hepato- and neuro-cytotoxicity, high stability in plasma and hydrolysis in the analyzed tissues (liver and brain lysate). Compound **2** displays an immunomodulation activity decreasing the expression of iNOS and increasing the expression of TREM2 in microglia cells. Importantly, this effect is displayed only by compound **2**, not for the reference compounds singularly, nor for the reference compounds in an equimolar concentration co-treatment. Finally, compound **2** displays a significative ability in the Oli-Neu differentiation assay of increasing the length of the filaments after its administration. This effect is appreciated only for the omega-3 FAs/VPA conjugate **2** and not for the reference compounds nor for their equimolar combination. Thus, we have demonstrated how the multitarget effect of compound **2** results in safer and more efficacious profiles compared the single treatment and the co-administration of the two single components.

2. In the second project, we applied a similar conjugation strategy to obtain FAs/$P2Y_6$ agonist conjugates for the treatment of AD. The molecules have been designed in order to potentially maintain the ability to interact with the $P2Y_6$ receptor, increase the anti-neuroinflammatory

profile and the PK properties. Indeed, the lipid-drug conjugate strategy represents a well-known alternative for the development of co/pro-drugs of drugs that generally suffer for their low BBB penetration ability. The synthetic strategy started with the synthesis of the $P2Y_6$ agonists and the stearic acid intermediate. The $P2Y_6$ agonist were prepared using the Ludwig procedure in order to obtain the uridine diphosphate derivatives. The FA intermediate was obtained starting from stearic acid and obtaining its 2-bromoethanolamide derivatives. Unfortunately, the reaction to obtain the final product failed by using the reported conditions.

3. In the third project, we focused on the design and synthesis of a small library of eight sustainable HDAC/ferroptosis inhibitors (**39-46**). These molecules, developed starting from food byproduct material might represents low cost and globally accessible drugs for the treatment of AD. The library of compounds has been obtained starting from CNSL, as a valid precursor for the synthesis of potential multipotent bioactive molecules. Thus, starting from CNSL-derived compounds we have modifyied their structures by introducing different zinc-binding groups able to interact with the HDAC enzymes and with potential ferroptosis inhibition activity. Final products **39-46** have been preliminary tested in MTT assays to evaluate their hepato- and neuro-toxicity. They resulted not cytotoxic at the tested concentration. In addition, the eight molecules have been tested for their HDAC inhibitor activity; however, they resulted very weak HDAC inhibitor binders. At the moment, the molecules are under evaluation to analyze their ferroptosis inhibition profiles using the ferroptosis-erastin model.

4. In the fourth project, we applied a hybridization strategy in order to design and synthesize the first class of hybrids between tacrine and its derivatives and CNSL-based compounds. These molecules, together with the previous ones, represents a good example of revalorization of food byproduct material for the production of globally accessible drugs for the treatment of AD. The obtained hybrids have been preliminary screened in order to filter out the more hepato- and neurotoxic compounds. Then, the most promising compounds have been tested for evaluating their neuroprotective/ neuroinflammatory effect after insults with LPS. From these assays it emerges that the most neuroprotective and anti-inflammatory molecules are the hybrids **72**, **74**, **75**, **82**, **85,** that also reduces the expression of IL-B and TNF-α. In parallel, the inhibition activity on BuChE has been evaluated using the Elmann

assay. From these data it emerges that hybrid **74** (synthesized by reacting the protected anacardic acid with tacrine) is endowed with a remarkable inhibitory activity BuChE IC_{50} = 35.2 ± 0.0077 pM and AChE IC_{50} = 17 ± 0.9 nM. The AChE inhibitory activity data will be confirmed soon.

Chapter 8

Experimental part

Chemistry

All the commercially available reagents and solvents were purchased from Sigma-Aldrich, Alpha Aesar, VWR, and TCI, and used without further purification. Reactions were followed by analytical thin layer chromatography (TLC), on pre-coated TLC plates (layer 0.20 mm silica gel60 with a fluorescent indicator UV254, from Sigma-Aldrich). Developed plates were air-dried and analyzed under a UV lamp (UV 254/365 nm). Nuclear magnetic resonance (NMR) experiments were run on Varian VXR 400 (400 MHz for 1H, 100 MHz for 13C). 1H and 13C NMR spectra were acquired at 300 K using deuterated dimethyl sulfoxide ((CD3)2SO) and chloroform (CDCl3) as solvents. Chemical shifts (δ) are reported in parts per million (ppm) relative to tetramethylsilane (TMS) as internal reference and coupling constants (J) are reported in hertz (Hz). The spin multiplicities are reported as s (singlet), br s (broad singlet), d (doublet), t (triplet), q (quartet), and m (multiplet). Due to the high level of carbon similarity several peaks in the 13C-NMR are overlapped especially for omega-3.[278, 279] Mass spectra were recorded on a VG707EH-F and Waters Xevo G2-XS QTOF apparatus, and electrospray ionization (ESI) both in positive and negative mode was applied when the 13C-NMR spectra were not completely exhaustive. Compounds were named following IUPAC rules as applied by ChemBioDraw Ultra (version 14.0). All of the final compounds showed ≥90% purity by analytical HPLC. The purity of compounds 1-35 was determined using a Kinetex® 5µm EVO C18 100 Å, LC column 150 x 4.6 mm and a HPLC Jasco Corporation (Tokyo, Japan) instrument (PU-1585 UV equipped with a 20 µL loop valve). HPLC parameters were the following: water with 0.05% trifluoroacetic acid (eluent A), and acetonitrile with 0.05% trifluoroacetic acid (eluent B); flow rate 1.00 mL/min; elution type isocratic with 75% of eluent A and 25% of eluent B; detection UV-Vis Abs at 254 nm. The samples were dissolved in MeOH or DMF (10 µg/mL).

Synthesis of omega-3 FAs/VPA conjugates

General procedure for the preparation of N-Boc linkers (14, 15)

To a solution of **11** or **12** (1 mmol) in DCM (10 ml), were added tert-butoxycarbonyl anhydride respectively (Boc_2O, 0.2 mmol and 1.1 mmol, respectively) and the resulting mixture was stirred at room temperature for 16 hours. The crude reaction was concentrated under reduce pressure and then was purified by using flash silica gel column chromatography using different eluent mixtures to give the title compounds **14**, **15.**

Tert-butyl (2-aminoethyl)carbamate (14)

The resulting residue was purified by flash chromatography (9:1:0.1 DCM/ MeOH/ NH_3 33%) affording **14** as pale-yellow oil. Yield 98%.

^{1}H-NMR ($CDCl_3$, 400 MHz) δ (ppm): 1.41 (s, 9H), 2.77 (t, 2H, J = 4 Hz), 3.14 (m, 2H), 5.01 (bs, 1H). ^{13}C-NMR ($CDCl_3$, 100 MHz) δ (ppm): 28.36, 41.79, 43.30, 79.67,156.19.

Tert-butyl (2-hydroxyethyl)carbamate (15)

The resulting residue was purified by flash chromatography (9:1:0.1 DCM/ MeOH/ NH_3 33%) affording **15** as pale-yellow oil. Yield 97%.

^{1}H-NMR ($CDCl_3$, 400 MHz) δ (ppm): 1.43 (s, 9H), 2.87 (bs, 1H), 3.24-3.28 (m, 2H), 3.65-3.69 (m, 2H), 5.04 (bs, 1H). ^{13}C-NMR ($CDCl_3$, 100 MHz) δ (ppm): 28.34, 43.05, 62.49, 79.67,156.80.

General procedure for the preparation of O-TBS linkers (16, 17)

To a solution of **12** or **13** (1 mmol) in DCM (10 ml), were added imidazole (1.2 mmol) tert-butyldimethylsilyl chloride respectively (TBS-Cl, 0.2 mmol or 1.1 mmol, respectively) and the resulting mixture was stirred at room temperature for 16 hours. The crude reaction was

concentrated under reduce pressure and then was purified by using flash silica gel column chromatography using different eluent mixtures to give the title compounds **16**, **17**.

2-((tert-butyldimethylsilyl)oxy)ethan-1-amine (16)

The resulting residue was purified by flash chromatography (9:1:0.1 DCM/ MeOH/NH_3 33%) affording **16** as pale-yellow oil. Yield 87%.

^{1}H-NMR ($CDCl_3$, 400 MHz) δ (ppm): 0.02 (t, 6H, J = 4 Hz), 0.87 (s, 9H), 1.72 (s, 2H), 2.73 (t, 2H, J = 4 Hz), 3.58 (t, 2H, J = 8 Hz). ^{13}C-NMR ($CDCl_3$, 100 MHz) δ (ppm): -5.38, 18.24, 25.85, 44.22, 65.16.

2-((tert-butyldimethylsilyl)oxy)ethan-1-ol (17)

The resulting residue was purified by flash chromatography (9:1 DCM/ MeOH) affording **17** as pale-white oil. Yield 92%.

^{1}H-NMR ($CDCl_3$, 400 MHz) δ (ppm): 0.07 (t, 6H, J = 4 Hz), 0.88-0.90 (m, 9H), 2.09 (bs, 1H), 3.61-3.41 (m, 2H), 3.69-3.71 (m, 2H). ^{13}C-NMR ($CDCl_3$, 100 MHz) δ (ppm): -5.38, 18.28, 25.85, 63.64, 64.07.

General procedure for the preparation compounds (18-21)

To a solution of VPA (1.2 mmol) in dry DCM (3 ml) under nitrogen, was added at 0°C, 1-etil-3 (3-dimetilaminopropil) carbodiimide chloride (EDC, 1.2 mmol) and the reaction was stirred at room temperature for 1 hour. Successively, a solution contained **14-17** (1 mmol) and 4-dimethylaminopyridine (DMAP, 10% mmol) in dry DCM (1 ml) were added in the activated solution. The resulting mixture was stirred at room temperature for 16 hours. The reaction was concentrated under reduce pressure and then was purified by using flash silica gel column chromatography using different eluent mixtures to give the title compounds **18-21**.

Tert-butyl (2-(2-propylpentanamido)ethyl)carbamate (18)

The resulting residue was purified by flash chromatography (9:1 DCM/ MeOH) affording **18** as pale-yellow oil. Yield 57%.

^{1}H-NMR ($CDCl_3$, 400 MHz) δ (ppm): 0.86-0.90 (m, 6H), 1.23-1.43 (m, 15H), 1.54-160 (m, 2H), 2.01-2.06 (m, 1H), 3.24-3-29 (m, 2H), 3.34-3.38 (m, 2H), 4.97 (bs, 1H), 6.18 (bs, 1H). ^{13}C-NMR ($CDCl_3$, 100 MHz) δ (ppm): 14.05, 20.72, 28.31, 35.13, 40.30, 40.43, 47.48, 79.47, 156.90, 176.90.

2-((tert-butoxycarbonyl)amino)ethyl 2-propylpentanoate (19)

The resulting residue was purified by flash chromatography (9:1 DCM/ MeOH) affording **19** as pale-yellow oil. Yield 63%.

^{1}H-NMR ($CDCl_3$, 400 MHz) δ (ppm): 0.84 (t, 6H, J = 8 Hz), 1.21-1.26 (m, 4H), 1.32-1.39 (s, 11H), 1.49-1.57 (m, 2H), 2.33 (q, 1H, J = 4 Hz), 3.31-3.35 (m, 2H), 4.08 (t, 2H, J = 8 Hz), 4.80 (bs, 1H). ^{13}C-NMR ($CDCl_3$, 100 MHz) δ (ppm): 13.88, 20.53, 28.26, 34.51, 39.74, 45.11, 62.89, 79.34, 155.66, 176.40.

N-(2-((tert-butyldimethylsilyl)oxy)ethyl)-2-propylpentanamide (20)

The resulting residue was purified by flash chromatography (9:1 DCM/ MeOH) affording **20** as pale-yellow oil. Yield 68%.

^{1}H-NMR ($CDCl_3$, 400 MHz) δ (ppm): 0.03 (s, 6H), 0.84-0.88 (m, 15H), 1.20-1.37 (m, 6H), 1.53-1.59 (m, 2H), 2.01 (q, 1H, J = 4 Hz), 3.30-3.37 (m, 2H), 3.64 (t, 2H, J = 4 Hz), 5.84 (bs, 1H). ^{13}C-NMR ($CDCl_3$, 100 MHz) δ (ppm): -5.48, 14.03, 18.17, 20.76, 25.78, 35.24, 41.33, 47.68, 61.95, 175.88.

2-((tert-butyldimethylsilyl)oxy)ethyl 2-propylpentanoate (21)

The resulting residue was purified by flash chromatography (9.5:0.5 DCM/ MeOH) affording **21** as pale-white oil. Yield 42%.

^{1}H-NMR ($CDCl_3$, 400 MHz) δ (ppm): 0.06 (m, 6H), 0.89 (m, 15H), 1.25-1.42 (m, 6H), 1.56-1.62 (m, 2H), 2.36 (q, 1H, J = 4 Hz), 3.77-3.80 (m, 2H), 4.10-4.13 (m, 2H). ^{13}C-NMR ($CDCl_3$, 100 MHz) δ (ppm): -5.41, 13.95, 18.23, 20.60, 25.76, 34.65, 45.27, 61.22, 65.36, 176.54.

General procedure for N-Boc deprotection (22, 23)

To a cold solution of **18** or **19** (1 mmol) in dry DCM (5 ml), was added dropwise trifluoroacetic acid (TFA, 20 mmol) under anhydrous condition. The resulting mixture was stirred at room temperature till the complete disappearance of the starting material (around 1.5-2.5 hours). The crude reaction was concentrated under reduce pressure and then was purified by using flash silica gel column chromatography using different eluent mixtures to give the title compounds **22**, **23**

N-(2-aminoethyl)-2-propylpentanamide (22)

The resulting residue was purified by flash chromatography (9:1:0.1 DCM/ MeOH/NH_3 33%) affording **22** as pale-yellow oil. Yield 98%.

^{1}H-NMR ($CDCl_3$, 400 MHz) δ (ppm): 0.86 (t, 6H, J = 8 Hz), 1.21-1.31 (m, 8H), 1.55 (m, 2H), 2.02 (q, 1H, J = 4 Hz), 2.79 (t, 2H, J = 4 Hz), 3.25-3.30 (m, 2H), 6.06 (bs, 1H). ^{13}C-NMR ($CDCl_3$, 100 MHz) δ (ppm): 14.06, 20.81, 35.20, 41.30, 41.56, 47.67, 176.26.

2-aminoethyl 2-propylpentanoate (23)

The resulting residue was purified by flash chromatography (9:1:0.1 DCM/ MeOH/NH_3 33%) affording **23** as pale-yellow oil. Yield 95%.

^{1}H-NMR ($CDCl_3$, 400 MHz) δ (ppm): 0.85 (t, 6H, J = 8 Hz), 1.21-1.37 (m, 6H), 1.51-156 (m, 2H), 2.07 (q, 1H, J = 4 Hz), 3.36-3.39 (t, 2H, J = 4 Hz), 3.66 (t, 2H, J = 4 Hz) 4.86 (bs, 2H). ^{13}C-NMR ($CDCl_3$, 100 MHz) δ (ppm): 13.65, 20.33, 33.98, 39.64, 44.79, 60.27, 177.40.

General procedure for O-TBS deprotection (**24**, **25**)

To a cold solution of **20** or **21** (1 mmol) in dry DCM (5 ml), was added dropwise tetrabutylammonium fluoride (TBAF, 5 mmol) under anhydrous condition. The resulting mixture was stirred at room temperature until the complete disappearance of the starting material (around 12-15 hours). The crude reaction was concentrated under reduce pressure and the crude was purified by using flash silica gel column chromatography using different eluent mixtures to give the title compounds **24**, **25**.

N-(2-hydroxyethyl)-2-propylpentanamide (24)

The resulting residue was purified by flash chromatography (9:1 DCM/ MeOH) affording **24** as pale-yellow oil. Yield 89%.

^{1}H-NMR ($CDCl_3$, 400 MHz) δ (ppm): 0.7 (m, 6H), 1.23-1.38 (m, 6H), 1.52-1.58 (m, 2H), 2.08 (q, 1H), 3.37-3.41 (m, 3H), 3.67 (t, 2H, J = 4 Hz), 6.42 (bs, 1H). ^{13}C-NMR ($CDCl_3$, 100 MHz) δ (ppm): 14.06, 20.73, 35.18, 42.31, 47.45, 62.37, 177.59.

2-hydroxyethyl 2-propylpentanoate (25)

The resulting residue was purified by flash chromatography (9:1 DCM/ MeOH) affording **25** as pale-white oil. Yield 92%.

^{1}H-NMR ($CDCl_3$, 400 MHz) δ (ppm): 0.85 (t, 6H, J = 4 Hz), 1.22-1.27 (m, 4H), 1.37-1.40 (m, 2H), 1.53-1.58 (m, 2H), 2.36 (q, 1H), 2.58 (bs, 1H), 3.74-3.77 (m, 2H), 4.14-4.17 (m, 2H). ^{13}C-NMR ($CDCl_3$, 100 MHz) δ (ppm): 13.89, 20.53, 34.53, 45.17, 61.10, 65.62, 177.07.

General procedure for the preparation of omega-3 FAs/VPA conjugates (1-8)

To a solution of ALA or DHA (1.2 mmol) in dry DCM (3 ml) under nitrogen, was added at 0°C, 1-etil-3 (3-dimetilaminopropil) carbodiimide chloride (EDC, 1.2 mmol) and the reaction was stirred at room temperature for 1 hour in the dark. Successively, a solution of one intermediate compound **22**-**25** (1 mmol) and 4-dimethylaminopyridine (DMAP, 10% mmol) in dry DCM (1 ml) were added in the activated solution. The resulting mixture was stirred at room

temperature around 4-6 hours. The crude reaction was concentrated under reduce pressure and then was purified by using flash silica gel column chromatography using different eluent mixtures to give the title compounds **1-8**.

(9*Z*,12*Z*,15*Z*)-*N*-(2-(2-propylpentanamido)ethyl)octadeca-9,12,15-trienamide (1)

The resulting residue was purified by flash chromatography (9.5:0.5 DCM/ MeOH) affording **1** as pale-yellow oil. Yield 32%.

^{1}H-NMR ($CDCl_3$, 400 MHz) δ (ppm): 0.87 (t, 6H, J = 8 Hz), 0.96 (t, 3H, J = 8 Hz), 1.23-1.35 (m, 14H), 1.53-1-58 (m, 4H), 2.03-2.08 (m, 5H), 2.15 (t, 2H, J = 8 Hz), 2.79 (m, 4H), 3.37 (s, 4H), 5.27-5.41 (m, 6H), 6.43 (bs, 1H), 6.52 (bs, 1H).^{13}C-NMR ($CDCl_3$, 100 MHz) δ (ppm): 14.07, 14.23, 20.51, 20.75, 25.49, 25.57, 25.67, 27.17, 29.11, 29.25, 29.28, 29.57, 35.18, 36.63, 39.83, 40.38, 47.47, 127.07, 127.69, 128.20, 128.25, 130.20, 131.92, 174.42, 177.55.

2-((9*Z*,12*Z*,15*Z*)-octadeca-9,12,15-trienamido)ethyl 2-propylpentanoate (2)

The resulting residue was purified by flash chromatography (9.5:0.5 DCM/ MeOH) affording **2** as pale-yellow oil. Yield 37%.

^{1}H-NMR ($CDCl_3$, 400 MHz) δ (ppm): 0.89 (t, 6H, J = 8 Hz), 0.96 (t, 3H, J = 8 Hz), 1.24-1.46 (m, 14H), 1.53-1-61 (m, 4H), 2.03-2.09 (m, 4H), 2.15 (t, 2H, J = 8 Hz), 2.35-2.39 (m, 1H), 2.79 (t, 4H, J = 4 Hz), 3.49-3.53 (m, 2H), 4.17 (m, 2H, J = 4 Hz), 5.28-5.40 (m, 6H), 5.77 (bs, 1H). ^{13}C-NMR ($CDCl_3$, 100 MHz, 2 overlapping peaks corresponding to the CH group present in the omega-3 fatty acid portion) δ (ppm): 13.96, 14.24, 20.51, 20.63, 25.49, 25.57, 25.62, 27.17, 29.09, 29.23, 29.56, 34.58, 36.69, 38.94, 45.17, 62.78, 127.07, 127.69, 128.20, 128.25, 130.21, 131.92, 173.15, 176.80.

2-(2-propylpentanamido)ethyl (9*Z*,12*Z*,15*Z*)-octadeca-9,12,15-trienoate (3)

The resulting residue was purified by flash chromatography (9.5:0.5 DCM/ MeOH) affording **3** as pale-yellow oil. Yield 28%.

^{1}H-NMR ($CDCl_3$, 400 MHz) δ (ppm): 0.88 (t, 6H, J = 4 Hz), 0.96 (t, 3H, J = 8 Hz), 1.24-1.35 (m, 14H), 1.56-1.62 (m, 4H), 2.03-2.06 (m, 5H), 2.30 (t, 2H, J = 8 Hz), 2.79 (s, 4H), 3.51-3.5 (m, 2H), 4.15 (t, 2H, J = 8 Hz), 5.29-5.40 (m, 6H), 5.76 (bs, 1H). ^{13}C-NMR ($CDCl_3$, 100 MHz) δ (ppm): 14.07, 14.23, 20.51, 20.74, 24.85, 25.49, 25.57, 27.15, 29.06, 29.09, 29.14, 29.54, 34.13, 35.19, 38.60, 47.64, 63.05, 127.06, 127.73, 128.19, 128.26, 130.17, 131.92, 173.91, 176.11.

2-((2-propylpentanoyl)oxy)ethyl (9*Z*,12*Z*,15*Z*)-octadeca-9,12,15-trienoate (4)

The resulting residue was purified by flash chromatography (9.8:0.2 DCM/ MeOH) affording **4** as pale-white oil. Yield 25%.

^{1}H-NMR ($CDCl_3$, 400 MHz) δ (ppm): 0.89 (t, 6H, J = 8 Hz), 0.97 (t, 3H, J = 8 Hz), 1.26-1.45 (m, 14H), 1.55-1.64 (m, 4H), 2.04-2.09 (m, 4H), 2.31 (t, 2H, J = 8 Hz), 2.39 (q, 1H, J = 4 Hz) , 2.79-2.80 (s, 4H), 4.27 (s, 4H), 5.29-5.43 (m, 6H). ^{13}C-NMR ($CDCl_3$, 100 MHz, 2 overlapping peaks corresponding to the CH group present in the omega-3 fatty acid portion) δ (ppm): 13.96, 14.24, 20.52, 20.55, 24.83, 25.50, 25.58, 27.17, 29.08, 29.14, 29.55, 34.10, 34.58, 45.14, 61.67, 62.02, 127.08, 127.71, 128.21, 128.26, 130.21, 131.93, 173.50, 176.27.

(4Z,7Z,10Z,13Z,16Z,19Z)-N-(2-(2-propylpentanamido)ethyl)docosa-4,7,10,13,16,19-hexaenamide (**5**)

The resulting residue was purified by flash chromatography (9.9:0.1 DCM/ MeOH) affording **5** as pale-white oil. Yield 48%.

^{1}H-NMR ($CDCl_3$, 400 MHz) δ (ppm): 0.87 (t, 6H, J = 8 Hz), 0.96 (t, 3H, J = 4 Hz), 1.21-1.39 (m, 6H), 1.50-1.59 (m, 2H), 2.02-2.10 (m, 3H), 2.21 (t, 2H, J = 4 Hz), 2.35-2.40 (m, 2H), 2.77-3.83 (m, 10H) 3.36 (m, 4H), 5.28-5.41 (m, 12H), 6.47 (bs, 1H), 6.62 (bs, 1H). ^{13}C-NMR ($CDCl_3$, 100 MHz, 3 overlapping peaks corresponding to the CH group present in the omega-3 fatty acid portion) δ (ppm): 14.07, 14.23, 20.52, 20.76, 23.31, 25.50, 25.55, 25.59, 35.16, 36.24,

39.77, 40.31, 47.44, 126.97, 127.83, 128.01, 128.04, 128.07, 128.08, 128.21, 128.24, 128.27, 128.53, 129.22, 131.99, 173.61, 177.54.

2-((4Z,7Z,10Z,13Z,16Z,19Z)-docosa-4,7,10,13,16,19-hexaenamido)ethyl 2-propylpentanoate (**6**)

The resulting residue was purified by flash chromatography (9.9:0.1 DCM/ MeOH) affording **6** as pale-white oil. Yield 45%.

^{1}H-NMR ($CDCl_3$, 400 MHz) δ (ppm): 0.87 (t, 6H, J = 8 Hz), 0.95 (t, 3H, J = 8 Hz), 1.21-1.38 (m, 6H), 1.52-1.61 (m, 2H), 1.99-2.08 (m, 3H), 2.37-2.38 (m, 4H), 2.78-2.84 (m, 10H), 3.49-3.53 (m, 2H), 4.15 (t, 2H J = 8), 5.26-5.43 (m, 12H), 5.79 (bs, 1H). ^{13}C-NMR ($CDCl_3$, 100 MHz, 3 overlapping peaks corresponding to the CH group present in the omega-3 fatty acid portion) δ (ppm): 14.06, 14.22, 20.51, 20.73, 22.66, 25.49, 25.55, 25.58, 25.59, 33.99, 35.17, 38.52, 47.60, 63.23, 126.96, 127.70, 127.81, 127.89, 128.01, 128.23, 128.25, 128.33, 128.53, 129.44, 131.99, 173.13, 176.13.

2-(2-propylpentanamido)ethyl (4Z,7Z,10Z,13Z,16Z,19Z)-docosa-4,7,10,13,16,19-hexaenoate (**7**)

The resulting residue was purified by flash chromatography (9.9:0.1 DCM/ MeOH) affording **7** as pale-white oil. Yield 33%.

^{1}H-NMR ($CDCl_3$, 400 MHz) δ (ppm): 0.87 (t, 6H, J = 8 Hz), 0.96 (t, 3H, J = 8 Hz), 1.22-1.40 (m, 6H), 1.52-1.62 (m, 2H), 1.99-2.08 (m, 3H), 2.38-2.49 (m, 4H), 2.78-2.85 (m, 10H), 3.49-3.53 (m, 2H), 4.16 (t, 2H J = 8), 5.28-5.42 (m, 12H), 5.75 (bs, 1H). ^{13}C-NMR ($CDCl_3$, 100 MHz, 3 overlapping peaks corresponding to the CH group present in the omega-3 fatty acid portion) δ (ppm): 14.07, 14.23, 20.52, 20.74, 22.66, 25.50, 25.56, 25.58, 25.60, 33.99, 35.18, 38.52, 47.62, 63.25, 126.96, 127.71, 127.82, 127.89, 128.01, 128.24, 128.26, 128.33, 128.54, 129.44, 132.00, 173.12, 176.10.

2-((2-propylpentanoyl)oxy)ethyl (4Z,7Z,10Z,13Z,16Z,19Z)-docosa-4,7,10,13,16,19-hexaenoate (**8**)

The resulting residue was purified by flash chromatography (9.9:0.1 DCM/ MeOH) affording **8** as pale-white oil. Yield 32%.

^{1}H-NMR ($CDCl_3$, 400 MHz) δ (ppm): 0.87 (t, 6H, J = 8 Hz), 0.96 (t, 3H, J = 8 Hz), 1.23-1.32 (m, 4H), 1.36-1.44 (m, 2H), 1.53-1.60 (m, 3H), 2.05 (t, 2H, J = 8 Hz), 2.39-2.49 (m, 4H), 2.78-2.84 (m, 10H), 4.16 (t, 4H J = 8), 5.28-5.42 (m, 12H). ^{13}C-NMR ($CDCl_3$, 100 MHz, 2 overlapping peaks corresponding to the CH group present in the omega-3 fatty acid portion) δ (ppm): 13.93, 14.21, 20.51, 20.54, 22.63, 25.49, 25.53, 25.59, 33.93, 34.55, 45.09, 61.60, 62.14, 126.97, 127.71, 127.82, 127.97, 128.02, 128.04, 128.18, 128.21, 128.24, 128.50, 129.33, 131.95, 172.67, 176.16.

General procedure for the preparation of compounds (26, **27)**

To a solution of ALA or DHA (1.2 mmol) in dry DCM (3 ml) under nitrogen, was added at 0°C, 1-etil-3 (3-dimetilaminopropil) carbodiimide chloride (EDC, 1.2 mmol) and the activation was stirred at room temperature for 1 hour in the dark. Successively, a solution contained **16** (1 mmol) and 4-dimethylaminopyridine (DMAP, 10% mmol) in dry DCM (1 ml) were added in the previous solution. The resulting mixture was stirred at room temperature around 4-6 hours. The residue was concentrated under reduce pressure and then was purified by using flash silica gel column chromatography using different eluent mixtures to give the title compounds **26**, **27**.

(9Z,12Z,15Z)-N-(2-((tert-butyldimethylsilyl)oxy)ethyl)octadeca-9,12,15-trienamide (**26**)

The resulting residue was purified by flash chromatography (9.5:0.5 DCM/ MeOH) affording **26** as pale-white oil. Yield 38%.

^{1}H-NMR ($CDCl_3$, 400 MHz) δ (ppm): 0.054 (s, 6H), 0.90 (s, 9H), 0.96 (t, 3H, J = 8 Hz), 1.30 (s, 8H), 1.61 (t, 2H, J = 8 Hz), 2.08-2.01 (m, 4H), 2.17 (t, 2H, J = 8 Hz), 2.79 (t, 4H, J = 4 Hz),

3.38-3.34 (m, 2H), 3,66 (t, 2H, J = 4 Hz), 5,40-5.29 (m, 6H), 5.80 (bs, 1H). ^{13}C-NMR ($CDCl_3$, 100 MHz) δ (ppm): -5.80, 14.25, 18.25, 20.52, 25.49, 25.58, 25.71, 25.86, 27.18, 29.10, 29.24, 29.57, 36.87, 41.50, 61.93, 127.08, 127.68, 128.22, 128.25, 130.23, 131.92, 173.00

(4Z,7Z,10Z,13Z,16Z,19Z)-N-(2-((tert-butyldimethylsilyl)oxy)ethyl)docosa-4,7,10,13,16,19-hexaenamide (**27**)

The resulting residue was purified by flash chromatography (9.8:0.2 DCM/ MeOH) affording **27** as pale-white oil. Yield 10%.

^{1}H-NMR ($CDCl_3$, 400 MHz) δ (ppm): 0.055 (s, 6H), 0.89 (s, 9H), 0.96 (t, 3H, J = 8 Hz), 2.06 (q, 2H, J = 8 Hz), 2.23 (t, 2H, J = 8 Hz), 2.40 (t, 2H, J = 8 Hz), 2.83-2.79 (m, 10H), 3.78-3.50 (m, 2H), 3.66 (t, 2H, J = 4 Hz), 5.40-5.31 (m, 12), 5.80 (bs, 1H). ^{13}C-NMR ($CDCl_3$, 100 MHz, 4 overlapping peaks corresponding to the CH group present in the omega-3 fatty acid portion) δ (ppm): -5.41, 14.16, 18.22, 20.49, 23.37, 25.50, 25.60, 25.61, 25.83, 36.49, 41.60, 61.90, 126.99, 127.84, 128.04, 128.08, 128.21, 128.23, 128.53, 129.25, 131.97, 172.11

General procedure for the preparation of compounds (9, 10)

To a cold solution of **26** or **27** (1 mmol) in dry DCM (5 ml), was added dropwise tetrabutylammonium fluoride (TBAF, 5 mmol) under anhydrous condition. The resulting mixture was stirred at room temperature until the complete disappearance of the starting material (around 12-15 hours). The reaction was directly concentrated under reduce pressure and the crude was purified by using flash silica gel column chromatography using different eluent mixtures to give the title compounds **9**, **10**.

(9Z,12Z,15Z)-N-(2-hydroxyethyl)octadeca-9,12,15-trienamide (**9**)

The resulting residue was purified by flash chromatography (9.8:0.2 DCM/ MeOH) affording **9** as pale-white oil. Yield 94%.

^{1}H-NMR ($CDCl_3$, 400 MHz) δ (ppm): 0.96 (t, 3H, J = 8 Hz), 1.29-1.24 (m, 8H), 1.61 (t, 2H, J = 8 Hz), 2.80-2.09 (m, 4H), 2.19 (t, 2H, J = 8 Hz), 2, 78 (t, 5H, J = 8 Hz), 3.93 (t, 2H, J = 8 Hz), 3.70 (t, 2H, J = 8 Hz), 5.40-5.28 (m, 6H), 6.11 (bs, 1H). ^{13}C-NMR ($CDCl_3$, 100 MHz, 2 overlapping peaks corresponding to the CH group present in the omega-3 fatty acid portion) δ (ppm): 14.25, 20.52, 25.49, 25.58, 25.68, 25.86, 27.17, 29.10, 29.22, 29.56, 36.62, 42.41, 62.38, 127.07, 127.71, 128.21, 128.26, 130.21, 131.94, 174.55.

(4Z,7Z,10Z,13Z,16Z,19Z)-N-(2-hydroxyethyl)docosa-4,7,10,13,16,19-hexaenamide (**10**)

The resulting residue was purified by flash chromatography (9.8:0.2 DCM/ MeOH) affording **10** as pale-white oil. Yield 98%.

^{1}H-NMR ($CDCl_3$, 400 MHz) δ (ppm): 0.96 (t, 3H, J = 8 Hz), 2.03-2.10 (m, 2H), 2.62 (t, 3H, J = 8 Hz), 2.39-2.44 (m, 2H), 2.84-2.74 (m, 10H), 3.43-3.39 (m, 2H), 3.71 (t, 2H, J = 8 Hz), 5.44-5.28(m, 12H), 5.96 (bs, 1H). ^{13}C-NMR ($CDCl_3$, 100 MHz, 3 overlapping peaks corresponding to the CH group present in the omega-3 fatty acid portion) δ (ppm): 14.24, 20.53, 23.36, 25.51, 25.58, 25.60, 25.62, 36.31, 42.46, 62.50, 126.98, 127.85, 127.96, 128.05, 128.26, 128.27, 128.32, 128.57, 129.47, 132.03, 173.60

Synthesis of FA/UDP-like conjugates

Chemistry

1-((2R,3R,4S,5R)-3,4-dihydroxy-5-(hydroxymethyl)tetrahydrofuran-2-yl)-3-(2-oxo-2-phenylethyl)pyrimidine-2,4(1H,3H)-dione (31)

Uridine (1 g, 4.09 mmol), anhydrous K_2CO_3 (0.960 g, 6.95 mmol), phenacyl chloride (2.03, 10.22 mmol), were dissolved in a mixture of DMF and acetone (1 : 1, 11 ml) and refluxed in an oil bath for 4 h at 120 °C. The acetone was evaporated, and 70 ml of ice was added followed by extraction with ethyl acetate. The organic phase was over anhydrous sodium sulfate and filtrated. The product was purified by using flash silica gel column chromatography using DCM: MeOH (20: 1). Yield 72%.

^{1}H NMR (600 MHz, DMSO) δ = 3.55-3.59 (m, 1H), 3.68-3.64 (m, 1H), 3.88-3.86 (m, 1H), 3.97-4.00 (m, 1H), 4.08-4.05 (m, 1H), 5.10 (d, J = 6 Hz, 1H), 5.13 (t, J = 6 Hz, 1H), 5.33 (d, J = 6 Hz, 2H), 5.40 (d, J = 6 Hz, 1H), 5.81 (d, J = 6 Hz, 1H), 5.88 (d, J = 6 Hz, 1H), 7.56-7-60 (m, 2H), 7,70-7,73 (m, 1H), 8.05-8.07 (m, 3H). ^{13}C NMR (151 MHz, DMSO) δ = 47.16, 60.88, 69.86, 73.87, 85.09, 89.14, 100.95, 128.15, 129.14, 134.22, 134.57, 139.93, 150.87, 161.76, 192.58. LC/ESI-MS: positive mode [M + H] 363, [M +NH_4] 380.

1-((2R,3R,4S,5R)-3,4-dihydroxy-5-(hydroxymethyl)tetrahydrofuran-2-yl)-5-iodo-3-(2-oxo-2-phenylethyl)pyrimidine-2,4(1H,3H)-dione (32)

In a solution of DCM (19.25 ml) containing 3.5 ml of HNO_3 (1M), was added I_2 and it was left solubilize for 5 minutes at room temperature. **31** was added to the reaction mixture (350 mg, 0.966 mmol) in little portions and the reaction was refluxed for 5 h at 50 °C. After 5 h a white precipitate was observed, and the reaction was cooled at 5 °C and filtrated. The white precipitate was filtrated and was the pure product **32**. The organic solution was composed by **32**, **31**, and

several side products. Thus, the organic solution was extract with a water solution of $Na_2S_2O_3$ (2 X 15 ml, 5%) in order to remove iodine and part of side products. Finally, the organic solvent was concentrated and purify by column chromatography using DCM: MeOH (9.5: 0.5). Yield 54% (pure product obtained after precipitation and column chromatography).

^{1}H NMR (600 MHz, DMSO) δ = 3.59-3.62 (m, 1H), 3.70-3.74 (m, 1H), 3.89-3.91 (M, 1H), 4.01-4.03 (m, 1H), 4.06-4.09 (m, 1H), 5.10 (d, J = 5 Hz, 1H), 5.30-5.32 (m, 1H), 5.39 (s, 2H), 5.44-5.45 (m, 1H), 5.76 (d, J = 6 Hz, 1H), 7.58-7.61 (m, 2H), 7.72-7.74 (m, 1H), 8.05-8.07 (m, 2H), 8.67 (s, 1H). ^{13}C NMR (151 MHz, DMSO) δ = 48.54, 60.19, 68.23, 69.34, 74.22, 84.98, 89.70, 128.17, 129.15, 134.30, 134.44, 144.33, 150.33, 159.38, 192.40. LC/ESI-MS: positive mode ([M + H] 489, [(M +NH_4] 506.

((2R,3S,4R,5R)-5-(2,4-dioxo-3-(2-oxo-2-phenylethyl)-3,4-dihydropyrimidin-1(2H)-yl)-3,4-dihydroxytetrahydrofuran-2-yl)methyl trihydrogen diphosphate (**33**)

Lyophilized nucleoside **31** (0.28 mmol) was dissolved in 1.4 mL of trimethyl phosphate (dried over 10 Å molecular sieves). The mixture was stirred at room temperature under argon and then cooled to 4 °C. Dry 1,8-bis(dimethylamino)naphthalene (Proton Sponge, 89 mg, 1.5 mmol) was added, followed by 55 mg (1.3 mmol) of $POCl_3$ 5 min later. After several hours of stirring at 0-4 °C, tri-n-butylamine (0.048 mL, 0.72 mmol) was added to the solution followed by 2.76 mL (5 mmol) of 0.5 M bis(tri-n-butylammonium) pyrophosphate in DMF. After 2-5 min the mixture was poured into a cold 0.5 M aqueous TEAC solution (30 mL, pH 7.5) and stirred at 0-4 °C for several minutes. The solution was allowed to reach room temperature upon stirring and then left standing for 1 h. Trimethylphosphate was extracted with tert-butyl methyl ether, and the aqueous solution was evaporated and lyophilized to yield glassy colorless oils. The reactions were controlled by TLC using a freshly prepared solvent system (2-propanol/NH_4OH/water) 6 : 3 : 1). The compound was purified by anion exchange chromatography (FPLC condition: the column was washed with deionized water, followed by

a solvent gradient of 5%−100% mM NH4HCO3 buffer (0.5 M) using approximately 1000 mL of solvent to elute the mono and diphosphates. Finally, to remove inorganic salts, such as inorganic phosphates and some buffer the product was further purified by reverse phase high-performance liquid chromatography (RP-HPLC column Knauer 20 mm ID, Eurospher-100 C18; condition: the column was eluted with a solvent gradient of 0−40% of acetonitrile in 50 mM aqueous NH_4HCO_3 buffer for 30 min at a flow rate of 5 mL/min). and purify as described before. Yield: 16%,

^{1}H NMR (600 MHz, D_2O) δ 4.06-4.09 (m, 1H), 4.15-4.18 (m, 1H), 4.28-4.30 (m, 1H), 4.36 (t, J = 6 Hz, 1H), 4.40 (t, J = 6 Hz, 1H), 5.51 (s, 2H), 6.00 (d, J = 6 Hz, 1H), 6.11 (m, 1H), 7.62 (t, J = 6 Hz, 2H), 7.75-7.78 (m, 1H), 8.07-8.09 (t, J = 6 Hz, 2H), 8.14 (d, J = 12 Hz, 1H). ^{13}C NMR (151 MHz, D_2O) δ 47.72, 63.56, 63.60, 69.52, 74.04, 83.43, 83.49, 89.56, 101.67, 128.24, 129.03, 133.89, 134.90, 140.33, 151.66, 164.56, 164.58, 196.00. ^{31}P NMR (243 MHz, D_2O) δ -6.56, -9.87 (J = 17.01 Hz). LC/ESI-MS: positive mode ([M + H] 523, [(M +NH_4] 540.

((2R,3S,4R,5R)-5-(2,4-dioxo-3-(2-oxo-2-phenylethyl)-3,4-dihydropyrimidin-1(2H)-yl)-3,4-dihydroxytetrahydrofuran-2-yl)methyl dihydrogen phosphate (**35**)

This product has been obtained as side product during the synthesis of compounds **33** and it has been purified and characterized. Yield 28%,

^{1}H NMR (600 MHz, D_2O) δ 4.05-4.08 (m, 1H), 4.14-4.17 (m, 1H), 4.28-4.29 (m, 1H), 4.36 (t, J = 6 Hz, 1H), 4.40-4.42 (m, 1H), 5.51 (s, 2H), 6.00 (d, J = 6 Hz, 1H), 6.11 (d, J = 6 Hz, 1H), 7.62 (t, J = 6 Hz, 2H), 7.75-7.78 (m, 1H), 8.08 (d, J = 12 Hz, 2H), 8.15 (d, J = 12 Hz, 1H). ^{13}C NMR (151 MHz, D_2O) δ 50.61, 66.37, 66.41, 72.45, 76.95, 86.41, 86.48, 92.42, 104.58, 131.14, 131.92, 136.78, 137.79, 143.27, 154.56, 163.58, 167.46, 198.90. ^{31}P NMR (243 MHz, D_2O) δ -10.78 (m). MicrOTOF-Q [M - H] 441.0707.

((2*R*,3*S*,4*R*,5*R*)-3,4-dihydroxy-5-(5-iodo-2,4-dioxo-3-(2-oxo-2-phenylethyl)-3,4-dihydropyrimidin-1(2*H*)-yl)tetrahydrofuran-2-yl)methyl trihydrogen diphosphate (34)

Lyophilized nucleoside **32** (0.28 mmol) was dissolved in 1.4 mL of trimethyl phosphate (dried over 10 Å molecular sieves). The mixture was stirred at room temperature under argon and then cooled to 4 °C. Dry 1,8-bis(dimethylamino)naphthalene (Proton Sponge, 89 mg, 1.5 mmol) was added, followed by 55 mg (1.3 mmol) of $POCl_3$ 5 min later. After several hours of stirring at 0-4 °C, tri-n-butylamine (0.048 mL, 0.72 mmol) was added to the solution followed by 2.76 mL (5 mmol) of 0.5 M bis(tri-n-butylammonium) pyrophosphate in DMF. After 2-5 min the mixture was poured into a cold 0.5 M aqueous TEAC solution (30 mL, pH 7.5) and stirred at 0-4 °C for several minutes. The solution was allowed to reach room temperature upon stirring and then left standing for 1 h. Trimethylphosphate was extracted with tert-butyl methyl ether, and the aqueous solution was evaporated and lyophilized to yield glassy colorless oils. The reactions were controlled by TLC using a freshly prepared solvent system (2-propanol/NH_4OH/water) 6 : 3 : 1) and purify as described before. The compound was purified by anion exchange chromatography (FPLC condition: the column was washed with deionized water, followed by a solvent gradient of 5%−100% mM NH_4HCO_3 buffer (0.5 M) using approximately 1000 mL of solvent to elute the mono and diphosphates. Finally, to remove inorganic salts, such as inorganic phosphates and some buffer the product was further purified by reverse phase high-performance liquid chromatography (RP-HPLC column Knauer 20 mm ID, Eurospher-100 C18; condition: the column was eluted with a solvent gradient of 0−40% of acetonitrile in 50 mM aqueous NH_4HCO_3 buffer for 30 min at a flow rate of 5 mL/min). and purify as described before. Yield: 0 %

((2R,3S,4R,5R)-3,4-dihydroxy-5-(5-iodo-2,4-dioxo-3-(2-oxo-2-phenylethyl)-3,4-dihydropyrimidin-1(2H)-yl)tetrahydrofuran-2-yl)methyl dihydrogen phosphate (36)

This product has been obtained as side product during the synthesis of compounds **34** and it has been purified and characterized. Yield 37%

^{1}H NMR (600MHz, D_2O) δ 4.09-4.12 (m, 1H), 4.15-4.18 (m, 1H), 4.28-4.30 (m, 1H), 4.34 (t, J = 6 Hz, 1H), 4.41 (t, J = 6 Hz, 1H), 5.58 (s, 2H), 5.95 (d, J = 6 Hz, 1H), 7.62 (t, J = 6 Hz, 2H), 7.77 (t, J = 6 Hz, 2H), 8,08 (d, J = 6 Hz, 2H), 8.41 (s, 1H). ^{13}C NMR (151 MHz, D_2O) δ 49.14, 63.89, 63.93, 67.15, 69.54, 73.98, 83.52, 83.58, 89.90, 128.25, 129.03, 133.86, 134.91, 144.69, 151.25, 161.73, 167.28, 195.67. ^{31}P NMR (243 MHz, D_2O) δ -11.02 (m). MicrOTOF-Q [M - H] 566.9650.

N-(2-hydroxyethyl)stearamide (**37**)

A solution of stearic acid (600 mg, 2.1 mmol) and NEt_3 (0.6 ml, 4.2 mmol) in DCM (50 ml) was stirred for 5 minutes at 0 °C. Then, ethyl chloroformate (0.4 ml, 4.2 mmol) was added dropwise slowly and the reaction was stirred for 1 hour at room temperature. Successively, ethanolamine (0.254 ml, 4.2 mmol) was added to the solution and the mixture was stirred overnight at room temperature. The white suspension obtained was concentrated at reduced pressure and the crude was purify by silica gel column chromatography using DCM: MeOH (9.5: 0.5). Yield 90%

^{1}H NMR (600 MHz, $CDCl_3$) δ 0.88 (t, J = 6 Hz, 3H), 1.25-1.32 (m, 28H), 1.63 (q, J = 6 Hz, 2H), 2.21 (t, J = 12 Hz, 2H), 2.49 (bs, 1H), 3.41-3.43 (m, 2 H), 4.72 (t, J = 6 Hz, 2H), 6.10 (bs, 1H). ^{13}C NMR (151 MHz, $CDCl_3$) δ 14.09, 25.73, 29.27, 29.33, 29.34, 29.47, 29.60, 29.64, 29.66, 29.68, 31.91, 36.60, 42.55, 62.50, 174.70. LC/ESI-MS: positive mode ([M + H] 328, [(M +Na] 350.

N-(2-bromoethyl)stearamide (**38**)

To a stirred suspension of **37** (200 mg, 0.6 mmol) in dry DCM (20 ml) was added dropwise PBr_3 (0.8 mmol) at 0 °C and the reaction was stirred overnight under argon. To the colorless

solution was added water (5 ml) and a white precipitate was formed and filtrated. The white solid was purified by silica gel column chromatography using petroleum ether: ethyl acetate (7: 3). Yield 54%.

^{1}H NMR (600 MHz, $CDCl_3$) δ 0.88 (t, J = 6 Hz, 3H), 1.25-1.32 (m, 28H), 1.61-1.65 (m, 2H), 2.20 (t, J = 12 Hz, 2H), 3.49 (t, J = 6 Hz, 2H), 3.65-3.68 (m, 2H), 5.86 (bs, 1H). ^{13}C NMR (151 MHz, $CDCl_3$) δ 14.07, 22.63, 25.61, 29.19, 29.28, 29.30, 29.42, 29.55, 29.59, 29.60, 29.62, 29.64, 31.86, 32.81, 36.65, 40.97, 173.23. Standard LC/ESI-MS cannot detect this molecule.

General procedure for compounds 28, **29**

To a solution of UDP or **33** (0.064 mmol) in 0.5 ml of dry DMF, was added a solution of **38** (0.93 mmol) in 1 ml of dry DMF and NBu_3 (1 mmol). The reaction was stirred for 24 hours at 45 °C, under argon atmosphere. After 24 hours a new molecule was detected by TLC (eluent iso-propanol/ NH_3 25% H_2O/ H_2O = 6/3/1). The crude of reaction is purify first using FPLC followed by RP-HPLC. Unfortunately, from micrOTOF-Q analysis the product obtained is not the target compounds.

Unfortunately, before the end of the Grant Period we did not finish to fully purify and characterize the two final products. Thus, to complete the first part of the project I prolongated my period for other two week out-side of the Grant Period in order to obtain at least the two final compounds.

Synthesis of dual sustainable HDAC/ferroptosis inhibitors

Chemistry

(E/Z)-1,16-bis(3-methoxyphenyl)hexadec-8-ene (**54**)

A solution of Grubbs I catalyst (0.075 mmol, 7.5% mol) in DCM (3 mL) was added at a 0.5 mL/h rate in a boiling solution of **47** (1.0 mmol, 1 eq) in DCM (3 mL). After complete addition, the solution was refluxed for 1 h. The reaction was directly concentrated under reduce pressure and the resulting yellow oil was purified by flash chromatography, ethyl acetate: pentane (0:100; 2.5:97.5; 5:95; 7.5:92.5 with 10:90) in order to obtain the dimer compounds (e/z).

Compounds **54** was obtained as a colorless oil. Yield 16%.

^{1}H-NMR ($CDCl_3$, 400 MHz) δ (ppm): 0.86-0.89 (m, 4H), 1.25-1-29 (m, 12H), 1.57-1.59 (m, 4H), 1.94-1.96 (m, 4H), 2.57 (t, 4H, J = 7.6 Hz), 3.79 (s, 6H), 5.37-5.40 (m, 2H), 6.71-6.78 (m, 6H), 7.17-7.21 (m, 2H). ^{13}C-NMR ($CDCl_3$, 100 MHz) δ (ppm): 14.2, 22.7, 29.4, 29.8, 31.4, 32.6, 36.0, 55.1, 110.8, 114.2, 120.9, 129.2, 129.9, 130.4, 144.6, 159.6. HRMS: $C_{35}H_{47}NO_8$ calc for [M+H$^+$] $C_{35}H_{47}NO_7$ 437.3431 found 437.3414; [M+Na$^+$] $C_{35}H_{47}NNaO_7$ 459.3235 found 459.3234

(Z)-1-(benzyloxy)-3-(pentadec-8-en-1-yl)-benzene (**56**)

To a solution of **47** (1.4g, 1 eq) in DMF (11ml) was added K_2CO_3 (0.767 g, 1.2 g) and the reaction was stirred 30 minutes. Then, to the solution was added benzyl bromide (0.870, 1.1 eq) and stirred for 24 h at room temperature. The reaction was quenched adding 20 ml of water and it was extracted with DCM (2 x 15 ml). The organic layer was concentrated under reduced pressure and it was purified by column chromatography with pentane / DCM (8.5/1.5).

Compound **56** was obtained as a pale-yellow oil. Yield 98%.

^{1}H-NMR ($CDCl_3$, 400 MHz) δ (ppm): 0.88 (q, 3H), 1.25-1.27 (m, 16H), 1.60-1.65 (m, 2H), 2.01 (t, 4H, J = 9 Hz), 2.57 (t, 2H, J = 9 Hz), 5.04 (s, 2H), 5.31-5.36 (m, 2H), 6.76-6.80 (m, 3H), 7.12-7.20 (m, 1H), 7.29-7.38 (m, 5H). ^{13}C-NMR ($CDCl_3$, 100 MHz) δ (ppm): 14.20, 22.75, 27.27, 20.07, 29.30, 29.37, 29.49, 29.60, 29.82, 31.43, 31.87, 36.08, 53.47, 69.91, 111.72, 115.19, 121.19, 127.57, 127.94, 128.22, 128.60, 129.22, 129.89, 130.00, 130.18, 137.25, 144.67, 158.88. HRMS: MW 392.31 $C_{28}H_{40}O$ calc for [M+Na^+] $C_{28}H_{40}NaO$ 415.2986 found 415.2971

General procedure for the cross-metathesis reaction (57-62)

Procedure A) In a boiling solution of **47**, **48**, **56** (1.0 mmol, 1 eq) and **50** (2.0 mmol, 2 eq) in DCM (3 ml) was added dropwise a solution of Grubbs I catalyst (0.075 mmol, 7.5% mol) in DCM (3 mL). The addition was completed in 6 hours (0.5 mL/h rate), after that it was refluxed 1 h. The reaction was directly concentrated under reduce pressure and the resulting yellow oil was purified by flash chromatography with ethyl acetate: pentane (0:100; 2.5:97.5; 5:95; 7.5:92.5 with 10:90) in order to obtain the dimer compounds (e/z).

Procedure B) In a boiling solution of **47**, **48**, **56** (1.0 mmol, 1 eq) and **51** (2.0 mmol, 2 eq) in DCM (3 ml) was added dropwise a solution of Grubbs I catalyst (0.075 mmol, 7.5% mol) in DCM (3 mL). The addition was completed in 6 hours (0.5 mL/h rate), after that it was refluxed 1 h. The reaction was directly concentrated under reduce pressure and the resulting yellow oil was purified by flash chromatography with ethyl acetate: pentane (0:100; 2.5:97.5; 5:95; 7.5:92.5 with 10:90) in order to obtain the dimer compounds (e/z).

(E/Z)-3-(12-((tert-butoxycarbonyl)((tert-butoxycarbonyl)oxy)amino)-12-oxododec-8-en-1-yl)phenyl benzoate (**57**)

Procedure A: Compound **57** was obtained as a pale-yellow oil. Yield 28%.

^{1}H-NMR ($CDCl_3$, 400 MHz) δ (ppm):1.27-1.30 (m, 8H), 1.54 (s, 18), 1.60-1.63 (m, 2H), 2.00-2.04 (m, 2H), 2.38 (m, 2H), 2.60-2.65 (m, 2H), 2.91-2.92 (m, 2H), 5.45 (s, 2H), 7.10-7.19 (m, 3H), 7-43-7.35 (m, 4H), 8.21-8.27 (m, 2H). ^{13}C-NMR ($CDCl_3$, 100 MHz) δ (ppm): 14.13, 27.31, 27.55, 27.60, 27.90, 28.06, 29.10, 29.27, 29.35, 29.44, 29.72, 31.26, 32.54, 35.79, 53.50, 118.85, 121.57, 126.05, 128.08, 128. 59,129.22, 129.69, 130.18, 133.55, 144.78, 150.92, 165.31. HRMS: $C_{35}H_{47}NO_8$ calc for [M+Na^+] $C_{35}H_{47}NNaO_7$ 609.3328 found 609.3332.

tert-butyl (E/Z)-((tert-butoxycarbonyl)oxy)(12-(3-methoxyphenyl)dodec-4-enoyl)carbamate (58)

Procedure A: Compound **58** was obtained as a pale-yellow oil. Yield 20%.

^{1}H-NMR ($CDCl_3$, 400 MHz) δ (ppm): 1.27-1.30 (m, 10H), 1.56 (s, 18H), 1,95-1.99 (m, 2H), 2.37-2.40 (m, 2H), 2.57 (t, 2H, J = 10.5Hz), 2.92-2.95 (m, 2H), 3.79 (s, 3H), 5.40-5.45 (m, 2H), 6.76-6.80 (m, 3H), 7.18-7.25 (m, 1H) ^{13}C-NMR ($CDCl_3$, 100 MHz) δ (ppm): 27.21, 27.94, 29.12, 29.72, 31.42, 32.53, 36.04, 36.97, 53.46, 55.13, 85.20, 85.94, 110.81, 114.15, 120.87, 127.83, 129.15, 131.93, 144.64, 149.59, 151.25, 159.54, 169.54. MW 519.32; HRMS: $C_{29}H_{45}NO_7$ calc for [M+Na^+] $C_{29}H_{45}NNaO_7$ 542.3088 found 542.3088.

tert-butyl(E/Z)-(12-(3-(benzyloxy)phenyl)dodec-4-enoyl)((tert-butoxycarbonyl)oxy)carbamate (**59**)

Procedure A: Compound **59** was obtained as a pale-yellow oil. Yield 38%.

^{1}H-NMR ($CDCl_3$, 400 MHz) δ (ppm): 1.28-1.30 (m, 10H), 1.57 (s, 18H), 1.96-2.00 (m, 2H), 2.37-2.40 (m, 2H), 2.57 (t, 2H, J = 8.5 Hz), 2.92-2.94 (m, 2H), 5.04 (s, 2H), 5.44 (m, 2H), 6.80-6.85 (m, 3H), 7.17-7.20 (m, 1H), 7.32-7.40 (m, 3H), 7.45-7.47 (m, 2H). ^{13}C-NMR ($CDCl_3$, 100 MHz) δ (ppm): 27.23, 27.41, 27.54, 27.89, 27.95, 29.13, 29.29, 29.38, 29.66, 31.39, 32.54, 34.14, 36.98, 69.89, 85.94, 111.71, 121.17, 126.10, 127.55, 127.90, 128.47, 129.18, 131.58,

137.21, 144.67, 149.60, 151.26, 158.82, 169.54. HRMS. MW 595.35; $C_{35}H_{49}NO_7$ calc for [M+Na^+] $C_{35}H_{49}NNaO_7$ 595.3547 found 595.3553

(E/Z)-3-(12-((2-((tert-butoxycarbonyl)amino)phenyl)amino)-12-oxododec-8-en-1-yl)phenyl benzoate (**60**)

Procedure B: Compound **60** was obtained as a pale-yellow oil. Yield 44%.

^{1}H-NMR ($CDCl_3$, 400 MHz) δ (ppm): 1.20-1.25 (m, 8H), 1.51 (s, 9H), 1.58-1.61 (m, 2H), 1.99-2.03 (m, 2H), 2.41 (s, 4H), 2.62 (t, 2H, 10.5 Hz), 5.50-5.54 (m, 2H), 6.91 (bs, 1H), 7.16-7.20 (m, 5H), 7.35-7.40 (m, 3H), 7.48-7.53 (m, 2H), 7.61-7.65 (m, 1H), 8.19-8.21 (bs, 1H), 8.21 (m, 2H). ^{13}C-NMR ($CDCl_3$, 100 MHz) δ (ppm): 23.51, 27,25, 28.33, 29.04, 29.63, 31.22, 32.56, 35.76, 37.23, 80.85, 118.86, 121.55, 124.34, 125.24, 125.42, 126.06, 127.23, 127.31, 127.93, 128.59, 129.23, 129.65, 129.75, 130.17, 131.96, 132.92, 133.60, 144.76, 150.91, 154.14, 165.29, 171.85. HRMS: MW 584.33; $C_{36}H_{44}N_2O_5$ calc for [M+Na^+] 607.3150 found $C_{36}H_{44}N_2NaO_5$ 607.3142.

tert-butyl (E/Z)-(2-(12-(3-methoxyphenyl)dodec-4-enamido)phenyl)carbamate (**61**)

Procedure B: Compound **61** was obtained as a pale-yellow oil. Yield 47%.

^{1}H-NMR ($CDCl_3$, 400 MHz) δ (ppm): 1.25-1.28 (m, 8H), 1.52 (s, 11H), 1.94-2.01 (m, 2H), 2.42 (s, 4H), 2.57 (t, 2H, J = 9 Hz), 5.46-5.51 (m, 2H), 6.71-6.77 (m, 3H), 6.87 (bs, 1H), 7.13-7.21 (m, 3H), 7.39-7.42 (m, 2H), 7.90 (t, 1H, J = 6 Hz). ^{13}C-NMR ($CDCl_3$, 100 MHz) δ (ppm): 28.31, 28.69, 29.10, 29.28, 29.46, 29.65, 31.40, 32.57, 36.02, 37.32, 53.46, 55.14, 80.94, 110.78, 114.22, 120.87, 124.41, 125.41, 126.26, 127.88, 129.17, 129.90, 130.75, 132.37, 144.59, 154.46, 159.39, 171.70. HRMS: MW 584.33; $C_{36}H_{44}N_2O_5$ calc for [M+Na^+] 607.3150 found $C_{36}H_{44}N_2NaO_5$: 607.3142 HRMS: MW 494.31; $C_{30}H_{42}N_2O_4$ calc for [M+Na^+] $C_{30}H_{42}N_2NaO_4$ 517.3045 found 517.3037

tert-butyl (E/Z)-(2-(12-(3-(benzyloxy)phenyl)dodec-4-enamido)phenyl)carbamate (**62**)

Procedure B: Compound **62** was obtained as a pale-yellow oil. Yield 46%.

^{1}H-NMR ($CDCl_3$, 400 MHz) δ (ppm): 1.26-1.28 (m, 8H), 1.51 (m, 11H), 1.98-1.99 (m, 2H), 2.40 (s, 4H), 2.56 (t, 2H, J = 11 Hz), 5. 04 (s, 2H), 5.45-5.50 (2H), 6.78-6.81 (m,3H), 6.93 (bs, 1H), 7.10-7.20 (m, 3H), 7.31-7.40 (m, 7H), 8.08 (bs, 1H). ^{13}C-NMR ($CDCl_3$, 100 MHz) δ (ppm): 27.28, 28.33, 29.12, 29.48, 31.37, 32.60, 34.68, 36.01, 37.26, 41.14, 69.90, 80.90, 111.68, 115,18, 121.17, 124.40, 125.33, 124.45, 126.26, 127.29, 127.93, 128.08, 129.21, 129.83, 130.83, 132.00, 132.34, 137.17, 144.64, 154.17, 158.83, 171.81. HRMS: MW 570,35 $C_{36}H_{46}N_2O_4$, calc for [M+Na^+] $C_{36}H_{46}N_2NaO_4$ 593.3360 found 593.3350

General procedure for the reduction reaction (63-70)

Pd/C 5% (0.9 mmol, 3 eq) was added to a solution of **57**-**62** (0.3 mmol, 1eq) in ethyl acetate (2 mL). After 3 h stirring under hydrogen atmosphere, the solution was diluted with DCM (10 mL) and filtered on silica with ethyl acetate : pentane (50:50) in order to obtain the desired compounds.

3-(12-((tert-butoxycarbonyl)((tert-butoxycarbonyl)oxy)amino)-12-oxododecyl)phenyl benzoate (**63**)

Compound **63** was obtained as a colorless oil. Yield 85%.

^{1}H-NMR ($CDCl_3$, 400 MHz) δ (ppm): 1.25-1.30 (m, 12H), 1.54 (s, 22H), 1.63-1.65 (m, 2H), 2.62-2.65 (m, 2H), 2.82-2.86 (m, 2H), 7.10-7.34 (m 4H), 7.47-7.53 (m, 2H), 7.61-7.65 (m, 1), 8.19-8.20 (m, 2H). ^{13}C-NMR ($CDCl_3$, 100 MHz) δ (ppm): 27.53, 27.88, 28.02, 29.04, 29.16, 29.32, 29.35, 29.46, 29.49, 31.27, 31.91, 36.12, 36.87, 85.36, 85.90, 118.83, 121.55, 126.04, 128.57, 129.19, 129.70, 130.16, 133.53, 144.81, 149.62, 150.92, 151.28, 165.28, 170.14. HRMS: MW 611.35; $C_{35}H_{49}NO_8$ calc for [M+Na^+] $C_{35}H_{49}NNaO_8$ 634.3371 found 634.3350.

tert-butyl ((tert-butoxycarbonyl)oxy)(12-(3-methoxyphenyl)dodecanoyl)carbamate (64)

Compound **64** was obtained as a colorless oil. Yield 91%.

^{1}H-NMR ($CDCl_3$, 400 MHz) δ (ppm): 1.26-1.29 (m, 14H), 1.54 (s, 18H) 1.65-1.67 (m, 4H), 2.57 (t, 2H, J = 10.5Hz), 2.84-2.86 (m, 2H), 3.79 (s, 3H), 6.70-6.78 (m, 3H), 7.16-7.20 (m, 1H). ^{13}C-NMR ($CDCl_3$, 100 MHz) δ (ppm): 27.53, 27.88, 29.04, 29.45, 29.52, 29.57, 30.96, 31.43, 36.05, 36.86, 55.12, 85.11, 85.89, 110.81, 114.13, 120.87, 129.14, 144.66, 149.62, 151.27, 159.54, 170.13, 207.21. HRMS: MW 496.33; $C_{30}H_{44}N_2O_4$ calc for [M+H$^+$] 497.3388 found $C_{30}H_{45}N_2O_4$ 497.3374; calc for [M+Na$^+$] 519.3206 found $C_{30}H_{44}N_2NaO_4$ 519.3193.

tert-butyl (12-(3-(benzyloxy)phenyl)dodecanoyl)((tert-butoxycarbonyl)oxy)carbamate (65)

Compound **65** was obtained as a colorless oil. Yield 50%.

^{1}H-NMR ($CDCl_3$, 400 MHz) δ (ppm): 1.28-1.30 (m, 14H), 1.52-1.68 (m, 22H), 2.57 (t, 2H, J = 9 Hz), 2.84 (t, 2H, J = 9 Hz), 5.05. (s, 2H), 6.78-6.81 (m, 3H), 7.16-7.20 (m, 1H), 7.31-7.36 (m, 1H), 7.40-7.45 (m, 4H). ^{13}C-NMR ($CDCl_3$, 100 MHz) δ (ppm): 27.54, 27.89, 27.94, 29.05, 29.35, 29.36, 29.47, 29.73, 31.40, 36.04, 36.87, 69.88, 85.11, 85.90, 111.72, 115.12, 121.17, 127.54, 127.89, 127.90, 129.18, 137.21, 144.69. 149.63, 151.29, 158,82, 170.137. HRMS: MW 597.37; $C_{35}H_{51}NO_7$ calc for [M+Na$^+$] $C_{35}H_{51}NNaO_7$ 620.3562 found 620.3558.

3-(12-((2-((tert-butoxycarbonyl)amino)phenyl)amino)-12-oxododecyl)phenyl benzoate (66)

Compound **66** was obtained as a colorless oil. Yield 92%.

^{1}H-NMR ($CDCl_3$, 400 MHz) δ (ppm): 1.30 (m, 14H), 1.50 (s, 9H), 1.66 (m, 4H), 2.33 (t, 2H, J = 10.5 Hz), 2.63 (t, 2H, J = 10.5 Hz), 6.99-7.11 (m, 6H), 7.29-7.38 (m, 1H), 7.48-7.52 (m, 2H), 7.60-7.64 (m, 1H), 8.12 (bs, 1H), 8.14-8.17 (m, 2H). ^{13}C-NMR ($CDCl_3$, 100 MHz) δ (ppm): 28.32, 29.23, 29.52, 29.55, 29.62, 30.96, 31.26, 35.69, 35.79, 37.33, 53.47, 60.45, 80.81, 118.85, 121.55, 124.49, 125.34, 126.05, 127.83, 128.37, 128.41, 128.59, 129.21, 129.66,

130.16, 130.81, 133.58, 144.79, 150.91, 154.22, 165.35, 172.49. HRMS: MW 486,29, $C_{31}H_{38}N_2O_3$ calc for $C_{31}H_{38}N_2NaO_3$ [M+Na^+] 509.2795 found 509.2775

tert-butyl (2-(12-(3-methoxyphenyl)dodecanamido)phenyl)carbamate (**67**)

Compound **67** was obtained as a colorless oil. Yield 100%.

^{1}H-NMR ($CDCl_3$, 400 MHz) δ (ppm): 1.25-1.30 (m, 12H), 1.51 (s, 11H), 1.58-1.60 (m, 2H), 1.68-1.70 (m, 2H), 2-36-2.36 (t, 2H, J = 9 Hz), 2.56-2.59 (t, 2H, J = 9.5 Hz), 3.80 (s, 3H), 6.78-6.78 (m, 3H), 6.95 (bs, 1H), 7.10-7.19 (m, 3H), 7.36-7.40 (m, 2H), 8.11 (bs, 1H). ^{13}C-NMR ($CDCl_3$, 100 MHz) δ (ppm): 25.80, 28.32, 29.20, 29.25, 29.36, 29.40, 29.53, 29.58, 29.64, 31.43, 36.05, 37.35, 55.13, 80.84, 110.784, 114.198, 120.88, 124.53, 125.40, 126.18, 128.37, 129.17, 130.05, 130.77, 144.63, 154.25, 159.55, 172.48. HRMS: MW 496.33; $C_{30}H_{44}N_2O_4$ calc for [M+H^+] 497.3388 found $C_{30}H_{45}N_2O_4$ 497.3374 calc for [M+Na^+] 519.3206 found $C_{30}H_{44}N_2NaO_4$ 519.3193.

tert-butyl (2-(12-(3-(benzyloxy)phenyl)dodecanamido)phenyl)carbamate (**68**)

Compound **68** was obtained as a colorless oil. Yield 50%.

^{1}H-NMR ($CDCl_3$, 400 MHz) δ (ppm):1.27-1.29 (m, 14H), 1.51 (s, 9H), 1.58-1.61 (m, 2H), 1.68-1.70 (m, 2H), 2.33 (t, 2H, J = 9.5 Hz), 2.60 (t, 2H, J = 9.5 Hz), 5.04 (s, 2H), 6.78-6.81 (m, 3H), 6.94 (bs, 1H), 7.10-7.20 (m, 2H), 7.31-7.38 (m, 6H), 8.07 (bs, 1H). ^{13}C-NMR ($CDCl_3$, 100 MHz) δ (ppm):22.67, 25.81, 28.33, 29.08, 29.26, 29.36, 29.42, 29.55, 29.59, 29.66, 31.40, 36.04, 37.36, 69.90, 80.85, 111.682, 115.168, 121.174, 124.53, 125.41, 126.19, 127.56, 127.93, 128.58, 129.20, 130.05, 130.77, 137.17, 144.67, 154.25, 158.83, 172.47. HRMS: MW 572,36 $C_{36}H_{48}N_2O_4$ calc for [M+Na^+] $C_{36}H_{48}N_2NaO_4$ 595.3519 found 595.3506.

tert-butyl ((tert-butoxycarbonyl)oxy)(12-(3-hydroxyphenyl)dodecanoyl)carbamate (**69**)

Compound **69** was obtained as a colorless oil. Yield 46%.

^{1}H-NMR ($CDCl_3$, 400 MHz) δ (ppm): 1-28-1.29 (m, 14H), 1.53-1.69 (s, 22H), 2.54 (t, 2H, J = 10.5Hz), 2.81-2.86 (m, 2H), 6.63-6.66 (m, 1H), 6.74-6.76 (m, 1H), 7.12 (t, 2H, J = 4.5 Hz). ^{13}C-NMR ($CDCl_3$, 100 MHz) δ (ppm): 24.39, 27.52, 27.88, 28.98, 29.16, 29.27, 29.36, 29.42, 29.59, 31.23, 35.81, 36.86, 85.25, 86.03, 112.48, 115.35, 120.77, 129.31, 144.87, 149.87, 151.30, 155.66, 170.34. HRMS: MW 507.32; $C_{28}H_{45}NO_7$ Calc for [M+Na^+] $C_{28}H_{45}NNaO_7$ 530.3106 found 530.3088.

tert-butyl (2-(12-(3-hydroxyphenyl)dodecanamido)phenyl)carbamate (**70**)

Compound **70** was obtained as a colorless oil. Yield 44%.

^{1}H-NMR ($CDCl_3$, 400 MHz) δ (ppm): 1.25-1.27 (m, 14H), 1.51-1.59 (m, 11H), 1.69-1.73 (m, 2H), 2.37 (t, 2H, J = 9.5 Hz), 2.53 (t, 2H, J = 9.5 Hz), 6.62-6.71 (m, 3H), 6.86 (bs, 1H), 7.10-7.16 (m, 3H), 7.35-7.39 (m, 1H), 7.46-7.49 (m, 1H), 8.12 (bs, 1H). ^{13}C-NMR ($CDCl_3$, 100 MHz) δ (ppm):25.77, 28.31, 28.90, 29.02, 29.11, 29.16, 29.22, 29.26, 29.28, 29.32, 31.13, 35.77, 37.43, 53.46, 81.11, 112.57, 115.39, 120.59, 124.61, 125.69, 126.31, 129.28, 130.14, 130.54, 154.34, 155.86, 172.70. HRMS: MW 482,31, $C_{29}H_{42}N_2O_4$ calc for [M+Na^+] $C_{29}H_{42}N_2NaO_4$ 505.3052 found 505.3037

General procedure for the deprotection reaction (39-46)

A compound **63-70** (0.2 mmol, 1 eq) was solubilized in DCM (1mL), then 0.5 mL of TFA (6.5 mmol, 30 eq) was added to the reaction mixture, and it was stirred at room temperature for 3 h. The resulting solution was dried under reduced pressure. The crude was resolubilized with of DCM and the product was precipitate adding some drops of pentane. The precipitate was purified removing the organic solvent. The white solid obtained was washed several times with pentane in order to obtain the desired product.

N-hydroxy-12-(3-methoxyphenyl)dodecanamide (**39**)

Compound **39** was obtained as a colorless oil. Yield 67%.

^{1}H-NMR (DMSO-d6, 400 MHz) δ (ppm): 1.23 (s, 14H), 1.46-1.54 (m, 4H), 1.94 (t, 2H, J = 11Hz), 2.54 (s, 2H), 3.73 (s, 3H), 6.718-6.76 (m, 3H), 7.15-7.19 (m, 1H), 8.67 (bs, 1H), 10.33 (bs, 1H). ^{13}C-NMR (DMSO-d6, 100 MHz) δ (ppm): 25.59, 29.06, 29.15, 29.23, 29.34, 29.41, 29.48, 30.18, 31.38, 32.72, 35.68, 55.30, 111.44, 114.35, 120.98, 129.63, 144.63, 144.40, 159.69, 169.56

3-(12-(hydroxyamino)-12-oxododecyl)phenyl benzoate (**40**)

Compound **40** was obtained as a colorless oil. Yield 25%.

^{1}H-NMR (DMSO-d6, 400 MHz) δ (ppm): 1.29 (s, 14H), 1.46-1.58 (m, 4H), 1.92 (t, 2H, J = 10Hz), 2.52-2.54 (m, 2H), 3.34 (s, 3H), 7.08-7.15 (m, 3H), 7.35-7.39 (m, 1H), 7.60-7-64 (m, 2H), 7.76-7.79 (m, 1H), 8.15 (m, 2H), 8.66 (s, 1H), 10.32 (s, 1H). ^{13}C-NMR (DMSO-d6, 100 MHz) δ (ppm): 25.58, 29.07, 29.22, 29.31, 29.41, 29.45, 31.06, 31.21, 32.71, 35.28, 119.58, 122.05, 126.41, 129.43, 129.48, 129.73, 130.20, 134.47, 144.73, 151.07, 165.06, 169.55. HRMS: MW 411,24, $C_{25}H_{33}NO_4$ calc for [M+Na^+] $C_{25}H_{33}NaNO_4$ 434.2309 found 434.2302.

12-(3-(benzyloxy)phenyl)-N-hydroxydodecanamide (**41**)

Compound **41**was obtained as a colorless oil. Yield 97%.

^{1}H-NMR (DMSO-d6, 400 MHz) δ (ppm):1.23 (s, 14H), 1.49-1.50 (m, 4H), 1.92 (t, 2H, J = 11 Hz), 2.52-2.56 (m, 2H), 5.07 (s, 2H), 6.80-6.87 (m, 3H), 7.15-7.19 (m, 1H), 7.39-7.44 (m, 5H), 8.68 (bs, 1H), 10.35 (bs, 1H). ^{13}C-NMR (DMSO-d6, 100 MHz) δ (ppm): 25.61, 29.05, 29,11, 29.34, 29.42, 29.47, 30.19, 31.31, 32.64, 34.60, 35.65, 39.32, 39.74, 39.95, 40.16, 40.37, 69.46, 112.34, 115.25, 121.24, 128.02, 128.13, 128.22, 128.74, 128.86, 128.92, 129.07, 129.66, 137.69, 144.44, 158.80. HRMS: MW 397.26; $C_{25}H_{35}NO_3$ Calc for [M+H^+] $C_{25}H_{36}NO_3$ 398.2693 found 398.2690

N-hydroxy-12-(3-hydroxyphenyl)dodecanamide (**42**)

Compound **42** was obtained as a colorless oil. Yield 88%.

^{1}H-NMR (DMSO-d6, 400 MHz) δ (ppm):1.23 (s, 16H), 1.51-1.53 (m, 4H), 1.93 (t, 2H, J = 9Hz), 6.56-6.60 (m, 3H), 7.04 (t, 1H, J = 10.5Hz), 8.68 (bs, 1H), 9.22 (bs, 1H), 10.35 (bs, 1H). ^{13}C-NMR (DMSO-d6, 100 MHz) δ (ppm): 25.90, 29.05, 29.13, 29.22, 29.36, 29.42, 29.48, 31.18, 31.35, 32.70, 35.61, 113.00, 114.68, 115.58, 119.38, 129.56, 144.19, 157.70. HRMS: MW 307,21; $C_{18}H_{29}NO_3$ calc for [M+Na^+] 330.2049 found $C_{18}H_{29}NNaO_3$ 330.2040

N-(2-aminophenyl)-12-(3-methoxyphenyl)dodecanamide (**43**)

Compound **43** was obtained as a colorless oil. Yield 57%.

^{1}H-NMR (DMSO-d6, 400 MHz) δ (ppm):1.26-1.30 (m,14H), 1.52-1.56 (m, 4H), 2.30 (t, 2H, J = 9.5 Hz), 2.51-2.54 (m, 2H), 3.73 (s, 3H), 4.82 (bs, 1H), 6.48-6.53 (m, 1H), 6.63-6.72 (m, 4H), 6.89-6.93 (m, 1H), 7.17-7.19 (m, 2H), 9.11 (bs, 1H). ^{13}C-NMR (DMSO-d6, 100 MHz) δ (ppm): 14.55, 21.22, 25.78, 29.15, 29.28, 29.35, 29.43, 29.48, 31.38, 35.68, 36.22, 55.30, 55.40, 60.23, 111.45, 114.35, 116.34, 116.60, 120.99, 124.04, 125.71, 126.13, 129.64, 142.34, 144.41, 159.69, 171.63.

3-(12-((2-aminophenyl)amino)-12-oxododecyl)phenyl benzoate (**44**)

Compound **44** was obtained as a colorless oil. Yield 64%.

^{1}H-NMR (DMSO-d6, 400 MHz) δ (ppm):1.29 (m, 14H), 1.58 (m, 4H), 2.29 (t, 2H, J = 10.5 Hz), 2.62 (t, 2H, J = 10.5 Hz), 4.84 (bs, 2H), 6.51 (t, 1H, J = 10.5 Hz), 6.72 (m, 1H), 6.90 (m, 1H), 7.10 (m, 4H), 7.39 (m, 1H), 7.62(m, 2H), 7.77 (m, 1H), 8.12 (m, 2H), 9.11 (bs, 1H). ^{13}C-NMR (DMSO-d6, 100 MHz) δ (ppm): 22.96, 25.78, 29.07, 29.14, 29.28, 29.45, 31.22, 35.28, 36.22, 55.90, 60.23, 116.35, 116.62, 119,59, 122.06, 124.04, 125.70, 126.13126.43, 129.45, 129.74, 130.21, 134.48, 142.32, 144.74, 151.06, 165.08, 170.82, 171,62

N-(2-aminophenyl)-12-(3-(benzyloxy)phenyl)dodecanamide (**45**)

Compound **45** was obtained as a colorless oil. Yield 64%.

^{1}H-NMR (DMSO-d6, 400 MHz) δ (ppm):1.24 (m, 14H), 1.52 (m,4H), 2.25 (t, 2H, J = 9.5 Hz), 2.46 (t, 2H, J = 9.5 Hz), 4.78 (bs, 2H), 5.03 (s, 2H), 6.47 (m, 1H), 6.78 (m, 5H), 7.09. (m, 2H), 7.36 (m, 5H), 9.06. (bs, 1H). ^{13}C-NMR (DMSO-d6, 100 MHz) δ (ppm):25.78, 29. 12, 29. 15, 29.29, 29.36, 29.44, 29.49, 31.32, 35.65, 36.22, 69.44, 112.33, 115.24, 116.34, 116.60, 121.25, 124.02, 125.71, 126.14, 128.14, 128.22, 128.86, 129.66, 135.24, 137.69, 142.35, 144.44, 158.80, 171.62

N-(2-aminophenyl)-12-(3-hydroxyphenyl)dodecanamide (**46**)

Compound **46 was obtained** as a colorless oil. Yield 91%.

^{1}H-NMR (DMSO-d6, 400 MHz) δ (ppm):1.26 (s, 14H), 1.58 (m, 4H), 2.30 (t, 2H, J = 9.5 Hz), 2.46 (t, 2H, J = 9.5 Hz), 4.82 (bs, 2H), 6.54 (m, 4H), 6.72 (m, 1H), 6.87 (m, 1H), 7.06 (m, 1H), 7.15 (m, 1H), 9.11 (bs, 1H), 9.25 (bs, 1H). ^{13}C-NMR (DMSO-d6, 100 MHz) δ (ppm): 25.78, 29.144, 29.28, 29.37, 29.44, 29.49, 31.36, 35.62, 36.22, 113.00, 115.58, 116.33, 116.60 119.36, 124.04, 125.71, 126.13, 129.55, 142.34, 144.177, 157.71, 171.64

Compound purity

HPLC were performed on Hitachi equipped with an auto-sampler, a diode array detection DAD L-2455 used in the range 230-400 nm and a column Kromasil C18 5uM, 4.6*150 mm. 5-20 □L of MeOH solution of compounds at 1-4mg/1.5mL concentrations was injected. Two eluents were used at 1 ml/mL flow rate to assess the compound purity >= 95%: Eluent A (for PBMR-1-45): Acetonitrile 0.1% TFA; eluent B (all compounds) MeOH 0.1% TFA.

Synthesis of cashew nut-shell liquid-derived compounds/tacrine hybrids

Chemistry

1,2,3,4-tetrahydroacridin-9-amine (Tacrine)

2-aminobenzonitril (0.553g, 4.68mmol) and $ZnCl_2$ (0.638g, 4.68mmol) were solubilized in cyclohexanone (5.62mL, 54,20mmol) and the reaction reflux for 3 h at 140 °C. After that, the reaction was cooled at room temperature and the jelly solid was filtrated. The crude solid was resuspended in NaOH 10% in water (pH 12) and refluxed for 1 h. Then, the suspension was filtrated, and then it was crystalized in ethanol / water mixture.

White solid, yield 70%

^{1}H NMR ($CDCl_3$, 400MHz) δ: 1.91 (m, 4H), 2.57 (t, 2H, J = 6.4Hz), 3.01 (t, 2H, J = 5.2), 4.65 (bs, 2H), 7.32 (t, 1H, J = 7.2), 7.54 (t, 1H, J = 7.6), 7.66 (d, 1H, J = 8.4), 7.88 (d, 1H, J = 8.4). ^{13}C NMR ($CDCl_3$, 100MHz) δ 22.77, 22.86, 23.74, 34.16, 110.39, 117.15, 119.61, 123.79, 128.37, 128.88, 146.32, 146.61, 158.60.

6-chloro-1,2,3,4-tetrahydroacridin-9-amine (Cl-6-THA)

2-amino-4-chlorobenzonitril (0.714g, 4.68mmol) and $ZnCl_2$ (0.638g, 4.68mmol) were solubilized in cyclohexanone (5.62mL, 54,20mmol) and the reaction reflux for 3 h at 140 °C. The reaction was cooled at room temperature and the jelly solid was filtrated. The crude solid was resuspended in NaOH 10% in water (pH 12) and refluxed for 1 h. Then, the suspension was filtrated, and then it was crystalized in ethanol / water mixture.

Pale yellow solid, yield 60%

^{1}H NMR (DMSO-d6, 400MHz) δ: 1.78 (m, 4H), 2.49 (t, 2H, J = 6Hz), 2.77 (t, 2H, J = 5.2Hz), 6.44 (bs, 2H), 7.25 (dd, 1H, J^1 = 9 Hz, J^2 = 2.4 Hz), 7.59 (d, 1H, J = 2.4 Hz), 8.15 (d, 1H, J =

8.8 Hz). ^{13}C NMR (DMSO-d6, 100MHz) δ: 22.81, 22.92, 24.04, 33.99, 109.90, 116.04, 123.21, 124.64, 126.82, 132.87, 147.48, 148.74, 159.32.

7-methoxy-1,2,3,4-tetrahydroacridin-9-amine (7-**MEOTA**)

The 7-methoxy-1,2,3,4-tetrahydroacridin-9-amine has been kindly donated from Professor Kamil Kuca of the department of pharmaceutical chemistry and drug control, faculty of pharmacy in Hradec Kralove, Charles University in Prague, Czech Republic. Pale yellow solid.

^{1}H NMR ($CDCl_3$, 400MHz) δ: 1.90 (m, 4H), 2.60 (t, 2H, J = 6.4 Hz), 2.98 (t, 2H, J = 5.2 Hz), 3.85 (s, 3H), 4.51 (s, NH_2), 6.90 (d, 1H, J = 2.4 Hz), 7.22 (dd, 1H, J^1 = 9.2 Hz, J^2 = 2.4 Hz), 7.79 (d, 1H, J = 9.2 Hz). ^{13}C NMR ($CDCl_3$, 100MHz) δ: 22.83, 22.92, 23.87, 33.90, 55.46, 98.60, 110.86, 117.55, 120.27, 130.49, 142.51, 145.34, 156.16, 156.17.

8-(3-(benzyloxy)phenyl)octan-1-ol (90)

LDT71 (0.165g, 0.74mmol) and K_2CO_3 (0.153g, 1.11mmol) were solubilized in acetone (7.40mL), then benzyl bromide (0.088mL, 0.74mmol) was added to the mixture. The mixture was stirred for 12 h refluxing. Then, the reaction mixture was cooled, and the solvent was removed under reduced pressure. The crude obtained was extracted with ethyl acetate/H_2O (3x, 10 ml), and it was purified using silica gel column chromatography with a mixture of eluent composed by petroleum ether / ethyl acetate / methanol (7.5/2/0.5). Colorless oil, yield: 92%

^{1}H NMR ($CDCl_3$, 400MHz) δ: 1.36 (s, 8H), 1.56-1.66 (m, 4H), 1.94 (s, OH), 2.62 (t, 2H, J = 7.6 Hz), 3.63 (t, 2H, J = 6.8Hz), 5.07 (s, 2H), 6.87-6.82 (m, 3H), 7.22 (s, 1H, J = 8 Hz), 7.35-7.48 (m, 5H). ^{13}C NMR ($CDCl_3$, 100MHz) δ: 25.79, 29.27, 29.41, 29.51, 31.36, 32.78, 36.03, 62.92, 69.93, 111.77, 115.232, 121.21, 127.56, 127.92, 128.58, 129.23, 137.24, 144.60, 158.88.

8-(3-(benzyloxy)phenyl)octyl methyl sulfate (89)

Compound **90** (0.212g, 0.68mmol) was solubilized in DCM (0.35mL) then, Et_3N (0.125mL, 0.88mmol) was added to the solution and stirred for 15 minutes DCM (0.35mL) at 0°C. Then, mesyl chloride (0.086mL, 0.88mmol) was added and the reaction was stirred 12 h, at room temperature. The reaction was quenched adding 10 ml of water and the crude was extracted with DCM/H_2O (3X 10 ml). The organic layer was collected and evaporated under reduced pression and the resulting crude was purified using silica gel column chromatography with a mixture of eluent composed by petroleum ether / DCM (3.5/6.5). Colorless oil, yield: 87%

^{1}H NMR ($CDCl_3$, 400MHz) δ: 1.35-1.41 (m, 8H), 1.64-1.76 (m, 4H), 2.61 (t, 2H, J = 7.6 Hz), 2.96 (s, 3H), 4.21 (t, 2H, J = 6.0 Hz), 5.06 (s, 2H), 6.81-6.85 (m, 3H), 7.22 (t, 1H, J = 8.0 Hz), 7.34-7.47 (m, 5H). ^{13}C NMR ($CDCl_3$, 100MHz) δ: 25.42, 28.96, 29.13, 29.14, 29.29, 31.28, 35.97, 37.26, 69.89, 70.27, 111.79, 115.21, 121.18, 127.55, 127.92, 128.57, 129.26, 137.24, 144.50, 158.88.

General Procedure for the synthesis of hybrids 71-78 and 91-93

In a microwave tube tacrine compounds (Tacrine or 6-Cl-THA or 7-MEOTA) was solubilized in dry DMSO (1.3mL), KOH (0.24mmol) and molecular sieves (4 Å, about 100mg) and stirred at room temperature for 1 h under N_2. Then, CNSL-derivatives **86-89** (0.18mmol) was added to the reaction mixture. The reaction was carried-out in a CEM microwave with the following condition: *pre-stirring* 15s, time 12minuti, temperature 120°C, pawer 100W. After that, the crude was extracted with DCM/H_2O (3X, 15 ml)/ and the organic layer was collected and evaporated under reduced pressure. Finally, the crude product was purified using silica gel column chromatography with different eluents.

N-(8-(3-methoxyphenyl)octyl)-1,2,3,4-tetrahydroacridin-9-amine (71)

Column chromatography eluent: petroleum ether / ethyl acetate / Et_3N (7/2.5/0.5). Sticky yellow-brown oil yield 24%, HPLC purity: 95%

^{1}H NMR ($CDCl_3$, 400MHz) δ: 1.30-1.39 (m, 8H) 1.55-1.66 (m, 4H), 1.92 (m, 4H), 2.53 (t, 2H, J = 8.0Hz), 2.70 (m, 2H), 3.06 (m, 2H), 3.47 (t, 2H, J = 7.6Hz), 3.77 (s, 3H), 6.70-6.75 (m, 3H), 7.17 (t, 1H, J = 7.6Hz,), 7.35 (t, 1H, J = 7.2Hz), 7.58 (t, 1H, J = 7.2Hz), 7.99 (d, 1H, J = 8.8Hz), 8.09 (d, 1H, J = 7.6Hz). ^{13}C NMR ($CDCl_3$, 100MHz) δ 21.51, 22.35, 22.65, 22.83, 24.01, 26.74, 29.10, 29.14, 29.30, 29.67, 31.23, 31.41, 35.91, 49.00, 55.09, 110.69, 114.28, 117.57, 120.81, 123.56, 124.44, 129.15, 130.62, 144.35, 153.45, 154.46, 159.55.

MS (ESI^+): cal. 416, found: m/z: $C_{28}H_{36}N_2O$ 417 [M + H^+].

6-chloro-N-(8-(3-methoxyphenyl)octyl)-1,2,3,4-tetrahydroacridin-9-amine (72)

The compounds 72 was purified by two subsequent column chromatography:
first column chromatography eluent: petroleum ether / ethyl acetate / Et_3N 8/1.5/0.5)
second column chromatography eluent: petroleum ether / ethyl acetate / methanol / ammonia (8/1.5/0.5/ 10%). Sticky yellow-brown oil yield 29%, HPLC purity: 91%

^{1}H NMR ($CDCl_3$, 400MHz) δ: 1.32-1.38 (m, 8H), 1.60-1.68 (m, 4H), 1.91 (m, 4H), 2.57 (t, 2H J = 7.6Hz), 2.65 (m, 2H), 3.05 (m, 2H), 3.51 (t, 2H, J = 7.6Hz), 3.79 (s, 3H), 6.72-6.77 (m, 3H), 7.19 (t, 1H, J = 8.4Hz), 7.27 (m, 1H), 7.90-7.93 (m, 2H).^{13}C NMR ($CDCl_3$, 100MHz) δ 22.46, 22.82, 24.45, 26.84, 29.12, 29.21, 29.32, 31.24, 31.70, 33.53, 35.93, 49.53, 55.10, 110.72, 114.26, 115.26, 118.02, 120.81, 124.31, 124.67, 126.92, 129.14, 134.34, 144.39, 151.17, 159.55. MS (ESI^+): cal. 450, found: m/z: $C_{28}H_{35}ClN_2O$ 451 [M + H^+].

7-methoxy-*N*-(8-(3-methoxyphenyl)octyl)-1,2,3,4-tetrahydroacridin-9-amine (73)

Column chromatography eluent: petroleum ether / ethyl acetate / Et_3N (8/1.5/0.5). Sticky yellow-brown oil yield 29%, HPLC purity: 96%

^{1}H NMR ($CDCl_3$, 400MHz) δ: 1.31-1.39 (m, 8H), 1.60-1.68 (m, 4H), 1.91 (m, 4H), 2.57 (t, 2H, J = 7.6Hz), 2.71 (m, 2H), 3.07 (m, 2H), 3.45 (t, 2H, J = 7.2Hz), 3.79 (s, 3H), 3.91 (s, 3H), 6.71-

6.77 (m, 3H), 7.19 (t, 1H, J = 8.4Hz,), 7.25 (m, 3H), 7.84 (d, 1H, J = 8.8Hz,). ^{13}C NMR ($CDCl_3$, 100MHz) δ: 22.57, 22.92, 24.58, 26.97, 29.13, 29.29, 29.37, 29.67, 31.25, 31.73, 31.90, 35.93, 49.12, 55.10, 55.47, 101.93, 110.71, 114.25, 120.65, 120.81, 129.14, 144.40, 155.99, 159.56. MS (ESI^+): cal. 446, found: m/z: $C_{29}H_{38}N_2O_2$ 447 [M + H^+].

methyl 2-methoxy-6-(8-((1,2,3,4-tetrahydroacridin-9-yl)amino)octyl)benzoate (74)

Column chromatography eluent: petroleum ether / ethyl acetate / Et_3N (6.5/3/0.5). Sticky yellow-brown oil yield 20%, HPLC purity: 95%

^{1}H NMR ($CDCl_3$, 400MHz) δ: 1.30-1.39 (m, 8H), 1.55-1.66 (m, 4H), 1.92 (m, 4H), 2.53 (t, 2H, J = 8.0Hz), 2.70 (m, 2H), 3.06 (m, 2H), 3.47 (t, 2H, J = 7.6Hz), 3.81 (s, 3H), 3.89 (s, 3H), 6.75 (d, 1H, J = 8.4Hz) 6.80 (d, 1H, J = 7.2Hz), 7.26 (t, 1H, J = 7.6Hz), 7.33 (t, 1H, J = 7.2Hz), 7.56 (t, 1H, J = 7.2Hz), 7.90-7.96 (m, 2H). ^{13}C NMR ($CDCl_3$, 100MHz) δ: 22.38, 22.83, 24.53, 26.81, 29.13, 29.18, 29.24, 29.30, 30.95, 31.00, 31.60, 32.89, 31.74, 33.37, 33.40, 49.31, 51.99, 55.86, 108.48, 113.49, 121.42, 121.46, 122.99, 123.56, 123.81, 127.32, 128.96, 130.19, 141.18, 156.26, 168.83. HRMS (ES+) calcd for $C_{30}H_{38}N_2O_3$ (M + H+) m/z, 475.29552; found, 475.29597.

methyl 2-(8-((6-chloro-1,2,3,4-tetrahydroacridin-9-yl)amino)octyl)-6-methoxybenzoate (75)

Column chromatography eluent: petroleum ether / ethyl acetate / Et_3N (7.5/2/0.5). Sticky yellow-brown oil yield 34%, HPLC purity: 98%

^{1}H NMR ($CDCl_3$, 400MHz) δ: 1.28-1.35 (m, 8H), 1.53-1.66 (m, 4H), 1.89 (s, 4H), 2.51 (t, 2H J = 7.6Hz), 2.63 (m, 2H), 3.04 (m, 2H), 3.50 (t, 2H, J = 7.2Hz), 3.79 (s, 3H), 3.87 (s, 3H), 6.72-6.79 (m, 2H) 7.24 (m, 2H), 7.89-7.93 (m, 2H). ^{13}C NMR ($CDCl_3$, 100MHz) δ: 22.34, 22.77,

24.43, 26.78, 29.10, 29.17, 29.22, 30.94, 31.62, 33.19, 33.36, 49.40, 51.99, 55.86, 108.49, 115.04, 117.84, 121.42, 123.56, 124.40, 124.68, 126.50, 130.24, 141.16, 151.40, 156.33, 168.83. HRMS (ES+) calcd for $C_{30}H_{37}ClN_2O_3$ (M + H+) m/z, 509.256547; found, 509.25651

methyl 2-methoxy-6-(8-((7-methoxy-1,2,3,4-tetrahydroacridin-9-yl)amino)octyl)benzoate (76)

Column chromatography eluent: petroleum ether / ethyl acetate / Et_3N (7.5/2/0.5) Sticky yellow-brown oil yield 23%, HPLC purity: 99%

^{1}H NMR ($CDCl_3$, 400MHz) δ: 1.29-1.37 (m, 8H), 1.55-1.66 (m, 4H), 1.90 (m, 4H), 2.51 (t, 2H, J = 7.6Hz), 2.69 (m, 2H), 3.05 (m, 2H), 3.42 (t, 2H, J = 6.8Hz), 3.79 (s, 3H), 3.87 (s, 3H), 3.89 (s, 3H), 6.73-6.80 (m, 2H) 7.24 (m, 4H), 7.99 (d, 1H, J = 7.2Hz). ^{13}C NMR ($CDCl_3$, 100MHz) δ: 20.90, 22.15, 24.20, 26.68, 28.88, 29.05, 29.16, 29.19, 30.95, 31.42, 33.35, 48.16, 52.13, 55.85, 103.34, 108.41, 117.81, 121.40, 122.97, 123.24, 130.26, 141.07, 154.09, 156.24, 156.65, 168.30. LRMS (ESI^+) cal. 504, found m/z: $C_{31}H_{40}N_2O_4$ 505 [M + H^+].

N-(8-(3,5-dimethoxyphenyl)octyl)-1,2,3,4-tetrahydroacridin-9-amine (77)

Column chromatography eluent: petroleum ether / ethyl acetate / dichloromethane /methanol / ammonia (7/2.5/0.5/1/10%). Sticky yellow-brown oil yield 25%, HPLC purity: 95%

^{1}H NMR (400 MHz, $CDCl_3$) δ: 1.46 – 1.13 (m, 8H), 1.73 – 1.46 (m, 4H), 1.91 (t, 4H, *J* = 6.6, Hz), 2.58 – 2.39 (m, 2H), 2.68 (s, 2H), 3.08 (s, 2H), 3.49 (t, 2H, *J* = 7.1 Hz), 3.61 (t, 2H, *J* = 6.6 Hz), 3.75 (s, 6H), 6.46 – 5.79 (m, 2H), 6.76 (m, 1H), 7.28 (m, 1H), 7.54 (t, 1H), 7.95 (d, 2H, *J* = 8.6 Hz), ^{13}C NMR (100 MHz, $CDCl_3$) δ: 22.61, 24.47, 25.21, 26.84, 29.11, 29.32, 31.64, 33.41, 39.64, 49.94, 52.20, 54.80, 55.19, 57.61, 97.44, 106.49, 107.09, 108.35, 119.94, 121.44, 123.02, 123.85, 130.19, 141.05, 141.26, 145.15, 159.22, 160.66.

6-chloro-N-(8-(3,5-dimethoxyphenyl)octyl)-1,2,3,4-tetrahydroacridin-9-amine (78)

Column chromatography eluent: petroleum ether / ethyl acetate / dichloromethane /methanol / ammonia (7/2.5/0.5/1/10%). Sticky yellow-brown oil yield 25%. HPLC purity: 95%

^{1}H NMR (400 MHz, $CDCl_3$) δ: 1.40-1.10 (m, 8H), 1.57-1.62 (m, 4H), 1.91 (t, 4H, J = 2.9 Hz), 2.58 – 2.47 (m, 2H), 2.65 (s, 2H), 3.02 (s, 2H), 3.45 (s, 2H), 3.77 (s, 6H), 6.46-6.16 (m, 3H), 7.57-6.97 (m, 2H), 7.8-7.90 (m, 2H). ^{13}C NMR (100 MHz, $CDCl_3$) δ: 22.61, 22.89, 24.51, 26.85, 29.12, 29.22, 29.33, 31.13, 31.74, 33.94, 36.20, 49.59, 55.20, 97.45, 106.47, 115.59, 118.32, 124.17, 124.60, 127.45, 133.98, 145.18, 148.03, 150.87, 159.39, 160.66,

***N*-(8-(3-(benzyloxy)phenyl)octyl)-1,2,3,4-tetrahydroacridin-9-amine (91)**

Column chromatography eluent: petroleum ether / ethyl acetate / Et_3N (6.5/3/0.5). Sticky yellow-brown oil yield 32%.

^{1}H NMR ($CDCl_3$, 400MHz) δ: 1.30-1.39 (m, 8H), 1.56-1.89 (m, 4H), 1.89 (m, 4H), 2.55 (t, 2H, J = 7.6Hz), 2.62 (m, 2H), 3.14 (m, 2H), 3.61 (t, 2H, J = 7.2Hz), 5.02 (s, 2H), 6.75-6.79 (m, 3H), 7.17 (t, 1H, J = 7.6Hz), 7.30-7.42 (m, 6H), 7.53 (t, 1H, J = 7.2Hz), 8.00 (d, 1H, J = 8.4Hz,), 8.12 (d, 1H, J = 8.00Hz). ^{13}C NMR ($CDCl_3$, 100MHz) δ: 22.74, 23.03, 24.74, 26.91, 29.14, 29.27, 29.37, 31.25, 31.76, 33.86, 35.94, 49.50, 69.88, 111.64, 115.19, 115.65, 120.09, 121.12, 122.90, 123.58, 127.50, 127.89, 128.36, 128.54, 129.19, 137.14, 144.47, 147.25, 150.93, 158.23, 158.82.

N-(8-(3-(benzyloxy)phenyl)octyl)-6-chloro-1,2,3,4-tetrahydroacridin-9-amine (92)

Column chromatography eluent: petroleum ether / ethyl acetate / Et_3N (7/2.5/0.5). Sticky yellow-brown oil yield 24%, HPLC purity 97%

^{1}H NMR (400 MHz, $CDCl_3$) δ: 1.36 - 1.24 (m, 8H), 1.64 - 1.59 (m, 4H), 1.91-1.88 (t, 4H, J = 8 Hz), 2.56 (t, 2H, J = 8 Hz), 2.63 (t, 2H, J = 8 Hz) , 3.02 (t, 2H, J = 8 Hz), 3.47 (t, 2H, J = 8

Hz), 5.03 (s, 2H), 6.81 - 6.76 (m, 3H), 7.43-7.15 (m, 8), 7.90 - 7.87 (m, 2H), ^{13}C NMR (100 MHz, $CDCl_3$) δ: 22.56, 22.87, 24.49, 26.85, 29.10, 29.22, 29.33, 31.21, 31.74, 33.81, 35.92, 49.58, 69.88, 111.63, 115.22, 121.11, 124.24, 124.63, 127.48, 127.88, 128.53, 129.17, 137.13, 144.44, 151.16, 158.83.

N-(8-(3-(benzyloxy)phenyl)octyl)-7-methoxy-1,2,3,4-tetrahydroacridin-9-amine (93)

Column chromatography eluent: petroleum ether / ethyl acetate / Et_3N (7/2.5/0.5). Sticky yellow-brown oil yield 24%. HPLC purity 94%

^{1}H NMR (400 MHz, $CDCl_3$) δ: 1.44 - 1.26 (m, 12H), 1.68 - 1.58 (m, 4H), 1.92 - 1.89 (m, 4H), 2.57 (t, 2H, J = 8 Hz), 2.71 (t, 2H, J = 4 Hz), 3.06 (t, 2H, J = 8 Hz), 3.43 (t, 2H, J = 8 Hz), 3.90 (s, 3H), 5.04 (s, 2H), 6.82-6.77 (m, 3H), 7.44 - 7.17 (m, 8H), 7.90 - 7.87 (m, 1H). ^{13}C NMR (100 MHz, $CDCl_3$) δ: 22.65, 22.98, 24.64, 26.98, 29.13, 29.30, 29.38, 29.68, 31.22, 31.74, 33.27, 35.92, 49.12, 55.47, 69.88, 101.85, 111.64, 115.21, 120.53, 121.11, 127.48, 127.88, 128.52, 129.17, 137.13, 144.44, 150.32, 155.96, 158.82.

General procedure for the reduction reaction

A solution 0.01 M of the intermediate compounds **91-93** (0.12-0.76 mmol) in EtOAc/MeOH (1/1) has been hydrogenate by H-Cube using Pd/C 10% as catalyst. The flow chemistry process was performed under the following conditions: flow 1mL/min, pressure H_2 5 Bar, and temperature 25°C. The crude reaction mixture has been purified with a very fast column chromatography

3-(8-((1,2,3,4-tetrahydroacridin-9-yl)amino)octyl)phenol (79)

Eluent column chromatography dichloromethane/methanol/ammonia (9.5/0.5/1%). Sticky yellow-brown oil yield 41%. HPLC purity: 95%

^{1}H NMR ($CDCl_3$, 400MHz) δ: 1.22-1.45 (m, 10H), δ 1.67 (q, 2H, J = 6.8Hz), δ 1.87 (m, 4H), δ 2.44 (t, 2H, J = 7.6Hz), δ 2.66 (m, 2H), δ 3.10 (m, 2H), δ 3.62 (t, 2H, J = 6.8Hz), δ 4.44 (br, NH), δ 6.62 (m, 2H) δ 6.73 (d, 1H, J = 8.0Hz,), δ 7.07 (t, 1H, J = 8.0Hz), δ 7.34 (t, 1H, J = 8.0Hz), δ 7.53 (t, 1H, J = 8.0Hz), δ 8.00-8.06 (m, 2H). ^{13}C NMR ($CDCl_3$, 100MHz) δ: 22.31, 22.76, 24.49, 26.41, 28.51, 28.64, 29.07, 29.67, 30.69, 31.39, 32.36, 35.49, 48.95, 113.04, 114.48, 115.38, 119.15, 119.56, 123.17, 123.80, 126.82, 129.16, 129.19, 144.19, 152.08, 157.10, 157.18. MS (ESI^+) cal. 402, found m/z: $C_{27}H_{34}N_2O$ 403 [M + H^+].

3-(8-((6-chloro-1,2,3,4-tetrahydroacridin-9-yl)amino)octyl)phenol (80)

Eluent column chromatography petroleum ether/ethyl acetate/methanol/ammonia (7/2.5/0.5/10%). Sticky yellow-brown oil yield 45%. HPLC purity: 97%

^{1}H NMR (400 MHz, CDCl3) δ: 1.40 – 1.13 (m, 8H), 1.51 (m, 2H), 1.69 (m, 4H), 2.00 – 1.84 (m, 2H), 2.55 – 2.43 (m, 2H), 2.73 – 2.63 (m, 2H), 3.17 – 3.02 (m, 2H), 3.64 – 3.51 (m, 2H), 4.36 – 4.00 (m, 1H), 6.70 (m, 3H), 7.12 (m, 1H), 7.28 (m, 1H), 7.97 (m, 2H). ^{13}C NMR (100 MHz, $CDCl_3$) δ: 22.31, 22.71, 24.36, 26.47, 28.60, 28.71, 29.13, 30.75, 31.47, 32.83, 35.55, 49.18, 112.99, 114.76, 115.40, 117.64, 119.75, 124.36, 124.89, 126,12, 129.23, 134.73, 144.30, 146.87, 151.75, 157.15, 158.63.

3-(8-((7-methoxy-1,2,3,4-tetrahydroacridin-9-yl)amino)octyl)phenol (81)

Eluent column chromatography petroleum ether/ethyl acetate/methanol/ammonia (7/2.5/0.5/10%). Sticky yellow-brown oil yield 44%. HPLC purity: 90%

^{1}H NMR (400 MHz, $CDCl_3$) δ: 1.40 – 1.19 (m, 8H), 1.72 – 1.44 (m, 4H), 1.90 (m, 2H), 2.59 – 2.47 (m, 2H), 2.68 (s, 2H), 3.08 (s, 2H), 3.49 (m, 2H), 3.60 (d, 2H, *J* = 6.6 Hz), 3.75 (s, 2H), 6.30 (t, 2H, *J* = 8.4 Hz), 7.26 – 7.15 (m, 1H), 7.33 (t, 1H, *J* = 7.6 Hz), 7.54 (t, 1H, *J* = 7.2 Hz), 7.95 (d, 1H, *J* = 8.6 Hz). ^{13}C NMR (100 MHz, $CDCl_3$) very low quantity to perform the experiment.

General procedure for the O-demethylation reaction

Compound **74** or **75** (0,25 mmol, 1 eq) was solubilized in DCM (3.03mL) then BBr_3 (1 mmol, 4 eq) drop wise was added at 0°C. The reaction mixture was left stirred for 40 min at room temperature. When the reaction was completed it was quenched with 1mL of saturated solution of $NaHCO_3$ and 20 mL of water. Then the crude solution was extracted with DCM/H_2O (3X10 mL) and the organic layers were collected and evaporated under reduced pressure. Finally, the crude. Obtained was purified using silica gel column chromatography with different eluents.

methyl 2-hydroxy-6-(8-((1,2,3,4-tetrahydroacridin-9-yl)amino)octyl)benzoate (82)

Eluent column chromatography petroleum ether/dichloromethane/methanol/ammonia (7/2.5/0.5/10%). Sticky colorless oil yield 25%. HPLC purity: 99%

^{1}H NMR (400 MHz, $CDCl_3$) δ: 1.25-1.38 (m, 8H), 1.50-1.52 (m, 2H), 1.64 (t, 2H, J^1 = 8 Hz), 1.91 (s, 4H), 2.69 (s, 2H), 2.85 (t, 2H, J^1 = 8 Hz), 3.06 (s, 2H), 3.48 (t, 2H, J = 7.1 Hz), 3.92 (s, 4H), 6.69 (d, 1H, J = 7.5 Hz), 6.83 (d, 1H, J = 8.2 Hz), 7.29 (dt, 2H, J = 15.8, 7.7 Hz), 7.54 (t, 1H, J = 7.5 Hz), 7.80-8.05 (m, 2H). ^{13}C NMR (100 MHz, $CDCl_3$) δ: 22.71, 23.00, 24.73, 26.91, 29.31, 29.38, 29.68, 31.75, 31.94, 33.81, 36.41, 49.46, 52.08, 112.19, 115.54, 115.63, 120.07, 122.28, 122.84, 123.58, 128.35, 128.48, 134.01, 145.81, 147.19, 150.90, 158.20, 162.29, 171.77.

methyl 2-(8-((6-chloro-1,2,3,4-tetrahydroacridin-9-yl)amino)octyl)-6-hydroxybenzoate (83)

Eluent column chromatography petroleum ether/dichloromethane/methanol/ammonia (7/2.5/0.5/10%). Sticky colorless oil yield 25%. HPLC purity: 97%

^{1}H NMR (400 MHz, $CDCl_3$) δ: 1.23-1.40 (m, 8H), 1.47-1.54 (m, 2H), 1.67 (dt, 2H, *J* = 8 Hz), 1.88-1.89 (m, 4H), 2.63 (s, 2H), 2.79-2.92 (m, 2H), 3.04 (s, 2H), 3.51 (t, 2H, *J* = 6.8 Hz,), 3.92

(s, 3H), 4.19 (s, 1H), 6.69 (d, 1H, J = 7.5 Hz), 6.75-6.98 (m, 1H), 7.11-7.33 (m, 2H), 7.92 (dd, 2H, J^1 = 16.0, J^2 = 5.2 Hz). ^{13}C NMR (100 MHz, $CDCl_3$) δ: 22.35, 22.76, 24.41, 26.86, 29.28, 29.38, 29.67, 31.70, 31.94, 33.25, 36.48, 49.46, 52.10, 111.01, 114.99, 115.62, 117.80, 122.37, 124.41, 124.72, 126.54, 134.12, 134.60, 145.89, 151.38, 158.51, 162.46, 171.81,

General procedure for the ester hydrolysis reaction

In a microwave tube the compound **82** or **83** (0.07mmol, 1eq) was solubilized in 2 ml of KOH solution 3.5M (composed by water/methanol 2:1). Then, the reaction was carried out in a CEM microwave with the following reaction condition: *pre-stirring* 15s, time 10 min, temperature 100°C, power 100W. Once cooled, a solution of HCl 2N was added dropwise until pH 2. A white precipitate was formed and collected by filtration obtaining the corresponding hydrochloride derivatives **84**, **85**.

2-hydroxy-6-(8-((1,2,3,4-tetrahydroacridin-9-yl)amino)octyl)benzoic acid (84)

White solid, yield 84%, HPLC purity: 92%

^{1}H NMR (400 MHz, CD_3OD) δ: 1.21-1.43 (m, 8H), 1.52 (s, 2H), 1.76-1.83 (m, 2H), 1.93 (s, 4H), 2.67 (s, 2H), 2.88-2.94 (m, 2H), 2.99 (s, 2H), 3.92 (t, 2H, J = 6.4 Hz,), 6.62 (dd, 2H, J^1 = 18.5, J^2= 7.7 Hz,), 7.11 (t, 1H, J = 7.8 Hz), 7.55 (t, 1H, J = 7.6 Hz), 7.74 (d, 1H, J = 8.4 Hz), 7.81 (t, 1H, J = 7.2 Hz), 8.35 (d, 1H, J = 8.7 Hz). ^{13}C NMR (100 MHz, CD_3OD) δ: 20.40, 21.53, 23.40, 26.04, 27.85, 28.50, 28.76, 29.09, 29.92, 31.26, 31.56, 34.93, 111.43, 113.90, 118.67, 121.04, 124.87, 125.04, 132.64, 137.75, 148.21 154.81, 159.89. HRMS (ES+) calcd for $C_{28}H_{34}N_2O_3$ (M + H+) m/z, 447.26422; found, 447.26436

2-(8-((6-chloro-1,2,3,4-tetrahydroacridin-9-yl)amino)octyl)-6-hydroxybenzoic acid (85)

White solid, yield 54%. HPLC purity: 95%

^{1}H NMR (400 MHz, $CDCl_3$) δ: 1.41 – 1.25 (m, 5H), 1.53 (s, 1H), 1.79 (dd, 1H, J^1= 14.1, J^2 = 6.8 Hz), 1.92 (d, 3H, J = 2.8 Hz), 2.64 (s, 1H), 2.89 – 2.77 (m, 1H), 2.97 (s, 1H), 3.31 – 3.24 (m, 1H), 3.91 (t, 2H, J = 7.3 Hz), 6.66 (dd, 2H, J^1 = 13.1, J^2 = 8.0 Hz,), 7.17 (t, 1H, J = 7.8 Hz,), 7.52 (dd, 1H, J = 9.3, J^2 = 1.9 Hz,), 7.75 (d, 1H, J = 1.9 Hz,), 8.35 (d, J = 9.3 Hz, 1H). ^{13}C NMR (100 MHz, $CDCl_3$) δ: 20.46, 21.92, 24.15, 25.90, 27.84, 27.89, 28.41, 28.65, 29.67, 30.75, 31.81, 36.28, 48.32, 110.65, 111.78, 115.38, 118.52, 122.24, 125.55, 126.64, 134.07, 138.32, 138.41, 147.19, 151.66, 155.35, 163.18, 173.25. HRMS (ES+) calcd for $C_{28}H_{33}ClN_2O_3$ (M + H+) m/z, 481.22525; found, 481.20619

Compounds purity.

The compounds purity was determined by using a Kinetex® 5µm EVO C18 100 Å, LC Column 150 x 4.6 mm and a HPLC Jasco Corporation (Tokyo, Japan) instrument, model PU-1580 UV equipped with 20 µL loop valve. HPLC parameters were the following: MeCN/H_2O/ trifluoroacetic acid 50/50/0.05%; flow rate: 0.6 ml/min; elution type: isocratic detection UV-Vis Abs at 254nm. The samples were dissolved in MeOH (100 µg/ml)

REFERENCES

1. Gilhus, N. E.; Deuschl, G. Neuroinflammation - a common thread in neurological disorders. *Nat Rev Neurol* **2019,** 15, 429-430.

2. Skaper, S. D.; Facci, L.; Zusso, M.; Giusti, P. An Inflammation-Centric View of Neurological Disease: Beyond the Neuron. *Front Cell Neurosci* **2018,** 12, 72.

3. Heneka, M. T.; Carson, M. J.; El Khoury, J.; Landreth, G. E.; Brosseron, F.; Feinstein, D. L.; Jacobs, A. H.; Wyss-Coray, T.; Vitorica, J.; Ransohoff, R. M.; Herrup, K.; Frautschy, S. A.; Finsen, B.; Brown, G. C.; Verkhratsky, A.; Yamanaka, K.; Koistinaho, J.; Latz, E.; Halle, A.; Petzold, G. C.; Town, T.; Morgan, D.; Shinohara, M. L.; Perry, V. H.; Holmes, C.; Bazan, N. G.; Brooks, D. J.; Hunot, S.; Joseph, B.; Deigendesch, N.; Garaschuk, O.; Boddeke, E.; Dinarello, C. A.; Breitner, J. C.; Cole, G. M.; Golenbock, D. T.; Kummer, M. P. Neuroinflammation in Alzheimer's disease. *Lancet Neurol* **2015,** 14, 388-405.

4. Torkildsen, O.; Wergeland, S.; Bakke, S.; Beiske, A. G.; Bjerve, K. S.; Hovdal, H.; Midgard, R.; Lilleås, F.; Pedersen, T.; Bjørnarå, B.; Dalene, F.; Kleveland, G.; Schepel, J.; Olsen, I. C.; Myhr, K. M. ω-3 fatty acid treatment in multiple sclerosis (OFAMS Study): a randomized, double-blind, placebo-controlled trial. *Arch Neurol* **2012,** 69, 1044-51.

5. DiSabato, D. J.; Quan, N.; Godbout, J. P. Neuroinflammation: the devil is in the details. *J Neurochem* **2016,** 139 Suppl 2, 136-153.

6. Lampron, A.; Elali, A.; Rivest, S. Innate immunity in the CNS: redefining the relationship between the CNS and Its environment. *Neuron* **2013,** 78, 214-32.

7. Voet, S.; Srinivasan, S.; Lamkanfi, M.; van Loo, G. Inflammasomes in neuroinflammatory and neurodegenerative diseases. *EMBO Mol Med* **2019,** 11.

8. Wyss-Coray, T.; Mucke, L. Inflammation in neurodegenerative disease--a double-edged sword. *Neuron* **2002,** 35, 419-32.

9. Hickman, S.; Izzy, S.; Sen, P.; Morsett, L.; El Khoury, J. Microglia in neurodegeneration. *Nat Neurosci* **2018,** 21, 1359-1369.

10. Bachiller, S.; Jiménez-Ferrer, I.; Paulus, A.; Yang, Y.; Swanberg, M.; Deierborg, T.; Boza-Serrano, A. Microglia in Neurological Diseases: A Road Map to Brain-Disease Dependent-Inflammatory Response. *Front Cell Neurosci* **2018,** 12, 488.

11. Crain, J. M.; Nikodemova, M.; Watters, J. J. Microglia express distinct M1 and M2 phenotypic markers in the postnatal and adult central nervous system in male and female mice. *J Neurosci Res* **2013,** 91, 1143-51.

12. Orihuela, R.; McPherson, C. A.; Harry, G. J. Microglial M1/M2 polarization and metabolic states. *Br J Pharmacol* **2016,** 173, 649-65.

13. Stein, M.; Keshav, S.; Harris, N.; Gordon, S. Interleukin 4 potently enhances murine macrophage mannose receptor activity: a marker of alternative immunologic macrophage activation. *J Exp Med* **1992,** 176, 287-92.

14. Bronzuoli, M. R.; Iacomino, A.; Steardo, L.; Scuderi, C. Targeting neuroinflammation in Alzheimer's disease. *J Inflamm Res* **2016,** 9, 199-208.

15. Lloyd, A. F.; Miron, V. E. The pro-remyelination properties of microglia in the central nervous system. *Nat Rev Neurol* **2019,** 15, 447-458.

16. Selkoe, D. J.; Hardy, J. The amyloid hypothesis of Alzheimer's disease at 25 years. *EMBO Mol Med* **2016,** 8, 595-608.

17. Schneider, L. S.; Mangialasche, F.; Andreasen, N.; Feldman, H.; Giacobini, E.; Jones, R.; Mantua, V.; Mecocci, P.; Pani, L.; Winblad, B.; Kivipelto, M. Clinical trials and late-stage drug development for

Alzheimer's disease: an appraisal from 1984 to 2014. *J Intern Med* **2014,** 275, 251-83.

18. Cummings, J. L.; Morstorf, T.; Zhong, K. Alzheimer's disease drug-development pipeline: few candidates, frequent failures. *Alzheimers Res Ther* **2014,** 6, 37.

19. Cummings, J.; Lee, G.; Ritter, A.; Sabbagh, M.; Zhong, K. Alzheimer's disease drug development pipeline: 2019. *Alzheimers Dement (N Y)* **2019,** 5, 272-293.

20. Akiyama, H.; Barger, S.; Barnum, S.; Bradt, B.; Bauer, J.; Cole, G. M.; Cooper, N. R.; Eikelenboom, P.; Emmerling, M.; Fiebich, B. L.; Finch, C. E.; Frautschy, S.; Griffin, W. S.; Hampel, H.; Hull, M.; Landreth, G.; Lue, L.; Mrak, R.; Mackenzie, I. R.; McGeer, P. L.; O'Banion, M. K.; Pachter, J.; Pasinetti, G.; Plata-Salaman, C.; Rogers, J.; Rydel, R.; Shen, Y.; Streit, W.; Strohmeyer, R.; Tooyoma, I.; Van Muiswinkel, F. L.; Veerhuis, R.; Walker, D.; Webster, S.; Wegrzyniak, B.; Wenk, G.; Wyss-Coray, T. Inflammation and Alzheimer's disease. *Neurobiol Aging* **2000,** 21, 383-421.

21. Zhang, B.; Gaiteri, C.; Bodea, L. G.; Wang, Z.; McElwee, J.; Podtelezhnikov, A. A.; Zhang, C.; Xie, T.; Tran, L.; Dobrin, R.; Fluder, E.; Clurman, B.; Melquist, S.; Narayanan, M.; Suver, C.; Shah, H.; Mahajan, M.; Gillis, T.; Mysore, J.; MacDonald, M. E.; Lamb, J. R.; Bennett, D. A.; Molony, C.; Stone, D. J.; Gudnason, V.; Myers, A. J.; Schadt, E. E.; Neumann, H.; Zhu, J.; Emilsson, V. Integrated systems approach identifies genetic nodes and networks in late-onset Alzheimer's disease. *Cell* **2013,** 153, 707-20.

22. Chow, V. W.; Mattson, M. P.; Wong, P. C.; Gleichmann, M. An overview of APP processing enzymes and products. *Neuromolecular Med* **2010,** 12, 1-12.

23. Cherry, J. D.; Olschowka, J. A.; O'Banion, M. K. Neuroinflammation and M2 microglia: the good, the bad, and the inflamed. *J Neuroinflammation* **2014,** 11, 98.

24. Venegas, C.; Kumar, S.; Franklin, B. S.; Dierkes, T.; Brinkschulte, R.; Tejera, D.; Vieira-Saecker, A.; Schwartz, S.; Santarelli, F.; Kummer, M. P.; Griep, A.; Gelpi, E.; Beilharz, M.; Riedel, D.; Golenbock, D. T.; Geyer, M.; Walter, J.; Latz, E.; Heneka, M. T. Microglia-derived ASC specks cross-seed amyloid-β in Alzheimer's disease. *Nature* **2017,** 552, 355-361.

25. Oddo, S.; Caccamo, A.; Kitazawa, M.; Tseng, B. P.; LaFerla, F. M. Amyloid deposition precedes tangle formation in a triple transgenic model of Alzheimer's disease. *Neurobiol Aging* **2003,** 24, 1063-70.

26. Michelucci, A.; Heurtaux, T.; Grandbarbe, L.; Morga, E.; Heuschling, P. Characterization of the microglial phenotype under specific pro-inflammatory and anti-inflammatory conditions: Effects of oligomeric and fibrillar amyloid-beta. *J Neuroimmunol* **2009,** 210, 3-12.

27. Yao, K.; Zu, H. B. Microglial polarization: novel therapeutic mechanism against Alzheimer's disease. *Inflammopharmacology* **2019**.

28. Filippi, M.; Bar-Or, A.; Piehl, F.; Preziosa, P.; Solari, A.; Vukusic, S.; Rocca, M. A. Multiple sclerosis. *Nat Rev Dis Primers* **2018,** 4, 43.

29. Chari, D. M. Remyelination in multiple sclerosis. *Int Rev Neurobiol* **2007,** 79, 589-620.

30. Frischer, J. M.; Bramow, S.; Dal-Bianco, A.; Lucchinetti, C. F.; Rauschka, H.; Schmidbauer, M.; Laursen, H.; Sorensen, P. S.; Lassmann, H. The relation between inflammation and neurodegeneration in multiple sclerosis brains. *Brain* **2009,** 132, 1175-89.

31. Finkelsztejn, A. Multiple sclerosis: overview of disease-modifying agents. *Perspect Medicin Chem* **2014,** 6, 65-72.

32. Küry, P.; Kremer, D.; Göttle, P. Drug repurposing for neuroregeneration in multiple sclerosis. *Neural Regen Res* **2018,** 13, 1366-1367.

33. Thompson, A. J.; Baranzini, S. E.; Geurts, J.; Hemmer, B.; Ciccarelli, O. Multiple sclerosis. *Lancet* **2018,** 391, 1622-1636.

34. Huynh, J. L.; Casaccia, P. Epigenetic mechanisms in multiple sclerosis: implications for pathogenesis and treatment. *Lancet Neurol* **2013,** 12, 195-206.

35. Pedre, X.; Mastronardi, F.; Bruck, W.; López-Rodas, G.; Kuhlmann, T.; Casaccia, P. Changed histone

acetylation patterns in normal-appearing white matter and early multiple sclerosis lesions. *J Neurosci* **2011,** 31, 3435-45.

36. Aguzzi, A.; Barres, B. A.; Bennett, M. L. Microglia: scapegoat, saboteur, or something else? *Science* **2013,** 339, 156-61.

37. Chu, F.; Shi, M.; Zheng, C.; Shen, D.; Zhu, J.; Zheng, X.; Cui, L. The roles of macrophages and microglia in multiple sclerosis and experimental autoimmune encephalomyelitis. *J Neuroimmunol* **2018,** 318, 1-7.

38. Prati, F.; Uliassi, E.; Bolognesi, M. Two diseases, one approach: multitarget drug discovery in Alzheimer's and neglected tropical diseases. *MedChemComm* **2014,** 5, 853-861.

39. Bolognesi, M. L.; Cavalli, A. Multitarget Drug Discovery and Polypharmacology. *ChemMedChem* **2016,** 11, 1190-2.

40. Patrick, G. L. History of Drug Discovery. *e LS* **2001**.

41. Kaufmann, S. H. Paul Ehrlich: founder of chemotherapy. *Nat Rev Drug Discov* **2008,** 7, 373.

42. Wermuth, C. G. Multitargeted drugs: the end of the "one-target-one-disease" philosophy? *Drug Discov Today* **2004,** 9, 826-7.

43. Tempini, N.; Leonelli, S. Human Genome Project, Personalised Medicine and Future Health Care. *eLS* **2001**, 1-5.

44. Scannell, J. W.; Blanckley, A.; Boldon, H.; Warrington, B. Diagnosing the decline in pharmaceutical R&D efficiency. *Nat Rev Drug Discov* **2012,** 11, 191-200.

45. Mullin, R. Tufts study finds big rise in cost of drug development. *Chemical and Engineering News* **2014,** 92, 6.

46. Morphy, R.; Kay, C.; Rankovic, Z. From magic bullets to designed multiple ligands. *Drug Discov Today* **2004,** 9, 641-51.

47. Barabási, A. L.; Gulbahce, N.; Loscalzo, J. Network medicine: a network-based approach to human disease. *Nat Rev Genet* **2011,** 12, 56-68.

48. Hopkins, A. L. Network pharmacology: the next paradigm in drug discovery. *Nat Chem Biol* **2008,** 4, 682-90.

49. Iyengar, R. Complex diseases require complex therapies. *EMBO Rep* **2013,** 14, 1039-42.

50. Levis, M. Midostaurin approved for FLT3-mutated AML. *Blood* **2017,** 129, 3403-3406.

51. Viayna, E.; Sabate, R.; Muñoz-Torrero, D. Dual inhibitors of β-amyloid aggregation and acetylcholinesterase as multi-target anti-Alzheimer drug candidates. *Curr Top Med Chem* **2013,** 13, 1820-42.

52. Marzo, A.; Dal Bo, L.; Monti, N. C.; Crivelli, F.; Ismaili, S.; Caccia, C.; Cattaneo, C.; Fariello, R. G. Pharmacokinetics and pharmacodynamics of safinamide, a neuroprotectant with antiparkinsonian and anticonvulsant activity. *Pharmacol Res* **2004,** 50, 77-85.

53. Morphy, R.; Rankovic, Z. Designed multiple ligands. An emerging drug discovery paradigm. *J Med Chem* **2005,** 48, 6523-43.

54. Cavalli, A.; Bolognesi, M. L.; Minarini, A.; Rosini, M.; Tumiatti, V.; Recanatini, M.; Melchiorre, C. Multi-target-directed ligands to combat neurodegenerative diseases. *J Med Chem* **2008,** 51, 347-72.

55. Morphy, R. Selectively nonselective kinase inhibition: striking the right balance. *J Med Chem* **2010,** 53, 1413-37.

56. Youdim, M. B.; Buccafusco, J. J. Multi-functional drugs for various CNS targets in the treatment of neurodegenerative disorders. *Trends Pharmacol Sci* **2005,** 26, 27-35.

57. Van der Schyf, C. J.; Geldenhuys, W. J.; Youdim, M. B. Multifunctional drugs with different CNS

targets for neuropsychiatric disorders. *J Neurochem* **2006,** 99, 1033-48.

58. Millan, M. J. Multi-target strategies for the improved treatment of depressive states: Conceptual foundations and neuronal substrates, drug discovery and therapeutic application. *Pharmacol Ther* **2006,** 110, 135-370.

59. Bolognesi, M. L. Polypharmacology in a single drug: multitarget drugs. *Curr Med Chem* **2013,** 20, 1639-45.

60. Nelson, D. R.; Nebert, D. W. Cytochrome P450 (CYP) gene superfamily. *eLS* **2001**, 1-19.

61. Preskorn, S. H.; Flockhart, D. 2006 guide to psychiatric drug interactions. *Primary Psychiatry* **2006,** 13, 35.

62. Seritan, A. L. How to prevent drug-drug interactions with cholinesterase inhibitors. *Current Psychiatry* **2008,** 7, 57.

63. Bolognesi, M. L. Harnessing Polypharmacology with Medicinal Chemistry. *ACS Med Chem Lett* **2019,** 10, 273-275.

64. Decker, M. *Design of hybrid molecules for drug development*. Elsevier: 2017.

65. Kumar, A. P.; Lukman, S.; Nguyen, M. N. Drug Repurposing and Multi-Target Therapies. **2019**.

66. Kibble, M.; Saarinen, N.; Tang, J.; Wennerberg, K.; Mäkelä, S.; Aittokallio, T. Network pharmacology applications to map the unexplored target space and therapeutic potential of natural products. *Nat Prod Rep* **2015,** 32, 1249-66.

67. Wink, M. Ecological roles of alkaloids. *Modern alkaloids* **2008**, 3-24.

68. Ji, H. F.; Li, X. J.; Zhang, H. Y. Natural products and drug discovery. Can thousands of years of ancient medical knowledge lead us to new and powerful drug combinations in the fight against cancer and dementia? *EMBO Rep* **2009,** 10, 194-200.

69. Viegas-Junior, C.; Danuello, A.; da Silva Bolzani, V.; Barreiro, E. J.; Fraga, C. A. Molecular hybridization: a useful tool in the design of new drug prototypes. *Curr Med Chem* **2007,** 14, 1829-52.

70. Morphy, J. R. Chapter 10:The Challenges of Multi-Target Lead Optimization. In *Designing Multi-Target Drugs*, Chemistry, T. R. S. o., Ed. 2012.

71. Prati, F.; Cavalli, A.; Bolognesi, M. L. Navigating the Chemical Space of Multitarget-Directed Ligands: From Hybrids to Fragments in Alzheimer's Disease. *Molecules* **2016,** 21, 466.

72. Ivasiv, V.; Albertini, C.; Goncalves, A. E.; Rossi, M.; Bolognesi, M. L. Molecular Hybridization as a Tool for Designing Multitarget Drug Candidates for Complex Diseases. *Curr Top Med Chem* **2019**.

73. Morphy, R.; Rankovic, Z. The physicochemical challenges of designing multiple ligands. *J Med Chem* **2006,** 49, 4961-70.

74. Wager, T. T.; Hou, X.; Verhoest, P. R.; Villalobos, A. Moving beyond rules: the development of a central nervous system multiparameter optimization (CNS MPO) approach to enable alignment of druglike properties. *ACS Chem Neurosci* **2010,** 1, 435-49.

75. Pajouhesh, H.; Lenz, G. R. Medicinal chemical properties of successful central nervous system drugs. *NeuroRx* **2005,** 2, 541-53.

76. Rankovic, Z. CNS drug design: balancing physicochemical properties for optimal brain exposure. *J Med Chem* **2015,** 58, 2584-608.

77. Baltzer, B.; Binderup, E.; von Daehne, W.; Godtfredsen, W. O.; Hansen, K.; Nielsen, B.; Sørensen, H.; Vangedal, S. Mutual pro-drugs of beta-lactam antibiotics and beta-lactamase inhibitors. *J Antibiot (Tokyo)* **1980,** 33, 1183-92.

78. Donovan, J. M.; Zimmer, M.; Offman, E.; Grant, T.; Jirousek, M. A Novel NF-κB Inhibitor, Edasalonexent (CAT-1004), in Development as a Disease-Modifying Treatment for Patients With Duchenne

Muscular Dystrophy: Phase 1 Safety, Pharmacokinetics, and Pharmacodynamics in Adult Subjects. *J Clin Pharmacol* **2017,** 57, 627-639.

79. Youdim, M. B. Multi target neuroprotective and neurorestorative anti-Parkinson and anti-Alzheimer drugs ladostigil and m30 derived from rasagiline. *Exp Neurobiol* **2013,** 22, 1-10.

80. Bottegoni, G.; Favia, A. D.; Recanatini, M.; Cavalli, A. The role of fragment-based and computational methods in polypharmacology. *Drug Discov Today* **2012,** 17, 23-34.

81. Bollag, G.; Tsai, J.; Zhang, J.; Zhang, C.; Ibrahim, P.; Nolop, K.; Hirth, P. Vemurafenib: the first drug approved for BRAF-mutant cancer. *Nat Rev Drug Discov* **2012,** 11, 873-86.

82. Souers, A. J.; Leverson, J. D.; Boghaert, E. R.; Ackler, S. L.; Catron, N. D.; Chen, J.; Dayton, B. D.; Ding, H.; Enschede, S. H.; Fairbrother, W. J.; Huang, D. C.; Hymowitz, S. G.; Jin, S.; Khaw, S. L.; Kovar, P. J.; Lam, L. T.; Lee, J.; Maecker, H. L.; Marsh, K. C.; Mason, K. D.; Mitten, M. J.; Nimmer, P. M.; Oleksijew, A.; Park, C. H.; Park, C. M.; Phillips, D. C.; Roberts, A. W.; Sampath, D.; Seymour, J. F.; Smith, M. L.; Sullivan, G. M.; Tahir, S. K.; Tse, C.; Wendt, M. D.; Xiao, Y.; Xue, J. C.; Zhang, H.; Humerickhouse, R. A.; Rosenberg, S. H.; Elmore, S. W. ABT-199, a potent and selective BCL-2 inhibitor, achieves antitumor activity while sparing platelets. *Nat Med* **2013,** 19, 202-8.

83. Davis, B. J.; Roughley, S. D. Fragment-based lead discovery. In *Annual Reports in Medicinal Chemistry*, Elsevier: 2017; Vol. 50, pp 371-439.

84. Prati, F.; De Simone, A.; Bisignano, P.; Armirotti, A.; Summa, M.; Pizzirani, D.; Scarpelli, R.; Perez, D. I.; Andrisano, V.; Perez-Castillo, A.; Monti, B.; Massenzio, F.; Polito, L.; Racchi, M.; Favia, A. D.; Bottegoni, G.; Martinez, A.; Bolognesi, M. L.; Cavalli, A. Multitarget drug discovery for Alzheimer's disease: triazinones as BACE-1 and GSK-3β inhibitors. *Angew Chem Int Ed Engl* **2015,** 54, 1578-82.

85. Prati, F.; De Simone, A.; Armirotti, A.; Summa, M.; Pizzirani, D.; Scarpelli, R.; Bertozzi, S. M.; Perez, D. I.; Andrisano, V.; Perez-Castillo, A.; Monti, B.; Massenzio, F.; Polito, L.; Racchi, M.; Sabatino, P.; Bottegoni, G.; Martinez, A.; Cavalli, A.; Bolognesi, M. L. 3,4-Dihydro-1,3,5-triazin-2(1H)-ones as the First Dual BACE-1/GSK-3β Fragment Hits against Alzheimer's Disease. *ACS Chem Neurosci* **2015,** 6, 1665-82.

86. LePage, K. T.; Dickey, R. W.; Gerwick, W. H.; Jester, E. L.; Murray, T. F. On the use of neuro-2a neuroblastoma cells versus intact neurons in primary culture for neurotoxicity studies. *Crit Rev Neurobiol* **2005,** 17, 27-50.

87. Nepovimova, E.; Uliassi, E.; Korabecny, J.; Peña-Altamira, L. E.; Samez, S.; Pesaresi, A.; Garcia, G. E.; Bartolini, M.; Andrisano, V.; Bergamini, C.; Fato, R.; Lamba, D.; Roberti, M.; Kuca, K.; Monti, B.; Bolognesi, M. L. Multitarget drug design strategy: quinone-tacrine hybrids designed to block amyloid-β aggregation and to exert anticholinesterase and antioxidant effects. *J Med Chem* **2014,** 57, 8576-89.

88. Gameiro, I.; Michalska, P.; Tenti, G.; Cores, Á.; Buendia, I.; Rojo, A. I.; Georgakopoulos, N. D.; Hernández-Guijo, J. M.; Teresa Ramos, M.; Wells, G.; López, M. G.; Cuadrado, A.; Menéndez, J. C.; León, R. Discovery of the first dual GSK3β inhibitor/Nrf2 inducer. A new multitarget therapeutic strategy for Alzheimer's disease. *Sci Rep* **2017,** 7, 45701.

89. Jeřábek, J.; Uliassi, E.; Guidotti, L.; Korábečný, J.; Soukup, O.; Sepsova, V.; Hrabinova, M.; Kuča, K.; Bartolini, M.; Peña-Altamira, L. E.; Petralla, S.; Monti, B.; Roberti, M.; Bolognesi, M. L. Tacrine-resveratrol fused hybrids as multi-target-directed ligands against Alzheimer's disease. *Eur J Med Chem* **2017,** 127, 250-262.

90. Calsolaro, V.; Edison, P. Neuroinflammation in Alzheimer's disease: Current evidence and future directions. *Alzheimers Dement* **2016,** 12, 719-32.

91. Peña-Altamira, E.; Prati, F.; Massenzio, F.; Virgili, M.; Contestabile, A.; Bolognesi, M. L.; Monti, B. Changing paradigm to target microglia in neurodegenerative diseases: from anti-inflammatory strategy to active immunomodulation. *Expert Opin Ther Targets* **2016,** 20, 627-40.

92. Szepesi, Z.; Manouchehrian, O.; Bachiller, S.; Deierborg, T. Bidirectional Microglia-Neuron Communication in Health and Disease. *Front Cell Neurosci* **2018,** 12, 323.

93. Chen, S.; Wu, H.; Klebe, D.; Hong, Y.; Zhang, J. Valproic acid: a new candidate of therapeutic application for the acute central nervous system injuries. *Neurochem Res* **2014,** 39, 1621-33.

94. Sousa, C.; Biber, K.; Michelucci, A. Cellular and Molecular Characterization of Microglia: A Unique Immune Cell Population. *Front Immunol* **2017,** 8, 198.

95. Roqué, P. J.; Costa, L. G. Co-Culture of Neurons and Microglia. *Curr Protoc Toxicol* **2017,** 74, 11.24.1-11.24.17.

96. Moraes, C. B.; Witt, G.; Kuzikov, M.; Ellinger, B.; Calogeropoulou, T.; Prousis, K. C.; Mangani, S.; Di Pisa, F.; Landi, G.; Iacono, L. D.; Pozzi, C.; Freitas-Junior, L. H.; Dos Santos Pascoalino, B.; Bertolacini, C. P.; Behrens, B.; Keminer, O.; Leu, J.; Wolf, M.; Reinshagen, J.; Cordeiro-da-Silva, A.; Santarem, N.; Venturelli, A.; Wrigley, S.; Karunakaran, D.; Kebede, B.; Pöhner, I.; Müller, W.; Panecka-Hofman, J.; Wade, R. C.; Fenske, M.; Clos, J.; Alunda, J. M.; Corral, M. J.; Uliassi, E.; Bolognesi, M. L.; Linciano, P.; Quotadamo, A.; Ferrari, S.; Santucci, M.; Borsari, C.; Costi, M. P.; Gul, S. Accelerating Drug Discovery Efforts for Trypanosomatidic Infections Using an Integrated Transnational Academic Drug Discovery Platform. *SLAS Discov* **2019,** 24, 346-361.

97. Bazinet, R. P.; Layé, S. Polyunsaturated fatty acids and their metabolites in brain function and disease. *Nat Rev Neurosci* **2014,** 15, 771-85.

98. Layé, S.; Nadjar, A.; Joffre, C.; Bazinet, R. P. Anti-Inflammatory Effects of Omega-3 Fatty Acids in the Brain: Physiological Mechanisms and Relevance to Pharmacology. *Pharmacol Rev* **2018,** 70, 12-38.

99. Gao, F.; Kiesewetter, D.; Chang, L.; Ma, K.; Bell, J. M.; Rapoport, S. I.; Igarashi, M. Whole-body synthesis-secretion rates of long-chain n-3 PUFAs from circulating unesterified alpha-linolenic acid in unanesthetized rats. *J Lipid Res* **2009,** 50, 749-58.

100. Lee, J. M.; Lee, H.; Kang, S.; Park, W. J. Fatty Acid Desaturases, Polyunsaturated Fatty Acid Regulation, and Biotechnological Advances. *Nutrients* **2016,** 8.

101. Kidd, P. M. Omega-3 DHA and EPA for cognition, behavior, and mood: clinical findings and structural-functional synergies with cell membrane phospholipids. *Altern Med Rev* **2007,** 12, 207-27.

102. Liu, J. J.; Green, P.; John Mann, J.; Rapoport, S. I.; Sublette, M. E. Pathways of polyunsaturated fatty acid utilization: implications for brain function in neuropsychiatric health and disease. *Brain Res* **2015,** 1597, 220-46.

103. Sledzinski, T.; Mika, A.; Stepnowski, P.; Proczko-Markuszewska, M.; Kaska, L.; Stefaniak, T.; Swierczynski, J. Identification of cyclopropaneoctanoic acid 2-hexyl in human adipose tissue and serum. *Lipids* **2013,** 48, 839-48.

104. Molfino, A.; Gioia, G.; Rossi Fanelli, F.; Muscaritoli, M. The role for dietary omega-3 fatty acids supplementation in older adults. *Nutrients* **2014,** 6, 4058-73.

105. Ferreri, C.; Masi, A.; Sansone, A.; Giacometti, G.; Larocca, A. V.; Menounou, G.; Scanferlato, R.; Tortorella, S.; Rota, D.; Conti, M.; Deplano, S.; Louka, M.; Maranini, A. R.; Salati, A.; Sunda, V.; Chatgilialoglu, C. Fatty Acids in Membranes as Homeostatic, Metabolic and Nutritional Biomarkers: Recent Advancements in Analytics and Diagnostics. *Diagnostics (Basel)* **2016,** 7.

106. Lauritzen, L.; Hansen, H. S.; Jørgensen, M. H.; Michaelsen, K. F. The essentiality of long chain n-3 fatty acids in relation to development and function of the brain and retina. *Prog Lipid Res* **2001,** 40, 1-94.

107. Chen, C. T.; Bazinet, R. P. β-oxidation and rapid metabolism, but not uptake regulate brain eicosapentaenoic acid levels. *Prostaglandins Leukot Essent Fatty Acids* **2015,** 92, 33-40.

108. Chen, C. T.; Liu, Z.; Ouellet, M.; Calon, F.; Bazinet, R. P. Rapid beta-oxidation of eicosapentaenoic acid in mouse brain: an in situ study. *Prostaglandins Leukot Essent Fatty Acids* **2009,** 80, 157-63.

109. Layé, S. Polyunsaturated fatty acids, neuroinflammation and well being. *Prostaglandins Leukot Essent Fatty Acids* **2010,** 82, 295-303.

110. Delpech, J. C.; Madore, C.; Joffre, C.; Aubert, A.; Kang, J. X.; Nadjar, A.; Layé, S. Transgenic increase

in n-3/n-6 fatty acid ratio protects against cognitive deficits induced by an immune challenge through decrease of neuroinflammation. *Neuropsychopharmacology* **2015,** 40, 525-36.

111. Orr, S. K.; Trépanier, M. O.; Bazinet, R. P. n-3 Polyunsaturated fatty acids in animal models with neuroinflammation. *Prostaglandins Leukot Essent Fatty Acids* **2013,** 88, 97-103.

112. Calder, P. C. n-3 polyunsaturated fatty acids, inflammation, and inflammatory diseases. *Am J Clin Nutr* **2006,** 83, 1505S-1519S.

113. Serhan, C. N. Pro-resolving lipid mediators are leads for resolution physiology. *Nature* **2014,** 510, 92-101.

114. Ferrucci, L.; Cherubini, A.; Bandinelli, S.; Bartali, B.; Corsi, A.; Lauretani, F.; Martin, A.; Andres-Lacueva, C.; Senin, U.; Guralnik, J. M. Relationship of plasma polyunsaturated fatty acids to circulating inflammatory markers. *J Clin Endocrinol Metab* **2006,** 91, 439-46.

115. Kiecolt-Glaser, J. K.; Belury, M. A.; Porter, K.; Beversdorf, D. Q.; Lemeshow, S.; Glaser, R. Depressive symptoms, omega-6:omega-3 fatty acids, and inflammation in older adults. *Psychosom Med* **2007,** 69, 217-24.

116. Vedin, I.; Cederholm, T.; Freund Levi, Y.; Basun, H.; Garlind, A.; Faxén Irving, G.; Jönhagen, M. E.; Vessby, B.; Wahlund, L. O.; Palmblad, J. Effects of docosahexaenoic acid-rich n-3 fatty acid supplementation on cytokine release from blood mononuclear leukocytes: the OmegAD study. *Am J Clin Nutr* **2008,** 87, 1616-22.

117. Ransohoff, R. M.; Cardona, A. E. The myeloid cells of the central nervous system parenchyma. *Nature* **2010,** 468, 253-62.

118. De Smedt-Peyrusse, V.; Sargueil, F.; Moranis, A.; Harizi, H.; Mongrand, S.; Layé, S. Docosahexaenoic acid prevents lipopolysaccharide-induced cytokine production in microglial cells by inhibiting lipopolysaccharide receptor presentation but not its membrane subdomain localization. *J Neurochem* **2008,** 105, 296-307.

119. Figueroa, J. D.; Cordero, K.; Baldeosingh, K.; Torrado, A. I.; Walker, R. L.; Miranda, J. D.; Leon, M. D. Docosahexaenoic acid pretreatment confers protection and functional improvements after acute spinal cord injury in adult rats. *J Neurotrauma* **2012,** 29, 551-66.

120. Hjorth, E.; Zhu, M.; Toro, V. C.; Vedin, I.; Palmblad, J.; Cederholm, T.; Freund-Levi, Y.; Faxen-Irving, G.; Wahlund, L. O.; Basun, H.; Eriksdotter, M.; Schultzberg, M. Omega-3 fatty acids enhance phagocytosis of Alzheimer's disease-related amyloid-β42 by human microglia and decrease inflammatory markers. *J Alzheimers Dis* **2013,** 35, 697-713.

121. Salem, N.; Litman, B.; Kim, H. Y.; Gawrisch, K. Mechanisms of action of docosahexaenoic acid in the nervous system. *Lipids* **2001,** 36, 945-59.

122. Stillwell, W.; Wassall, S. R. Docosahexaenoic acid: membrane properties of a unique fatty acid. *Chem Phys Lipids* **2003,** 126, 1-27.

123. Murphy, M. G. Membrane fatty acids, lipid peroxidation and adenylate cyclase activity in cultured neural cells. *Biochem Biophys Res Commun* **1985,** 132, 757-63.

124. Nicolas, C.; Lacasa, D.; Giudicelli, Y.; Demarne, Y.; Agli, B.; Lecourtier, M. J.; Lhuillery, C. Dietary (n-6) polyunsaturated fatty acids affect beta-adrenergic receptor binding and adenylate cyclase activity in pig adipocyte plasma membrane. *J Nutr* **1991,** 121, 1179-86.

125. Green, J. T.; Orr, S. K.; Bazinet, R. P. The emerging role of group VI calcium-independent phospholipase A2 in releasing docosahexaenoic acid from brain phospholipids. *J Lipid Res* **2008,** 49, 939-44.

126. Stella, N. Endocannabinoid signaling in microglial cells. *Neuropharmacology* **2009,** 56 Suppl 1, 244-53.

127. Kim, H. Y.; Spector, A. A. Synaptamide, endocannabinoid-like derivative of docosahexaenoic acid with cannabinoid-independent function. *Prostaglandins Leukot Essent Fatty Acids* **2013,** 88, 121-5.

128. Piomelli, D.; Sasso, O. Peripheral gating of pain signals by endogenous lipid mediators. *Nat Neurosci* **2014,** 17, 164-74.

129. Castillo, P. E.; Younts, T. J.; Chávez, A. E.; Hashimotodani, Y. Endocannabinoid signaling and synaptic function. *Neuron* **2012,** 76, 70-81.

130. Grueter, B. A.; Brasnjo, G.; Malenka, R. C. Postsynaptic TRPV1 triggers cell type-specific long-term depression in the nucleus accumbens. *Nat Neurosci* **2010,** 13, 1519-25.

131. Kim, H. Y.; Moon, H. S.; Cao, D.; Lee, J.; Kevala, K.; Jun, S. B.; Lovinger, D. M.; Akbar, M.; Huang, B. X. N-Docosahexaenoylethanolamide promotes development of hippocampal neurons. *Biochem J* **2011,** 435, 327-36.

132. Kim, H. Y.; Spector, A. A.; Xiong, Z. M. A synaptogenic amide N-docosahexaenoylethanolamide promotes hippocampal development. *Prostaglandins Other Lipid Mediat* **2011,** 96, 114-20.

133. Cao, D.; Kevala, K.; Kim, J.; Moon, H. S.; Jun, S. B.; Lovinger, D.; Kim, H. Y. Docosahexaenoic acid promotes hippocampal neuronal development and synaptic function. *J Neurochem* **2009,** 111, 510-21.

134. Fedorova, I.; Salem, N. Omega-3 fatty acids and rodent behavior. *Prostaglandins Leukot Essent Fatty Acids* **2006,** 75, 271-89.

135. Calderon, F.; Kim, H. Y. Docosahexaenoic acid promotes neurite growth in hippocampal neurons. *J Neurochem* **2004,** 90, 979-88.

136. Kim, H. Y.; Akbar, M.; Lau, A.; Edsall, L. Inhibition of neuronal apoptosis by docosahexaenoic acid (22:6n-3). Role of phosphatidylserine in antiapoptotic effect. *J Biol Chem* **2000,** 275, 35215-23.

137. Zimmermann, S.; Moelling, K. Phosphorylation and regulation of Raf by Akt (protein kinase B). *Science* **1999,** 286, 1741-4.

138. Lo Van, A.; Sakayori, N.; Hachem, M.; Belkouch, M.; Picq, M.; Lagarde, M.; Osumi, N.; Bernoud-Hubac, N. Mechanisms of DHA transport to the brain and potential therapy to neurodegenerative diseases. *Biochimie* **2016,** 130, 163-167.

139. Bannenberg, G.; Serhan, C. N. Specialized pro-resolving lipid mediators in the inflammatory response: An update. *Biochim Biophys Acta* **2010,** 1801, 1260-73.

140. Spite, M.; Clària, J.; Serhan, C. N. Resolvins, specialized proresolving lipid mediators, and their potential roles in metabolic diseases. *Cell Metab* **2014,** 19, 21-36.

141. Rashid, M. A.; Kim, H. Y. N-Docosahexaenoylethanolamine ameliorates ethanol-induced impairment of neural stem cell neurogenic differentiation. *Neuropharmacology* **2016,** 102, 174-85.

142. Kim, H. Y.; Spector, A. A. N-Docosahexaenoylethanolamine: A neurotrophic and neuroprotective metabolite of docosahexaenoic acid. *Mol Aspects Med* **2018,** 64, 34-44.

143. Park, T.; Chen, H.; Kevala, K.; Lee, J. W.; Kim, H. Y. N-Docosahexaenoylethanolamine ameliorates LPS-induced neuroinflammation via cAMP/PKA-dependent signaling. *J Neuroinflammation* **2016,** 13, 284.

144. Lee, J. W.; Huang, B. X.; Kwon, H.; Rashid, M. A.; Kharebava, G.; Desai, A.; Patnaik, S.; Marugan, J.; Kim, H. Y. Orphan GPR110 (ADGRF1) targeted by N-docosahexaenoylethanolamine in development of neurons and cognitive function. *Nat Commun* **2016,** 7, 13123.

145. Park, S. W.; Hah, J. H.; Oh, S. M.; Jeong, W. J.; Sung, M. W. 5-lipoxygenase mediates docosahexaenoyl ethanolamide and N-arachidonoyl-L-alanine-induced reactive oxygen species production and inhibition of proliferation of head and neck squamous cell carcinoma cells. *BMC Cancer* **2016,** 16, 458.

146. Meijerink, J.; Poland, M.; Balvers, M. G.; Plastina, P.; Lute, C.; Dwarkasing, J.; van Norren, K.; Witkamp, R. F. Inhibition of COX-2-mediated eicosanoid production plays a major role in the anti-inflammatory effects of the endocannabinoid N-docosahexaenoylethanolamine (DHEA) in macrophages. *Br J Pharmacol* **2015,** 172, 24-37.

147. Cicero, A. F.; Reggi, A.; Parini, A.; Borghi, C. Application of polyunsaturated fatty acids in internal

medicine: beyond the established cardiovascular effects. *Arch Med Sci* **2012,** 8, 784-93.

148. Rationalizing combination therapies. *Nat Med* **2017,** 23, 1113.

149. Morris, M. C.; Evans, D. A.; Bienias, J. L.; Tangney, C. C.; Bennett, D. A.; Wilson, R. S.; Aggarwal, N.; Schneider, J. Consumption of fish and n-3 fatty acids and risk of incident Alzheimer disease. *Arch Neurol* **2003,** 60, 940-6.

150. Reitz, C.; Brayne, C.; Mayeux, R. Epidemiology of Alzheimer disease. *Nat Rev Neurol* **2011,** 7, 137-52.

151. Quinn, J. F.; Raman, R.; Thomas, R. G.; Yurko-Mauro, K.; Nelson, E. B.; Van Dyck, C.; Galvin, J. E.; Emond, J.; Jack, C. R.; Weiner, M.; Shinto, L.; Aisen, P. S. Docosahexaenoic acid supplementation and cognitive decline in Alzheimer disease: a randomized trial. *JAMA* **2010,** 304, 1903-11.

152. Freund-Levi, Y.; Basun, H.; Cederholm, T.; Faxén-Irving, G.; Garlind, A.; Grut, M.; Vedin, I.; Palmblad, J.; Wahlund, L. O.; Eriksdotter-Jönhagen, M. Omega-3 supplementation in mild to moderate Alzheimer's disease: effects on neuropsychiatric symptoms. *Int J Geriatr Psychiatry* **2008,** 23, 161-9.

153. DeGiorgio, C. M.; Taha, A. Y. Omega-3 fatty acids (ϖ-3 fatty acids) in epilepsy: animal models and human clinical trials. *Expert Rev Neurother* **2016,** 16, 1141-5.

154. Xiao, Y. F.; Kang, J. X.; Morgan, J. P.; Leaf, A. Blocking effects of polyunsaturated fatty acids on Na+ channels of neonatal rat ventricular myocytes. *Proc Natl Acad Sci U S A* **1995,** 92, 11000-4.

155. Xiao, Y. F.; Gomez, A. M.; Morgan, J. P.; Lederer, W. J.; Leaf, A. Suppression of voltage-gated L-type Ca2+ currents by polyunsaturated fatty acids in adult and neonatal rat ventricular myocytes. *Proc Natl Acad Sci U S A* **1997,** 94, 4182-7.

156. Taha, A. Y.; Huot, P. S.; Reza-López, S.; Prayitno, N. R.; Kang, J. X.; Burnham, W. M.; Ma, D. W. Seizure resistance in fat-1 transgenic mice endogenously synthesizing high levels of omega-3 polyunsaturated fatty acids. *J Neurochem* **2008,** 105, 380-8.

157. El-Mowafy, A. M.; Abdel-Dayem, M. A.; Abdel-Aziz, A.; El-Azab, M. F.; Said, S. A. Eicosapentaenoic acid ablates valproate-induced liver oxidative stress and cellular derangement without altering its clearance rate: dynamic synergy and therapeutic utility. *Biochim Biophys Acta* **2011,** 1811, 460-7.

158. Abdel-Dayem, M. A.; Elmarakby, A. A.; Abdel-Aziz, A. A.; Pye, C.; Said, S. A.; El-Mowafy, A. M. Valproate-induced liver injury: modulation by the omega-3 fatty acid DHA proposes a novel anticonvulsant regimen. *Drugs R D* **2014,** 14, 85-94.

159. Abdel-Wahab, B. A.; Shaikh, I. A.; Khateeb, M. M.; Habeeb, S. M. Omega 3 polyunsaturated fatty acids enhance the protective effect of levetiracetam against seizures, cognitive impairment and hippocampal oxidative DNA damage in young kindled rats. *Pharmacol Biochem Behav* **2015,** 135, 105-13.

160. Ramirez-Ramirez, V.; Macias-Islas, M. A.; Ortiz, G. G.; Pacheco-Moises, F.; Torres-Sanchez, E. D.; Sorto-Gomez, T. E.; Cruz-Ramos, J. A.; Orozco-Aviña, G.; Celis de la Rosa, A. J. Efficacy of fish oil on serum of TNF α , IL-1 β , and IL-6 oxidative stress markers in multiple sclerosis treated with interferon beta-1b. *Oxid Med Cell Longev* **2013,** 2013, 709493.

161. Meinig, J. M.; Ferrara, S. J.; Banerji, T.; Sanford-Crane, H. S.; Bourdette, D.; Scanlan, T. S. Targeting Fatty-Acid Amide Hydrolase with Prodrugs for CNS-Selective Therapy. *ACS Chem Neurosci* **2017,** 8, 2468-2476.

162. Irby, D.; Du, C.; Li, F. Lipid-Drug Conjugate for Enhancing Drug Delivery. *Mol Pharm* **2017,** 14, 1325-1338.

163. Taresco, V.; Alexander, C.; Singh, N.; Pearce, A. K. Stimuli-Responsive Prodrug Chemistries for Drug Delivery. *Advanced Therapeutics* **2018,** 1.

164. Gong, X.; Moghaddam, M. J.; Sagnella, S. M.; Conn, C. E.; Danon, S. J.; Waddington, L. J.; Drummond, C. J. Lamellar crystalline self-assembly behaviour and solid lipid nanoparticles of a palmityl prodrug analogue of Capecitabine--a chemotherapy agent. *Colloids Surf B Biointerfaces* **2011,** 85, 349-59.

165. Jin, Y.; Lian, Y.; Du, L.; Wang, S.; Su, C.; Gao, C. Self-assembled drug delivery systems. Part 6: in vitro/in vivo studies of anticancer N-octadecanoyl gemcitabine nanoassemblies. *Int J Pharm* **2012,** 430, 276-81.

166. Tamargo, J.; Tamargo, M. Pharmacokinetics and Safety Profile of Omega-3 Polyunsaturated Fatty Acids. In *Omega-3 Fatty Acids*, Springer: 2016; pp 541-584.

167. Vu, C. B.; Bemis, J. E.; Benson, E.; Bista, P.; Carney, D.; Fahrner, R.; Lee, D.; Liu, F.; Lonkar, P.; Milne, J. C.; Nichols, A. J.; Picarella, D.; Shoelson, A.; Smith, J.; Ting, A.; Wensley, A.; Yeager, M.; Zimmer, M.; Jirousek, M. R. Synthesis and Characterization of Fatty Acid Conjugates of Niacin and Salicylic Acid. *J Med Chem* **2016,** 59, 1217-31.

168. Wang, Y.; Plastina, P.; Vincken, J. P.; Jansen, R.; Balvers, M.; Ten Klooster, J. P.; Gruppen, H.; Witkamp, R.; Meijerink, J. N-Docosahexaenoyl Dopamine, an Endocannabinoid-like Conjugate of Dopamine and the n-3 Fatty Acid Docosahexaenoic Acid, Attenuates Lipopolysaccharide-Induced Activation of Microglia and Macrophages via COX-2. *ACS Chem Neurosci* **2017,** 8, 548-557.

169. Seitz, J.; Ojima, I. Drug conjugates with polyunsaturated fatty acids. In Wiley-VCH, Weinheim, Germany: 2011; pp 1323-1360.

170. Wachira, J. K.; Larson, M. K.; Harris, W. S. n-3 Fatty acids affect haemostasis but do not increase the risk of bleeding: clinical observations and mechanistic insights. *Br J Nutr* **2014,** 111, 1652-62.

171. Blondeau, N.; Lipsky, R. H.; Bourourou, M.; Duncan, M. W.; Gorelick, P. B.; Marini, A. M. Alpha-linolenic acid: an omega-3 fatty acid with neuroprotective properties-ready for use in the stroke clinic? *Biomed Res Int* **2015,** 2015, 519830.

172. Zhang, X. Z.; Li, X. J.; Zhang, H. Y. Valproic acid as a promising agent to combat Alzheimer's disease. *Brain Res Bull* **2010,** 81, 3-6.

173. Nielsen, N. M.; Svanström, H.; Stenager, E.; Magyari, M.; Koch-Henriksen, N.; Pasternak, B.; Hviid, A. The use of valproic acid and multiple sclerosis. *Pharmacoepidemiol Drug Saf* **2015,** 24, 262-8.

174. Durham, B. S.; Grigg, R.; Wood, I. C. Inhibition of histone deacetylase 1 or 2 reduces induced cytokine expression in microglia through a protein synthesis independent mechanism. *J Neurochem* **2017,** 143, 214-224.

175. Gibbons, H. M.; Smith, A. M.; Teoh, H. H.; Bergin, P. M.; Mee, E. W.; Faull, R. L.; Dragunow, M. Valproic acid induces microglial dysfunction, not apoptosis, in human glial cultures. *Neurobiol Dis* **2011,** 41, 96-103.

176. Fleisher, A. S.; Truran, D.; Mai, J. T.; Langbaum, J. B.; Aisen, P. S.; Cummings, J. L.; Jack, C. R.; Weiner, M. W.; Thomas, R. G.; Schneider, L. S.; Tariot, P. N.; Study, A. s. D. C. Chronic divalproex sodium use and brain atrophy in Alzheimer disease. *Neurology* **2011,** 77, 1263-71.

177. Chen, S.; Ye, J.; Chen, X.; Shi, J.; Wu, W.; Lin, W.; Li, Y.; Fu, H.; Li, S. Valproic acid attenuates traumatic spinal cord injury-induced inflammation via STAT1 and NF-κB pathway dependent of HDAC3. *J Neuroinflammation* **2018,** 15, 150.

178. Zhang, Z.; Zhang, Z. Y.; Wu, Y.; Schluesener, H. J. Valproic acid ameliorates inflammation in experimental autoimmune encephalomyelitis rats. *Neuroscience* **2012,** 221, 140-50.

179. Hooijmans, C. R.; Hlavica, M.; Schuler, F. A. F.; Good, N.; Good, A.; Baumgartner, L.; Galeno, G.; Schneider, M. P.; Jung, T.; de Vries, R.; Ineichen, B. V. Remyelination promoting therapies in multiple sclerosis animal models: a systematic review and meta-analysis. *Sci Rep* **2019,** 9, 822.

180. Bozzatello, P.; Rocca, P.; Bellino, S. Combination of Omega-3 Fatty Acids and Valproic Acid in Treatment of Borderline Personality Disorder: A Follow-Up Study. *Clin Drug Investig* **2018,** 38, 367-372.

181. Aljuffali, I. A.; Lin, C. F.; Chen, C. H.; Fang, J. Y. The codrug approach for facilitating drug delivery and bioactivity. *Expert Opin Drug Deliv* **2016,** 13, 1311-25.

182. Contestabile, A. Cerebellar granule cells as a model to study mechanisms of neuronal apoptosis or

survival in vivo and in vitro. *Cerebellum* **2002,** 1, 41-55.

183. Niculescu, M. D.; Lupu, D. S.; Craciunescu, C. N. Perinatal manipulation of α-linolenic acid intake induces epigenetic changes in maternal and offspring livers. *FASEB J* **2013,** 27, 350-8.

184. Chen, X.; Chen, C.; Fan, S.; Wu, S.; Yang, F.; Fang, Z.; Fu, H.; Li, Y. Omega-3 polyunsaturated fatty acid attenuates the inflammatory response by modulating microglia polarization through SIRT1-mediated deacetylation of the HMGB1/NF-κB pathway following experimental traumatic brain injury. *J Neuroinflammation* **2018,** 15, 116.

185. Takahashi, K.; Prinz, M.; Stagi, M.; Chechneva, O.; Neumann, H. TREM2-transduced myeloid precursors mediate nervous tissue debris clearance and facilitate recovery in an animal model of multiple sclerosis. *PLoS Med* **2007,** 4, e124.

186. Kipp, M.; van der Star, B.; Vogel, D. Y.; Puentes, F.; van der Valk, P.; Baker, D.; Amor, S. Experimental in vivo and in vitro models of multiple sclerosis: EAE and beyond. *Mult Scler Relat Disord* **2012,** 1, 15-28.

187. Ransohoff, R. M. How neuroinflammation contributes to neurodegeneration. *Science* **2016,** 353, 777-83.

188. Wolf, S. A.; Boddeke, H. W.; Kettenmann, H. Microglia in Physiology and Disease. *Annu Rev Physiol* **2017,** 79, 619-643.

189. Fu, W. Y.; Wang, X.; Ip, N. Y. Targeting Neuroinflammation as a Therapeutic Strategy for Alzheimer's Disease: Mechanisms, Drug Candidates, and New Opportunities. *ACS Chem Neurosci* **2019,** 10, 872-879.

190. Heppner, F. L.; Ransohoff, R. M.; Becher, B. Immune attack: the role of inflammation in Alzheimer disease. *Nat Rev Neurosci* **2015,** 16, 358-72.

191. Koizumi, S.; Shigemoto-Mogami, Y.; Nasu-Tada, K.; Shinozaki, Y.; Ohsawa, K.; Tsuda, M.; Joshi, B. V.; Jacobson, K. A.; Kohsaka, S.; Inoue, K. UDP acting at P2Y6 receptors is a mediator of microglial phagocytosis. *Nature* **2007,** 446, 1091-5.

192. Inoue, K.; Koizumi, S.; Kataoka, A.; Tozaki-Saitoh, H.; Tsuda, M. P2Y(6)-Evoked Microglial Phagocytosis. *Int Rev Neurobiol* **2009,** 85, 159-63.

193. Rafehi, M.; Müller, C. E. Tools and drugs for uracil nucleotide-activated P2Y receptors. *Pharmacol Ther* **2018,** 190, 24-80.

194. Costanzi, S.; Mamedova, L.; Gao, Z. G.; Jacobson, K. A. Architecture of P2Y nucleotide receptors: structural comparison based on sequence analysis, mutagenesis, and homology modeling. *J Med Chem* **2004,** 47, 5393-404.

195. Abbracchio, M. P.; Burnstock, G.; Boeynaems, J. M.; Barnard, E. A.; Boyer, J. L.; Kennedy, C.; Knight, G. E.; Fumagalli, M.; Gachet, C.; Jacobson, K. A.; Weisman, G. A. International Union of Pharmacology LVIII: update on the P2Y G protein-coupled nucleotide receptors: from molecular mechanisms and pathophysiology to therapy. *Pharmacol Rev* **2006,** 58, 281-341.

196. Kawashita, E.; Tsuji, D.; Kanno, Y.; Tsuchida, K.; Itoh, K. Enhancement by Uridine Diphosphate of Macrophage Inflammatory Protein-1 Alpha Production in Microglia Derived from Sandhoff Disease Model Mice. *JIMD Rep* **2016,** 28, 85-93.

197. Kim, B.; Jeong, H. K.; Kim, J. H.; Lee, S. Y.; Jou, I.; Joe, E. H. Uridine 5'-diphosphate induces chemokine expression in microglia and astrocytes through activation of the P2Y6 receptor. *J Immunol* **2011,** 186, 3701-9.

198. Jacobson, K. A.; Costanzi, S.; Joshi, B. V.; Besada, P.; Shin, D. H.; Ko, H.; Ivanov, A. A.; Mamedova, L. Agonists and antagonists for P2 receptors. *Novartis Found Symp* **2006,** 276, 58-68; discussion 68-72, 107-12, 275-81.

199. Chetty, A.; Sharda, A.; Warburton, R.; Weinberg, E. O.; Dong, J.; Fang, M.; Sahagian, G. G.; Chen, T.; Xue, C.; Castellot, J. J.; Haydon, P. G.; Nielsen, H. C. A purinergic P2Y6 receptor agonist prodrug modulates airway inflammation, remodeling, and hyperreactivity in a mouse model of asthma. *J Asthma Allergy* **2018,**

11, 159-171.

200. Boswell-Casteel, R. C.; Hays, F. A. Equilibrative nucleoside transporters-A review. *Nucleosides Nucleotides Nucleic Acids* **2017,** 36, 7-30.

201. Pradere, U.; Garnier-Amblard, E. C.; Coats, S. J.; Amblard, F.; Schinazi, R. F. Synthesis of nucleoside phosphate and phosphonate prodrugs. *Chem Rev* **2014,** 114, 9154-218.

202. El-Tayeb, A.; Qi, A.; Nicholas, R. A.; Müller, C. E. Structural modifications of UMP, UDP, and UTP leading to subtype-selective agonists for P2Y2, P2Y4, and P2Y6 receptors. *J Med Chem* **2011,** 54, 2878-90.

203. El-Tayeb, A.; Qi, A.; Müller, C. E. Synthesis and structure-activity relationships of uracil nucleotide derivatives and analogues as agonists at human P2Y2, P2Y4, and P2Y6 receptors. *J Med Chem* **2006,** 49, 7076-87.

204. Besada, P.; Shin, D. H.; Costanzi, S.; Ko, H.; Mathé, C.; Gagneron, J.; Gosselin, G.; Maddileti, S.; Harden, T. K.; Jacobson, K. A. Structure-activity relationships of uridine 5'-diphosphate analogues at the human P2Y6 receptor. *J Med Chem* **2006,** 49, 5532-43.

205. Hacker, S. M.; Mex, M.; Marx, A. Synthesis and stability of phosphate modified ATP analogues. *J Org Chem* **2012,** 77, 10450-4.

206. Gollnest, T.; de Oliveira, T. D.; Schols, D.; Balzarini, J.; Meier, C. Lipophilic prodrugs of nucleoside triphosphates as biochemical probes and potential antivirals. *Nat Commun* **2015,** 6, 8716.

207. Gollnest, T.; Dinis de Oliveira, T.; Rath, A.; Hauber, I.; Schols, D.; Balzarini, J.; Meier, C. Membrane-permeable Triphosphate Prodrugs of Nucleoside Analogues. *Angew Chem Int Ed Engl* **2016,** 55, 5255-8.

208. Aisen, P. S.; Cummings, J.; Jack, C. R.; Morris, J. C.; Sperling, R.; Frölich, L.; Jones, R. W.; Dowsett, S. A.; Matthews, B. R.; Raskin, J.; Scheltens, P.; Dubois, B. On the path to 2025: understanding the Alzheimer's disease continuum. *Alzheimers Res Ther* **2017,** 9, 60.

209. Wimo, A.; Guerchet, M.; Ali, G. C.; Wu, Y. T.; Prina, A. M.; Winblad, B.; Jönsson, L.; Liu, Z.; Prince, M. The worldwide costs of dementia 2015 and comparisons with 2010. *Alzheimers Dement* **2017,** 13, 1-7.

210. International, A. s. D. *World Alzheimer Report, 2019, https://www.alz.co.uk/research/WorldAlzheimerReport2019.pdf*.

211. UK, A. s. R. *Dementia Statistic Hub, https://www.dementiastatistics.org/statistics/global-prevalence/*.

212. GROUP, T. W. B. *World Bank Country and Lending Groups, https://datahelpdesk.worldbank.org/knowledgebase/articles/906519-world-bank-country-and-lending-groups*.

213. International, A. D. *World Alzheimer report 2015 - the global impact of dementia: an analysis of prevalence, incidence, cost and trends. https://www.alz.co.uk/research/world-report-2015*

214. Marciani, D. J. Facing Alzheimer's disease in the developing countries. *Revista de Neuro-Psiquiatría* **2017,** 80, 105-110.

215. It's Time for Pharmaceutical Companies to Have Their Tobacco Moment. *The New York Times* **2019**, 22.

216. Pollack, A. *Drug Goes From $13.50 a Tablet to $750, Overnight*. *The New York Time* **2015**.

217. Cummings, J.; Reiber, C.; Kumar, P. The price of progress: Funding and financing Alzheimer's disease drug development. *Alzheimers Dement (N Y)* **2018,** 4, 330-343.

218. Prasad, V.; Mailankody, S. Research and Development Spending to Bring a Single Cancer Drug to Market and Revenues After Approval. *JAMA Intern Med* **2017,** 177, 1569-1575.

219. Deardorff, W. J.; Grossberg, G. T. A fixed-dose combination of memantine extended-release and donepezil in the treatment of moderate-to-severe Alzheimer's disease. *Drug Des Devel Ther* **2016,** 10, 3267-3279.

220. M.D. https://www.pfizer.com/news/featured_stories/featured_stories_detail/learn_more_about_our_neuroscience_r_d_decision. In.

221. Lin, C. S. K.; Pfaltzgraff, L. A.; Herrero-Davila, L.; Mubofu, E. B.; Abderrahim, S.; Clark, J. H.; Koutinas, A. A.; Kopsahelis, N.; Stamatelatou, K.; Dickson, F. Food waste as a valuable resource for the production of chemicals, materials and fuels. Current situation and global perspective. *Energy & Environmental Science* **2013,** 6, 426-464.

222. Socaci, S. A.; Fărcaş, A. C.; Vodnar, D. C.; Tofană, M. Food wastes as valuable sources of bio-active molecules. *Superfood and Functional Food—The Development of Superfoods and Their Roles as Medicine. Rijeka, Croatia: InTech* **2017**, 75-93.

223. Mubofu, E. B.; Mgaya, J. E. Chemical Valorization of Cashew Nut Shell Waste. *Top Curr Chem (Cham)* **2018,** 376, 8.

224. Phani Kumar, P.; Paramashivappa, R.; Vithayathil, P. J.; Subba Rao, P. V.; Srinivasa Rao, A. Process for isolation of cardanol from technical cashew (Anacardium occidentale L.) nut shell liquid. *J Agric Food Chem* **2002,** 50, 4705-8.

225. Hemshekhar, M.; Sebastin Santhosh, M.; Kemparaju, K.; Girish, K. S. Emerging roles of anacardic acid and its derivatives: a pharmacological overview. *Basic Clin Pharmacol Toxicol* **2012,** 110, 122-32.

226. Baader, S.; Podsiadly, P. E.; Cole-Hamilton, D. J.; Goossen, L. J. Synthesis of tsetse fly attractants from a cashew nut shell extract by isomerising metathesis. *Green Chemistry* **2014,** 16, 4885-4890.

227. Cerone, M.; Uliassi, E.; Prati, F.; Ebiloma, G. U.; Lemgruber, L.; Bergamini, C.; Watson, D. G.; de A M Ferreira, T.; Roth Cardoso, G. S. H.; Soares Romeiro, L. A.; de Koning, H. P.; Bolognesi, M. L. Discovery of Sustainable Drugs for Neglected Tropical Diseases: Cashew Nut Shell Liquid (CNSL)-Based Hybrids Target Mitochondrial Function and ATP Production in Trypanosoma brucei. *ChemMedChem* **2019**.

228. Lemes, L. F. N.; de Andrade Ramos, G.; de Oliveira, A. S.; da Silva, F. M. R.; de Castro Couto, G.; da Silva Boni, M.; Guimarães, M. J. R.; Souza, I. N. O.; Bartolini, M.; Andrisano, V.; do Nascimento Nogueira, P. C.; Silveira, E. R.; Brand, G. D.; Soukup, O.; Korábečný, J.; Romeiro, N. C.; Castro, N. G.; Bolognesi, M. L.; Romeiro, L. A. S. Cardanol-derived AChE inhibitors: Towards the development of dual binding derivatives for Alzheimer's disease. *Eur J Med Chem* **2016,** 108, 687-700.

229. Soares Romeiro, L. A.; da Costa Nunes, J. L.; de Oliveira Miranda, C.; Simões Heyn Roth Cardoso, G.; de Oliveira, A. S.; Gandini, A.; Kobrlova, T.; Soukup, O.; Rossi, M.; Senger, J.; Jung, M.; Gervasoni, S.; Vistoli, G.; Petralla, S.; Massenzio, F.; Monti, B.; Bolognesi, M. L. Novel Sustainable-by-Design HDAC Inhibitors for the Treatment of Alzheimer's Disease. *ACS Med Chem Lett* **2019,** 10, 671-676.

230. Graham, W. V.; Bonito-Oliva, A.; Sakmar, T. P. Update on Alzheimer's Disease Therapy and Prevention Strategies. *Annu Rev Med* **2017,** 68, 413-430.

231. Huang, Y. M.; Shen, J.; Zhao, H. L. Major Clinical Trials Failed the Amyloid Hypothesis of Alzheimer's Disease. *J Am Geriatr Soc* **2019,** 67, 841-844.

232. Alzheimer's Drug Discovery Foundation. https://www.alzdiscovery.org/research-and-grants/funding-opportunities/drug-discovery. In.

233. Iqbal, K.; Grundke-Iqbal, I. Alzheimer's disease, a multifactorial disorder seeking multitherapies. *Alzheimers Dement* **2010,** 6, 420-4.

234. Chouliaras, L.; Rutten, B. P.; Kenis, G.; Peerbooms, O.; Visser, P. J.; Verhey, F.; van Os, J.; Steinbusch, H. W.; van den Hove, D. L. Epigenetic regulation in the pathophysiology of Alzheimer's disease. *Prog Neurobiol* **2010,** 90, 498-510.

235. Pal, S.; Tyler, J. K. Epigenetics and aging. *Sci Adv* **2016,** 2, e1600584.

236. Yang, S. S.; Zhang, R.; Wang, G.; Zhang, Y. F. The development prospection of HDAC inhibitors as a potential therapeutic direction in Alzheimer's disease. *Transl Neurodegener* **2017,** 6, 19.

237. Closing In On A Cure: 2017 Alzheimer's Clinical Trials Report. https://www.alzdiscovery.org/assets/content/static/ADDF-2017-Alzheimers-Clinical-Trials-Report.pdf.

238. Kilgore, M.; Miller, C. A.; Fass, D. M.; Hennig, K. M.; Haggarty, S. J.; Sweatt, J. D.; Rumbaugh, G. Inhibitors of class 1 histone deacetylases reverse contextual memory deficits in a mouse model of Alzheimer's disease. *Neuropsychopharmacology* **2010,** 35, 870-80.

239. Xu, K.; Dai, X. L.; Huang, H. C.; Jiang, Z. F. Targeting HDACs: a promising therapy for Alzheimer's disease. *Oxid Med Cell Longev* **2011,** 2011, 143269.

240. Doraiswamy, P. M.; Finefrock, A. E. Metals in our minds: therapeutic implications for neurodegenerative disorders. *Lancet Neurol* **2004,** 3, 431-4.

241. Dixon, S. J.; Lemberg, K. M.; Lamprecht, M. R.; Skouta, R.; Zaitsev, E. M.; Gleason, C. E.; Patel, D. N.; Bauer, A. J.; Cantley, A. M.; Yang, W. S.; Morrison, B.; Stockwell, B. R. Ferroptosis: an iron-dependent form of nonapoptotic cell death. *Cell* **2012,** 149, 1060-72.

242. Beard, J. L. Iron biology in immune function, muscle metabolism and neuronal functioning. *J Nutr* **2001,** 131, 568S-579S; discussion 580S.

243. Belaidi, A. A.; Bush, A. I. Iron neurochemistry in Alzheimer's disease and Parkinson's disease: targets for therapeutics. *J Neurochem* **2016,** 139 Suppl 1, 179-197.

244. Stockwell, B. R.; Friedmann Angeli, J. P.; Bayir, H.; Bush, A. I.; Conrad, M.; Dixon, S. J.; Fulda, S.; Gascón, S.; Hatzios, S. K.; Kagan, V. E.; Noel, K.; Jiang, X.; Linkermann, A.; Murphy, M. E.; Overholtzer, M.; Oyagi, A.; Pagnussat, G. C.; Park, J.; Ran, Q.; Rosenfeld, C. S.; Salnikow, K.; Tang, D.; Torti, F. M.; Torti, S. V.; Toyokuni, S.; Woerpel, K. A.; Zhang, D. D. Ferroptosis: A Regulated Cell Death Nexus Linking Metabolism, Redox Biology, and Disease. *Cell* **2017,** 171, 273-285.

245. Dolma, S.; Lessnick, S. L.; Hahn, W. C.; Stockwell, B. R. Identification of genotype-selective antitumor agents using synthetic lethal chemical screening in engineered human tumor cells. *Cancer Cell* **2003,** 3, 285-96.

246. Yang, W. S.; Stockwell, B. R. Synthetic lethal screening identifies compounds activating iron-dependent, nonapoptotic cell death in oncogenic-RAS-harboring cancer cells. *Chem Biol* **2008,** 15, 234-45.

247. Yagoda, N.; von Rechenberg, M.; Zaganjor, E.; Bauer, A. J.; Yang, W. S.; Fridman, D. J.; Wolpaw, A. J.; Smukste, I.; Peltier, J. M.; Boniface, J. J.; Smith, R.; Lessnick, S. L.; Sahasrabudhe, S.; Stockwell, B. R. RAS-RAF-MEK-dependent oxidative cell death involving voltage-dependent anion channels. *Nature* **2007,** 447, 864-8.

248. Hofmans, S.; Vanden Berghe, T.; Devisscher, L.; Hassannia, B.; Lyssens, S.; Joossens, J.; Van Der Veken, P.; Vandenabeele, P.; Augustyns, K. Novel Ferroptosis Inhibitors with Improved Potency and ADME Properties. *J Med Chem* **2016,** 59, 2041-53.

249. Devisscher, L.; Van Coillie, S.; Hofmans, S.; Van Rompaey, D.; Goossens, K.; Meul, E.; Maes, L.; De Winter, H.; Van Der Veken, P.; Vandenabeele, P.; Berghe, T. V.; Augustyns, K. Discovery of Novel, Drug-Like Ferroptosis Inhibitors with in Vivo Efficacy. *J Med Chem* **2018,** 61, 10126-10140.

250. Zille, M.; Kumar, A.; Kundu, N.; Bourassa, M. W.; Wong, V. S. C.; Willis, D.; Karuppagounder, S. S.; Ratan, R. R. Ferroptosis in Neurons and Cancer Cells Is Similar But Differentially Regulated by Histone Deacetylase Inhibitors. *eNeuro* **2019,** 6.

251. Sartori, L.; Minucci, S. Tackling oxidative stress by a direct route: a new job for HDAC inhibitors? *Chem Biol* **2015,** 22, 431-432.

252. Zwick, V.; Nurisso, A.; Simões-Pires, C.; Bouchet, S.; Martinet, N.; Lehotzky, A.; Ovadi, J.; Cuendet, M.; Blanquart, C.; Bertrand, P. Cross metathesis with hydroxamate and benzamide BOC-protected alkenes to access HDAC inhibitors and their biological evaluation highlighted intrinsic activity of BOC-protected dihydroxamates. *Bioorg Med Chem Lett* **2016,** 26, 154-9.

253. Bouchet, S.; Linot, C.; Ruzic, D.; Agbaba, D.; Fouchaq, B.; Roche, J.; Nikolic, K.; Blanquart, C.; Bertrand, P. Extending Cross Metathesis To Identify Selective HDAC Inhibitors: Synthesis, Biological Activities, and Modeling. *ACS Med Chem Lett* **2019,** 10, 863-868.

254. Francis, P. T.; Palmer, A. M.; Snape, M.; Wilcock, G. K. The cholinergic hypothesis of Alzheimer's disease: a review of progress. *J Neurol Neurosurg Psychiatry* **1999,** 66, 137-47.

255. Mesulam, M.; Guillozet, A.; Shaw, P.; Quinn, B. Widely spread butyrylcholinesterase can hydrolyze acetylcholine in the normal and Alzheimer brain. *Neurobiol Dis* **2002,** 9, 88-93.

256. Bazelyansky, M.; Robey, E.; Kirsch, J. F. Fractional diffusion-limited component of reactions catalyzed by acetylcholinesterase. *Biochemistry* **1986,** 25, 125-30.

257. Mushtaq, G.; Greig, N. H.; Khan, J. A.; Kamal, M. A. Status of acetylcholinesterase and butyrylcholinesterase in Alzheimer's disease and type 2 diabetes mellitus. *CNS Neurol Disord Drug Targets* **2014,** 13, 1432-9.

258. Maurya, S. S.; Khan, S. I.; Bahuguna, A.; Kumar, D.; Rawat, D. S. Synthesis, antimalarial activity, heme binding and docking studies of N-substituted 4-aminoquinoline-pyrimidine molecular hybrids. *Eur J Med Chem* **2017,** 129, 175-185.

259. Greig, N. H.; Lahiri, D. K.; Sambamurti, K. Butyrylcholinesterase: an important new target in Alzheimer's disease therapy. *Int Psychogeriatr* **2002,** 14 Suppl 1, 77-91.

260. Greig, N. H.; Utsuki, T.; Ingram, D. K.; Wang, Y.; Pepeu, G.; Scali, C.; Yu, Q. S.; Mamczarz, J.; Holloway, H. W.; Giordano, T.; Chen, D.; Furukawa, K.; Sambamurti, K.; Brossi, A.; Lahiri, D. K. Selective butyrylcholinesterase inhibition elevates brain acetylcholine, augments learning and lowers Alzheimer beta-amyloid peptide in rodent. *Proc Natl Acad Sci U S A* **2005,** 102, 17213-8.

261. Pezzementi, L.; Nachon, F.; Chatonnet, A. Evolution of acetylcholinesterase and butyrylcholinesterase in the vertebrates: an atypical butyrylcholinesterase from the Medaka Oryzias latipes. *PLoS One* **2011,** 6, e17396.

262. Bartus, R. T.; Dean, R. L.; Beer, B.; Lippa, A. S. The cholinergic hypothesis of geriatric memory dysfunction. *Science* **1982,** 217, 408-14.

263. Sampath, D.; Sathyanesan, M.; Newton, S. S. Cognitive dysfunction in major depression and Alzheimer's disease is associated with hippocampal-prefrontal cortex dysconnectivity. *Neuropsychiatr Dis Treat* **2017,** 13, 1509-1519.

264. Ezoulin, M. J.; Dong, C. Z.; Liu, Z.; Li, J.; Chen, H. Z.; Heymans, F.; Lelièvre, L.; Ombetta, J. E.; Massicot, F. Study of PMS777, a new type of acetylcholinesterase inhibitor, in human HepG2 cells. Comparison with tacrine and galanthamine on oxidative stress and mitochondrial impairment. *Toxicol In Vitro* **2006,** 20, 824-31.

265. Girek, M.; Szymański, P. Tacrine hybrids as multi-target-directed ligands in Alzheimer's disease: influence of chemical structures on biological activities. *Chemical Papers* **2019,** 73, 269-289.

266. Kozurkova, M.; Hamulakova, S.; Gazova, Z.; Paulikova, H.; Kristian, P. Neuroactive multifunctional tacrine congeners with cholinesterase, anti-amyloid aggregation and neuroprotective properties. *Pharmaceuticals* **2011,** 4, 382-418.

267. Spilovska, K.; Korabecny, J.; Nepovimova, E.; Dolezal, R.; Mezeiova, E.; Soukup, O.; Kuca, K. Multitarget Tacrine Hybrids with Neuroprotective Properties to Confront Alzheimer's Disease. *Curr Top Med Chem* **2017,** 17, 1006-1026.

268. Pang, Y. P.; Quiram, P.; Jelacic, T.; Hong, F.; Brimijoin, S. Highly potent, selective, and low cost bis-tetrahydroaminacrine inhibitors of acetylcholinesterase. Steps toward novel drugs for treating Alzheimer's disease. *J Biol Chem* **1996,** 271, 23646-9.

269. Rosini, M.; Andrisano, V.; Bartolini, M.; Bolognesi, M. L.; Hrelia, P.; Minarini, A.; Tarozzi, A.; Melchiorre, C. Rational approach to discover multipotent anti-Alzheimer drugs. *J Med Chem* **2005,** 48, 360-

3.

270. Muñoz-Ruiz, P.; Rubio, L.; García-Palomero, E.; Dorronsoro, I.; del Monte-Millán, M.; Valenzuela, R.; Usán, P.; de Austria, C.; Bartolini, M.; Andrisano, V.; Bidon-Chanal, A.; Orozco, M.; Luque, F. J.; Medina, M.; Martínez, A. Design, synthesis, and biological evaluation of dual binding site acetylcholinesterase inhibitors: new disease-modifying agents for Alzheimer's disease. *J Med Chem* **2005,** 48, 7223-33.

271. Chen, Y.; Sun, J.; Peng, S.; Liao, H.; Zhang, Y.; Lehmann, J. Tacrine-flurbiprofen hybrids as multifunctional drug candidates for the treatment of Alzheimer's disease. *Arch Pharm (Weinheim)* **2013,** 346, 865-71.

272. Keri, R. S.; Quintanova, C.; Marques, S. M.; Esteves, A. R.; Cardoso, S. M.; Santos, M. A. Design, synthesis and neuroprotective evaluation of novel tacrine-benzothiazole hybrids as multi-targeted compounds against Alzheimer's disease. *Bioorg Med Chem* **2013,** 21, 4559-69.

273. Camps, P.; Formosa, X.; Galdeano, C.; Gómez, T.; Muñoz-Torrero, D.; Scarpellini, M.; Viayna, E.; Badia, A.; Clos, M. V.; Camins, A.; Pallàs, M.; Bartolini, M.; Mancini, F.; Andrisano, V.; Estelrich, J.; Lizondo, M.; Bidon-Chanal, A.; Luque, F. J. Novel donepezil-based inhibitors of acetyl- and butyrylcholinesterase and acetylcholinesterase-induced beta-amyloid aggregation. *J Med Chem* **2008,** 51, 3588-98.

274. de Souza, M. Q.; Teotônio, I. M. S. N.; de Almeida, F. C.; Heyn, G. S.; Alves, P. S.; Romeiro, L. A. S.; Pratesi, R.; de Medeiros Nóbrega, Y. K.; Pratesi, C. B. Molecular evaluation of anti-inflammatory activity of phenolic lipid extracted from cashew nut shell liquid (CNSL). *BMC complementary and alternative medicine* **2018,** 18, 181.

275. Nordberg, A.; Ballard, C.; Bullock, R.; Darreh-Shori, T.; Somogyi, M. A review of butyrylcholinesterase as a therapeutic target in the treatment of Alzheimer's disease. *Prim Care Companion CNS Disord* **2013,** 15.

276. Zha, X.; Lamba, D.; Zhang, L.; Lou, Y.; Xu, C.; Kang, D.; Chen, L.; Xu, Y.; De Simone, A.; Samez, S.; Pesaresi, A.; Stojan, J.; Lopez, M. G.; Egea, J.; Andrisano, V.; Bartolini, M. Novel Tacrine-Benzofuran Hybrids as Potent Multitarget-Directed Ligands for the Treatment of Alzheimer's Disease: Design, Synthesis, Biological Evaluation, and X-ray Crystallography. *J Med Chem* **2016,** 59, 114-31.

277. Nachon, F.; Carletti, E.; Ronco, C.; Trovaslet, M.; Nicolet, Y.; Jean, L.; Renard, P. Y. Crystal structures of human cholinesterases in complex with huprine W and tacrine: elements of specificity for anti-Alzheimer's drugs targeting acetyl- and butyryl-cholinesterase. *Biochem J* **2013,** 453, 393-9.

278. Vu, C. B.; Bridges, R. J.; Pena-Rasgado, C.; Lacerda, A. E.; Bordwell, C.; Sewell, A.; Nichols, A. J.; Chandran, S.; Lonkar, P.; Picarella, D.; Ting, A.; Wensley, A.; Yeager, M.; Liu, F. Fatty Acid Cysteamine Conjugates as Novel and Potent Autophagy Activators That Enhance the Correction of Misfolded F508del-Cystic Fibrosis Transmembrane Conductance Regulator (CFTR). *J Med Chem* **2017,** 60, 458-473.

279. Kim, I. H.; Kanayama, Y.; Nishiwaki, H.; Sugahara, T.; Nishi, K. Structure-Activity Relationships of Fish Oil Derivatives with Antiallergic Activity in Vitro and in Vivo. *J Med Chem* **2019,** 62, 9576-9592.